Y-12

Y/EN-4683

OAK RIDGE
Y-12
PLANT

MARTIN MARIETTA

SEISMIC HAZARD EVALUATION FOR DEPARTMENT OF ENERGY OAK RIDGE RESERVATIONS OAK RIDGE, TENNESSEE

R. K. McGuire, Risk Engineering, Inc.
G. F. Toro, Risk Engineering, Inc.
R. J. Hunt, Center for Natural Phenomena Engineering, Engineering Division

SEPTEMBER 30, 1992

Prepared by

Oak Ridge Y-12 Plant
Oak Ridge, Tennessee 37831

managed by
Martin Marietta Energy Systems, Inc.

Prepared for the
U.S. Department of Energy under
U.S. Government contract DE-AC05-84OR21400

MANAGED BY
MARTIN MARIETTA ENERGY SYSTEMS, INC.
FOR THE UNITED STATES
DEPARTMENT OF ENERGY

DISCLAIMER

EXECUTIVE SUMMARY

This study presents the results of an investigation of seismic hazard at the Department of Energy Oak Ridge Reservations (K-25 Site, Oak Ridge National Laboratories, and Oak Ridge Y-12 Plant)[1], located in Oak Ridge Tennessee. Oak Ridge is located in eastern Tennessee, in an area of moderate to high historical seismicity.

Results from two separate seismic hazard analyses are presented here. The EPRI/SOG analysis uses the input data and methodology developed by the Electric Power Research Institute, under the sponsorship of several electric utilities, for the evaluation of seismic hazard in the central and eastern United States. Section 2 of this report documents the application of the EPRI/SOG methodology to the Oak Ridge site. The LLNL analysis uses the input data and methodology developed by the Lawrence Livermore National Laboratory for the Nuclear Regulatory Commission. This analysis was performed by LLNL and results were transmitted to us. Section 3 of this report contains a summary of LLNL inputs and results (considering 4 and 5 LLNL ground motion experts).

Both the EPRI/SOG and LLNL studies characterize earth-science uncertainty on the causes and characteristics of earthquakes in the central and eastern United States. This is accomplished by considering multiple hypotheses on the locations and parameters of seismic source zones and by considering multiple attenuation functions for the prediction of ground shaking given earthquake size and location. These hypotheses were generated by multiple expert teams and experts. Furthermore, each team and expert was asked to generate multiple hypotheses in order to characterize his own internal uncertainty. The seismic-hazard calculations are performed for all hypotheses. Combining the results from each hypothesis with the weight associated to that hypothesis, one obtains an overall representation of the seismic hazard at the Oak Ridge site and its uncertainty.

Combining the EPRI/SOG and LLNL results with equal weights—while considering their respective uncertainties—provides another set of seismic-hazard results. Section 4 explains the combination process and presents results (for both rock and soil conditions, and considering 4 and 5 LLNL ground motion experts).

The following table summarizes results from the EPRI/SOG and LLNL analyses, and the combined results, for peak ground acceleration and spectral velocity at 1 Hz (5% damping).

[1]Managed by Martin Marietta Energy Systems, Inc. for the U.S. Department of Energy under contract DE-AC05-840R21400.

Ground-Motion Amplitudes for Selected Values of
the Median Annual Exceedance Probability

Ground Motion Measure	Annual Exceedance Probability	EPRI	LLNL (4 GX†)	LLNL (5 GX†)	Combined EPRI+LLNL (4 GX†)	Combined EPRI+LLNL (5 GX†)
Peak Ground Acceleration (g)	2×10^{-3} (500 yr)	0.041	0.050	0.068	0.043	0.051
	1×10^{-3} (1000 yr)	0.068	0.073	0.100	0.068	0.076
	2×10^{-4} (5000 yr)	0.153	0.162	0.209	0.153	0.170
1-Hz Spectral Velocity (cm/sec)	2×10^{-3} (500 yr)	0.96	2.46	3.38	1.42	1.60
	1×10^{-3} (1000 yr)	1.45	3.38	4.74	2.01	2.37
	2×10^{-4} (5000 yr)	3.67	7.03	10.2	4.55	5.76

† 4GX and 5GX denote results obtained considering 4 and 5 LLNL ground-motion experts

The EPRI/SOG and LLNL are also used to calculate site-specific design spectra for the Oak Ridge site, using the Department of Energy interim procedure for combining the EPRI/SOG and LLNL seismic hazard results. Section 5 documents the calculation of design spectra; Section 6 documents the generation of artificial ground motions compatible with these spectra.

CONTENTS

LIST OF FIGURES

LIST OF TABLES

Section 1

INTRODUCTION

This study investigates the probabilistic hazard of earthquake-induced ground shaking at the U. S. Department of Energy Oak Ridge Reservations (K-25 Site, Oak Ridge National Laboratories, and Oak Ridge Y-12 Plant), in Oak Ridge, Tennessee.[1] These results will be used to make decisions regarding seismic safety and levels of seismic design at the facility. An express purpose of this study is to make use of the most recent studies of seismic hazard in the central and eastern United States, which represent uncertainty in the seismic hazard caused by multiple, alternative hypotheses on the causes and characteristics of earthquakes.

Recent intensive studies of seismic hazard in the central and eastern United States (CEUS) have been completed by the Electric Power Research Institute (EPRI), funded by the Seismicity Owners Group (1), and by the Lawrence Livermore National Laboratory (LLNL), funded by the U.S. Nuclear Regulatory Commission (2). These studies represent major efforts to characterize the seismic hazard for nuclear power plants in the CEUS, and use the most recent, up-to-date understandings of seismicity and ground motion relations for the region. With these studies as a resource, the current effort relies exclusively on the seismicity and ground motion assumptions therein to formulate seismic hazard curves for the Oak Ridge complex. The interpretation of these studies to derive seismic hazard curves in a format suitable for evaluation of the facility is described in this report.

Both the EPRI/SOG and LLNL studies utilize a point-source representation of earthquakes, thereby ignoring the non-zero dimensions of earthquake ruptures. This simplification is appropriate for Oak Ridge and for most other sites in CEUS, because earthquakes with large ruptures are highly unlikely to occur near these sites (due to low values of maximum magnitude).

The coordinates used to represent the Oak Ridge reservations are latitude 35.95 north and longitude 84.33 west.[2] Structures at the site are founded on rock. Consistent with other

[1]The remainder of this report will use the term "Oak Ridge site" to refer to the Oak Ridge Reservations

[2]These coordinates correspond to the High-Flux Isotope Reactor (HFIR) site, but the results are applicable to the entire Oak Ridge site. Some of the hazard results presented here were obtained for HFIR under a separate study (3).

recent seismic hazard analyses, we report the distribution of peak horizontal ground acceleration (PGA) and spectral velocities at multiple frequencies; we also show constant percentile hazard curves to demonstrate a typical spectral shape that might apply for the ground motions of interest.

Section 2 of this report summarizes the application of the EPRI methodology for the Oak Ridge site. The LLNL methodology was applied by LLNL, who transmitted results to us for use in the HFIR study. Their results and our interpretation of them are described in Section 3. The synthesis of the results of the two studies is described in Section 4, in the form of multiple hazard curves that represent the distribution of frequency of exceedance of PGA levels. Section 5 documents the use of the EPRI/SOG and LLNL results to calculate the site-specific design spectra, using an interim procedure developed by the Department of Energy (4). Section 6 investigates the characteristics of earthquakes associated with the design spectra and generates corresponding artificial ground motions. Finally, Section 7 presents conclusions of the study and some important qualifications to these results.

1.1 REFERENCES

1. *Seismic Hazard Methodology for the Central and Eastern United States.* Technical Report NP-4726-A, Electric Power Research Institute, July 1986. Revised, 1988. Vol. 1, Part 1: Methodology, Vol. 1, Part 2: Theory, Vol. 2: EQHAZARD Programmer's Manual, Vol. 3: EQHAZARD User's Manual, Vol. 4: Applications, Vols. 5 through 10: Tectonic Interpretations, Vol. 11: Nuclear Regulatory Commission Safety Review.

2. D. L. Bernreuter, J. B. Savy, R. W. Mensing, and J. C. Chen. *Seismic Hazard Characterization of 69 Plant Sites East of the Rocky Mountains.* Technical Report NUREG/CR5250, UCID-21517, U. S. Nuclear Regulatory Commission, 1988.

3. Risk Engineering, Inc. *Seismic Hazard Evaluation for the High-Flux Isotope Reactor (HFIR): Oak Ridge National Laboratory, Oak Ridge, Tennessee.* Final Report to Pickard, Lowe and Garrick, Inc., February 1991.

4. Department of Energy Seismic Working Group. Use of LLNL and EPRI Probabilistic Seismic Hazard Curves: Interim Position. Attachment to Memorandum of W.H. Young to Program Secretarial Officers, dated March 19, 1992. U.S. Department of Energy, 1992.

Section 2

EPRI/SOG METHODOLOGY AND RESULTS

2.1 INTRODUCTION

This Section describes the EPRI/SOG methodology and inputs for seismic-hazard analysis in the central and eastern United States, documents the application of these for the Oak Ridge site, and presents the results obtained from this application.

These results will be combined in Sections 4 and 5 with the corresponding results from the LLNL analysis, to generate aggregate seismic-hazard results and design spectra for the Oak Ridge site.

The EPRI/SOG methodology calculates ground-motion exceedance probabilities using earth-science hypotheses about the causes and characteristics of earthquakes in the central and eastern United States. Scientific uncertainty about the causes of earthquakes and about the physical characteristics of potentially active tectonic features lead to uncertainties in the inputs to the seismic hazard calculations. These uncertainties are quantified by using the tectonic interpretations developed by six Earth-Science Teams, who quantified the likelihood associated with alternative tectonic features and the likelihood associated with alternative characteristics of these potential sources.

These and other uncertainties are carried through the entire analysis. The result of the analysis is a suite of hazard curves and their associated weights; they quantify the seismic hazard at the site and its uncertainty.

Each team was comprised of at least four members with expertise in different earth-science disciplines. Table 2–1 lists the six teams and their members.

2.2 EPRI/SOG METHODOLOGY

2.2.1 Basic Seismic Hazard Model

The methodology to calculate seismic hazard at a site is well established in the literature (1,2,3,4,5). In the EPRI/SOG methodology, calculation of the hazard contributed by one source requires specification of three inputs:

Table 2-1

EPRI/SOG Earth-Science Teams

Team	Members
Bechtel Group, Inc.	Thomas Buschbach Robert D. Hatcher, Jr. Joseph Litehiser† Rolfe Stanley Isidore Zietz
Dames and Moore	Charles Fairhurst Robert Herrmann Lyle McGinnis James McWhorter† Rene Rodriguez
Law Engineering Testing Company	Robert Butler Martin Chapman John Dwyer Arch Johnston Timothy Long Malcolm Schaeffer William Seay Robert White†
Rondout Associates, Inc.	Noël Barstow† William Hinze Pradeep Talwani Barry Voight
Weston Geophysical Corporation	Richard Holt George Klimkiewicz† Gabriel LeBlanc Donald Wise
Woodward-Clyde Consultants	Terry Engelder John Kelleher Richard Quittmeyer Thomas Statton† Thomas Turcotte

†TeamLeader

1. Source geometry: the geographic description of the seismic source. A seismic source is a portion of the earth's crust, associated with a tectonic feature or with a concentration of historic seismicity, which may be capable of producing earthquakes. Source geometry determines the probability distribution of distance from the earthquake to the site: $f_R(r)$. In the EPRI/SOG methodology, each seismic source is divided into cells of 1 degree latitude by 1 degree longitude and $f_{R(i)}(r)$ is computed for each cell.

2. Seismicity: the rate of occurrence ν_i and magnitude distribution $f_{M(i)}(m)$ of earthquakes within each cell. Magnitude is characterized by the body-wave magnitude m_b.

3. Attenuation functions: a relationship that allows the estimation of ground motion at the site as a function of earthquake magnitude and distance.

These inputs are illustrated in Figure 2–1, parts a through c. Figure 2–1a shows the geometry of a seismic source and a cell within that source. From the cell's geometry, $f_{R(i)}(r)$, can be derived. The density function on magnitude $f_{M(i)}(m)$ is the doubly truncated exponential distribution as shown in figure 2-1b. Seismicity in a cell is completely specified by a minimum magnitude m_0, a maximum magnitude m_{max}, and parameters a and b. a is a measure of seismic activity per unit area, b is a measure of relative frequency of large versus small events, and $\log[\nu_i f_{M(i)}(m)]$ is proportional to $a + b\ m$ for $m_0 < m \leq m_{max}$. The ground motion is modeled by an attenuation function, as illustrated in figure 2-1c. Attenuation functions are usually of the form $\ln[Y] = f(M, R) + \epsilon$, where Y is ground-motion amplitude, M is magnitude, R is distance, and ϵ is a random variable that represents scatter. The attenuation function is used to calculate $G_{Y|m,r}(y) = P[Y > y|m, r]$: the probability that the ground-motion amplitude be larger than y, for given M and R. The seismic hazard contributed by a source is calculated as :

$$\frac{P[Y > y \text{ in time } t]}{t} \simeq \sum_i \nu_i \int\int P[Y > y|m, r]\ f_{M(i)}(m)\ f_{R(i)}(r)\ dm\ dr \qquad (2-1)$$

in which the summation is performed over all cells that comprise the source.

Equation 2-1 is formulated using the assumption that earthquakes (most particularly, successive earthquakes) are independent in size and location. In all seismic hazard applications, primary interest is focused on computing probabilities for high (rare) ground motions (as a result, the probability of two exceedances in time t is negligible). Thus, the quantity on the right side of Equation 2-1 — which is the rate of earthquakes with $Y > y$ — is a good approximation to the probability of exceeding amplitude y in time t. The same argument

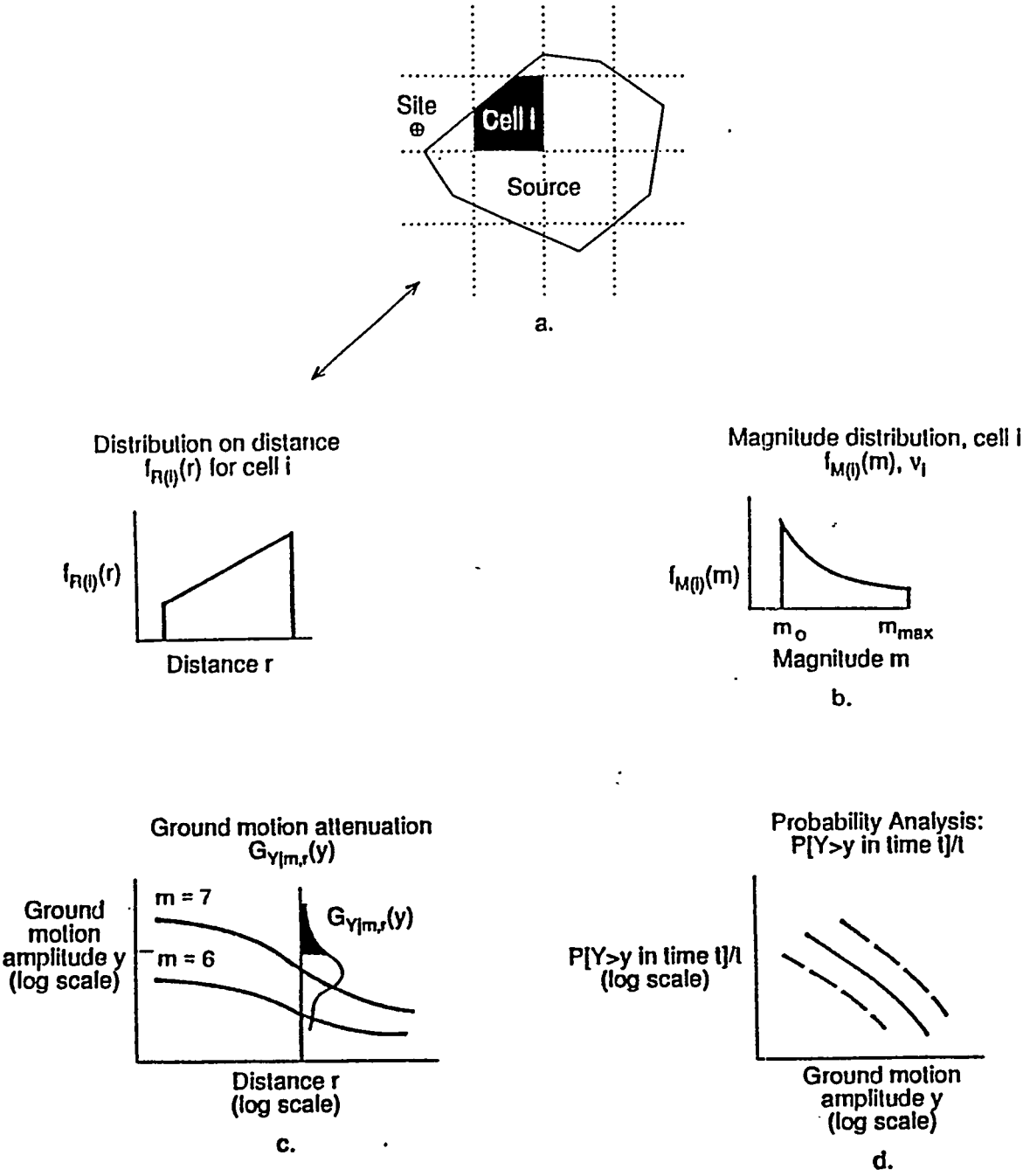

Figure 2-1. Seismic hazard computational model. Source: (6).

holds when considering hazard at a site from multiple sources. Terms similar to the right hand side of equation 2-1 are summed to compute, to very good approximation, the total hazard at the site (see Figure 2-1d).

The calculation of hazard from all sources is performed for multiple values of y in order to generate the hazard curve, which gives the annual probability of exceedance as a function of y. This calculation is performed for 6 different measures of ground motion: peak ground acceleration and spectral velocities at 5 frequencies (1, 2.5, 5, 10, 25 Hz; 5% damping).

2.2.2 Treatment of Uncertainty

Most recent seismic-hazard studies distinguish between two types of variability: randomness and uncertainty. Randomness is probabilistic variability that results from natural physical processes. The size, location and time of the next earthquake on a fault and the details of the ground motion are examples of random events. In concept, these elements cannot be predicted even with collection of additional data, so the randomness component of variability is irreducible. The second category of variability is "uncertainty" which is the statistical or modeling variability that result from lack of knowledge about the true state of nature. In principle, this variability can be reduced with the collection of additional data.

These two types of variability are treated differently in advanced seismic hazard studies, as follows: integration is carried out over probabilistic variabilities to get a single hazard curve (see equation 2–1), whereas modeling uncertainties are expressed by multiple assumptions, hypotheses, or parameter values. These multiple interpretations result in a suite of hazard curves and their associated weights.

There are uncertainties associated with each of the three inputs to the seismic-hazard evaluation, as follows:

- Uncertainty about seismic sources (i.e., which tectonic features in a region are actually earthquake sources) arises because there are multiple hypotheses about the causes of earthquakes in CEUS and because there is incomplete knowledge about the physical characteristics of tectonic features. Uncertainty may also arise about the geometry of a seismic source.
- Uncertainty in seismicity is generally divided into uncertainty in maximum magnitude and uncertainty in seismicity parameters a and b. Uncertainty about, m_{max}, the maximum magnitude that a given source can generate arises for the same reasons

described above. Estimates of m_{max} are obtained from physical characteristics of the source and from historic seismicity. Uncertainty in seismicity parameters a and b arises from statistical uncertainty and from uncertainty about the variability of a and b between cells in a given source.

- Uncertainty in the attenuation functions arises from alternative hypotheses about the dynamic characteristics of earthquakes in CEUS. This uncertainty has been large because there have been few strong-motion recordings from earthquakes of engineering interest in CEUS.

The EPRI/SOG methodology quantifies seismic hazard and its uncertainty by using as inputs the tectonic interpretations developed by six multidisciplinary Earth-Science Teams. In addition, each team quantified its uncertainty about seismic sources, maximum magnitudes, and seismicity parameters, as follows:

- Uncertainty about seismic sources was characterized by specifying an activity probability P^a to each seismic source and specifying activity dependencies among sources in the same region.

- Uncertainty about maximum magnitude is characterized by a discrete distribution of m_{max} for each source. That is, multiple values of m_{max} are specified and given weights.

- Uncertainty about seismicity parameters is characterized by considering multiple sets of parameter values of each source, and giving them weights. Each set of parameters is computed, for instance, using different assumptions about spatial continuity of a and b, or using different portions of the earthquake catalog.

Ground-motion attenuation in CEUS, and its uncertainty, is quantified by considering three alternative attenuation functions for each ground-motion measure, and giving them weights (see Section 2.4). The development and selection of these attenuation equations is documented in (7) and in Appendix A of (6).

In order to organize and display the multiple hypotheses, assumptions, parameter values, and their possible combinations, a logic tree approach is used. Logic trees are a convenient means to express alternative interpretations and their probabilities.

Each level of the logic tree represents one source of uncertainty. The branches emanating from one node represent possible values of a parameter. The probability assigned to a branch represents the likelihood of the parameter value associated with that branch, given certain values of the preceding parameters.

The logic tree in Figure 2–2 represents the treatment of parameter uncertainty in the EPRI/SOG methodology, for one team. Associated with each terminal node, there is one hazard curve, which corresponds to certain sources being active, each active source having a certain m_{max} and certain seismicity parameters, and a certain attenuation function being the true attenuation model. The probability associated with that end branch is the product of the probabilities of all branches traversed to reach that terminal node.

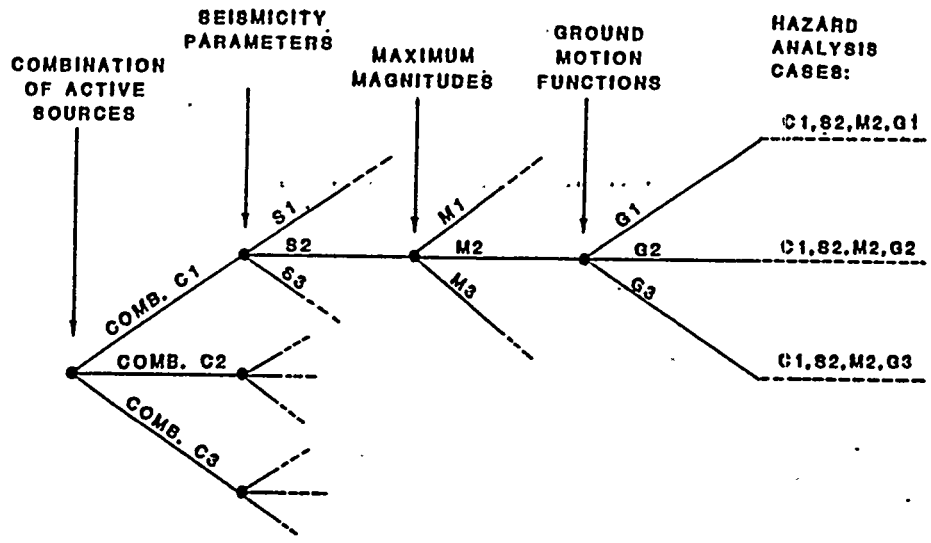

Figure 2-2. Logic tree representation of uncertain parameters in the EPRI/SOG methodology

The hazard curves obtained by the 6 teams are given equal weights and then combined. The resulting family of hazard curves and their associated probabilities, corresponding to all end branches of the six teams' logic trees, contains all the information about seismic hazard at the site, its uncertainty, and the different contributors to that uncertainty.

2.2.3 Development of Seismological Interpretations

This section briefly describes the development of the EPRI/SOG seismic sources and the estimation of their their parameters; a complete description is found in Volume 1, Sections 3 and 4, of (8). Volumes 5 through 10 of (8) document the seismological interpretations by

the six Earth-Science Teams. Section 2.3 describes the seismic sources that contribute to hazard at the Oak Ridge site, and the characteristics of these sources.

Seismic Sources. In the EPRI/SOG methodology, seismic sources have the following characteristics:

- A seismic source is associated with potentially active tectonic features or with a cluster of seismicity.
- The entire source is either active or inactive.
- Every point within the source has the same maximum magnitude.
- The seismic source is composed of individual cells (1 degree latitude by 1 degree longitude). Seismicity parameters a and b may be specified separately for each cell within the source.

The EPRI/SOG seismic sources were developed using the tectonic framework: a structured approach to identify tectonic features that may be capable of generating earthquakes, interpret scientific knowledge concerning the causative mechanisms of earthquakes in CEUS, delineate seismic sources, and assess probabilities of activity (P^a) for these sources.

In addition, the teams assessed joint activity probabilities for multiple sources in the same region. In most cases, the Teams specified joint activity probabilities through simple forms of dependence, such as perfect dependence or mutual exclusivity. Activity dependencies have no effect on the mean hazard (because the total hazard is a linear combination of source hazards), but they have an effect on uncertainty. Perfect dependence produces the highest uncertainty, mutual exclusivity produces the lowest uncertainty.

Seismicity Parameters. Seismicity parameters a and b are estimated using the maximum likelihood method. Parameters a and b (especially a) may be allowed to vary spatially within a seismic source. For computational convenience, they are assumed to be constant within each 1-degree cell within the source. The degree of spatial variability (or smoothing) of a and b between adjacent cells in each source is controlled by the seismicity option. Each team captured uncertainty on the appropriate degree of smoothing for each source (i.e., whether the source has homogeneous seismicity or if the activity rates follow the within-source pattern of historic activity) by specifying alternative seismicity options, with associated probabilities.

In addition, the teams could specify a prior distribution (in the Bayesian sense) on b, and other parameters of the estimation algorithm, with each seismicity option.

Maximum Magnitudes. To calculate seismic hazard at a site, the largest possible earthquake magnitude that can occur in each seismic source must be estimated. This maximum magnitude m_{max} is generally uncertain. This uncertainty is represented by a probability distribution on the maximum magnitude that the source can generate.

Each team estimated a probability distribution of m_{max} for each active source that the team had identified. The following considerations were used to constrain the maximum-magnitude estimates:

- Physical Constraints. These approaches relate m_{max} to the size of the source or the thickness of the earth's crust.
- Historic Seismicity. These approaches involve the addition of an increment to the maximum historical magnitude, extrapolation of the magnitude-recurrence relation to some justified frequency of occurrence, and the statistical treatment of the earthquake catalog.
- Analogies With Other Sources or Regions. If one is able to identify a number of analogous sources, so that one can assume that they all have the same value of m_{max}, one can improve the precision of m_{max} estimates obtained from statistical analyses. The analyses of earthquakes in other intraplate regions of the world is another way to increase sample size. A study of this type was performed by EPRI (9,10); m_{max} values were obtained for various types of tectonic features.

The EPRI/SOG methodology uses discrete distributions to represent uncertainty in m_{max}. When a team specified continuous distributions or discrete distributions with excessive numbers of values, equivalent discrete distributions were developed.

Minimum Magnitude. The minimum magnitude m_0 introduced in Section 2.2.1 represents the smallest magnitude of interest in the hazard calculations. It is assumed that earthquakes with magnitudes lower than m_0 are incapable of causing damage. Therefore, the choice of m_0 is related to the type of facility being analyzed.

Based on the seismological characteristics of small earthquakes, analysis of structural response, and field studies of structural performance during low-intensity ground motions, it

has been concluded that it is appropriate to use moment magnitude 5.0 (which corresponds to m_b approximately equal to 5.5) as the minimum magnitude for seismic-hazard calculations (11,12). As an added measure of conservatism, the EPRI/SOG methodology uses m_b 5.0 as the minimum magnitude. This value is considered more than sufficiently conservative to compensate for the small probability that an earthquake with $m_b < 5.0$ could cause damage to a well-engineered structure.

2.2.4 Computer Codes

The computer package EQHAZARD performs seismic-hazard calculations using the EPRI/SOG methodology and seismological interpretations. This section provides a brief description of the various modules in EQHAZARD and their functions (see Figure 2–3). Volumes 2 and 3 of (8) contain a detailed description of these computer codes.

Modules for the Development of a Homogeneous Earthquake Catalog. The development of a homogeneous earthquake catalog is performed by five modules: CREINP, EQCONVERT, UNIMAG, EQCLUSTER, and CRECAT. These programs perform two main functions: (1) calculate a uniform value of m_b for each earthquake, using all size measures available (e.g., m_b, M_L, epicentral intensity, felt area); and (2) identify and eliminate secondary events (e.g., aftershocks). The result is a catalog of main events in which earthquake size is measured by the uniform m_b.

Module for the estimation of seismicity parameters—EQPARAM. EQPARAM estimates seismicity parameters for area seismic sources, using as basic inputs the earthquake catalog, the source geometries and seismicity parameters specified by one Earth-Science team, and catalog incompleteness information.

Modules for the calculation of seismic hazard. EQHAZ calculates the seismic hazard at one site from each source specified by one Earth-Science team. Hazard is simultaneously calculated for several measures of ground motion. EQPOST calculates the total hazard at the site and its uncertainty for one or more Earth-Science Teams, and calculates the sensitivity of seismic hazard to attenuation function, maximum magnitudes, seismicity options, and earth-science teams. EQAG calculates the group-consensus mean log hazard as a weighted sum of the teams' results for that site. Module EQAG was not used in this study.

2.3 TECTONIC AND SEISMICITY INTERPRETATIONS

The specification of potential sources of future earthquakes is the first step in the evaluation of earthquake hazards. Seismic sources indicate where earthquakes may occur; analysis of

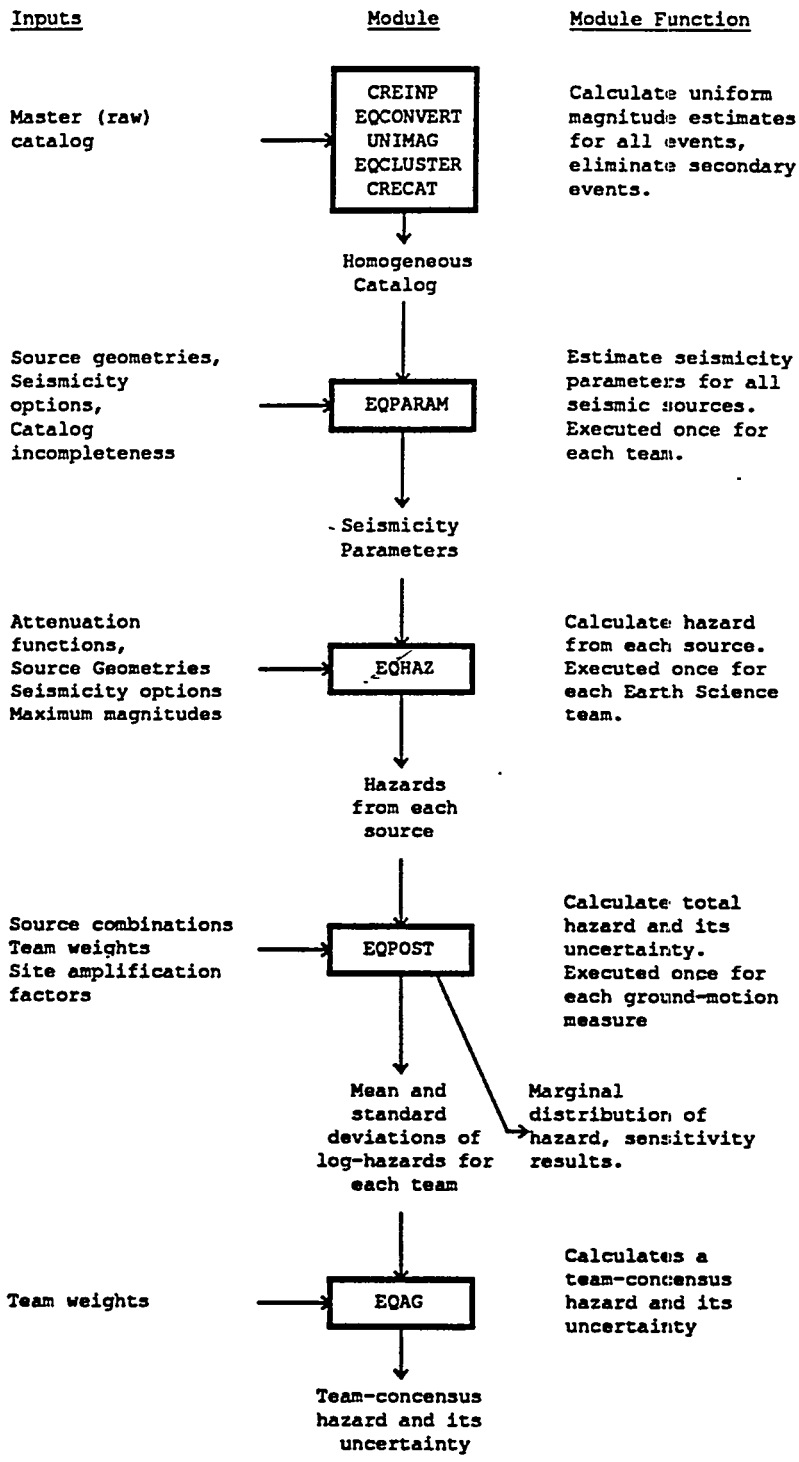

Figure 2-3. EQHAZARD modules: their functions and data flow. Source: (6).

historical seismicity within those defined sources indicates the probabilities of occurrence and characteristics of future earthquakes (i.e., we fit a magnitude distribution to historical data within the source, once the source is defined).

In the EPRI/SOG methodology, a seismic source is defined as a region with a single probability of activity P^a and a single maximum magnitude (which may be uncertain). Within a seismic source the seismicity (quantified by parameters a and b) can vary in space.

In general, the sources derived by the six Teams are based on tectonic features and other evidence (including, in some cases, merely a spatial cluster of historical seismicity). Because of this derivation there is, conceptually, some causal association of earthquakes within a source: they are releasing crustal stresses of the same orientation and amplitude, and/or they are caused by slip on faults with the same general depth, orientation, and sense of slip. Because of these similarities the delineation conforms to the seismic source definition with regard to maximum magnitude and probability of activity.

This section reviews the characteristics of seismic sources in the EPRI/SOG methodology and briefly summarizes the interpretations by the 6 Teams. Volumes 5 through 10 of (8) describe and document these interpretations.

2.3.1 Seismic Sources

Sets of seismic sources were derived for the central and eastern US by the six Earth Science Teams, using the project data bases of geologic, geophysical, and seismological evidence (including historical seismicity). The bases for these derivations are given in detail in Volumes 5 through 10 of (8). During the project, multiple interpretations were encouraged, to express uncertainty on the causes of earthquakes and their physical expression in the form of seismic sources. In other words, if there were multiple theories on the physical causes of earthquakes, and these theories had different implications in terms of the regions within which future earthquakes were thought possible, the Teams were encouraged to express these uncertainties with multiple tectonic features and seismic sources. Each Team's uncertainty was quantified through its assessments of P^a for each source and a specification of the interdependency of activity (whether the state of activity of one source affects the activity of another). Five of the six Teams specified interdependencies among sources.

Joint activity probabilities were often specified through the following simple forms of dependence:

- Perfect Dependence (PD). Two sources A and B are perfectly dependent if the probability that A is active, given that B is active, is unity. This form of dependency arises between tectonic features with the same physical characteristics (e.g., multiple faults with identical orientations).

- Independence. Two sources a and b are independent if the state of activity of source A does not affect the state of activity of source B. Mathematically, $P^a[A \text{ and } B] = P^a[A]P^a[B]$.

- Mutual Exclusivity (ME). Two sources A and B are mutually exclusive if the probability of A being active, given that B is active, is zero. Mutually exclusive sources are used to represent alternative hypotheses for the causes of seismicity in a region or uncertainty on the geographic extent of a seismic source.

- Default Sources. This is a special form of mutual exclusivity. It arises when an earthquake is known to have occurred in a region, but the tectonic features (say, the features represented by sources A, B, and C) do not make a collectively exhaustive set (i.e., $P^a[A \text{ or } B \text{ or } C] < 1$). A default source D, with $P^a[D] = 1 - P^a[A \text{ or } B \text{ or } C]$ and $P[D|(A \text{ or } B \text{ or } C)] = 0$, must be added in order to have a model of seismicity that is consistent with historical seismicity.

The Weston and Woodward-Clyde teams characterized the probability of activity using P^*: the probability that the source is capable of generating earthquakes with magnitudes larger than 5. P^* and P^a are related through the distribution of maximum magnitude.

Background sources and their probabilities of activity P^a_{BG} require special description, as the interpretation is slightly different from that for primary sources. A background source represents a region where specific causes of earthquakes cannot be identified, but where a Team feels that earthquakes will occur. The regions of background sources are defined so that there is one maximum-magnitude (m_{max}) distribution for the entire source, but the interpretation of P^a_{BG} is not that the background is active with probability P^a_{BG} and inactive with probability 1 - P^a_{BG}. Rather, P^a_{BG} represents the fraction of area of the background that is active. In the hazard calculations if the background contributes significantly the background hazard is weighted by P^a_{BG} to calculate the correct average contribution of hazard from the background.

All Teams except Dames and Moore and Rondout used background sources to some extent. P^a_{BG} was set to unity by all teams except Law Engineering. The Woodward-Clyde Consultants Team used local background sources centered at each EPRI/SOG site. For the Oak Ridge site, we used the Watts Bar background. (This is accurate because the two sites are close relative to the size of the background.)

2.3.2 Maximum Magnitudes and Seismicity Options

Each team specified maximum magnitudes and seismicity options for each source it had identified.

Most teams specified maximum magnitudes in the form of discrete distributions with 2 to 4 values (i.e., they specified multiple alternative values of m_{max} with associated weights). The Law Engineering Team specified only one value of maximum magnitude for some sources. The Woodward-Clyde Team specified a larger number of values for all sources; these values were transformed into an equivalent discrete distribution with three values.

Each seismicity option specifies the assumptions used in the estimation of seismicity parameters a and b for that source. Each option specifies the cell-to-cell variability of a and b, the prior distribution of b, and the weight (or importance) given to small-magnitude earthquakes in the estimation process. Alternatively, a seismicity option may directly specify the values of a and b. All teams except Law and Rondout specified 2 to 4 alternative seismicity options (with associated weights) for most sources.

2.3.3 Seismic Sources near the Oak Ridge Site

Figures 2–4 through 2–9 show the seismic sources near the Oak Ridge site, as identified by the six Earth-Science Teams. Tables 2–2 through 2–7 list those seismic sources near Oak Ridge that contribute to seismic hazard at the site. These tables also include the sources' maximum magnitudes, seismicity options, and activity probabilities.

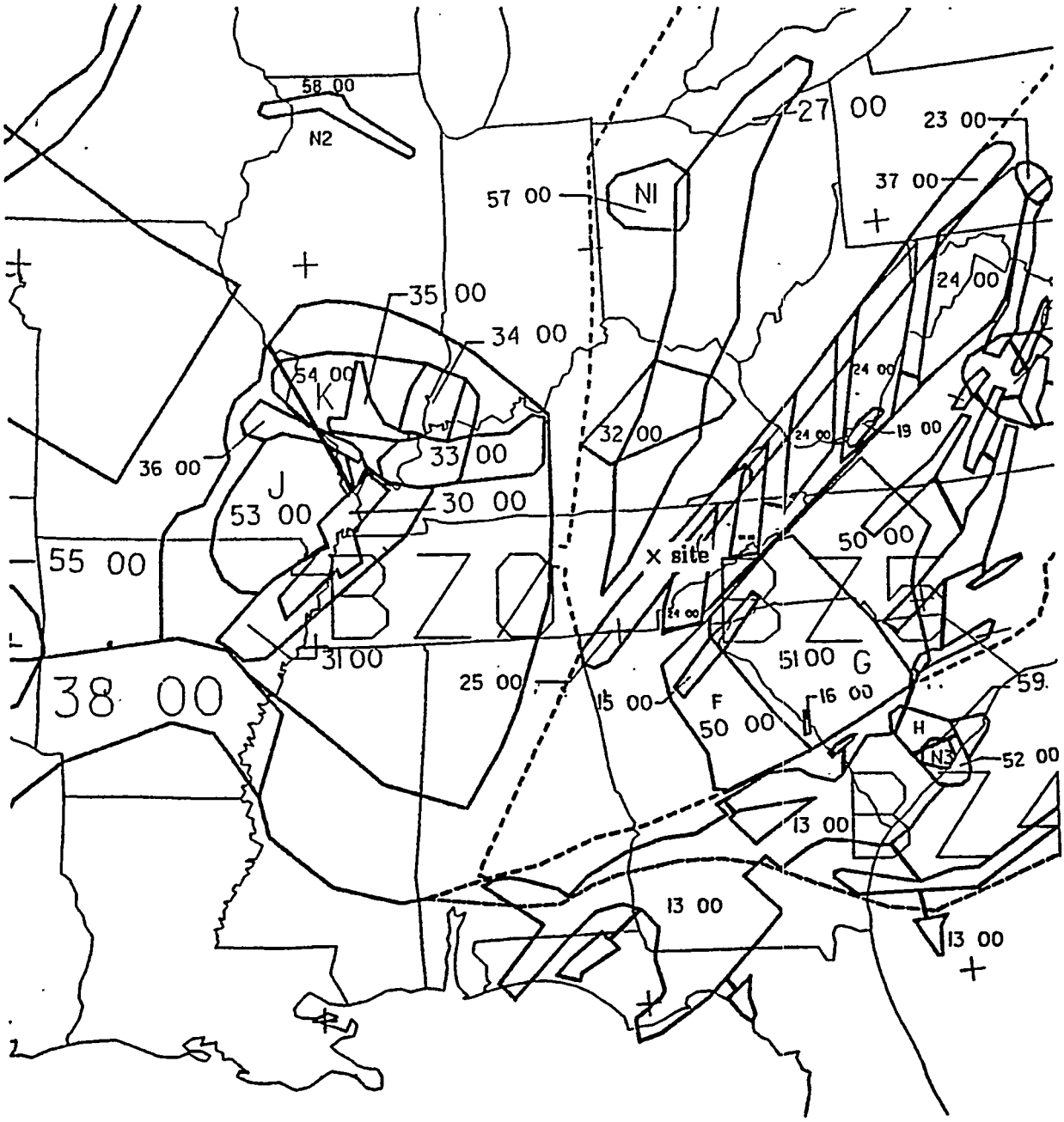

Figure 2-4. Map showing the seismic sources specified by the Bechtel team in the region around Oak Ridge.

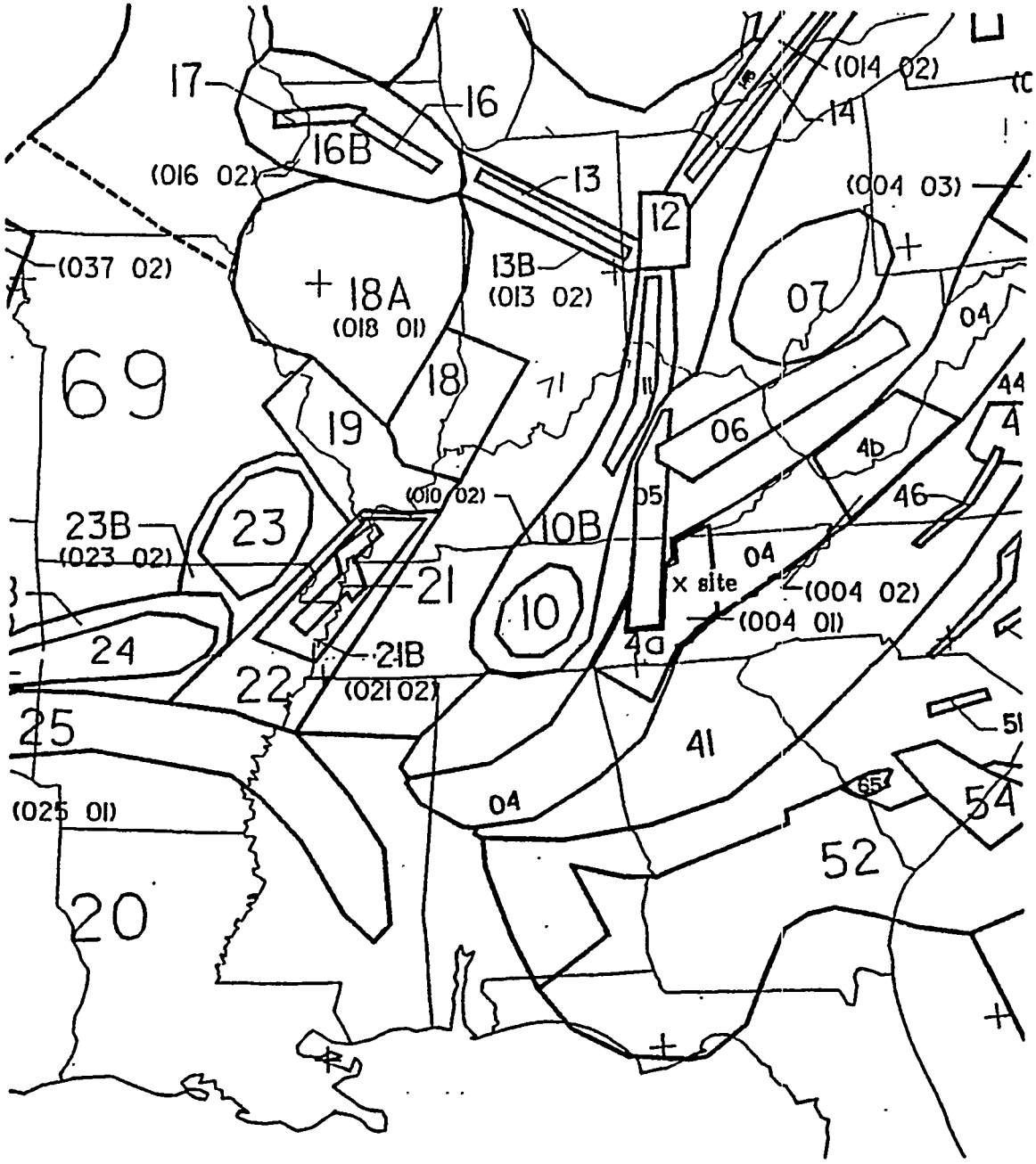

Figure 2-5. Map showing the seismic sources specified by the Dames and Moore team in the region around the Oak Ridge Site.

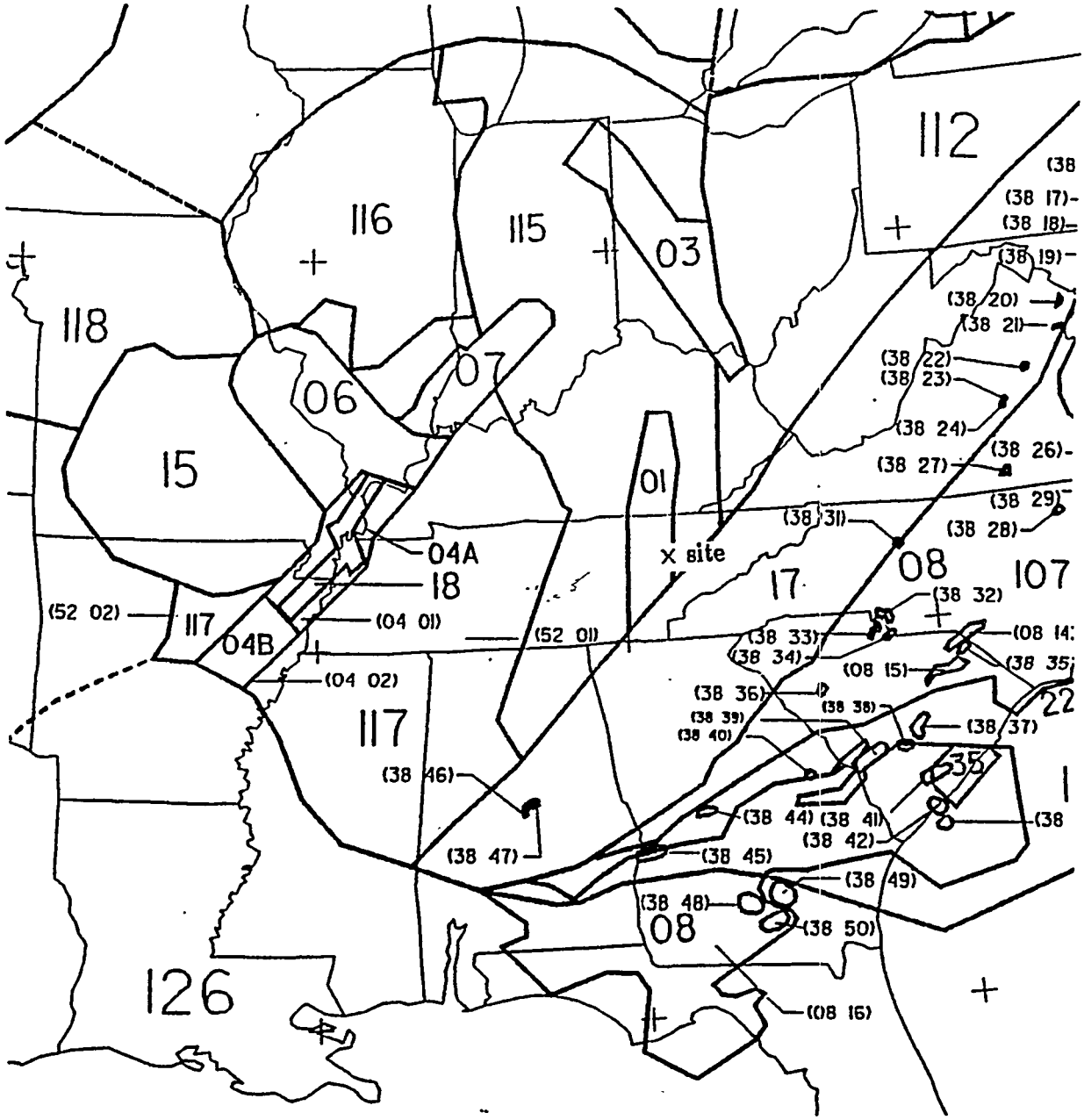

Figure 2-6. Map showing the seismic sources specified by the Law team in the region around the Oak Ridge Site.

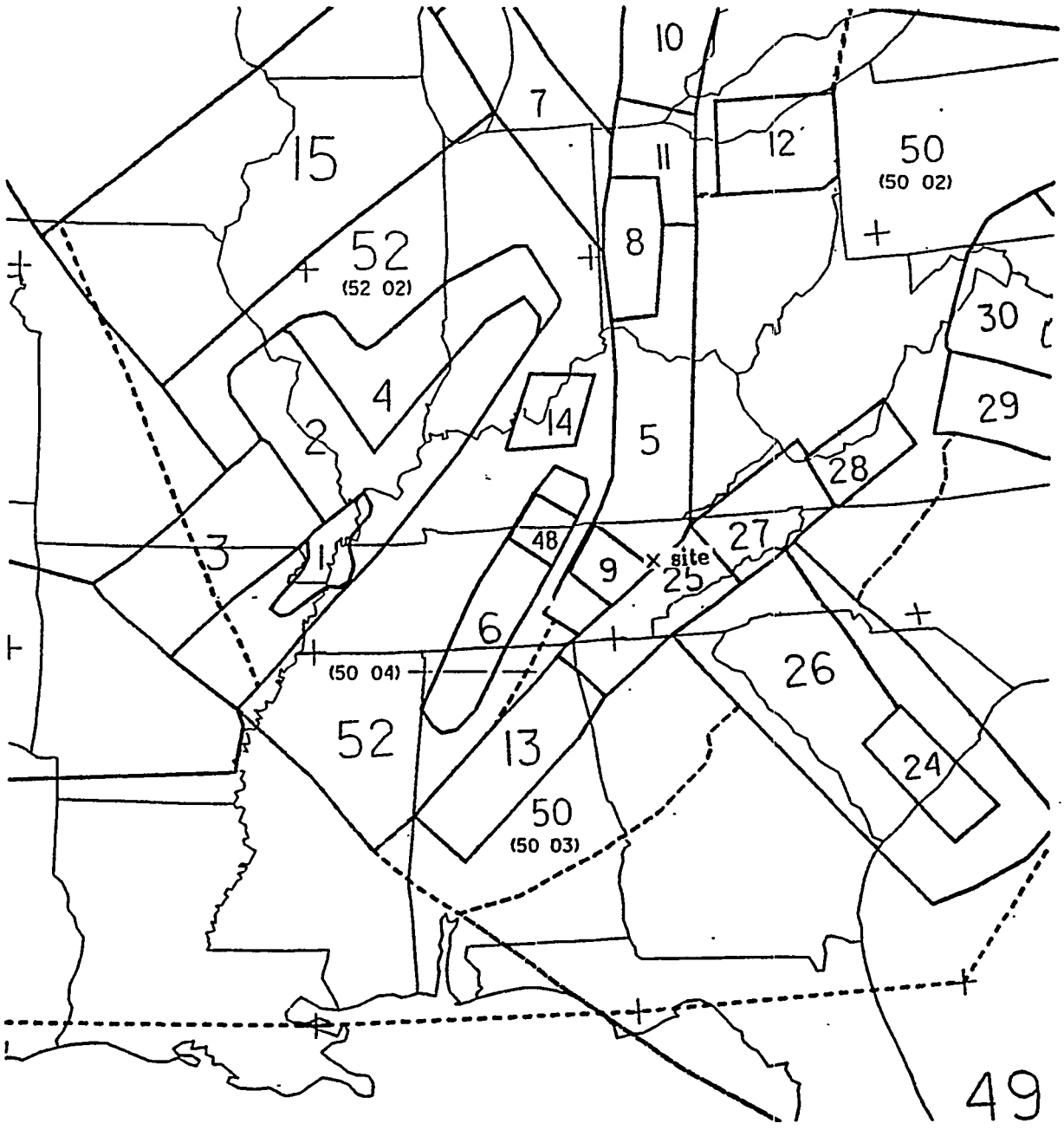

Figure 2-7. Map showing the seismic sources specified by the Rondout team in the region around the Oak Ridge Site.

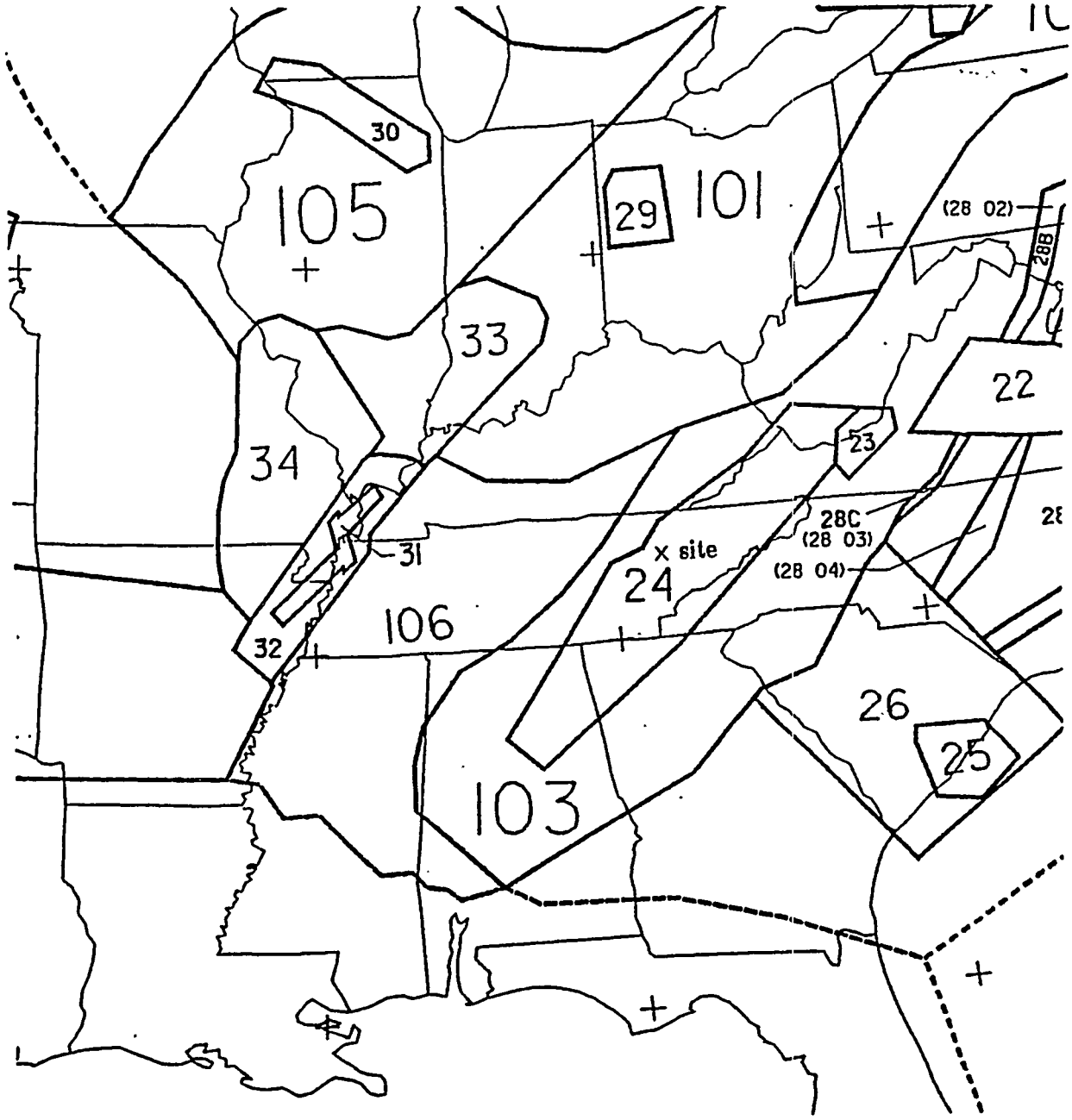

Figure 2-8. Map showing the seismic sources specified by the Weston team in the region around the Oak Ridge Site.

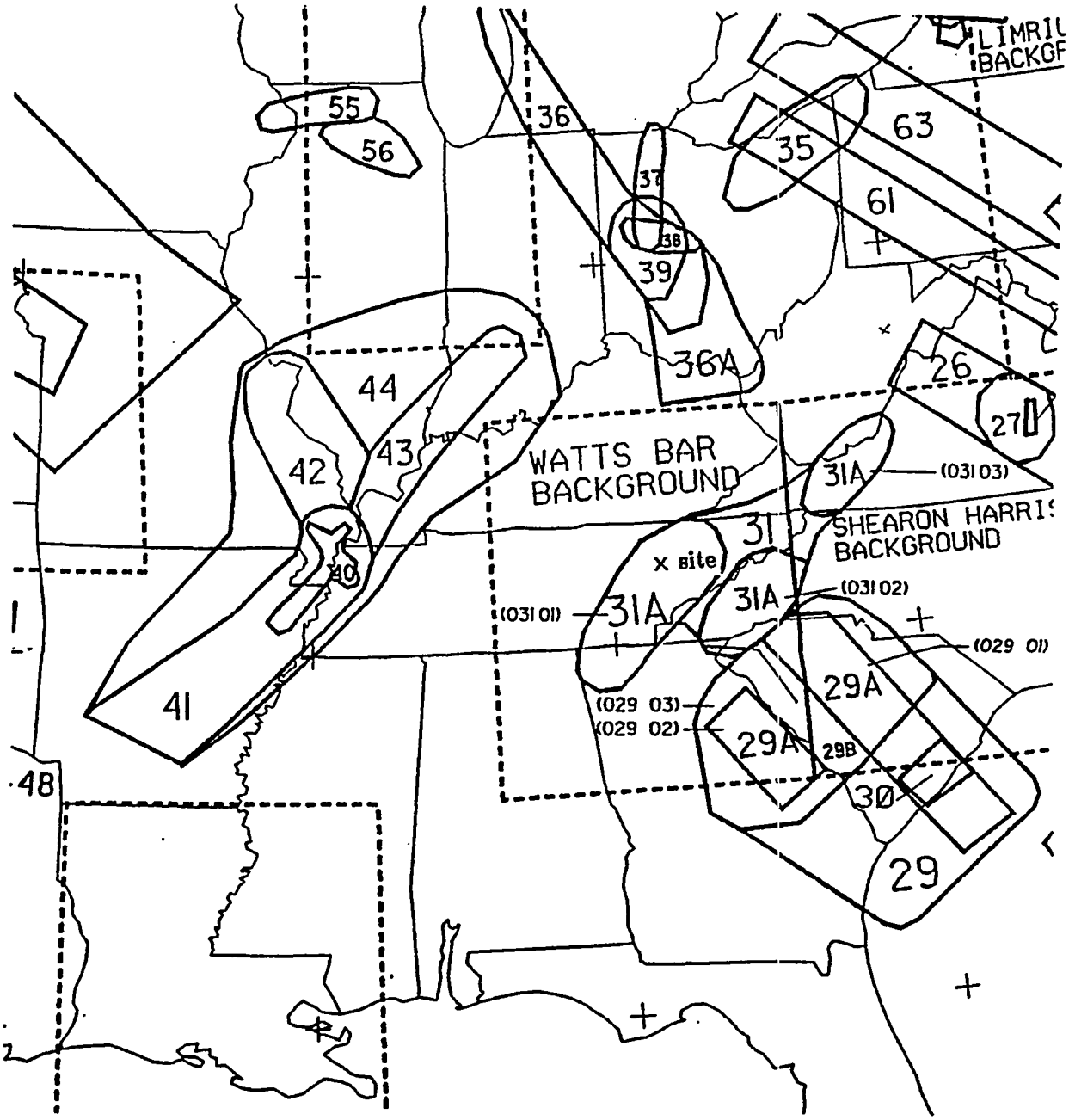

Figure 2-9. Map showing the seismic sources specified by the Woodward-Clyde team in the region around the Oak Ridge Site.

Table 2-2

Summary of Bechtel Team Sources Near the Oak Ridge Site

Source	Description	Seis. Opts.[1] and Probs.	Max. Mags. and Probs.	P^a	Inter-dependencies
24	Bristol Trends	1[0.33] 2[0.34] 4[0.33]	5.7[0.10] 6.0[0.40] 6.3[0.40] 6.6[0.10]	0.25	ME with 24 and 25A
25	NY-Alabama lineament (short)	1[0.33] 2[0.34] 4[0.33]	5.4[0.10] 5.7[0.40] 6.0[0.40] 6.6[0.10]	0.30	ME with 24 and 25A
25A	NY-Alabama lineament (long)	1[0.33] 2[0.34] 4[0.33]	5.4[0.10] 5.7[0.40] 6.0[0.40] 6.6[0.10]	0.45	ME with 24 and 25
30	New Madrid	1[0.33] 2[0.34] 4[0.33]	7.4[0.10] 7.5[0.90]	1.00	Not contained in BZ0
F	S.E. Appalachians	1[0.33] 2[0.34] 4[0.33]	5.4[0.10] 5.7[0.40] 6.0[0.40] 6.6[0.10]	0.35	none
H	Charleston	1[0.33] 2[0.34] 4[0.33]	6.8[0.20] 7.1[0.40] 7.4[0.40]	0.50	none
BZ0	New Madrid Region	1[0.33] 2[0.34] 3[0.33]	5.7[0.10] 6.0[0.40] 6.3[0.40] 6.6[0.10]	1.00	Background $P^a_{BG} = 1.00$
BZ5	S. Appalachians	1[0.33] 2[0.34] 3[0.33]	5.7[0.10] 6.0[0.40] 6.3[0.40] 6.6[0.10]	1.00	Background $P^a_{BG} = 1.00$

Table 2–2 (continued)

Summary of Bechtel Team Sources Near the Oak Ridge Site

Source	Description	Seis. Opts.[1] and Probs.	Max. Mags. and Probs.	P^a	Inter-dependencies
BZ6	S.E. Craton Region	1[0.33] 2[0.34] 3[0.33]	5.7[0.10] 6.0[0.40] 6.3[0.40] 6.6[0.10]	1.00	Background $P^a_{BG} = 1.00$

[1] Seismicity options are defined as follows:
1 = constant a, constant b (no prior b);
2 = low smoothing on a, high smoothing on b (no prior b);
3 = low smoothing on a, low smoothing on b (no prior b);
4 = low smoothing on a, low smoothing on b (weak prior of 1.05).

Weights on magnitude intervals are [1.0,1.0,1.0,1.0,1.0,1.0,1.0]

Table 2-3

Summary of Dames and Moore Team Sources Near the Oak Ridge Site

Source	Description	Seis. Opts.[1] and Probs.	Max. Mags. and Probs.	P^a	Inter-dependencies
04	Appalachian Fold Belt	1[0.75] 2[0.25]	6.0[0.80] 7.2[0.20]	0.35	ME with 4A
4A	Kink in Fold Belts	3[0.75] 4[0.75]	6.8[0.75] 7.2[0.25]	0.65	ME with 04
05	E. Continent Gravity High	3[0.75] 4[0.75]	5.7[0.75] 7.2[0.25]	0.30	none
21	New Madrid	(Use params. from 21B‡) 3[0.75] 4[0.25]	7.2[0.25] 7.5[0.75]	1.0	none
41	Default	1[0.75] 2[0.75]	6.1[0.80] 7.2[0.20]	0.12	Default for 42, 43, and 46

[1] Seismicity options are defined as follows:
1 = no smoothing on a, no smoothing on b (strong prior of 1.04);
2 = no smoothing on a, no smoothing on b (weak prior of 1.04);
3 = constant a, constant b (strong prior of 1.04);
4 = constant a, constant b (weak prior of 1.04);

Weights on magnitude intervals are [0.1,0.2,0.4,1.0,1.0,1.0,1.0]

‡ To account for differences in areas, the value of a in source 21 is equal to the value of a in source 21B plus the quantity $\log_{10}(\text{Area}_{21B}/\text{Area}_{21})$.

Table 2-4

Summary of Law Engineering Team Sources Near the Oak Ridge Site

Source	Description	Seis. Opts.[1] and Probs.	Max. Mags. and Probs.	P^a	Inter-dependencies
01	E. Continent Gravity High	1a[1.00]	5.4[1.00]	0.32	none
17	Eastern Basement	1b[1.00]	5.7[0.20] 6.8[0.80]	0.62	none
18	Postulated Faults in Reelfoot Rift	2d[1.00]	7.4[1.00]	1.00	none
115	Indiana Block	1a[1.00]	5.2[0.50] 5.5[0.50]	1.00	Background $P^a_{BG} = 1.00$
217	Eastern Basement Background	1b[1.00]	4.9[0.50] 5.7[0.50]	1.00	Background $P^a_{BG} = 0.29$; same geometry as 17

[1] Seismicity options are defined as follows:

1a = high smoothing on a, constant b (strong prior of 1.05);
1b = high smoothing on a, constant b (strong prior of 1.00);
1c = high smoothing on a, constant b (strong prior of 0.95);
1d = high smoothing on a, constant b (strong prior of 0.90);
2a = constant a, constant b (strong prior of 1.05);
2c = constant a, constant b (strong prior of 0.95);
2d = constant a, constant b (strong prior of 0.90);

Weights on magnitude intervals are all 1.0 for the above options

3a = high smoothing on a, constant b (strong prior of 1.05)

Weights on magnitude intervals are [0.0,1.0,1.0,1.0,1.0,1.0,1.0] for option 3a.

Table 2-5

Summary of Rondout Associates Team Sources Near the Oak Ridge Site

Source	Description	Seis. Opts.[1] and Probs.	Max. Mags. and Probs.	P^a	Inter-dependencies
1	New Madrid	5[1.00] (A=3.85, b=1.00)	7.1[0.10] 7.3[0.80] 7.4[0.10]	1.00	none
5	East Continent Geoph. Anomaly	1[1.00] (a=−1.66, b=0.96)	5.2[0.30] 6.3[0.55] 6.5[0.15]	1.00	none
9	Eastern Tennessee	1[0.70] (a=−1.38, b=0.89) 6[0.30] (a=−1.08, b=0.81)	5.8[0.15] 6.5[0.60] 6.8[0.25]	0.99	none
25	S. Appalachians	1[1.00] (a=−0.63, b=1.15)	6.6[0.30] 6.8[0.60] 7.0[0.10]	0.99	none
26	S. Carolina Zone	1[1.00] (a=−1.39, b=0.97)	5.8[0.15] 6.5[0.60] 6.8[0.25]	1.00	none
27	Tennessee-Va. Border Zone	1[1.00] (a=−1.12, b=0.93)	5.2[0.30] 6.3[0.55] 6.5[0.15]	0.99	none

[1] Seismicity options are defined as follows:
1,6 = a and b as listed above;
3 = low smoothing on a, constant b (strong prior of 1.00);
5 = A and b as listed above;

Weights on magnitude intervals are [1.0,1.0,1.0,1.0,1.0,1.0,1.0]

Table 2-6

Summary of Weston Geophysical Team Sources Near the Oak Ridge Site

Source	Description	Seis. Opts.[1] and Probs.	Max. Mags. and Probs.	P^*	Inter-dependencies
24	New York-Alabama Clingman	1b[1.00]	5.4[0.26] 6.0[0.58] 6.6[0.16]	0.90	Contained in 103
31	New Madrid	1b[1.00]	7.2[1.00]	0.95	none
32	Reelfoot Rift	1b[0.80] 2b[0.30]	7.2[1.00]	1.00	
C11	32–31	1b[1.00]	6.0[0.13] 6.6[0.77] 7.2[0.10]	NA	Donut source
C17	103–23	1a[0.70] 2a[0.30]	5.4[0.26] 6.0[0.58] 6.6[0.16]	NA	Donut source
C19	103–23–24	1a[1.00]	5.4[0.26] 6.0[0.58] 6.6[0.16]	NA	Donut source

[1] Seismicity options are defined as follows:

1a = constant a, constant b (medium prior of 1.00);
1b = constant a, constant b (medium prior of 0.90);
1c = constant a, constant b (medium prior of 0.70);
2a = medium smoothing on a, medium smoothing on b (medium prior of 1.00);
2b = medium smoothing on a, medium smoothing on b (medium prior of 0.90);
2c = medium smoothing on a, medium smoothing on b (medium prior of 0.70);

Weights on magnitude intervals are all 1.0 for the above options

Table 2-7

Summary of Woodward-Clyde Consultants Team Sources Near the Oak Ridge Site

Source	Description	Seis. Opts.[1] and Probs.	Max. Mags. and Probs.	P^*	Inter-dependencies
29	So. Carolina Gravity Saddle (extended)	2[0.25] 3[0.25] 4[0.25] 5[0.25]	6.7[0.33] 7.0[0.34] 7.4[0.33]	0.122	ME with 29A, 30
29A	So. Carolina Gravity Saddle #2	2[0.25] 3[0.25] 4[0.25] 5[0.25]	6.7[0.33] 7.0[0.34] 7.4[0.33]	0.305	ME with 29, 30
29B	So. Carolina Gravity Saddle #3	2[0.25] 3[0.25] 4[0.25] 5[0.25]	5.4[0.33] 6.0[0.34] 7.0[0.33]	0.183	ME with 29, 29A
31	Blue Ridge Combo	2[0.25] 3[0.25] 4[0.25] 5[0.25]	5.9[0.33] 6.3[0.34] 7.0[0.33]	0.024	ME with 31A
31A	Blue Ridge Combo (alternate configuration)	2[0.25] 3[0.25] 4[0.25] 5[0.25]	5.9[0.33] 6.3[0.34] 7.0[0.33]	0.211	ME with 31
40	Disturbed Zone of Reelfoot Rift	2[0.33] 3[0.34] 4[0.33]	7.2[0.33] 7.5[0.34] 7.9[0.33]	1.000	none

Table 2–7 (continued)

Summary of Woodward-Clyde Team Sources Near the Oak Ridge Site

Source	Description	Seis. Opts.[1] and Probs.	Max. Mags. and Probs.	P^*	Inter-dependencies
B29	Watts Bar Background	1[0.25] 6[0.25] 7[0.25] 8[0.25]	4.9[0.17] 5.4[0.28] 5.8[0.27] 6.5[0.28]	1.000	Background $P^a_{BG} = 1.00$

[1] Seismicity options are defined as follows:

1 = low smoothing on a, high smoothing on b (no prior);
2 = high smoothing on a, high smoothing on b (no prior);
3 = high smoothing on a, high smoothing on b (medium prior of 1.00);
4 = high smoothing on a, high smoothing on b (medium prior of 0.90);
5 = high smoothing on a, high smoothing on b (medium prior of 0.80);
6 = low smoothing on a, high smoothing on b (medium prior of 1.00);
7 = low smoothing on a, high smoothing on b (medium prior of 0.90);
8 = low smoothing on a, high smoothing on b (medium prior of 0.80);

Weights on magnitude intervals are all 1.0.

2.4 GROUND-MOTION ATTENUATION

This section presents the ground-motion attenuation functions used in the EPRI/SOG calculations. The attenuation functions predict six measures of rock-site ground motions: peak acceleration and spectral velocities at six frequencies. Three sets of attenuation functions, with associated weights, characterize uncertainty in ground-motion predictions. The NRC has stated that these attenuation functions are acceptable for computations of seismic hazard (13).

The attenuation functions used in the EPRI/SOG seismic-hazard calculations are based on simplified physical models of energy release at the seismic source and of wave propagation. The model of energy release describes the Fourier spectrum and duration of shaking at a hypothetical site close to the earthquake, and how these vary with seismic moment (seismic moment is a measure of earthquake size). The model of wave propagation describes how the spectrum and duration of shaking vary as the waves travel through the crust. This model contains the effects of geometric spreading (including *Lg* waves at longer distances), anelastic attenuation, and dispersion. The combined predictions of these models are consistent with seismograph and accelerograph data from the region.

Uncertainty on attenuation functions arises from uncertainty on the parameters of these models and on the derivation of peak time-domain amplitudes from Fourier spectra. The most important of these are uncertainty on source scaling, on the magnitude-moment relation, and on the spectra to time-domain derivation. These uncertainties are captured by considering three alternative formulations of these models, as follows:

1. The attenuation functions obtained by McGuire et al. (7) using an ω-square model with stress drop of 100 bars. This set of attenuation functions is assigned a weight of 0.5.

2. The attenuation functions obtained by Boore and Atkinson (14) using an ω-square model. This set of attenuation functions is assigned a weight of 0.25.

3. The attenuation function obtained from the velocity and acceleration attenuation equations obtained by Nuttli (15) using the "increasing stress-drop" assumption coupled with the dynamic amplification factors by Newmark and Hall (16). The attenuation functions in (15) were derived using a procedure analogous to that of Herrmann and Nuttli (17). This set of attenuation functions is given a weight of 0.25.

Table 2–8 contains the coefficients of these models. Figure 2–10 shows their predictions for magnitudes 5 and 6. The attenuation functions for 0.5-Hz spectral velocity from the models by McGuire et al. (7) and Nuttli (15) were calculated for this study, by using these models' assumptions.

Table 2-8

Attenuation Equations Used in the EPRI/SOG Calculations

$$(\ln[Y] = a + bm_b + c\ln[R] + dR)$$

MODEL	WEIGHT	Y†	a	b	c	d
McGuire et al. (7)	0.5	PSV(0.5 Hz)	-12.36	2.81	-1.00	-0.0015
		PSV(1 Hz)	-7.95	2.14	-1.00	-0.0018
		PSV(2.5 Hz)	-3.82	1.49	-1.00	-0.0024
		PSV(5 Hz)	-2.11	1.20	-1.00	-0.0031
		PSV(10 Hz)	-1.55	1.05	-1.00	-0.0039
		PSV(25 Hz)	-1.63	0.98	-1.00	-0.0053
		Accel.	2.55	1.00	-1.00	-0.0046
Boore and Atkinson (14)	0.25	All Frequencies and Acceleration	More complicated functional form; see Equations 12 and 13 and Table 3 of (14).			
Nuttli (15), Newmark-Hall Amplification Factors	0.25	PSV(0.5 Hz) ‡	0.99	1.15	-0.83	-0.0028
		PSV(1 Hz) ‡	0.29	1.15	-0.83	-0.0028
		PSV(2.5 Hz) ‡	-0.62	1.15	-0.83	-0.0028
		PSV(5 Hz) ‡	-1.32	1.15	-0.83	-0.0028
		PSV(10 Hz) ‡	-2.13	1.15	-0.83	-0.0028
		PSV(25 Hz) ‡	-3.53	1.15	-0.83	-0.0028
		Accel.	1.38	1.15	-0.83	-0.0028

† Spectral velocities have units of *cm/sec*; acceleration has units of cm/sec^2; R has units of km. Variability of $\ln[Y]$ around the predicted value is characterized by a normal distribution with $\sigma = 0.5$.

‡ For given m_b and R, $\ln[Y]$ is the smaller of $a + bm_b + c\ln[R] + dR$ and $-8.3 + 2.3m_b - 0.83\ln[R] - 0.0012R$.

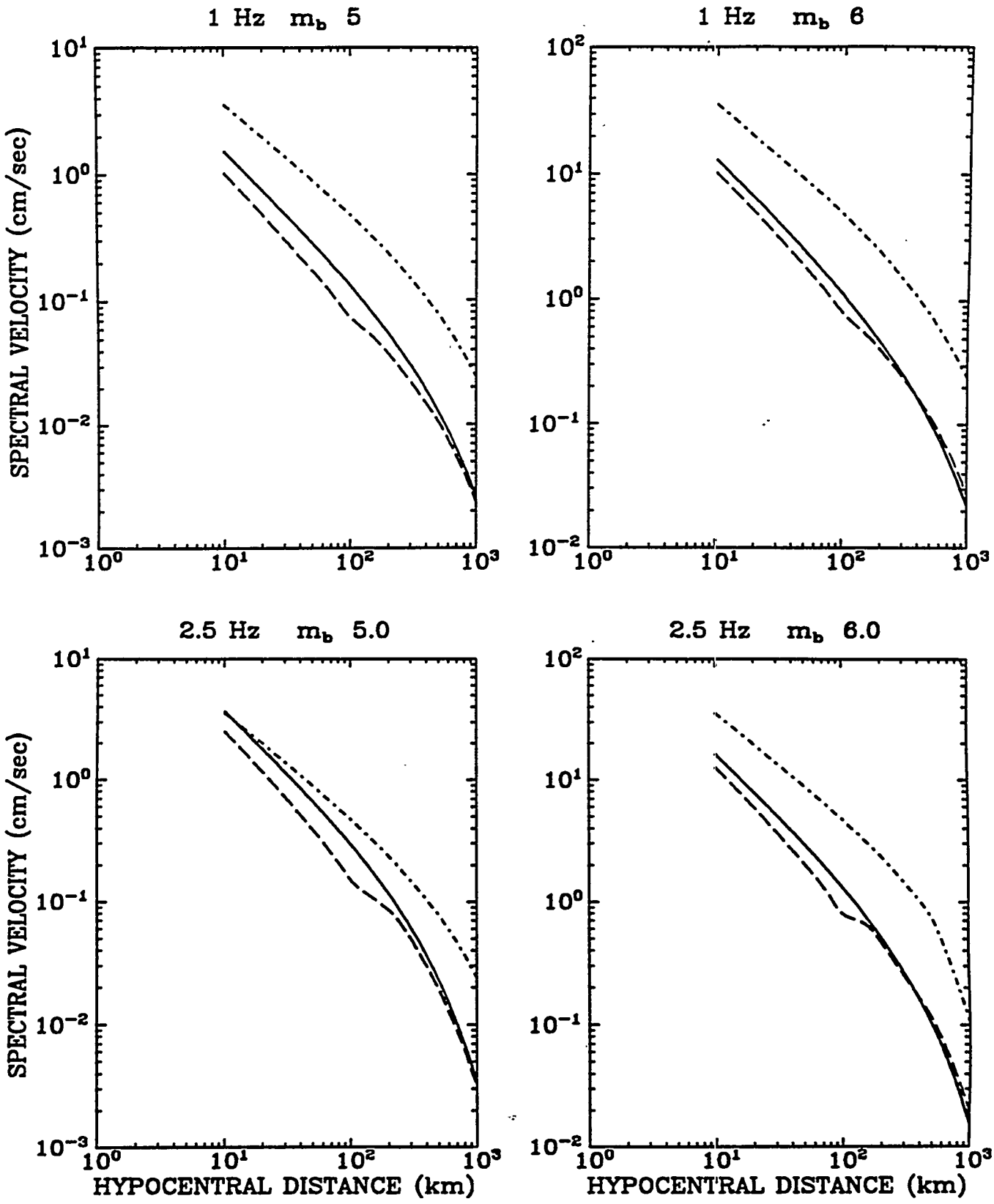

Figure 2-10. Ground motions predicted by the EPRI/SOG attenuation equations for m_b 5 and 6. Key: McGuire et al. (7) (solid), Boore and Atkinson (14) (– – –), and Nuttli (15) (– · –).

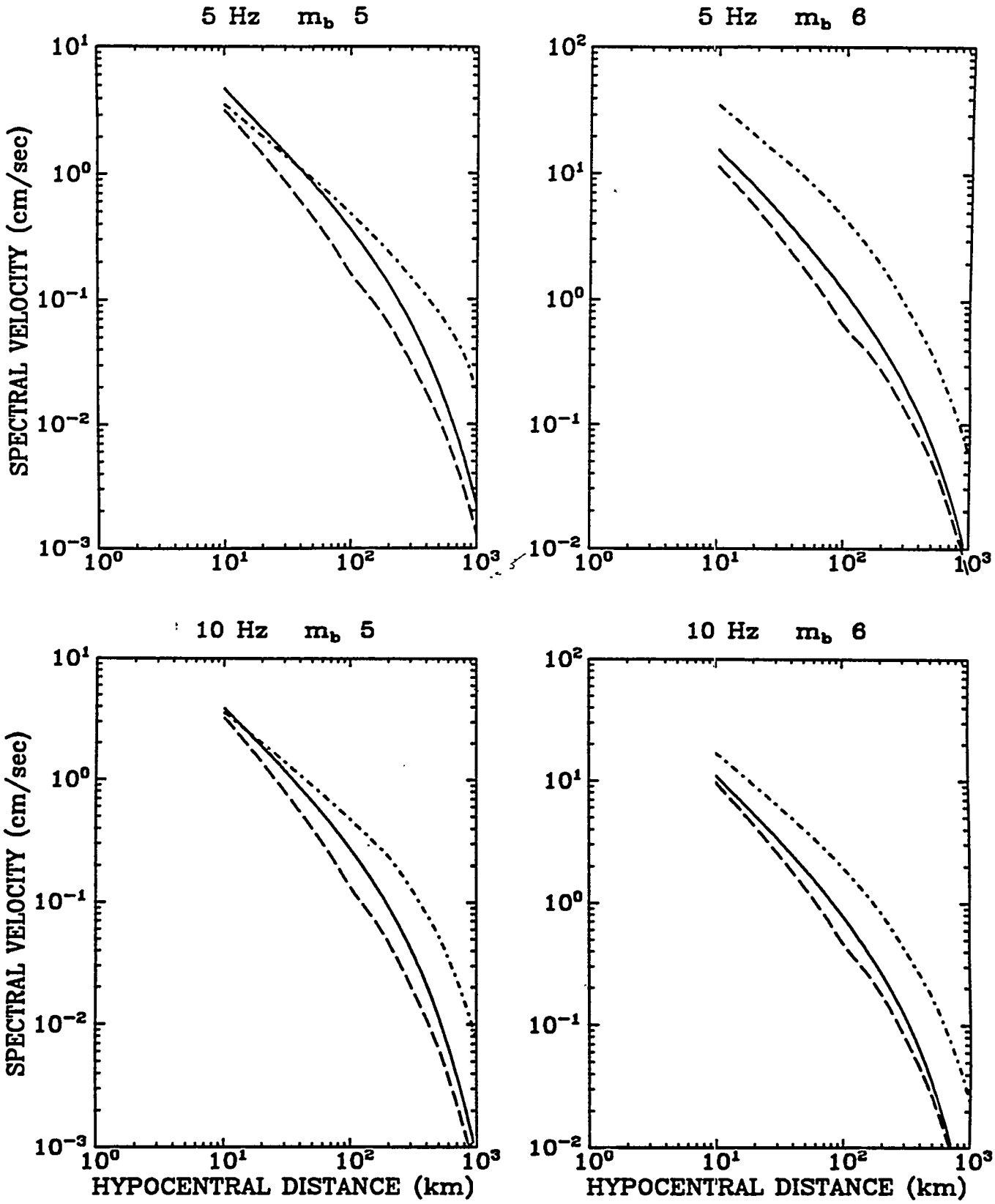

Figure 2–10 (continued). Ground motions predicted by the EPRI/SOG attenuation equations for m_b 5 and 6. Key: McGuire et al. (7) (solid), Boore and Atkinson (14) (– – –), and Nuttli (15) (– · –).

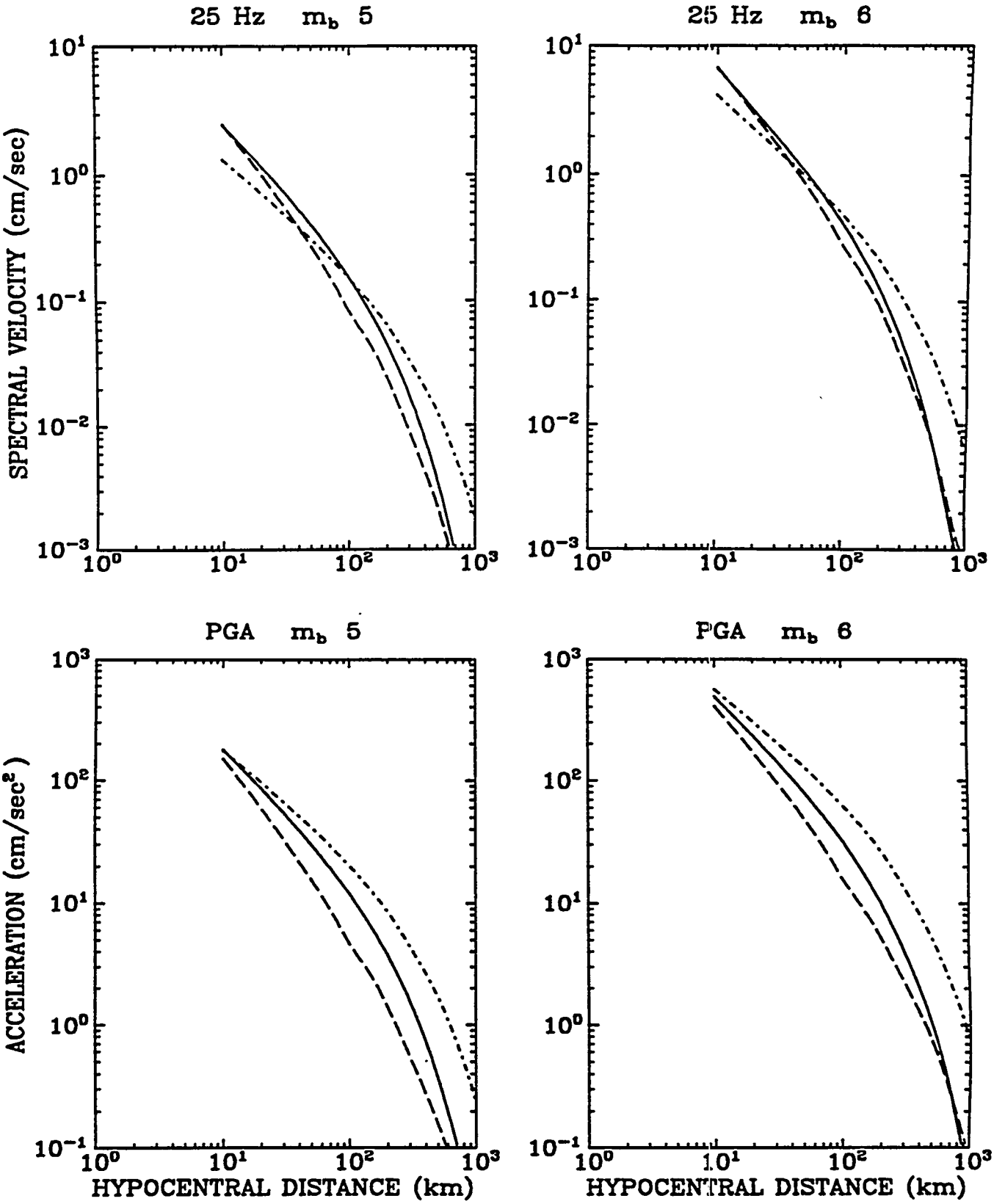

Figure 2–10 (continued). Ground motions predicted by the EPRI/SOG attenuation equations for m_b 5 and 6. Key: McGuire et al. (7) (solid), Boore and Atkinson (14) (– – –), and Nuttli (15) (– · –).

2.5 CALCULATIONS

2.5.1 Overview

The seismic-hazard calculations for the Oak Ridge site used the EPRI/SOG methodology and inputs, and followed the same steps as the EPRI/SOG calculations documented in(6). These steps are as follows:

1. Identify all sources within 200 km of the site and include them in the screening calculations (step 2). Include also the New Madrid and Charleston sources if they are within 500 km of the site.

2. Use EQHAZ to perform screening calculations for each team considering one PGA amplitude (0.25 g) and one 1-Hz amplitude (10 cm/sec) and using the Nuttli attenuation functions (see Section 4.2). Evaluate the mean hazard from each source, and its percent contribution to the total hazard considering the source's P^a. Eliminate those sources that make negligible contributions to the hazard for both ground-motion measures, so that the combined hazards from all excluded sources is less than 1% of the total hazard.

3. Perform EQHAZ calculations for all amplitudes and 6 measures of ground motion (i.e., peak acceleration and 5% damped spectral velocity at 1., 2.5, 5, 10, and 25 Hz) using all attenuation functions. These calculations are performed separately for each team.

4. Develop source combinations for each team, considering all sources included in step 2, their activity probabilities and dependencies. These source combinations are sometimes simplified as described in Volume 3 of (8), while maintaining the conservative criteria of step 2.

5. Simplify the logic trees for some sites and teams, by considering only 1 seismicity option for each source. (The hazard associated with that one seismicity option is the weighted average of hazards from the original seismicity options.) This simplification was performed for the Bechtel team only, because the number of sources selected in step 2 was too large and EQPOST runs with the full logic trees would require excessive computer time. Test runs indicate that the effect of this simplification is insignificant.

6. Perform EQPOST calculations using the source-hazard results from step 3 and the source combinations from step 4. These calculations are performed separately for each ground-motion measure. For soil sites, introduce site-amplification factors and their uncertainty.

This study used the source geometries and seismicity parameters that were generated during the EPRI/SOG project. These data were used to develop the geometry and seismicity input files for the EQHAZ calculations in steps 2 and 3.

2.5.2 Screening of Seismic Sources

The screening of seismic sources is performed in order to reduce the number of sources considered in the analysis, thereby simplifying the development of source combinations and reducing the computer time required for the final calculations. The screening is performed using the Nuttli attenuation functions — which have the strongest magnitude dependence and the slowest decay with distance — thus avoiding the possibility of erroneously excluding a distant source that makes a significant contribution to seismic hazard at the site.

The screening is based on the contribution of each source to the mean value of total hazard. Tables 2–9 through 2–14 show the results of the screening calculations. Results for each team contain one table for peak ground acceleration and one table for 1-Hz spectral velocity. Each table shows the contribution to the total hazard from each source within 200 km of the site. A source's contribution to the total hazard depends on the mean hazard when the source is active (column 2) and on the activity probability P^a or P^* of the source (column 3).[1] Donut sources do not have activity probabilities and cannot be included in the computation of total hazard. The decision to include or exclude these sources must be made by considering which sources form the donut and considering the hazard in column 2. Table 2–15 lists the sources selected for final calculations.

2.5.3 Development of Source Combinations

The source combinations represent all possible states of activity of the seismic sources that contribute to hazard at the site (i.e., all the sources selected in the screening process above). The source combinations are developed considering the following three types of information: (1) the activity probabilities P^a or P^* of the various sources, (2) the interdependencies of source activities, and (3) the geographic relationships among sources.

The most common geographic relationship occurs with background sources. If the site is within a background source and within a standard source, the background is included only in source combinations where the standard source is not active. In some instances, "donut" sources of the type *BACKGROUND – STANDARD SOURCE* have also been digitized and analyzed. In those instances, the appropriate donut should be included in each source combination, depending on which standard sources are active.

[1] In the headings of Tables 2–9 through 2–14 we do not distinguish between P^a and P^*.

Table 2–16 shows the source combinations and their probabilities, for the six Earth-Science Teams.

2.5.4 Results

Seismic hazard calculations were performed for peak acceleration and 6 spectral velocities, using the ERPI/SOG software modules EQHAZ and EQPOST, and considering the seismic sources and source combinations in Tables 2–15 and 2–16.

Results for rock are presented in Figures 2–11 through 2–18 in the form of hazard curves and uniform-hazard spectra.

The highest frequency shown in the response spectra in Figures 2–11 through 2–18 is 25 Hz. Studies of the frequency content of ground motions in the central and eastern United States (18, for example) indicate that the maximum spectral acceleration occurs at approximately 30 Hz and that the spectral acceleration approaches the peak ground acceleration at frequencies near 80 Hz.

2.6 REFERENCES

1. C. A. Cornell. "Engineering Seismic Risk Analysis". *Bulletin of the Seismological Society of America*, 58(5):1583–1606, October 1968.
2. C. A. Cornell. *Dynamic Waves in Civil Engineering*, chapter 27: "Probabilistic Analysis of Damage to Structures under Seismic Loads". Wiley Interscience, 1971.
3. A. Der Kiureghian and A. H. S. Ang. *A Line Source Model for Seismic Risk Analysis.* Technical Report UILU-ENG-75-2023, Univ. of Illinois, October 1975. pp. 134.
4. R. K. McGuire. *FORTRAN Computer Program for Seismic Risk Analysis.* Open File Report 76-67, U. S. Geological Survey, 1976. pp. 1-90.
5. D. L. Bernreuter, J. B. Savy, R. W. Mensing, J. C. Chen, and B. C. Davis. *Seismic Hazard Characterization of the Eastern United States.* Technical Report LLNL UCID-20421, Volumes 1 and 2, Lawrence Livermore National Laboratory, Livermore, Ca., 1985.
6. R. K. McGuire, G. R. Toro, J. P. Jacobson, T. F. O'Hara, and W. J. Silva. *Probabilistic Seismic Hazard Evaluations in the Central and Eastern United States: Resolution of the Charleston Earthquake Issue.* Special Report NP-6395-D, Electric Power Research Institute, April 1989.
7. R. K. McGuire, G. R. Toro, and W. J. Silva. *Engineering Model of Earthquake Ground Motion for Eastern North America.* Technical Report NP-6074, Electric Power Research Institute, 1988.

8. *Seismic Hazard Methodology for the Central and Eastern United States.* Technical Report NP-4726-A, Electric Power Research Institute, July 1986. Revised, 1988. Vol. 1, Part 1: Methodology, Vol. 1, Part 2: Theory, Vol. 2: EQHAZARD Programmer's Manual, Vol. 3: EQHAZARD User's Manual, Vol. 4: Applications, Vols. 5 through 10: Tectonic Interpretations, Vol. 11: Nuclear Regulatory Commission Safety Review.

9. K. J. Coppersmith, A. C. Johnston, and W. J. Arabasz. "Assessment of Maximum Earthquake Magnitudes in the Eastern United States". *Earthquake Notes*, 57–1:12, 1986.

10. A. C. Johnston, A. G. Metzger, K. J. Coppersmith, and W. J. Arabasz. "A Systematic Global Overview of Large Intraplate Earthquakes". *Earthquake Notes*, 57–1:12, 1986.

11. M. W. McCann and J. W. Reed. *Selection of a Lower Bound Magnitude for Seismic Hazard Assessment.* Technical Report, Electric Power Research Institute, Palo Alto, California, 1988.

12. M. W. McCann and J. W. Reed, editors. *Engineering Characterization of Small-Magnitude Earthquakes*, Electric Power Research Institute, Palo Alto, California, 1988.

13. L. Reiter. EPRI Ground Motion Models for Eastern North America. NRC Letter to R.A. Thomas, August 3, 1988.

14. D. M. Boore and G. M. Atkinson. "Stochastic Prediction of Ground Motion and Spectral Response Parameters at Hard-Rock Sites in Eastern North America". *Bulletin of the Seismological Society of America*, 77(2):440–467, 1987.

15. O. W. Nuttli. Letter dated September 19, 1986 to J. B. Savy. Reproduced in: D. Bernreuter, J. Savy, R. Mensing, J. Chen, and B. Davis. *Seismic Hazard Characterization of 69 Nuclear Plant Sites East of the Rocky Muntains: Questionnaires.* U. S. Nuclear Regulatory Commission, Technical Report NUREG/CR-5250, UCID-21517, Volume 7, 1989. Prepared by the Lawrence Livermore National Laboratory.

16. N. M. Newmark and W. J. Hall. *Earthquake Spectra and Design.* Earthquake Engineering Research Institute, Berkeley, CA, 1982.

17. R. B. Herrmann and O. W. Nuttli. "Strong Motion Investigations in the Central United States". In *Proceedings: 7th World Conference on Earthquake Engineering, Istanbul*, pp. 533–536, 1980.

18. W. J. Silva and R. K. Green. "Magnitude and Distance Scaling of Response Spectral Shapes for Rock sites with Application to North American Tectonic Environments". *Earthquake Spectra*, 5(4):591–624, 1989.

Table 2-9

Screening of Seismic Sources: Bechtel Team

SCREENING OF SEISMIC SOURCES

site: OAK RIDGE team: BEC peak accel.

Source	Hazard	P*	Haz.P*	%	Acum. %	Include
BZ5	7.53E-05	1.000	7.53E-05	50.7	50.7	Y
BZ6	2.70E-05	1.000	2.70E-05	18.2	69.0	Y
25A	5.17E-05	0.450	2.33E-05	15.7	84.6	Y
25	6.50E-05	0.300	1.95E-05	13.1	97.8	Y
24	1.28E-05	0.250	3.20E-06	2.2	99.9	Y
27	2.64E-07	0.200	5.28E-08	0.0	100.0	N
F	7.32E-08	0.350	2.56E-08	0.0	100.0	N
G	5.77E-08	0.350	2.02E-08	0.0	100.0	N
BZ0	1.23E-08	1.000	1.23E-08	0.0	100.0	N
32	2.19E-08	0.350	7.67E-09	0.0	100.0	N
BZ3	4.75E-09	1.000	4.75E-09	0.0	100.0	N
30	2.40E-09	1.000	2.40E-09	0.0	100.0	N
N3	1.00E-10	0.530	5.31E-11	0.0	100.0	N
H	1.00E-10	0.500	5.01E-11	0.0	100.0	N
15	1.00E-10	0.050	5.01E-12	0.0	100.0	N
donut sources, etc.						
C09	2.86E-07					
C06	1.21E-06					
C10	1.27E-06					

SCREENING OF SEISMIC SOURCES

site: OAK RIDGE team: BEC 1-Hz psv

Source	Hazard	P*	Haz.P*	%	Acum. %	Include
BZ5	1.91E-04	1.000	1.91E-04	42.8	42.8	Y
30	1.31E-04	1.000	1.31E-04	29.2	72.0	Y
BZ6	3.32E-05	1.000	3.32E-05	7.4	79.4	Y
25A	6.14E-05	0.450	2.76E-05	6.2	85.6	Y
25	7.71E-05	0.300	2.31E-05	5.2	90.8	Y
24	6.33E-05	0.250	1.58E-05	3.5	94.3	Y
BZ0	8.99E-06	1.000	8.99E-06	2.0	96.3	Y
F	1.25E-05	0.350	4.37E-06	1.0	97.3	Y
G	8.34E-06	0.350	2.92E-06	0.7	98.0	Y
H	5.55E-06	0.500	2.78E-06	0.6	98.6	Y
N3	4.91E-06	0.530	2.60E-06	0.6	99.2	Y
32	7.43E-06	0.350	2.60E-06	0.6	99.8	N
BZ3	9.29E-07	1.000	9.29E-07	0.2	100.0	N
27	8.02E-07	0.200	1.60E-07	0.0	100.0	N
15	1.00E-10	0.050	5.01E-12	0.0	100.0	N
donut sources, etc.						
C09	8.99E-07					
C06	4.07E-06					
C10	4.49E-06					

Table 2-10

Screening of Seismic Sources: Dames and Moore Team

SCREENING OF SEISMIC SOURCES

site: OAK RIDGE team: DAM peak accel.

Source	Hazard	P*	Haz.P*	%	Acum. %	Include
4A	3.31E-04	0.650	2.15E-04	80.6	80.6	Y
04	1.44E-04	0.350	5.02E-05	18.8	99.4	Y
05	4.07E-06	0.300	1.22E-06	0.5	99.8	N
08	3.01E-06	0.080	2.40E-07	0.1	99.9	N
41	1.83E-06	0.120	2.20E-07	0.1	100.0	N
10B	4.72E-08	0.390	1.84E-08	0.0	100.0	N
10	1.99E-08	0.300	5.96E-09	0.0	100.0	N
21	1.10E-09	1.000	1.10E-09	0.0	100.0	N
06	3.19E-09	0.240	7.67E-10	0.0	100.0	N
11	1.74E-09	0.310	5.40E-10	0.0	100.0	N
54	1.00E-10	1.000	1.00E-10	0.0	100.0	N
donut sources, etc.						
C15	1.36E-10					
C03	2.03E-08					
C02	3.00E-06					
C01	3.67E-06					

SCREENING OF SEISMIC SOURCES

site: OAK RIDGE team: DAM 1-Hz psv

Source	Hazard	P*	Haz.P*	%	Acum. %	Include
4A	5.77E-04	0.650	3.75E-04	67.4	67.4	Y
04	2.38E-04	0.350	8.34E-05	15.0	82.4	Y
21	8.24E-05	1.000	8.24E-05	14.8	97.3	Y
41	6.40E-05	0.120	7.68E-06	1.4	98.6	Y
05	8.56E-06	0.300	2.57E-06	0.5	99.1	Y
54	2.50E-06	1.000	2.50E-06	0.4	99.6	N
08	1.28E-05	0.080	1.02E-06	0.2	99.7	N
10B	2.20E-06	0.390	8.57E-07	0.2	99.9	N
10	1.11E-06	0.300	3.32E-07	0.1	99.9	N
11	5.39E-07	0.310	1.67E-07	0.0	100.0	N
06	5.04E-07	0.240	1.21E-07	0.0	100.0	N
donut sources, etc.						
C03	7.86E-07					
C15	1.08E-05					
C02	1.27E-05					
C01	2.77E-05					

Table 2-11

Screening of Seismic Sources: Law Engineering Team

SCREENING OF SEISMIC SOURCES

site: OAK RIDGE team: LAW peak accel.

Source	Hazard	P*	Haz.P*	%	Acum. %	Include
17	3.92E-05	0.620	2.43E-05	59.1	59.1	Y
115	1.37E-05	1.000	1.37E-05	33.2	92.4	Y
01	7.89E-06	0.320	2.52E-06	6.1	98.5	Y
217	2.14E-06	0.290	6.22E-07	1.5	100.0	Y
18	1.22E-09	1.000	1.22E-09	0.0	100.0	N
117	1.00E-10	1.000	1.00E-10	0.0	100.0	N
C07	1.00E-10	1.000	1.00E-10	0.0	100.0	N
112	1.00E-10	0.850	8.52E-11	0.0	100.0	N
35	1.00E-10	0.450	4.51E-11	0.0	100.0	N
donut sources, etc.						
117A	1.00E-10					

SCREENING OF SEISMIC SOURCES

site: OAK RIDGE team: LAW 1-Hz psv

Source	Hazard	P*	Haz.P*	%	Acum. %	Include
17	3.19E-04	0.620	1.98E-04	58.4	58.4	Y
18	1.36E-04	1.000	1.36E-04	40.0	98.4	Y
115	3.74E-06	1.000	3.74E-06	1.1	99.5	Y
01	1.87E-06	0.320	5.99E-07	0.2	99.7	N
217	1.87E-06	0.290	5.44E-07	0.2	99.9	N
35	9.12E-07	0.450	4.10E-07	0.1	100.0	N
117	2.40E-10	1.000	2.40E-10	0.0	100.0	N
C07	2.38E-10	1.000	2.38E-10	0.0	100.0	N
112	1.00E-10	0.850	8.52E-11	0.0	100.0	N
donut sources, etc.						
117A	2.38E-10					

Table 2-12

Screening of Seismic Sources: Rondout Associates Team

SCREENING OF SEISMIC SOURCES

site: OAK RIDGE team: RND peak accel.

Source	Hazard	P*	Haz.P*	%	Acum. %	Include
25	1.12E-04	0.990	1.10E-04	58.6	58.6	Y
9	7.05E-05	0.990	6.98E-05	37.0	95.6	Y
5	7.80E-06	1.000	7.80E-06	4.1	99.7	Y
26	2.97E-07	1.000	2.97E-07	0.2	99.9	N
27	2.73E-07	0.990	2.71E-07	0.1	100.0	N
48	7.12E-09	0.870	6.19E-09	0.0	100.0	N
6	1.03E-09	0.830	8.57E-10	0.0	100.0	N
1	6.82E-10	1.000	6.82E-10	0.0	100.0	N
13	5.98E-10	1.000	5.98E-10	0.0	100.0	N
C02	2.25E-10	1.000	2.25E-10	0.0	100.0	N
52	2.19E-10	1.000	2.19E-10	0.0	100.0	N
24	1.00E-10	1.000	1.00E-10	0.0	100.0	N
donut sources, etc.						
C07	2.02E-10					

SCREENING OF SEISMIC SOURCES

site: OAK RIDGE team: RND 1-Hz psv

Source	Hazard	P*	Haz.P*	%	Acum. %	Include
25	2.74E-04	0.990	2.71E-04	43.5	43.5	Y
1	1.54E-04	1.000	1.54E-04	24.7	68.2	Y
9	1.37E-04	0.990	1.35E-04	21.7	89.8	Y
26	2.60E-05	1.000	2.60E-05	4.2	94.0	Y
5	2.12E-05	1.000	2.12E-05	3.4	97.4	Y
27	1.23E-05	0.990	1.22E-05	2.0	99.4	Y
24	2.23E-06	1.000	2.23E-06	0.4	99.7	N
48	8.50E-07	0.870	7.39E-07	0.1	99.9	N
13	7.21E-07	1.000	7.21E-07	0.1	100.0	N
6	2.28E-07	0.830	1.89E-07	0.0	100.0	N
52	1.60E-09	1.000	1.60E-09	0.0	100.0	N
C02	1.34E-09	1.000	1.34E-09	0.0	100.0	N
donut sources, etc.						
C07	1.08E-09					

Table 2-13

Screening of Seismic Sources: Weston Geophysical Team

SCREENING OF SEISMIC SOURCES

site: OAK RIDGE team: WGC peak accel.

Source	Hazard	P*	Haz.P*	%	Acum. %	Include
24	1.54E-04	0.900	1.38E-04	59.0	59.0	Y
103	9.63E-05	1.000	9.63E-05	41.0	100.0	Y
106	2.44E-08	1.000	2.44E-08	0.0	100.0	N
101	1.42E-09	1.000	1.42E-09	0.0	100.0	N
31	2.09E-10	0.950	1.98E-10	0.0	100.0	N
C11	1.67E-10	0.950	1.59E-10	0.0	100.0	N
25	1.00E-10	0.990	9.92E-11	0.0	100.0	N
32	1.25E-09	0.050	6.23E-11	0.0	100.0	N
donut sources, etc.						
C16	1.40E-09					
C12	1.52E-09					
C15	1.52E-09					
C14	1.72E-09					
C13	1.80E-09					
C19	1.53E-06					
C18	1.63E-06					
C17	6.44E-05					

SCREENING OF SEISMIC SOURCES

site: OAK RIDGE team: WGC 1-Hz psv

Source	Hazard	P*	Haz.P*	%	Acum. %	Include
24	2.41E-04	0.900	2.17E-04	44.9	44.9	Y
103	1.69E-04	1.000	1.69E-04	34.9	79.9	Y
31	7.93E-05	0.950	7.53E-05	15.6	95.5	Y
32	1.86E-04	0.050	9.31E-06	1.9	97.4	Y
C11	9.69E-06	0.950	9.21E-06	1.9	99.3	Y
25	1.17E-06	0.990	1.15E-06	0.2	99.5	N
106	1.15E-06	1.000	1.15E-06	0.2	99.8	N
101	1.11E-06	1.000	1.11E-06	0.2	100.0	N
donut sources, etc.						
C16	9.48E-07					
C12	1.08E-06					
C15	1.08E-06					
C14	1.20E-06					
C13	1.28E-06					
C19	1.12E-05					
C18	1.46E-05					
C17	1.13E-04					

Table 2-14

Screening of Seismic Sources: Woodward-Clyde Team

SCREENING OF SEISMIC SOURCES

site: OAK RIDGE team: WCC peak accel.

Source	Hazard	P*	Haz.P*	%	Acum. %	Include
B29	1.27E-04	1.000	1.27E-04	58.8	58.8	Y
31A	3.80E-04	0.211	8.01E-05	37.2	96.0	Y
31	3.56E-04	0.024	8.53E-06	4.0	100.0	Y
29	2.98E-07	0.122	3.63E-08	0.0	100.0	N
29A	7.60E-08	0.305	2.32E-08	0.0	100.0	N
29B	5.25E-08	0.183	9.60E-09	0.0	100.0	N
40	6.31E-09	1.000	6.31E-09	0.0	100.0	N
30	1.00E-10	0.573	5.74E-11	0.0	100.0	N

SCREENING OF SEISMIC SOURCES

site: OAK RIDGE team: WCC 1-Hz psv

Source	Hazard	P*	Haz.P*	%	Acum. %	Include
B29	2.76E-04	1.000	2.76E-04	45.3	45.3	Y
31A	8.44E-04	0.211	1.78E-04	29.1	74.4	Y
40	9.78E-05	1.000	9.78E-05	16.0	90.4	Y
31	8.48E-04	0.024	2.04E-05	3.3	93.7	Y
29A	4.90E-05	0.305	1.49E-05	2.4	96.2	Y
29	1.09E-04	0.122	1.33E-05	2.2	98.4	Y
29B	3.71E-05	0.183	6.79E-06	1.1	99.5	Y
30	5.72E-06	0.573	3.27E-06	0.5	100.0	N

Table 2-15

Sources used for Seismic Hazard Calculations

Team	Sources
Bechtel	24, 25, 25A, 30, F, H, BZ0, BZ5, BZ6
Dames and Moore	04, 4A, 05, 21, 41
Law Engineering	01, 17, 18, 115, 217
Rondout	1, 5, 9, 25, 26, 27
Weston Geophysical	24, 31, 32, C11, C17, C19
Woodward-Clyde	29, 29A, 29B, 31, 31A, 40, B29

Table 2-16

Source Combinations and Their Probabilities

Team	Prob.	Active Sources					
Bechtel	0.09970	30	BZ0	BZ5	BZ6	25	H F
	0.18530	30	BZ0	BZ5	BZ6	25	H
	0.00530	30	BZ0	BZ5	BZ6	25	F
	0.00980	30	BZ0	BZ5	BZ6	25	
	0.14960	30	BZ0	BZ5	BZ6	25A	H F
	0.27790	30	BZ0	BZ5	BZ6	25A	H
	0.00790	30	BZ0	BZ5	BZ6	25A	F
	0.01460	30	BZ0	BZ5	BZ6	25A	
	0.08310	30	BZ0	BZ5	BZ6	24	H F
	0.15440	30	BZ0	BZ5	BZ6	24	H
	0.00440	30	BZ0	BZ5	BZ6	24	F
	0.00810	30	BZ0	BZ5	BZ6	24	
Dames & Moore	0.01260	21	04	05	41		
	0.09240	21	04	05			
	0.02940	21	04	41			
	0.21560	21	04				
	0.02340	21	4A	05	41		
	0.17160	21	4A	05			
	0.05460	21	4A	41			
	0.40040	21	4A				
Law Engineering	0.19840	18	115	01	17		
	0.12160	18	115	01	217		
	0.42160	18	115	17			
	0.25840	18	115	217			
Rondout Associates	0.98010	1	5	26	27	9	25
	0.00990	1	5	26	27	9	
	0.00990	1	5	26	27	25	
	0.00010	1	5	26	27		
Weston Geophysical	0.85500	24	C19	31	C11		
	0.04500	24	C19	32			
	0.09500	C17	31	C11			
	0.00500	C17	32				
Woodward-Clyde	0.00290	40	31	29			
	0.00730	40	31	29A			
	0.00440	40	31	29B			
	0.00940	40	31				
	0.02570	40	31A	29			
	0.06440	40	31A	29A			
	0.03860	40	31A	29B			
	0.08230	40	31A				
	0.09330	40	B29	29			
	0.23330	40	B29	29A			
	0.14000	40	B29	29B			
	0.29830	40	B29				

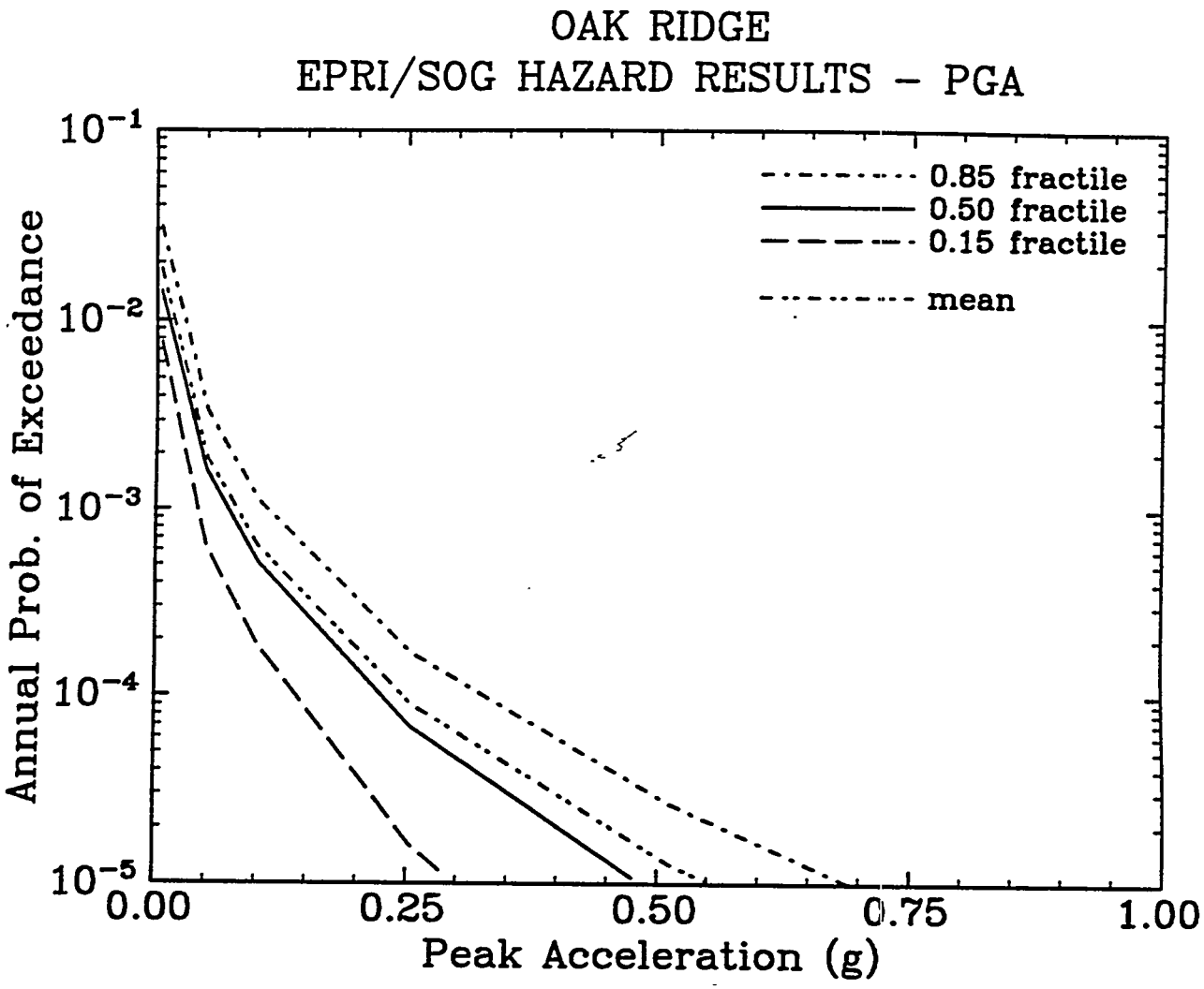

Figure 2-11. Peak ground acceleration hazard curves for Oak Ridge computed using the EPRI/SOG methodology.

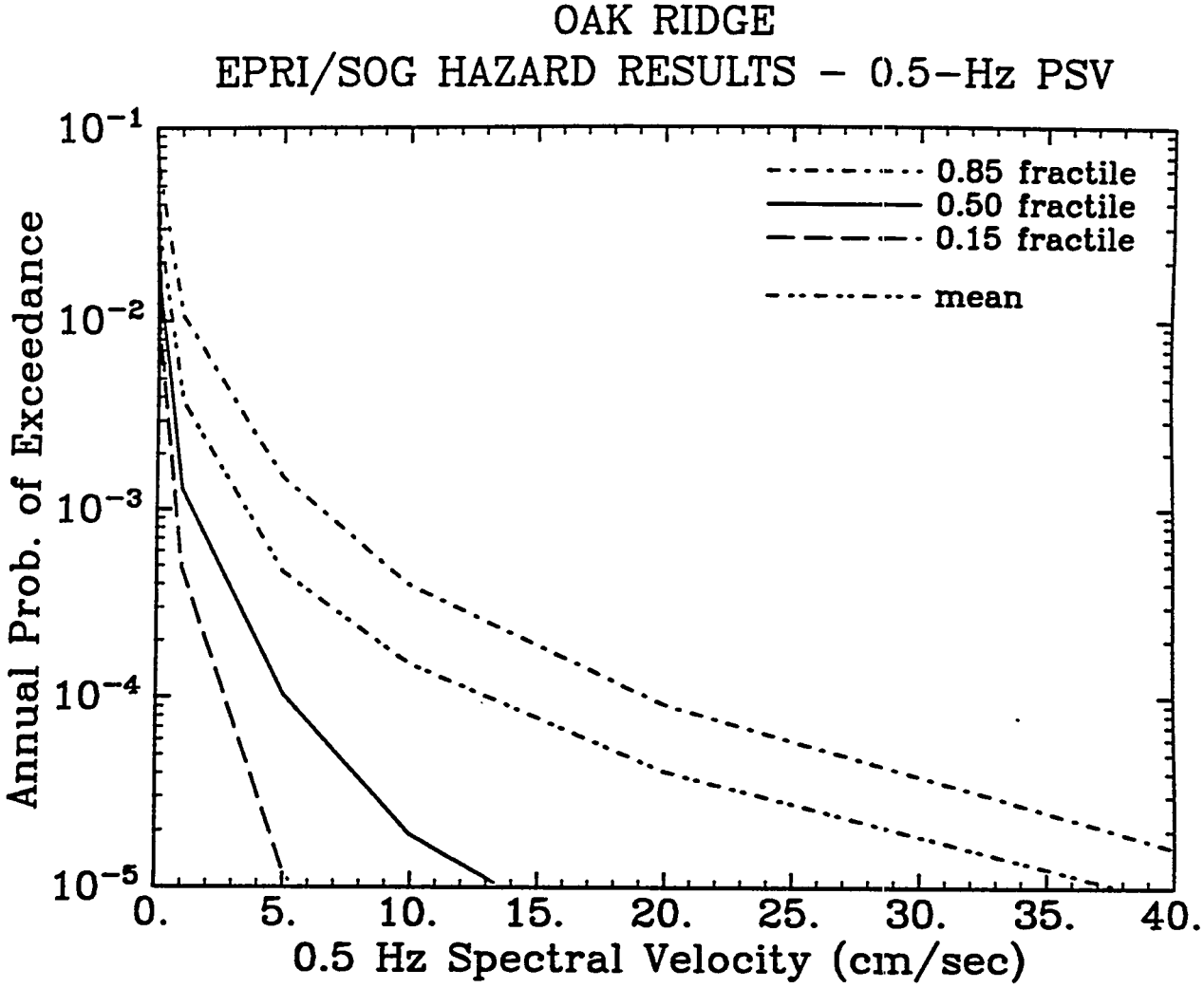

Figure 2-12. 0.5-Hz spectral velocity hazard curves for Oak Ridge computed using the EPRI/SOG methodology.

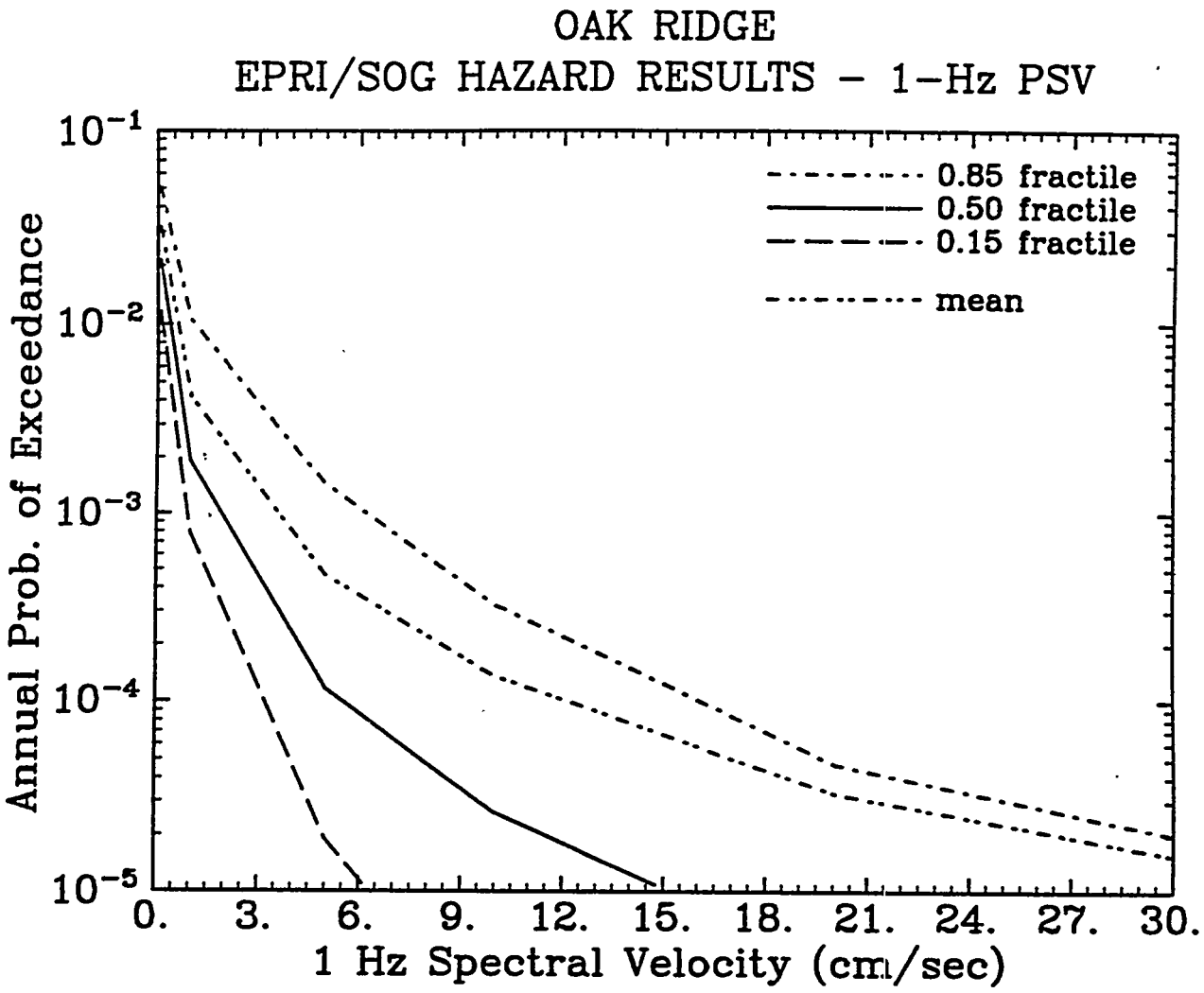

Figure 2-13. 1-Hz spectral velocity hazard curves for Oak Ridge computed using the EPRI/SOG methodology.

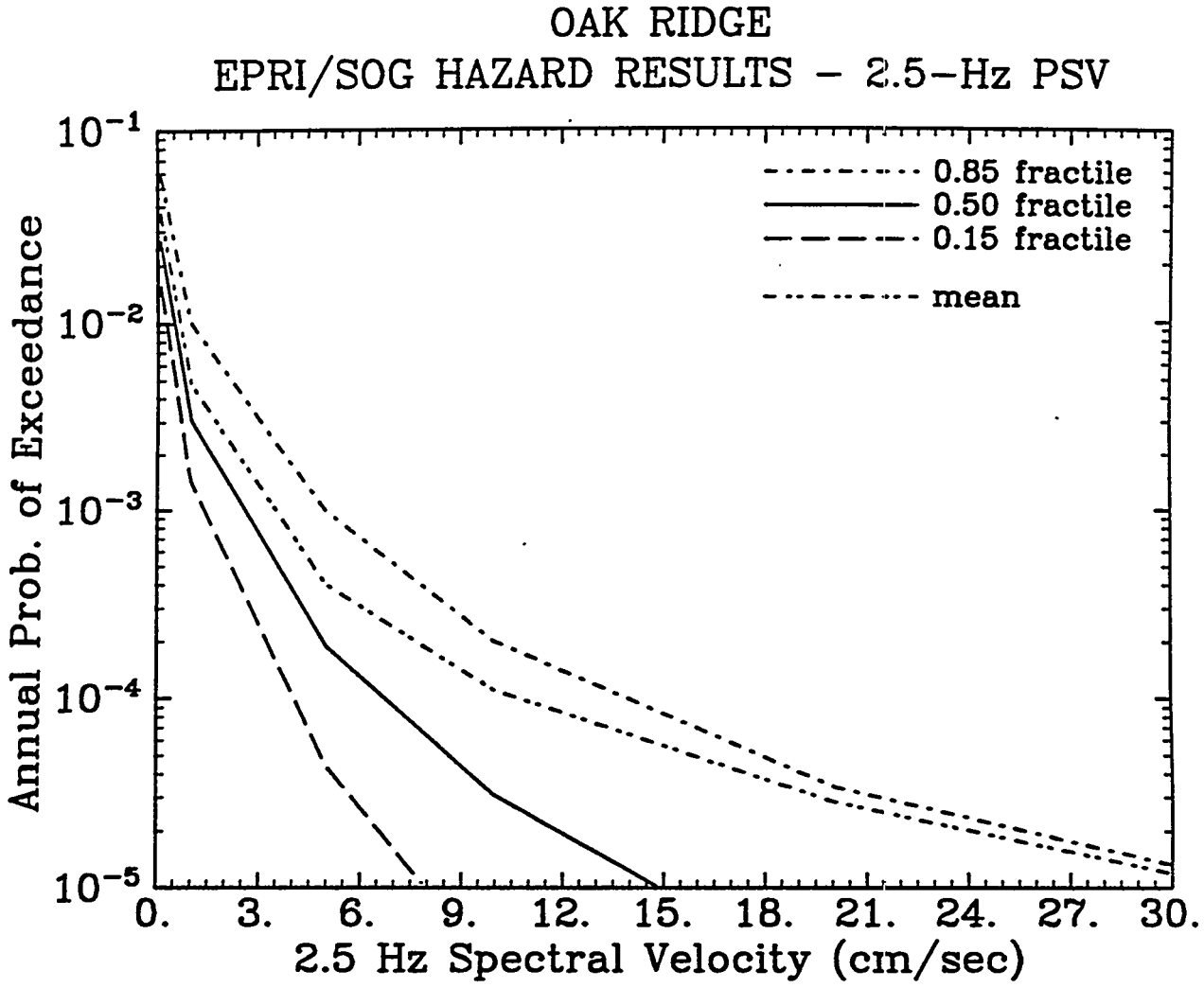

Figure 2-14. 2.5-Hz spectral velocity hazard curves for Oak Ridge computed using the EPRI/SOG methodology.

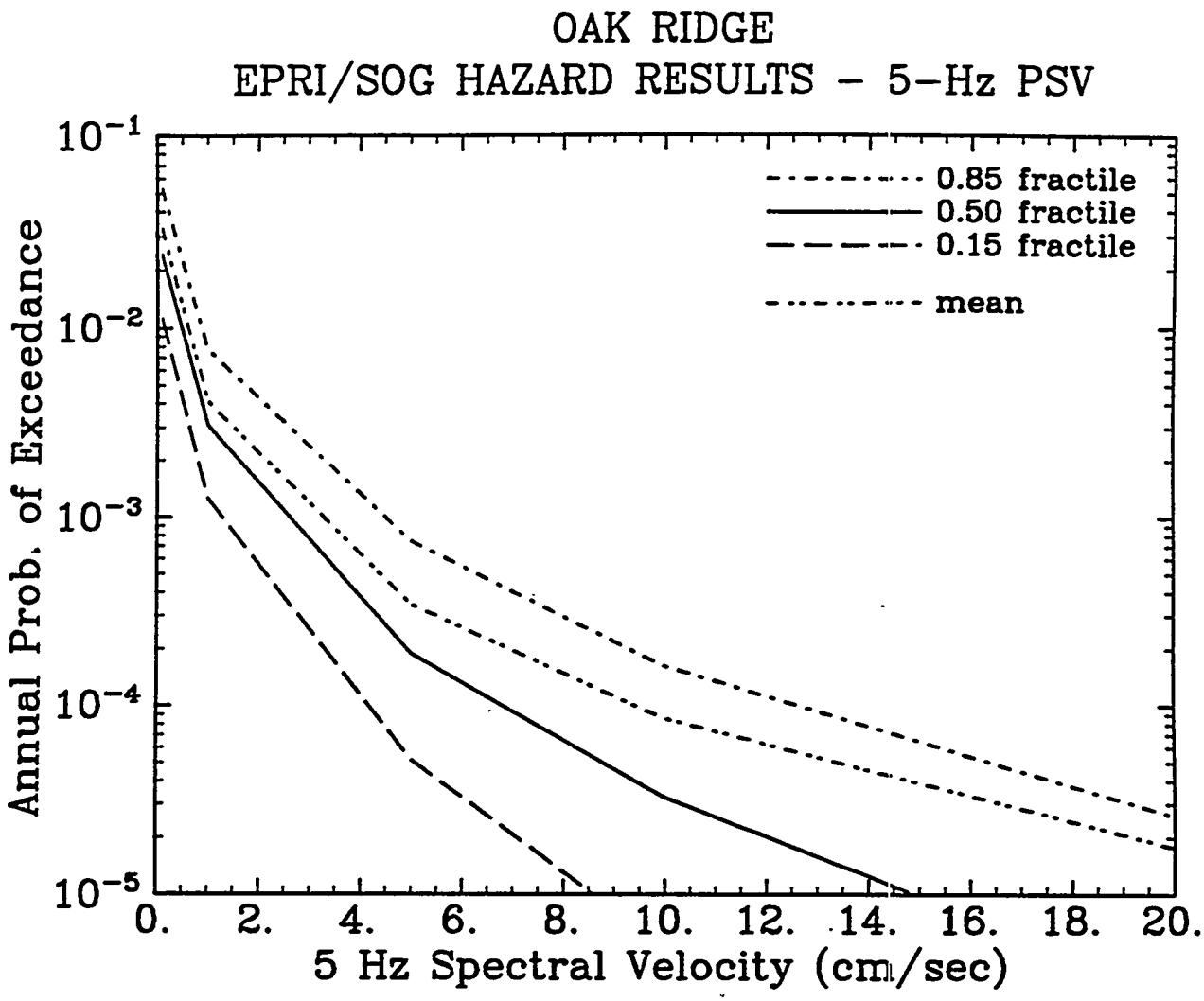

Figure 2-15. 5-Hz spectral velocity hazard curves for Oak Ridge computed using the EPRI/SOG methodology.

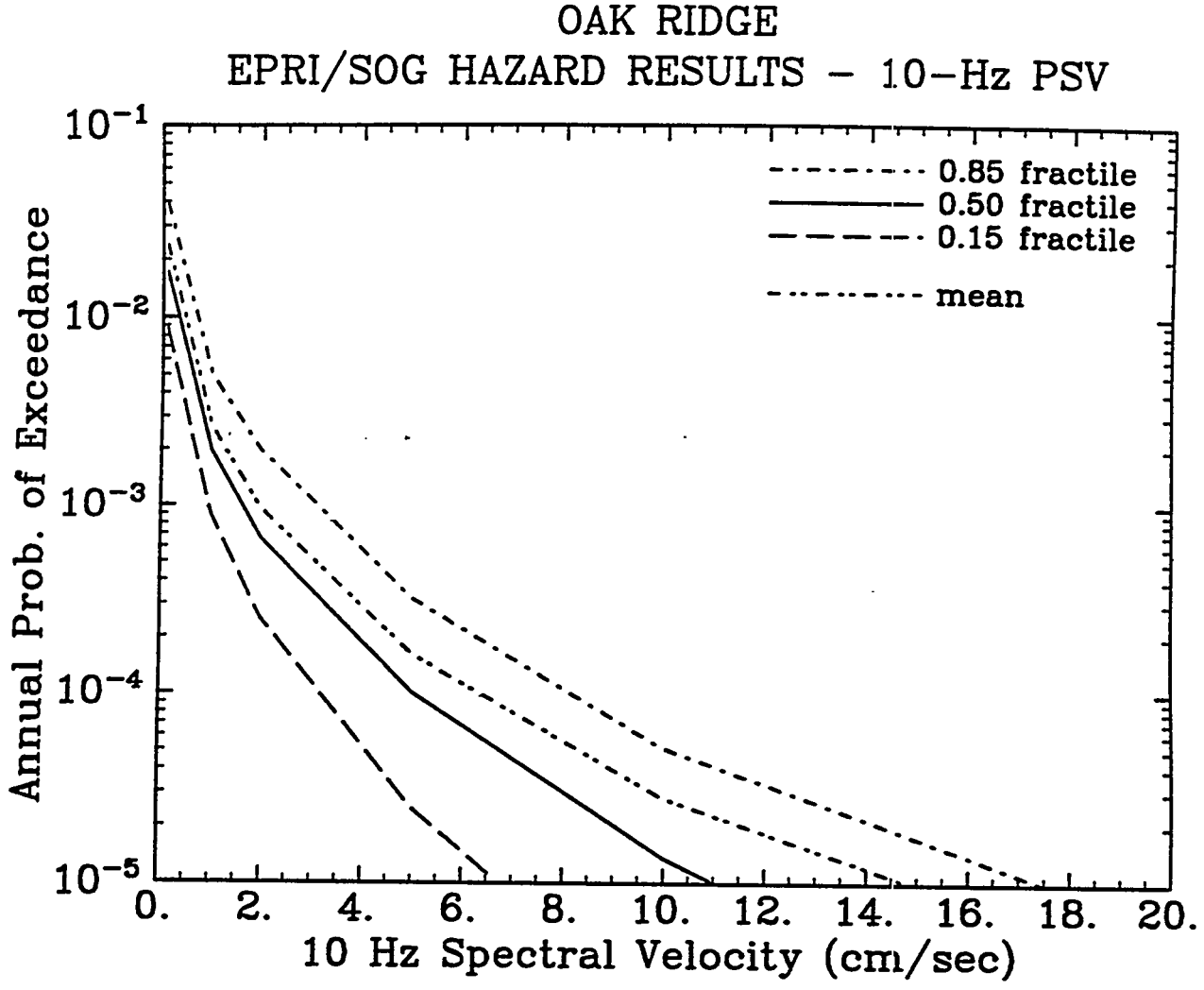

Figure 2-16. 10-Hz spectral velocity hazard curves for Oak Ridge computed using the EPRI/SOG methodology.

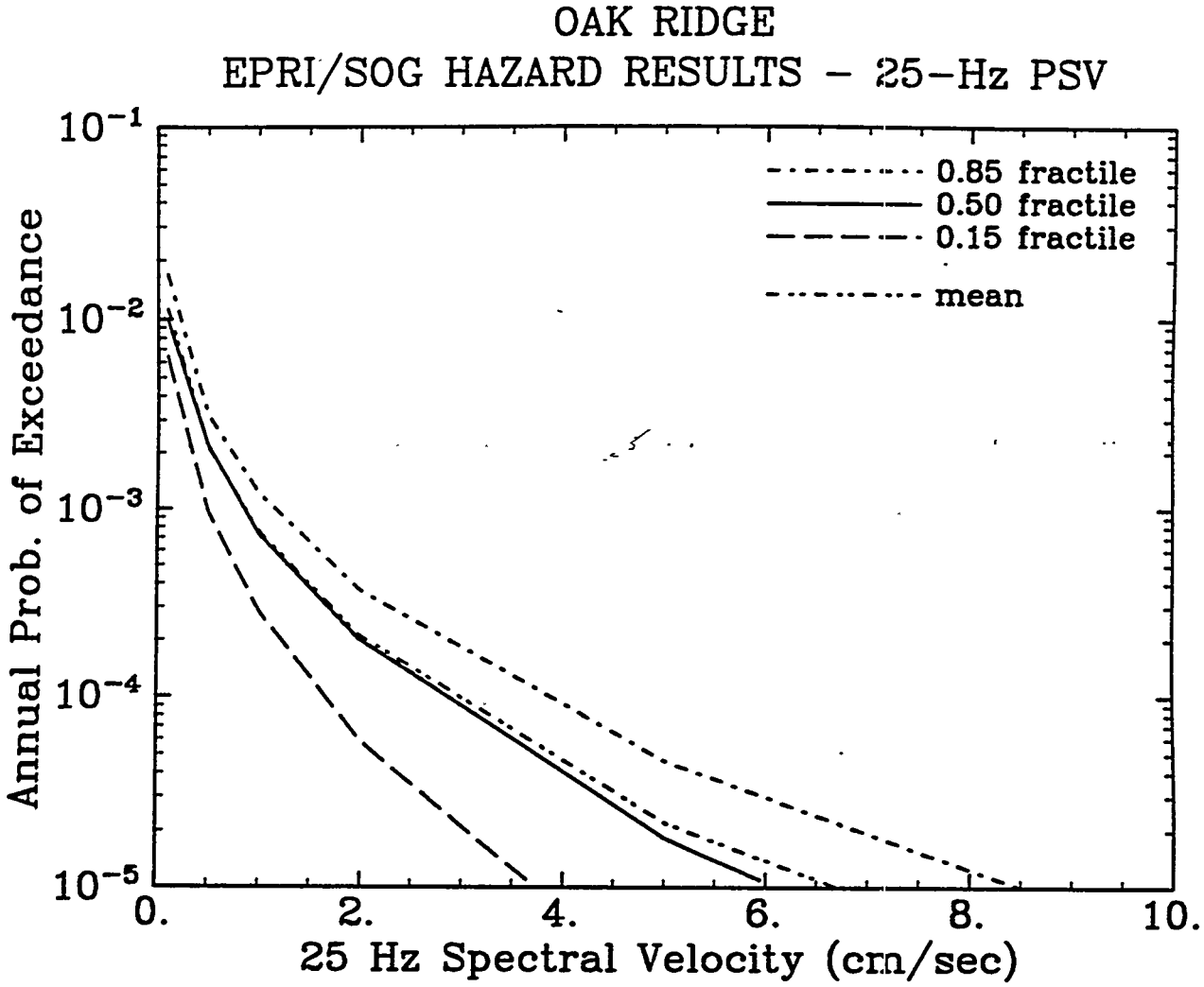

Figure 2-17. 25-Hz spectral velocity hazard curves for Oak Ridge computed using the EPRI/SOG methodology.

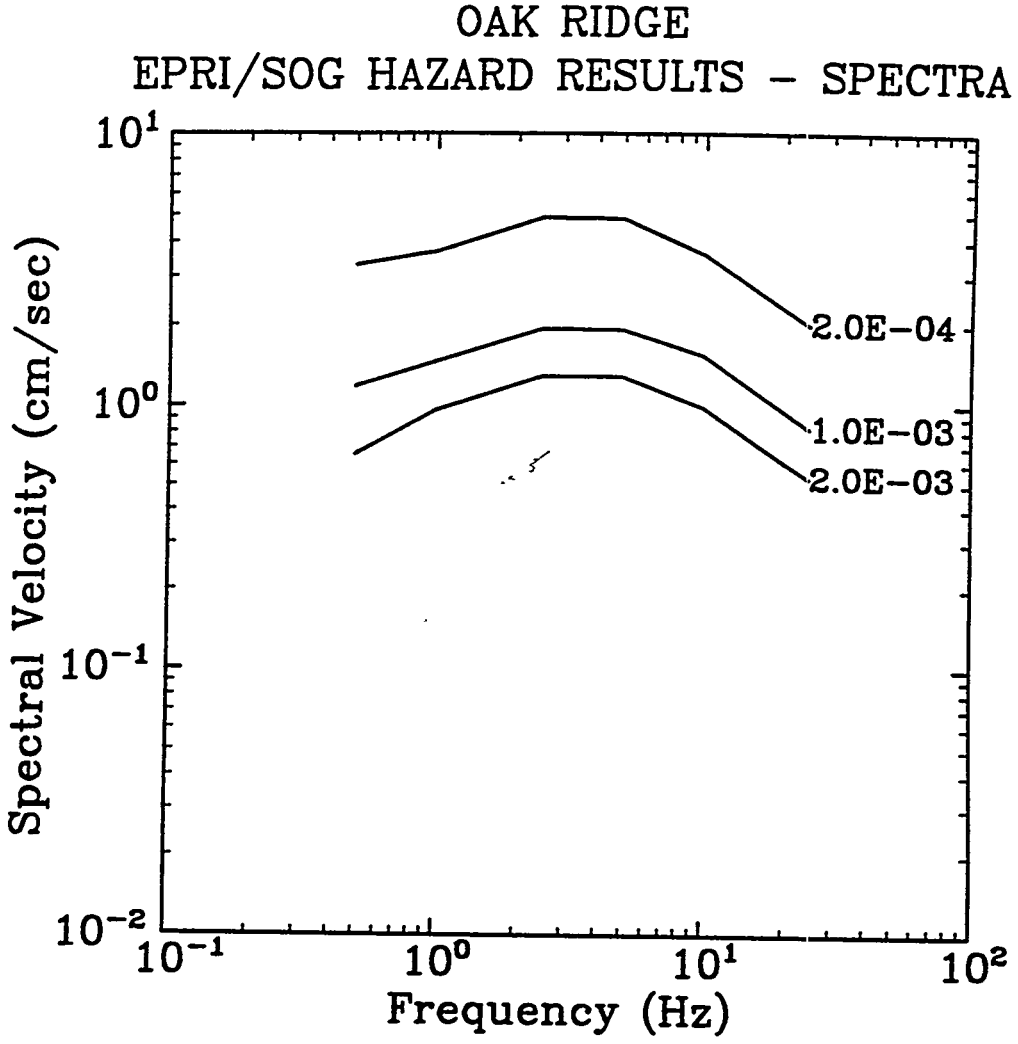

Figure 2-18. Seismic hazard at Oak Ridge computed using the EPRI/SOG methodology. Results shown as uniform hazard spectra for four values of the annual probability of exceedance.

Section 3

LLNL METHODOLOGY AND RESULTS

3.1 METHODOLOGY

The second source of interpretations for this study consists of the study of seismic hazard in the CEUS conducted by LLNL (1). This study culminates a decade of effort funded by the U.S. Nuclear Regulatory Commission to characterize earthquake sources, seismicity parameters, and ground-motion estimates for the region, for the purpose of evaluating seismic hazard at nuclear plant sites. Two panels of experts were formed. Eleven seismicity experts familiar with the region were polled for interpretations of seismic sources and ground-motion parameter values, and five ground-motion experts were polled for opinions on appropriate attenuation equations to estimate PGA and response spectrum amplitudes. Uncertainties in the interpretations were represented by discrete and continuous distributions, and uncertainty in the seismic hazard was derived by Monte Carlo sampling of the input distributions, producing a seismic hazard curve for each set of simulated variables and thus representing the uncertainty in the seismic hazard as a function of uncertainty in expert interpretation.

LLNL performed its methodology for the HFIR site under a separate agreement, and provided results for use in this study. We summarize herein some of the important inputs to the LLNL analysis and our interpretations of them for this study.

3.2 SEISMICITY INTERPRETATIONS

The eleven seismicity experts provided sets of seismic sources for the CEUS; the basic set of sources for the region are reproduced in Figures 3–1 through 3–11, for comparison to the EPRI sources. Some LLNL experts also specified alternative geometries of sources; these are not reproduced here but are available in the LLNL documentation (1). By contrast to the EPRI study, which specified uncertainty on the seismic activity of each source separately, the LLNL experts specified global alternatives for sets of sources that might be active simultaneously.

Seismicity parameters (rates of activity and Richter b-values) for the sources were provided by the seismicity experts, although the LLNL team made available the results of calculations of these parameters using a standard method and an earthquake catalog specified by the

expert. Distributions and correlations were also specified to represent the uncertainty of these parameters. In addition, the distribution of maximum possible earthquake size was specified for each source by each expert. (Most of them used magnitude to characterize earthquake size; one used MM intensity, and a second used a combination of the two.)

3.3 GROUND-MOTION MODELS

Five earth scientists and engineers were asked to derive ground-motion estimation equations for the CEUS for the LLNL study. These equations were to estimate PGA and response spectrum amplitude as a function of earthquake magnitude and distance. Estimating such equations for the CEUS is problematic because of the lack of recorded strong earthquake motions in the area with which to calibrate empirical techniques or validate theoretical models. Any method thought to be adequate by the five experts was acceptable. The five participants were asked to specify uncertainty in their choice of ground-motion equations by designating multiple models with subjective weights.

One of the models selected gives substantially higher ground-motion estimates than the others for PGA and response spectrum amplitudes. For PGA this model is designated "G16-A3" in the LLNL report (1); it is a combination of two equations, a correlation between PGA and MM intensity published by Trifunac from California data (2), and an MM intensity attenuation equation published by Gupta and Nuttli (3). A similar procedure was followed for spectral velocities; the resulting model is designated "TL." This selection received 100% weight from Expert 5, and zero weight from the other panelists. Comparing the predictions from this equation to data available from CEUS seismographs and accelerographs indicates that equation G16-A3 severely over-estimates ground-motions in the CEUS, particularly at distances greater than 20 km from the earthquake source. [See Figures 5–123 through 5–125 of (4) and for these comparisons and Figures 3–2 through 3–13 of (5) for comparisons with data from the Saguenay earthquake.]

There are good reasons why equations G16-A3 and TL might lead to poor estimates of ground-motion in the CEUS. This function was obtained by substitution of a stochastic relationship between instrumental ground-motion and intensity into a stochastic intensity-attenuation relation. This type of substitution of one regression into another is mathematically incorrect and has been demonstrated to produce significant biases when applied to intensity-attenuation data (6). In particular, after such a substitution the dependent variable does not appear to be as strongly correlated to the independent variable as it should be, which is the behavior evident in comparisons of data with estimates from G16-A3. For example, the data in Figures 5-123 through 5-125 of (4) show a much stronger dependence

on distance than do the estimates. Further, this model was given zero weight by four of the LLNL panelists (and 100% weight by the fifth), an indication that the model has a small following in the scientific community [see Tables 3.5 and 3.6 in Volume 1 of (1)]. Because of the theoretical problems in the derivation of equation G16-A3 and its lack of agreement with available data from the CEUS, it appears that this equation lacks credibility and should not be included in results used from the LLNL study.

An important set of earthquake ground-motion data became available on November 25, 1988 when the Saguenay earthquake (magnitude m_{bLg} 6.5) occurred in Quebec. This earthquake generated more accelerograph records than any previous earthquake in eastern North America. We have performed a detailed comparison of Saguenay ground-motions to predictions by the LLNL and EPRI attenuation functions, a review of seismological studies on the Saguenay earthquake, and an examination of the assumptions and substitution methods employed by LLNL ground-motion expert 5 (5). We conclude from the above study that the attenuation functions proposed by LLNL ground-motion expert 5 should not be used for seismic hazard calculations in eastern North America, because these attenuation functions are inconsistent with all instrumental ground motion data from eastern North America, they are based on assumptions about intensity that are incorrect, and they were obtained using a substitution procedure that is invalid.

3.4 COMPUTATIONS

The Monte Carlo simulation procedure used by LLNL to express uncertainty in seismic hazard as a function of uncertain input was conducted as follows. There were 55 possible combinations of the eleven seismicity experts and the five ground-motion experts, and each combination was considered separately. For each, 50 simulations of uncertain parameters were made, drawing from the distributions on seismicity parameters, ground-motion equations, and attenuation randomness terms specified by each expert. This resulted in 2750 combinations of parameters from which a family of 2750 seismic hazard curves could be calculated. Each of these seismic hazard curves was then assigned a weight based on a self-weighting provided by the experts. This led to an uncertainty distribution on the frequency of exceedance for any PGA level, from which fractiles of seismic hazard can be computed and plotted as fractile seismic hazard curves.

3.5 RESULTS

LLNL calculated two sets of seismic hazard results, i.e., with and without ground-motion Expert 5. These results are presented in Figures 3-12 through 3-15, in the form of PGA hazard curves and median uniform-hazard spectra.

3.6 REFERENCES

1. D. L. Bernreuter, J. B. Savy, R. W. Mensing, and J. C. Chen. *Seismic Hazard Characterization of 69 Plant Sites East of the Rocky Mountains.* Technical Report NUREG/CR5250, UCID-21517, U. S. Nuclear Regulatory Commission, 1988.

2. M. D. Trifunac. "A Note on the Range of Peak Amplitudes of Recorded Accelerations, Velocities, and Displacements With Respect to the Modified Mercalli Intensity Scale". *Earthquake Notes*, 47:9–24, 1976.

3. I. N. Gupta and O. W. Nuttli. "Spatial Attenuation of Intensities for Central U.S. Earthquakes". *Bulletin of the Seismological Society of America*, 743–751, June 1976. Number 66–3.

4. R. K. McGuire, G. R. Toro, and W. J. Silva. *Probabilistic Seismic Hazard Evaluations in the Central and Eastern United States — Appendix A: Model of Earthquake Ground Motion for the Central and Eastern United States.* Technical Report, Electric Power Research Institute, 1989. EPRI Project RP101-53, prepared by Risk Engineering, Inc.

5. Risk Engineering, Inc. *Assessment of the 1988 Saguenay Earthquake – Implications on Attenuation Functions for Seismic Hazard Analysis.* Report to Pickard, Lowe and Garrick, Inc, February 1991.

6. C. A. Cornell, H. Banon, and A. F. Shakal. "Seismic Motion and Response Prediction Alternatives". *Earthquake Engineering and Structural Dynamics*, 7:295–315, 1979.

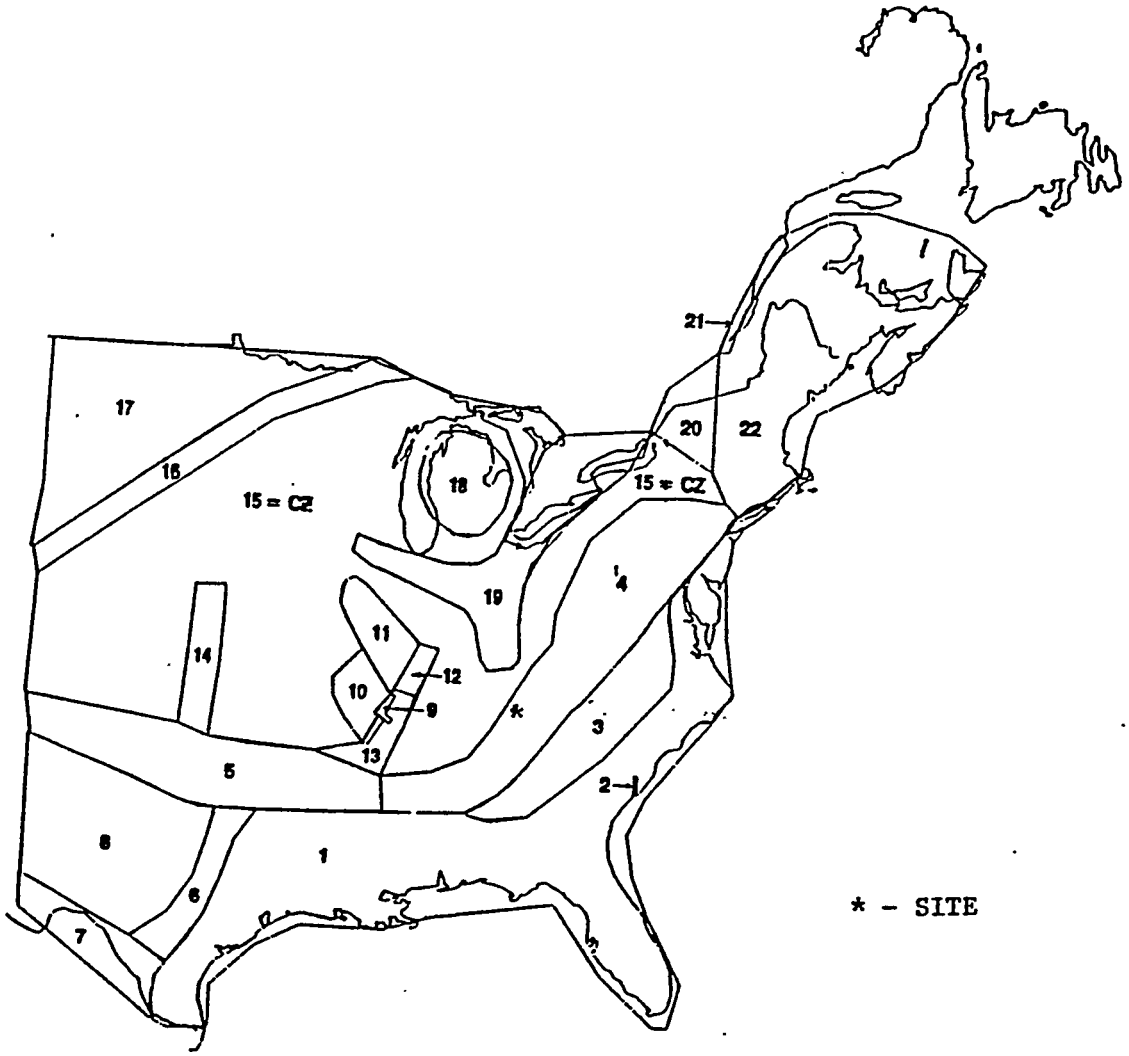

Figure 3-1. Main set of seismic sources provided by LLNL seismicity expert 1. Source: Volume 1 of (1).

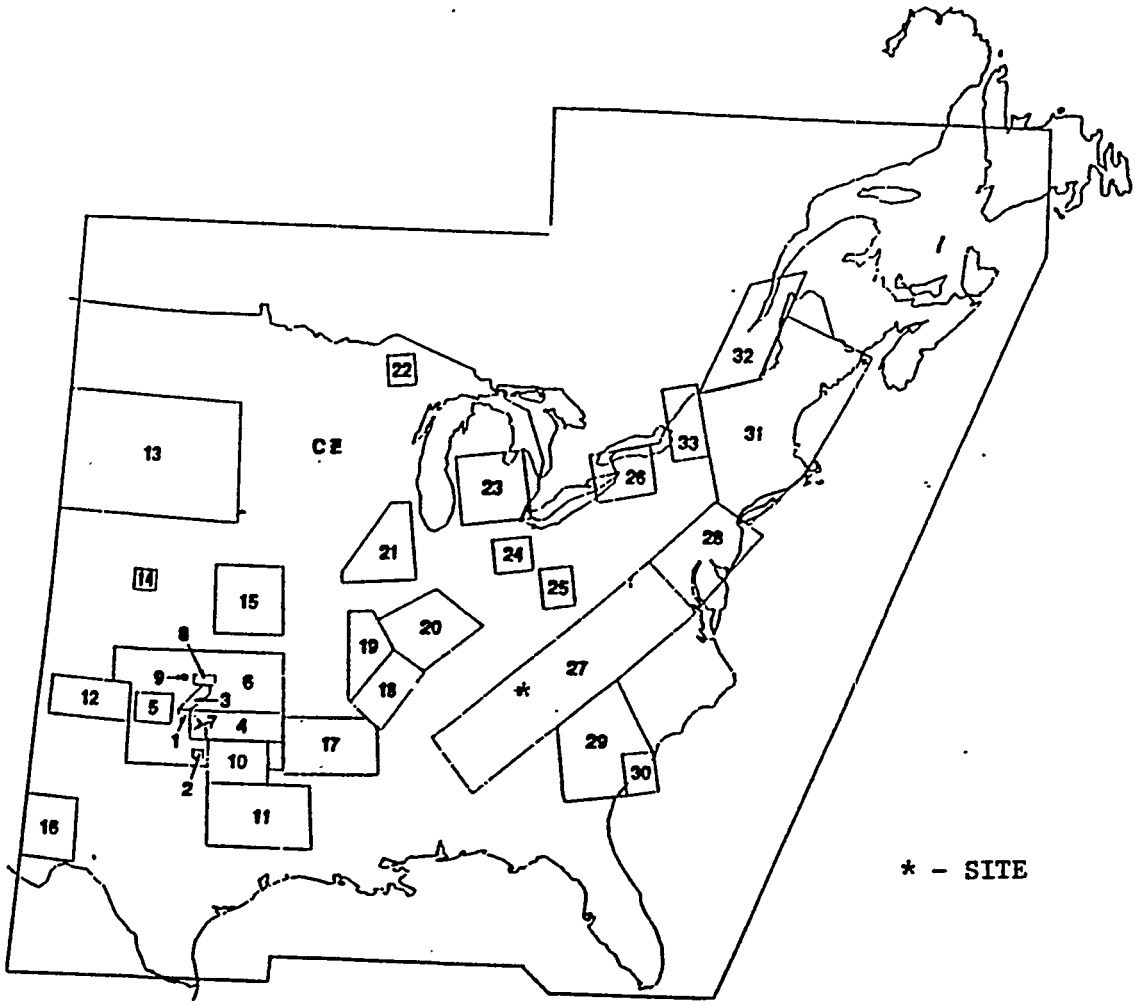

Figure 3-2. Main set of seismic sources provided by LLNL seismicity expert 2. Source: Volume 1 of (1).

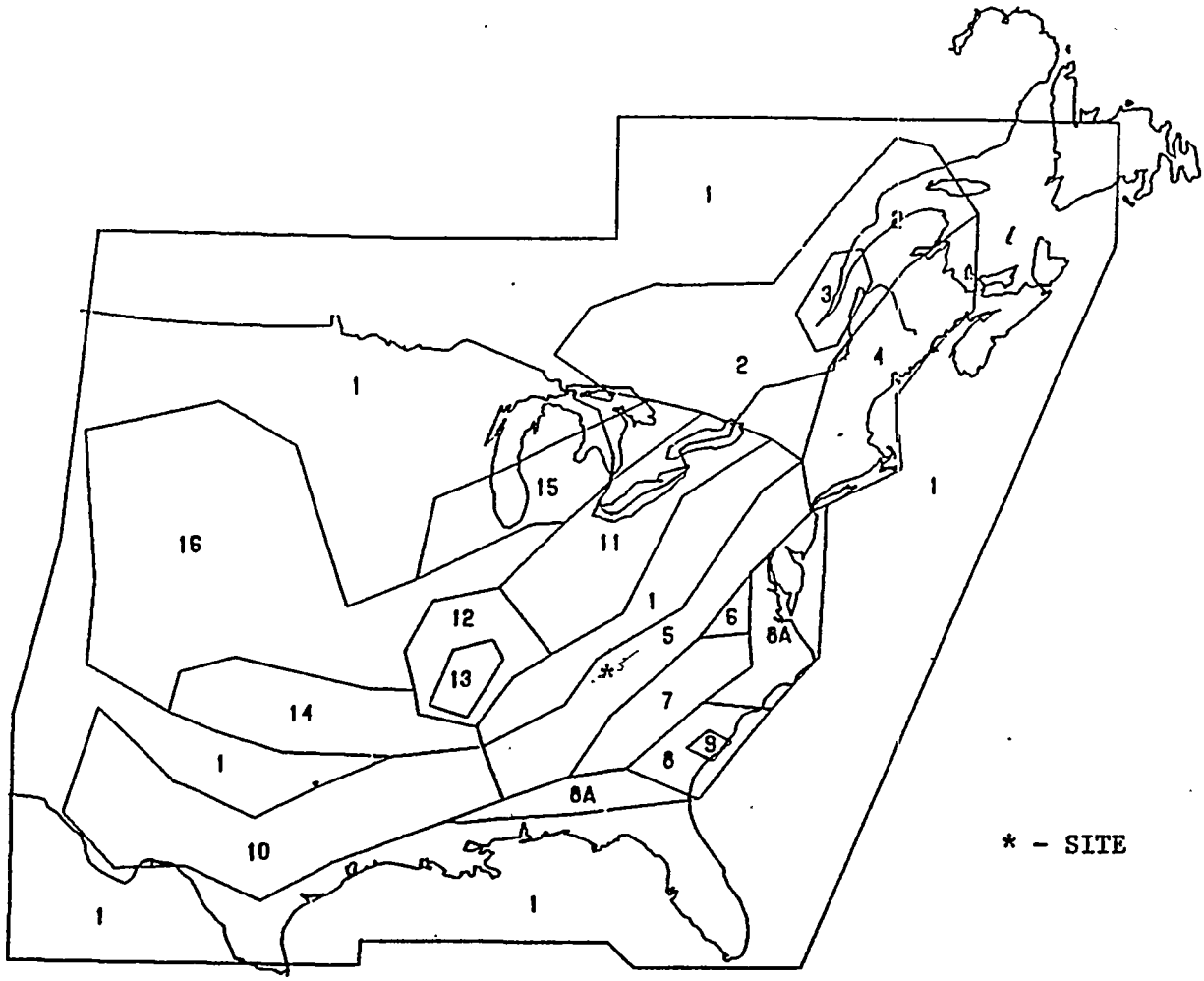

Figure 3-3. Main set of seismic sources provided by LLNL seismicity expert 3. Source: Volume 1 of (1).

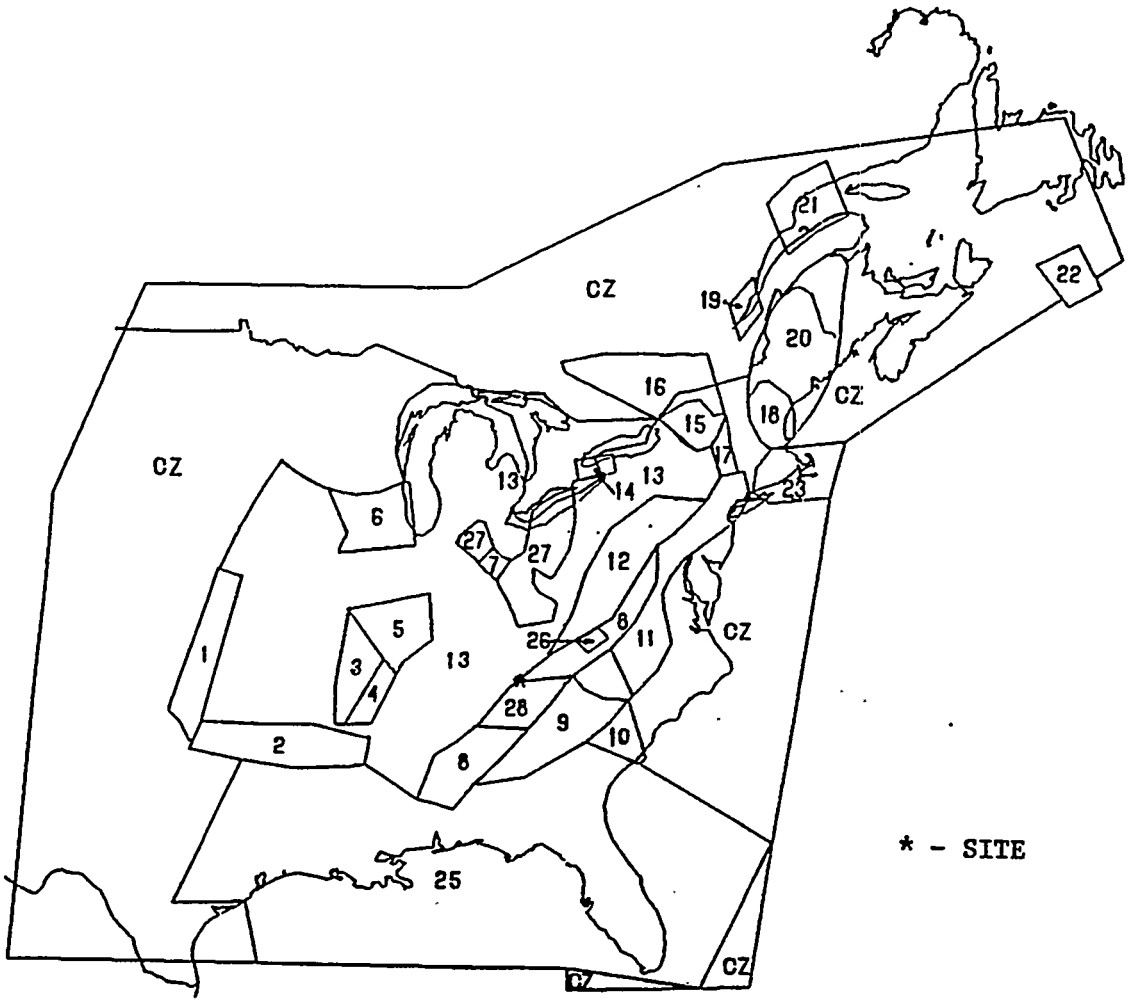

Figure 3-4. Main set of seismic sources provided by LLNL seismicity expert 4. Source: Volume 1 of (1).

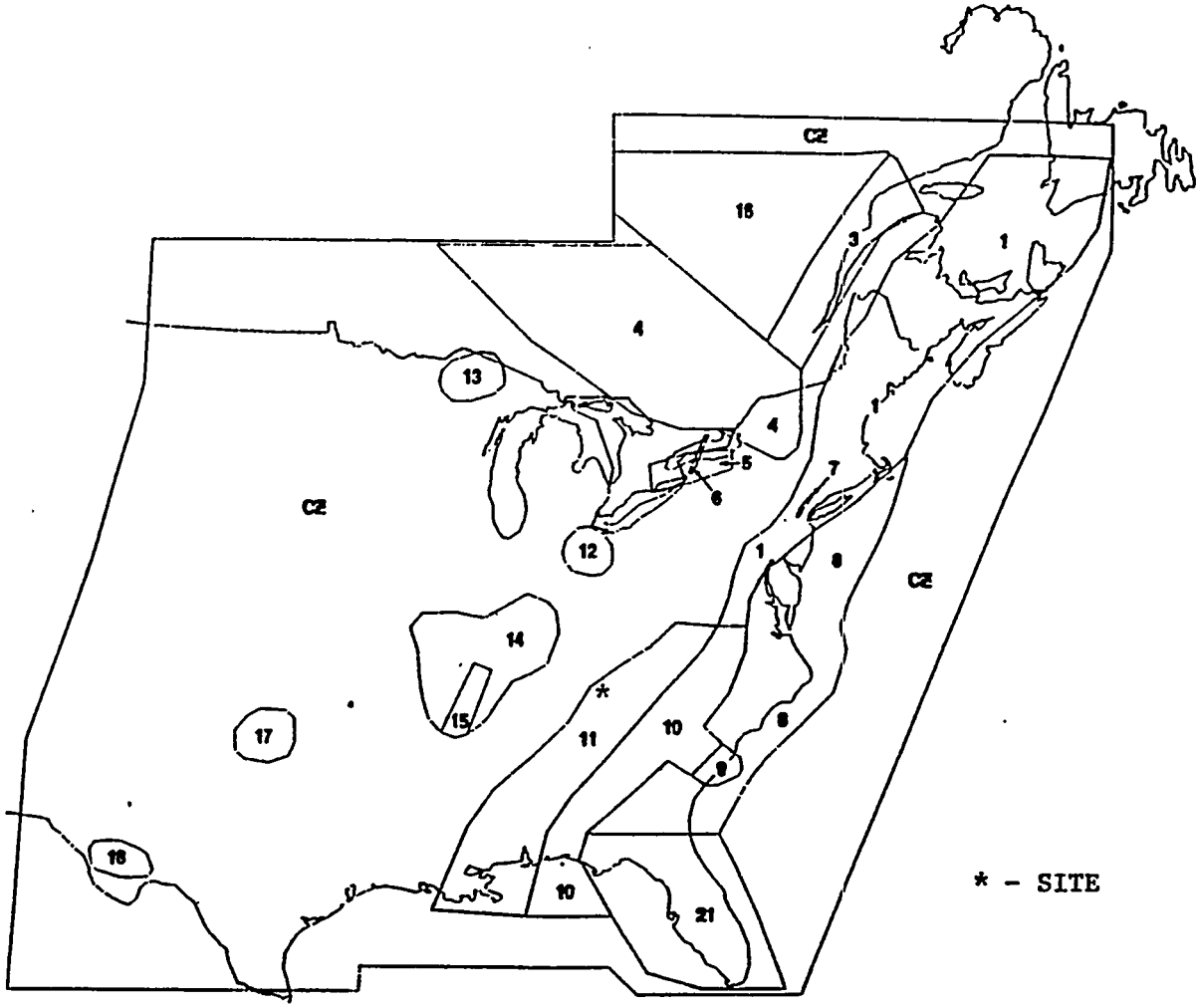

Figure 3-5. Main set of seismic sources provided by LLNL seismicity expert 5. Source: Volume 1 of (1).

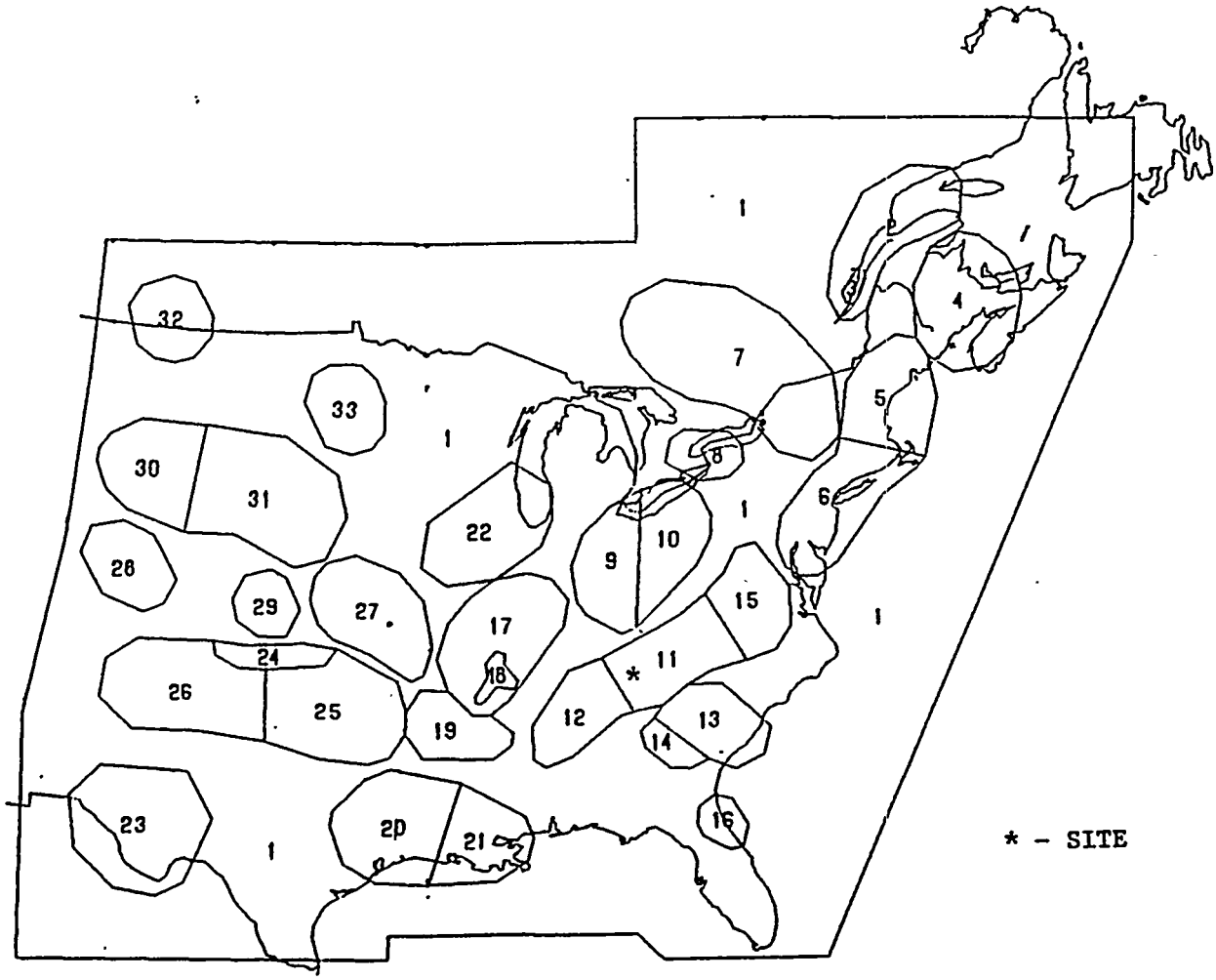

Figure 3-6. Main set of seismic sources provided by LLNL seismicity expert 6. Source: Volume 1 of (1).

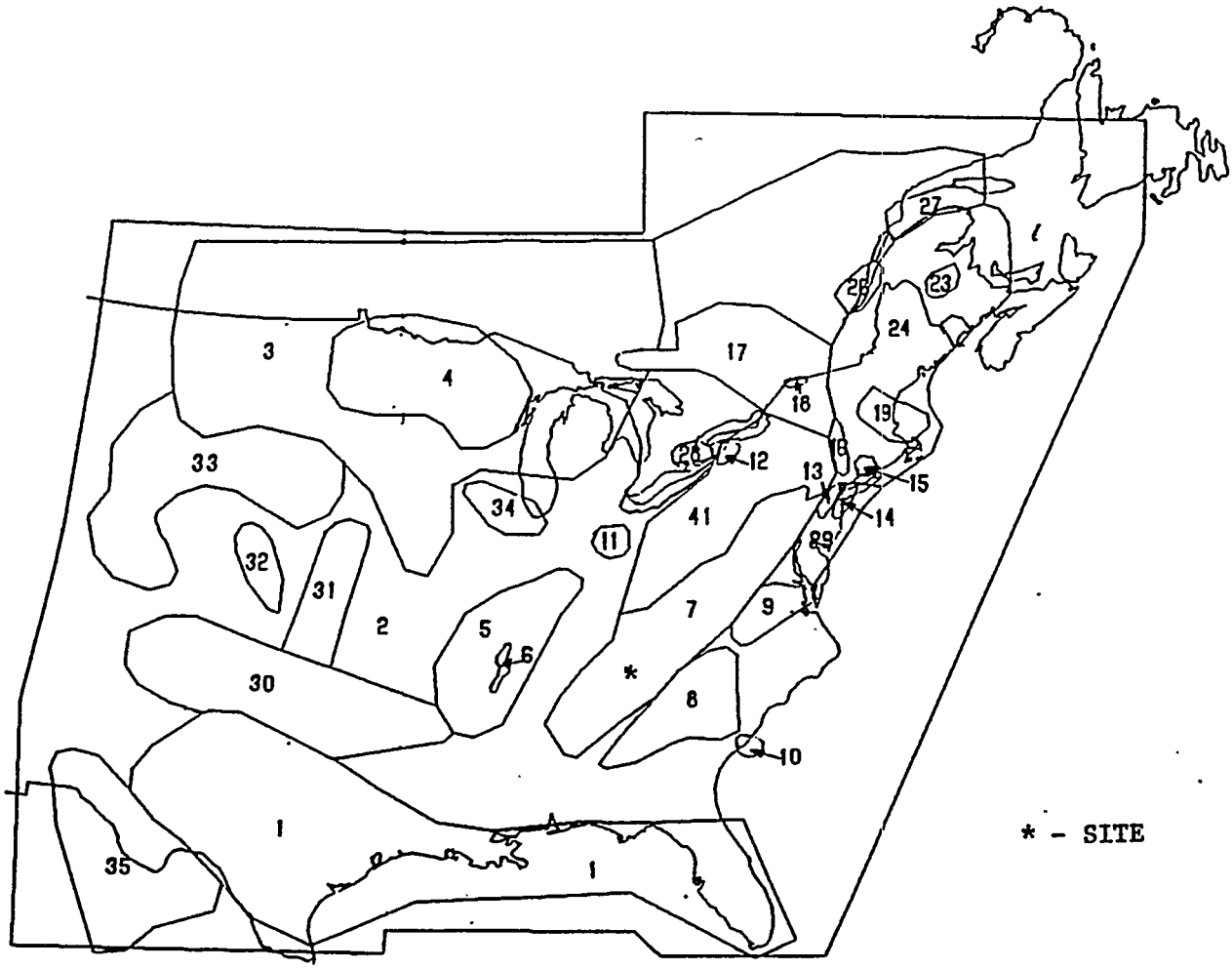

Figure 3-7. Main set of seismic sources provided by LLNL seismicity expert 7. Source: Volume 1 of (1).

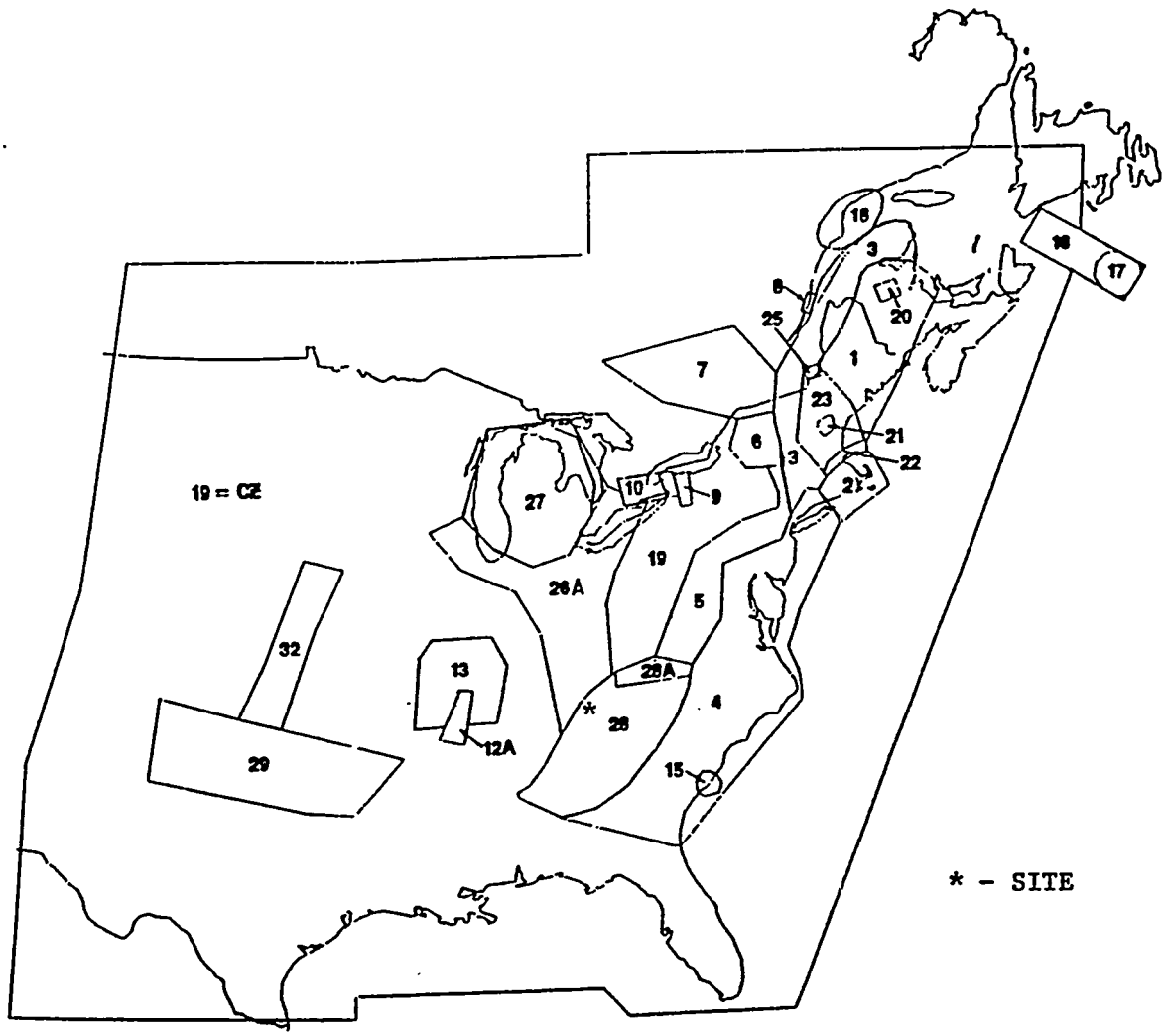

Figure 3-8. Main set of seismic sources provided by LLNL seismicity expert 10. Source: Volume 1 of (1).

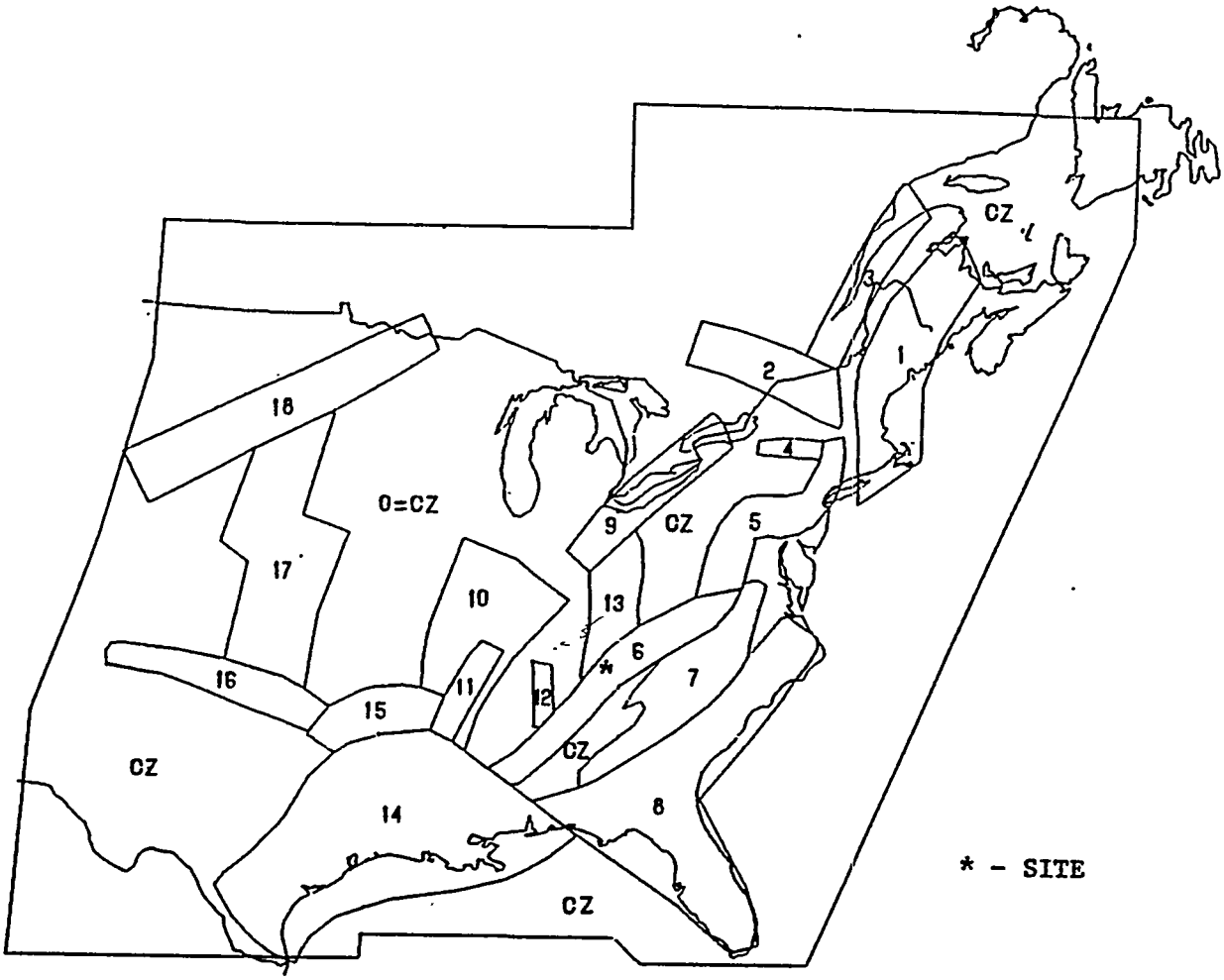

Figure 3-9. Main set of seismic sources provided by LLNL seismicity expert 11. Source: Volume 1 of (1).

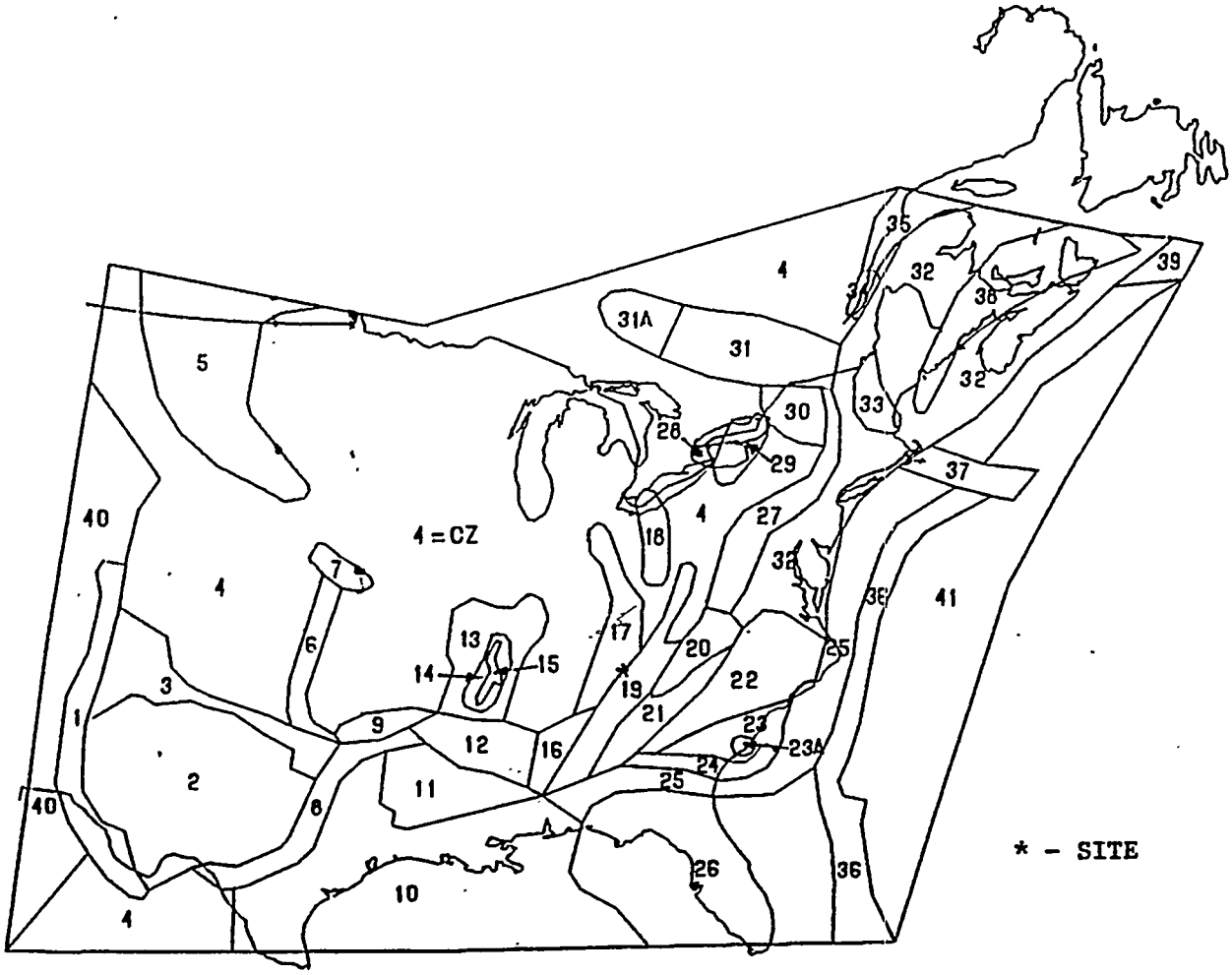

Figure 3-10. Main set of seismic sources provided by LLNL seismicity expert 12. Source: Volume 1 of (1).

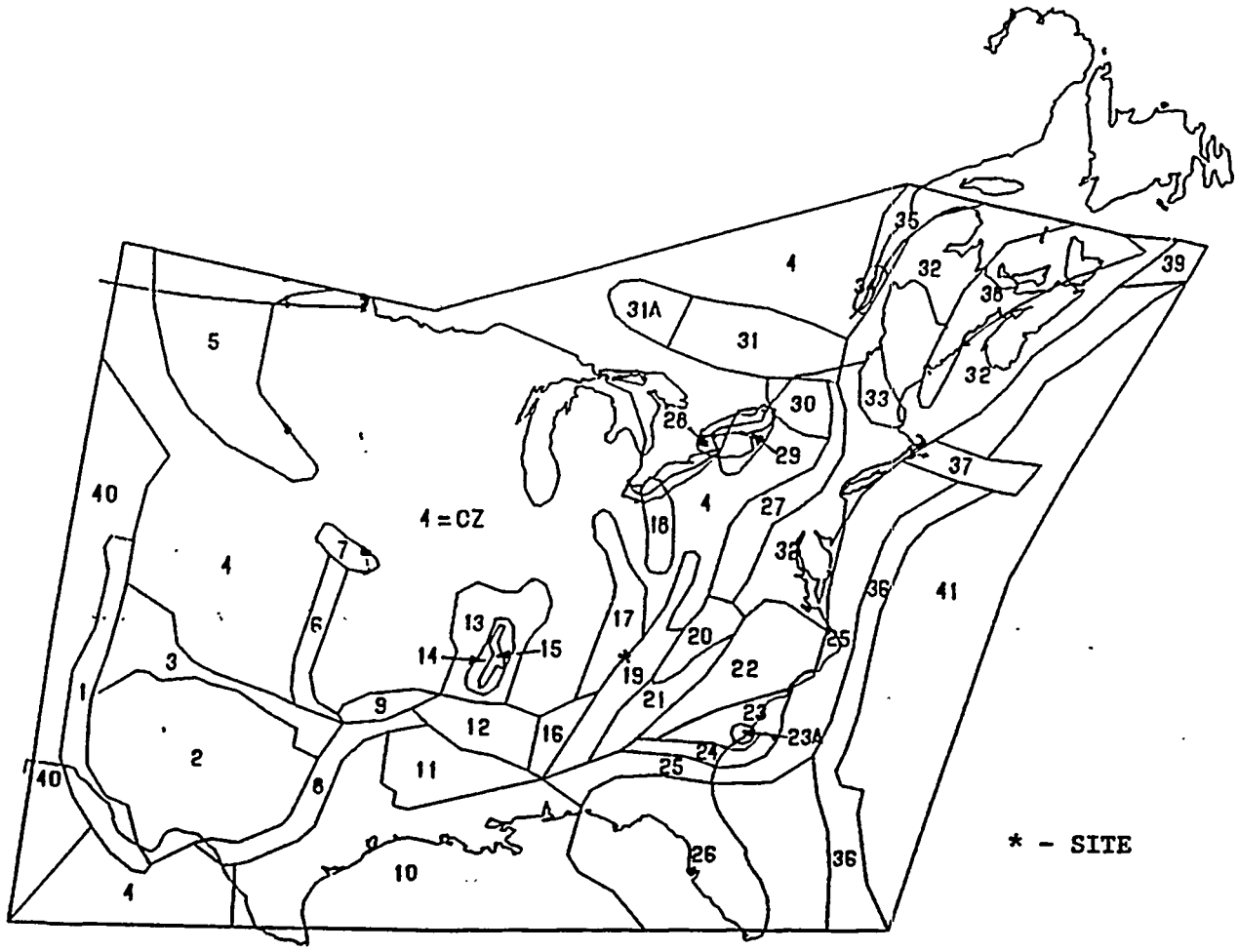

Figure 3-10. Main set of seismic sources provided by LLNL seismicity expert 12. Source: Volume 1 of (1).

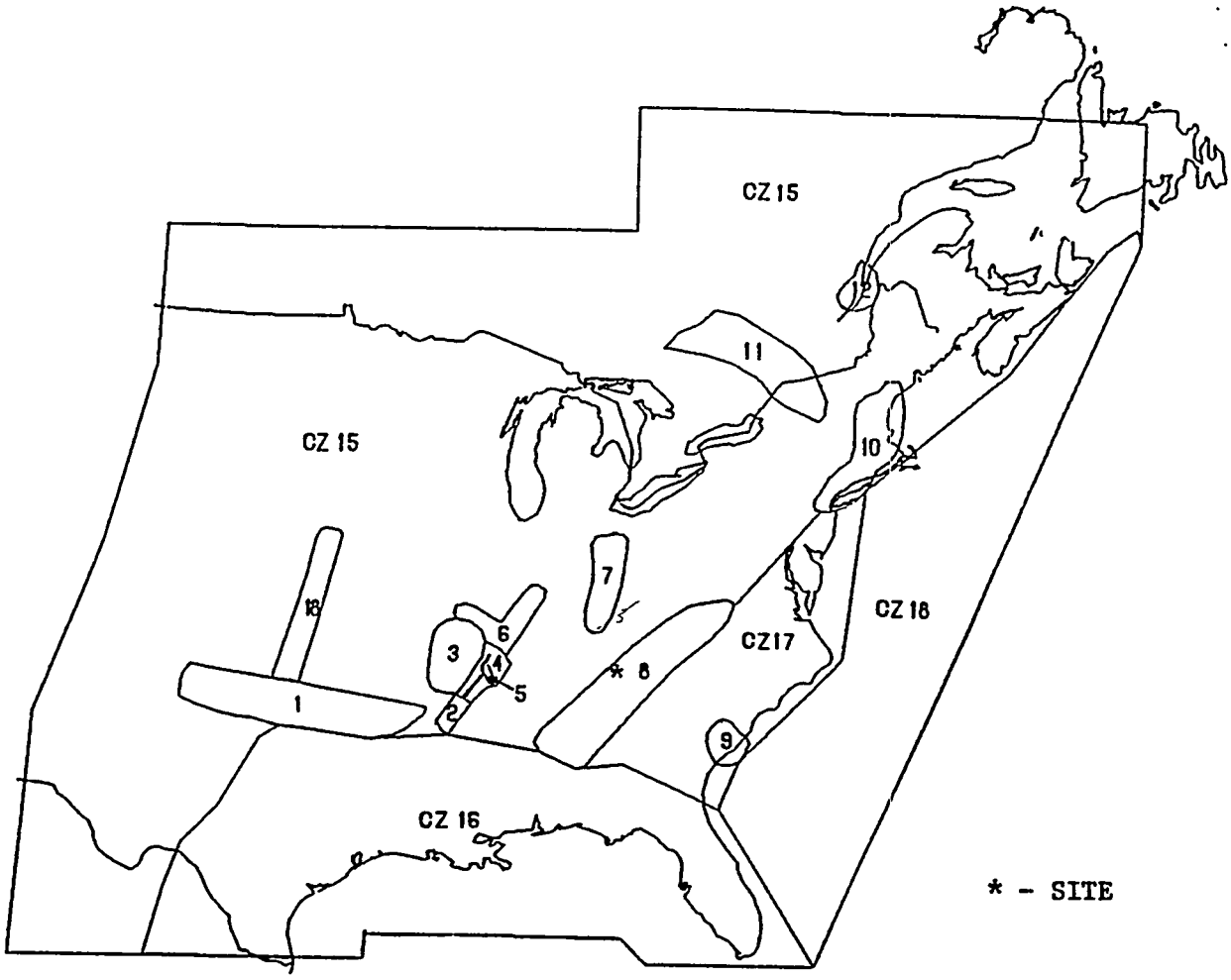

Figure 3-11. Main set of seismic sources provided by LLNL seismicity expert 13. Source: Volume 1 of (1).

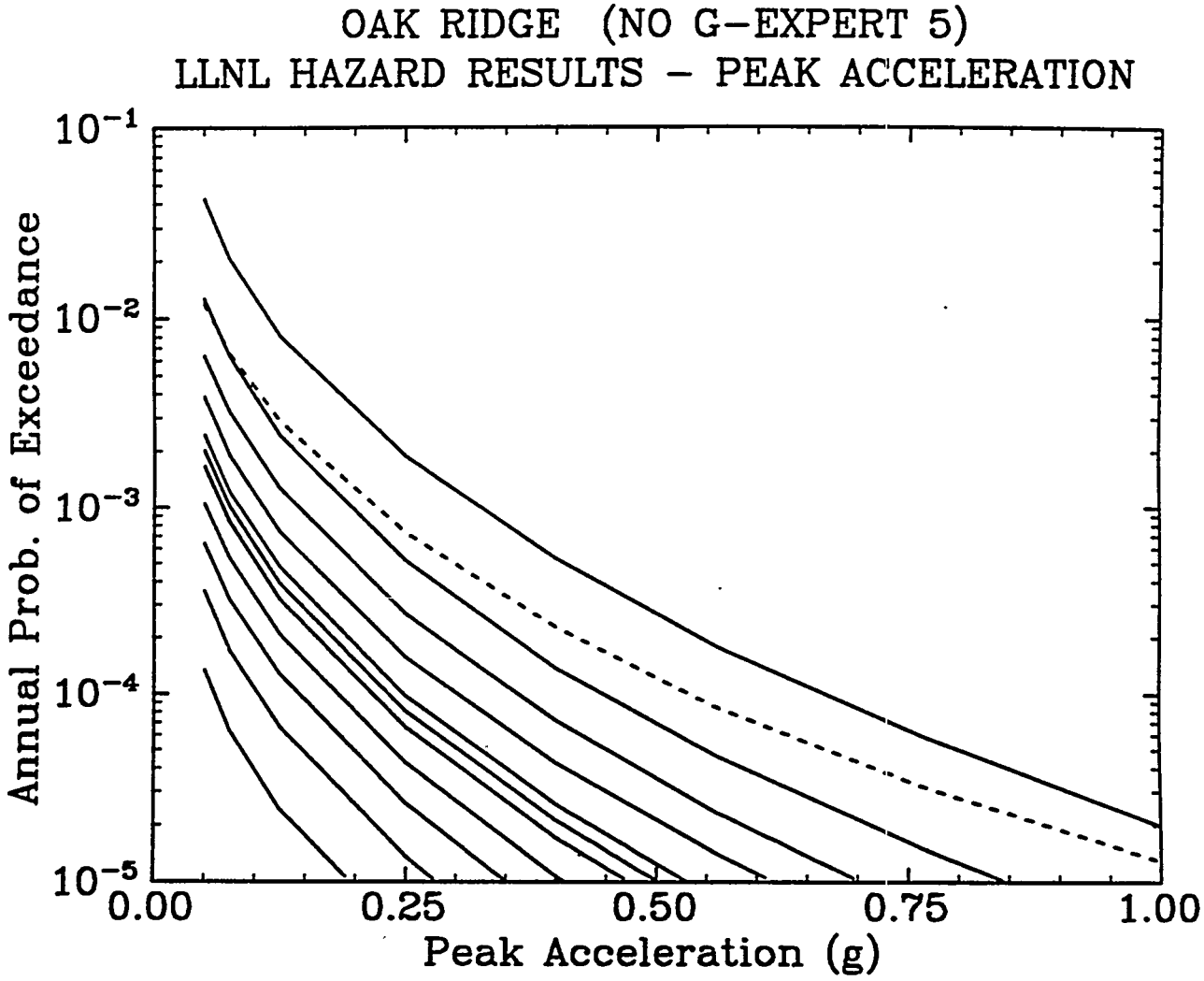

Figure 3-12. Seismic hazard at Oak Ridge computed by LLNL using the LLNL methodology (excluding LLNL ground-motion expert 5). Results shown as fractile hazard curves for peak acceleration. The solid curves shown represent the following fractiles: 0.05 (bottom), 0.15, 0.25, 0.35, 0.45, 0.50, 0.55, 0.65, 0.75, 0.85, 0.95 (top). The dashed curve represents the mean hazard curve.

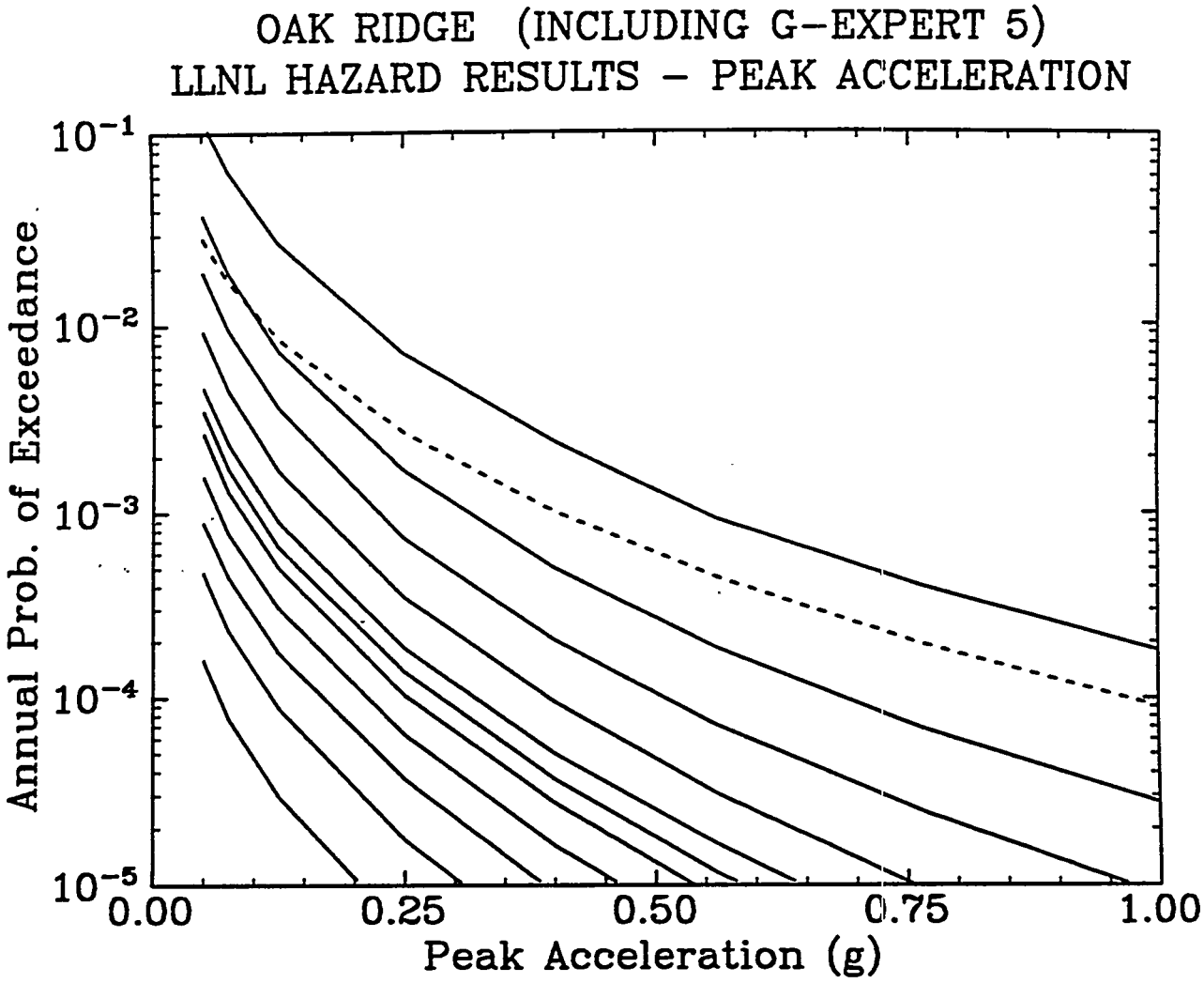

Figure 3-13. Seismic hazard at Oak Ridge computed by LLNL using the LLNL methodology (including LLNL ground-motion expert 5). Results shown as fractile hazard curves for peak acceleration. The solid curves shown represent the following fractiles: 0.05 (bottom), 0.15, 0.25, 0.35, 0.45, 0.50, 0.55, 0.65, 0.75, 0.85, 0.95 (top). The dashed curve represents the mean hazard curve.

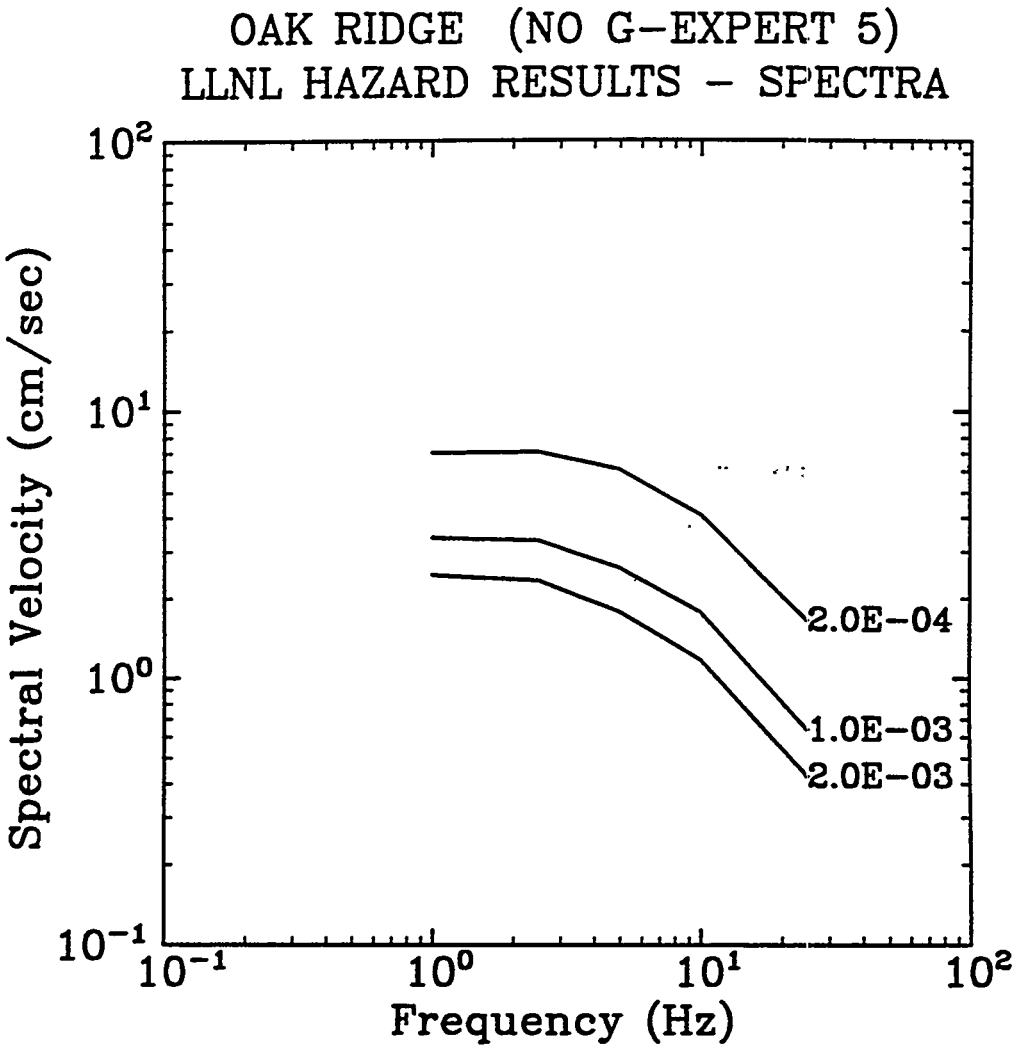

Figure 3-14. Seismic hazard at Oak Ridge computed by LLNL using the LLNL methodology (excluding LLNL ground-motion expert 5). Results shown as median uniform hazard spectra.

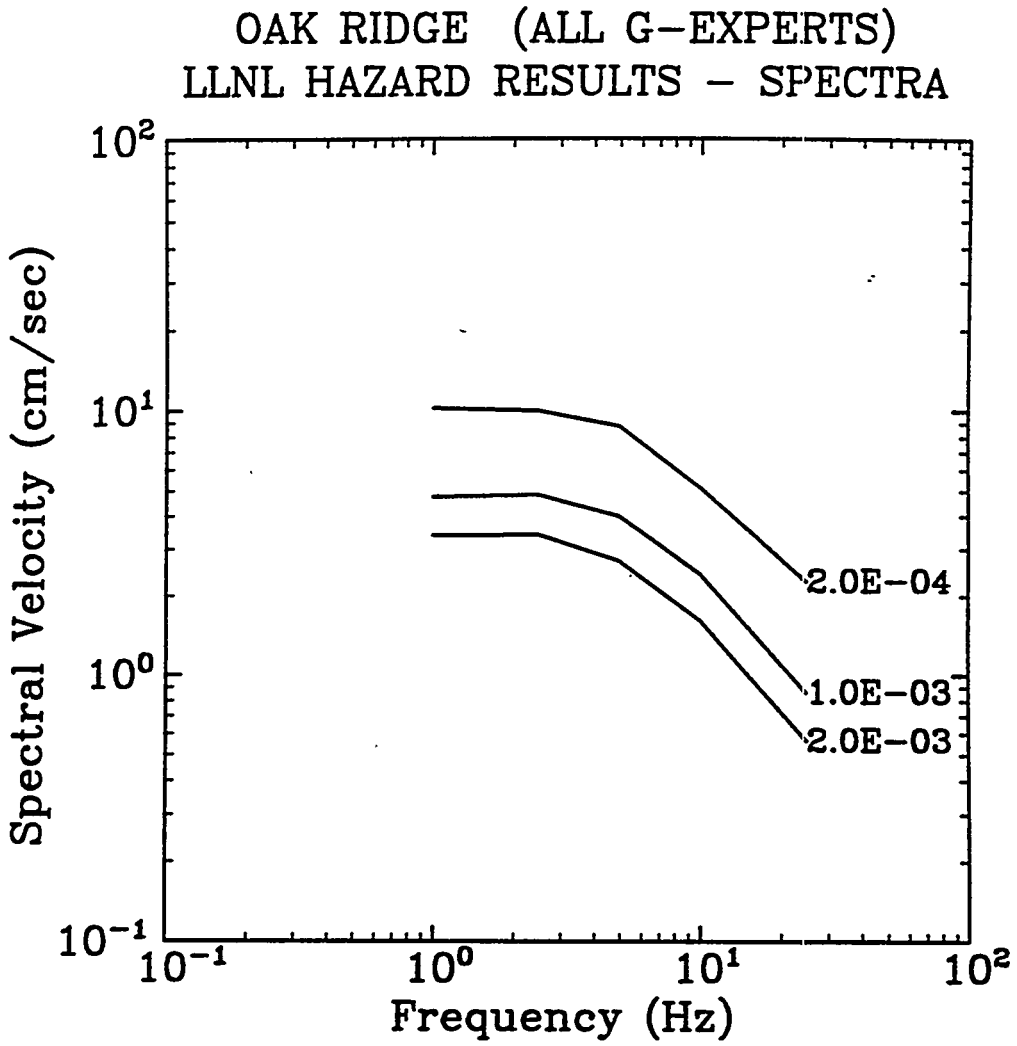

Figure 3-15. Seismic hazard at Oak Ridge computed by LLNL using the LLNL methodology (including LLNL ground-motion expert 5). Results shown as median uniform hazard spectra.

Section 4

COMBINATION OF EPRI/SOG AND LLNL RESULTS

4.1 OVERVIEW

This Section describes the procedure used to combine the EPRI/SOG and LLNL seismic hazard results presented in Sections 2 and 3, in order to obtain a synthesized representation of seismic hazard and its uncertainty at the Oak Ridge site. Results are then presented as fractile hazard curves, mean hazard curve, and median uniform-hazard spectra.

4.2 COMBINATION OF EPRI/SOG AND LLNL RESULTS

The EPRI/SOG and LLNL results are given equal weights to obtain an overall representation of the seismic hazard and its uncertainty. The choice of equal weights is justified given the comparable caliber of the two studies. Both studies elicited interpretations by multiple experts—in order to capture all hypotheses with scientific validity—and both studies underwent extensive peer reviews.

For the development of combined hazard results, the EPRI/SOG results are represented by 30 equally weighted hazard curves. The LLNL results are represented by 10 equally weighted hazard curves, which correspond to the 0.05, 0.15, ... 0.95 fractile curves shown in Section 3.

We combine these 40 hazard curves, giving a weight of 1/60 to each EPRI/SOG curve and 1/20 to each LLNL curve. We then compute fractile and mean curves[1] from these combined curves.

4.2.1 Mechanics of the Combination Process

We combine the EPRI/SOG and LLNL seismic hazard results by operating with their uncertainty distributions on the hazard at each calculated ground-motion amplitude. This section contains a detailed description of this process and gives some insights about its results. To

[1]We deliberately use the mean curve computed from these 40 hazard curves—instead of combining the original mean hazard curves shown in Sections 2 and 3—in order to avoid the well-known instabilities in the mean LLNL hazard curves.

illustrate this process, we will consider the evaluation of combined hazard estimates for one value of peak acceleration.[2]

For the purposes of the combination process, the EPRI/SOG results are represented by 30 equally weighted hazard curves. These curves are constructed from each team's 0.10, 0.30, 0.50, 0.70, and 0.90 fractile curves.

For each ground-motion amplitude (e.g., each value of PGA), a discrete probability distribution of hazard is constructed by reading the hazard curves at this amplitude. Figure 4–1 shows the distribution of hazard at 0.2 g (PGA), as obtained from the EPRI/SOG analysis. Each spike in the probability mass function in Figure 4–1 (top) represents one hazard curve; all spikes have heights of 0.0333=1/30 because all hazard curves carry equal weights. The bottom portion of Figure 4–1 shows the corresponding cumulative distribution, and illustrates the process of evaluating the median (or 0.50 fractile).

We follow a similar process for the LLNL results, which are represented by 10 equally weighted fractile hazard curves (corresponding to 0.05, 0.15, 0.25, 0.35, 0.45, 0.55, 0.65, 0.75, 0.85, and 0.95 fractiles). Figure 4–2 shows the distribution of hazard at 0.2 g, as obtained from the LLNL fractile hazard curves.

We combine the EPRI/SOG and LLNL results by combining their corresponding probability mass functions, with equal weights, as shown in Figure 4–3. Each of 30 spikes from the EPRI/SOG results gets a weight of 1/60, while each of 10 spikes from the LLNL results gets a weight of 1/20. We then construct the combined cumulative distribution and use it to evaluate the median and other fractiles (see bottom of Figure 4–3). We also use this combined distribution to evaluate the mean hazard.

Figure 4–3 shows that, unlike the mean, the median of the combined results depends on the distributions of the EPRI/SOG and LLNL results (i.e., it is impossible to calculate the median of the combined results from the EPRI/SOG and LLNL medians). Because the EPRI/SOG results have a tighter distribution of uncertainty, the median of the combined results tends to fall closer to the EPRI/SOG median.

We follow a similar procedure for spectral velocities, the only difference being that LLNL reported only the 0.05, 0.15, 0.50, 0.85, and 0.95 fractile hazard curves. Other LLNL fractile

[2]The results that we will show in Figures 4–1 through 4–3 were obtained for another site; they will shown here for the sake of illustration.

hazard curves were generated from the above fractile hazard curves assuming that each half of the body of the uncertainty distribution is approximately lognormal. The combined PSV hazard curves are then used to generate uniform-hazard spectra. Because LLNL did not generate results for 0.5-Hz spectral velocities, it was assumed that the ratio of 0.5 Hz to 1-Hz ordinates is the same for LLNL and for EPRI/SOG.

4.3 RESULTS

Two sets of combined EPRI/SOG–LLNL hazard results are generated, as follows: using all LLNL ground-motion Experts (Figs. 4–4 and 4–5), and using 4 LLNL ground-motion Experts (Figs. 4–6 and 4–7).

4.3.1 Uniform Hazard Spectra for Additional Damping Ratios

We calculate approximate uniform hazard spectra for damping ratios of 2, 7, 10, 12, and 15 % from the 5% results presented in Figures 4–5 for all LLNL Ground-Motion experts. We use the expression:

$$\frac{\mathrm{PSV}(f,\zeta)}{\mathrm{PSV}(f,0.05)} \simeq \left[\frac{1+4.9\zeta fT}{1+4.9\times 0.05 fT}\right]^{-0.41} \qquad (4-1)$$

in which f is frequency (Hz), ζ is damping ratio (as a fraction of critical damping, not as a percentage), and T is the duration of the strongest phase of the ground motion. Equation 4-1 is based on a semi-empirical expression by Rosenblueth (1, Equation 1.11). The PSV ratios predicted by Equation $4-1$ agree with results from random-vibration theory for large values of fT, and with real and artificial records for all interesting values of fT. Comparisons with records also show that the ratio $\mathrm{PSV}(f,\zeta)/\mathrm{PSV}(f,0.05)$ has a low variability from record to record.

We use Equation 4–1, together with the strong-motion duration determined in Section 5. Figures 4–6 through 4–10 present the calculated uniform hazard spectra for the additional damping ratios.

4.4 REFERENCES

1. E. Rosenblueth. "Characteristics of Earthquakes". In E. Rosenblueth, editor, *Design of Earthquake Resistant Structures*, chapter 1, Wiley, 1980.

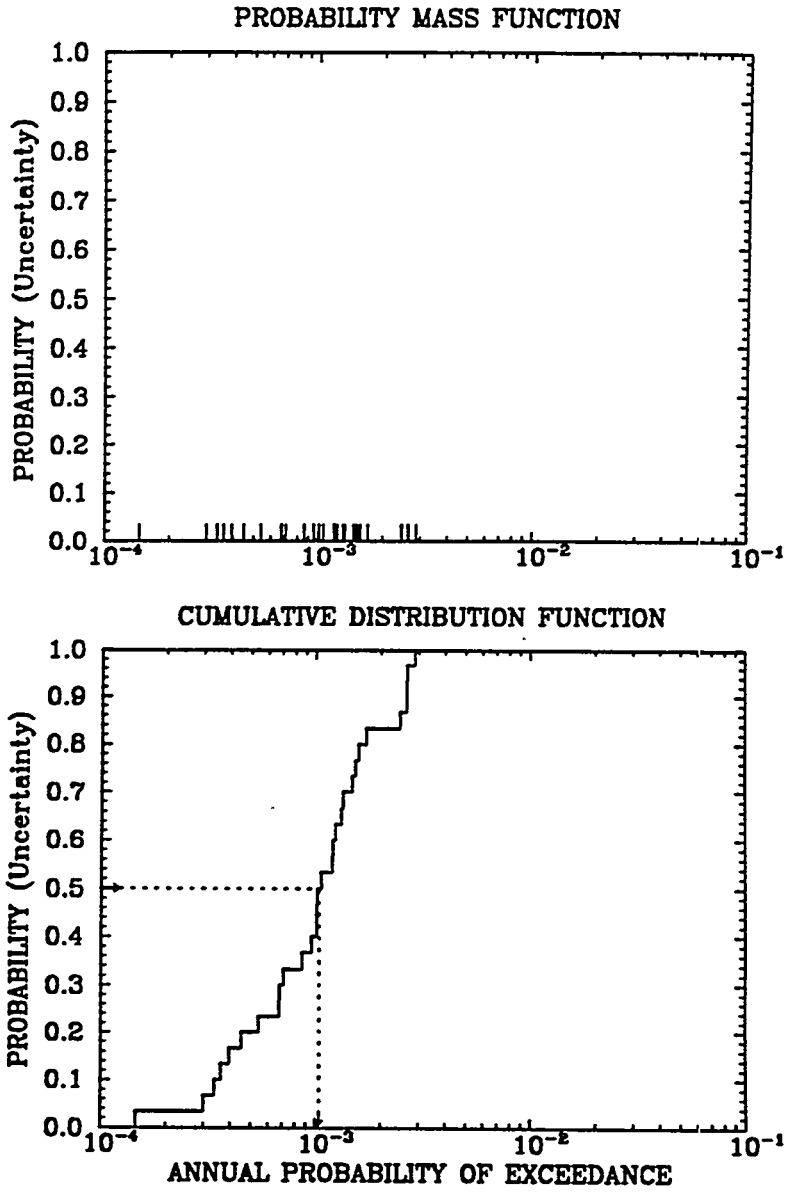

Figure 4-1. Discrete distribution representing uncertainty in the annual probability of exceeding 0.2 g PGA, as evaluated by the EPRI/SOG methodology. Top: probability mass function; bottom: cumulative distribution function. The dashed lines illustrate the evaluation of the median.

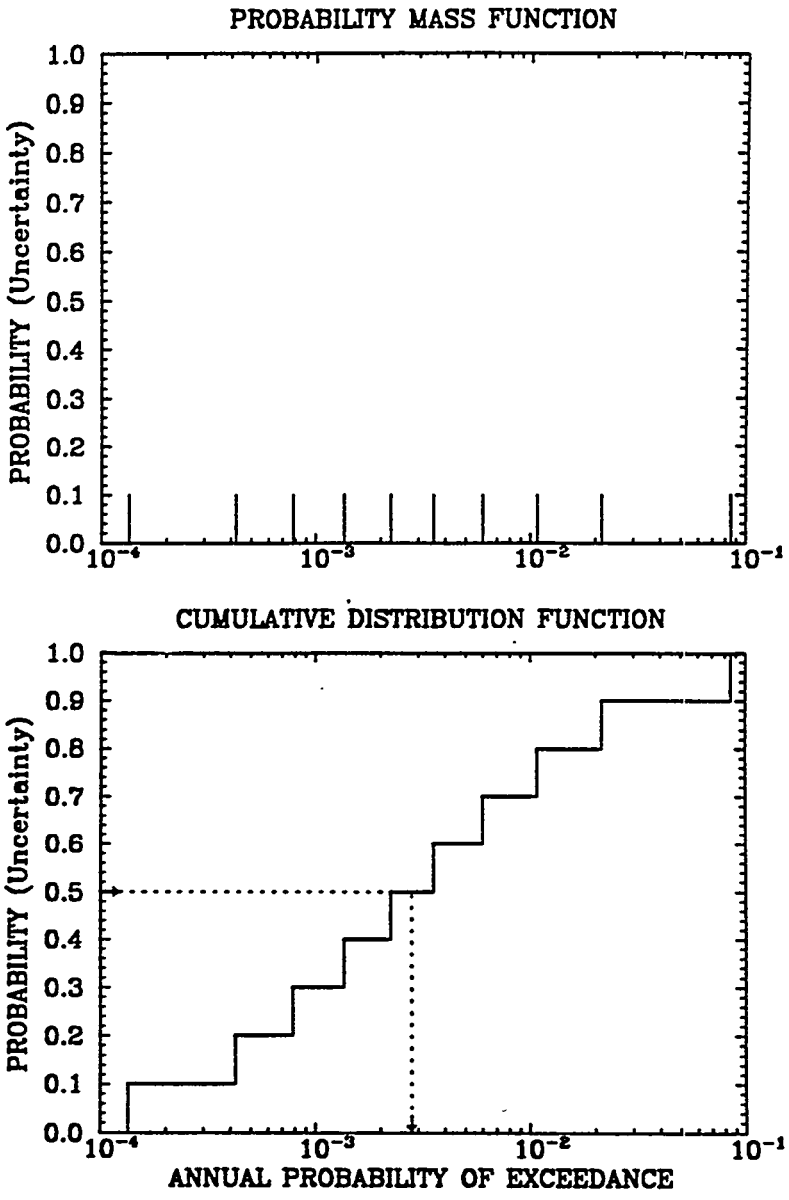

Figure 4-2. Discrete distribution representing uncertainty in the annual probability of exceeding 0.2 g PGA, as evaluated by the LLNL methodology. Top: probability mass function; bottom: cumulative distribution function. The dashed lines illustrate the evaluation of the median.

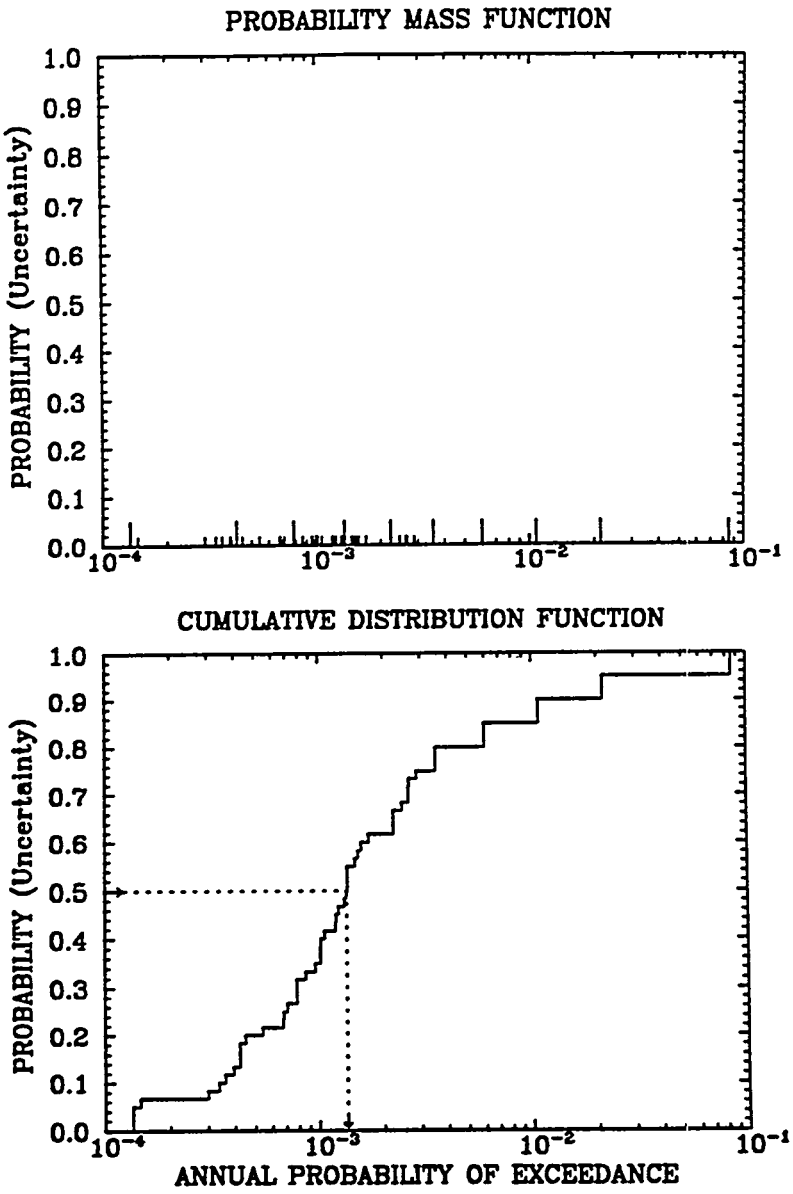

Figure 4-3. Discrete distribution representing uncertainty in the annual probability of exceeding 0.2 g PGA, as obtained by combining the EPRI/SOG and LLNL methodologies with equal weights. Top: probability mass function; bottom: cumulative distribution function. The dashed lines illustrate the evaluation of the median.

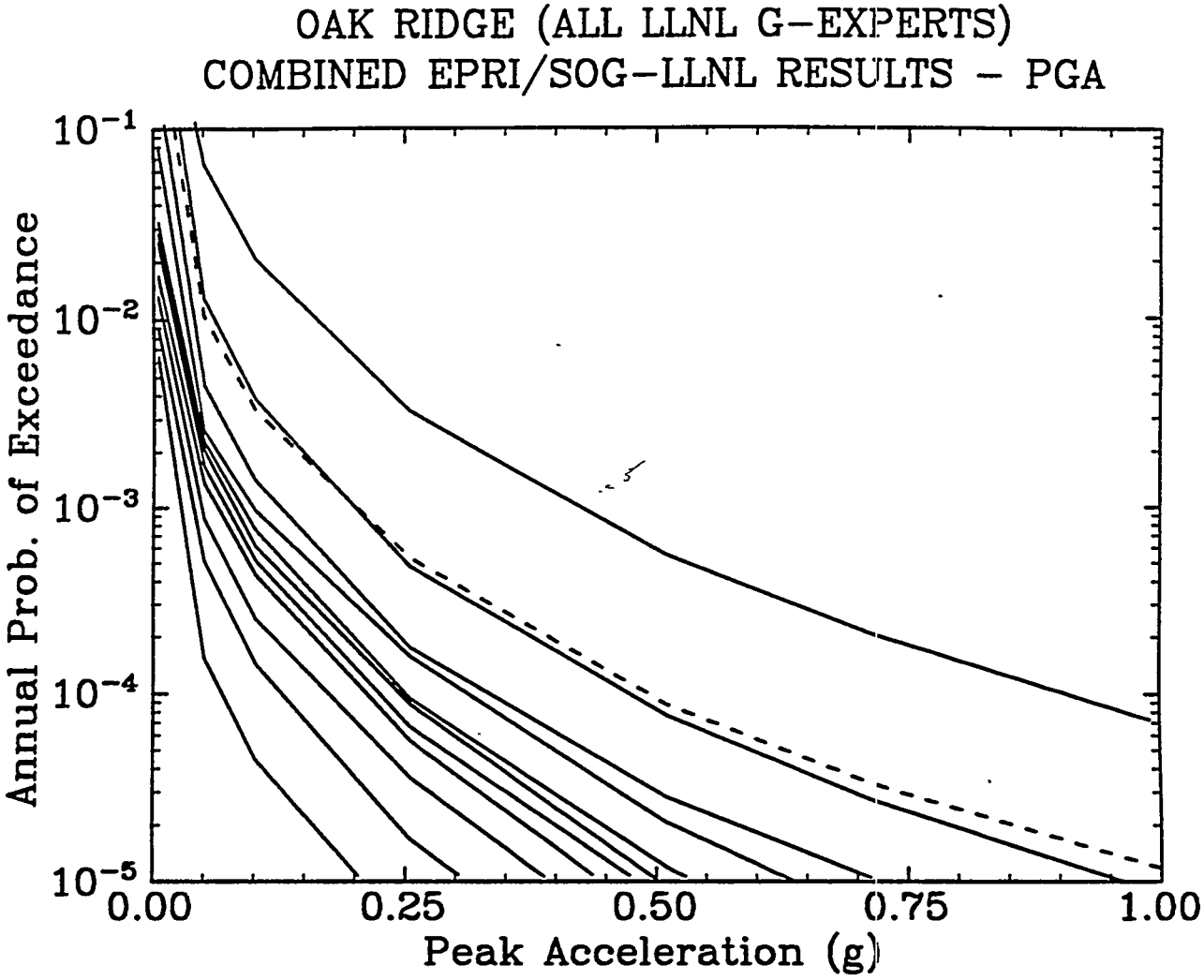

Figure 4-4. Peak-acceleration hazard curves for Oak Ridge obtained by combining results from the EPRI/SOG and LLNL (all ground-motion Experts) methodologies. The solid curves correspond to the following fractile hazard curves: 0.05 (bottom), 0.15, 0.25, 0.35, 0.45, 0.50, 0.55, 0.65, 0.75, 0.85, 0.95 (top); the dashed curve represents the mean hazard curve.

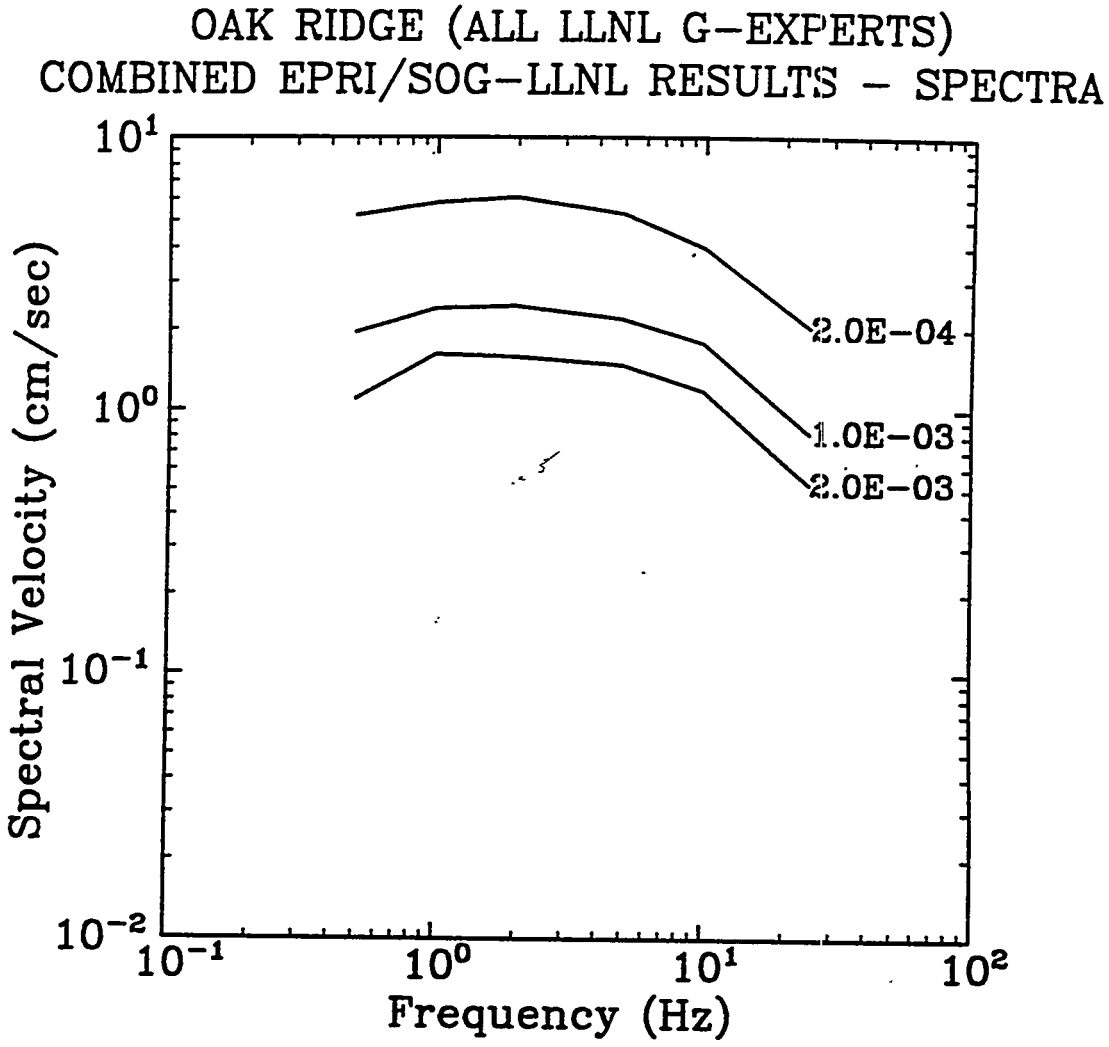

Figure 4-5. Median uniform-hazard spectra (5 % damping) for Oak Ridge obtained by combining results from the EPRI/SOG and LLNL (all ground-motion Experts) methodologies.

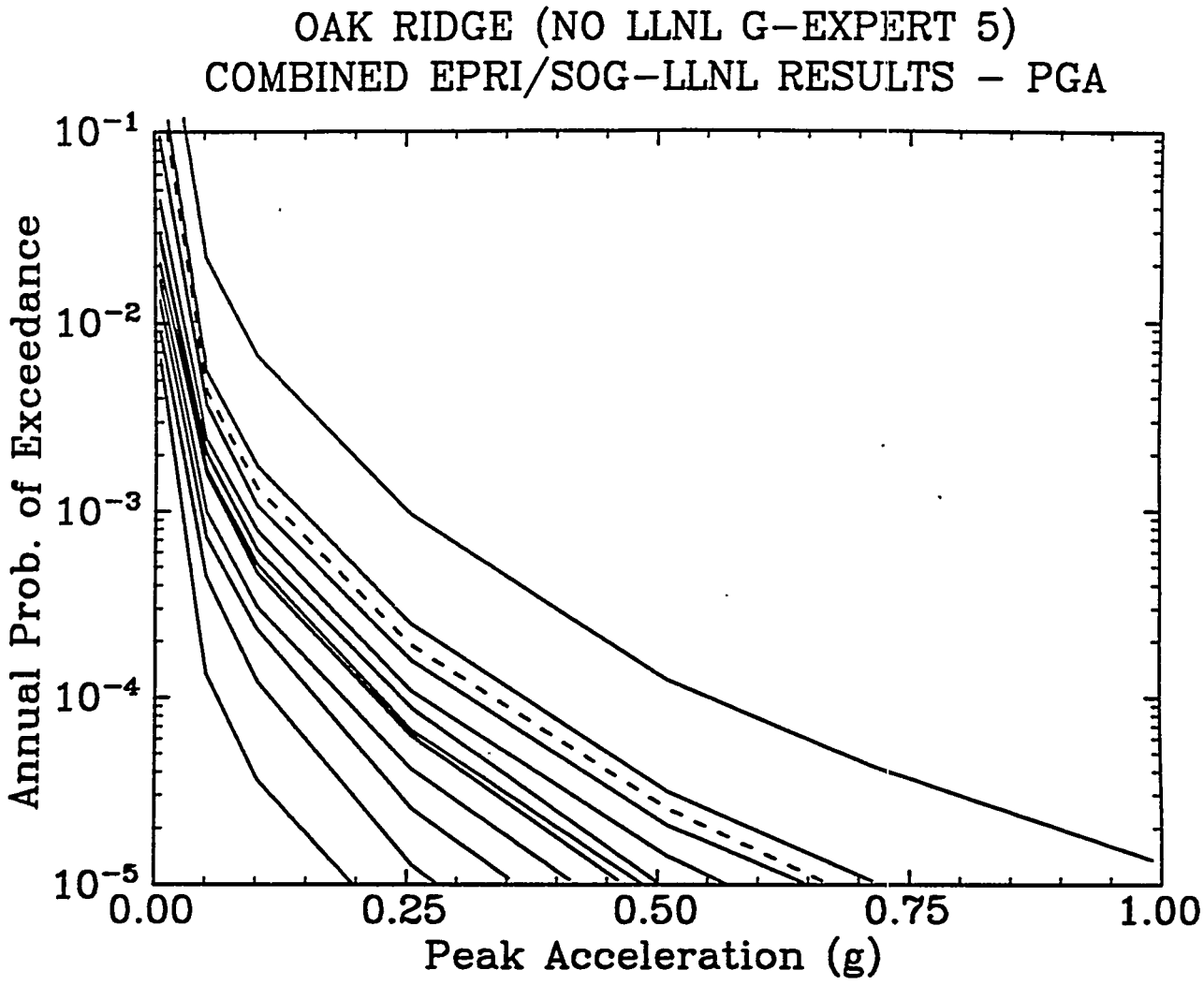

Figure 4-6. Peak-acceleration hazard curves for Oak Ridge obtained by combining results from the EPRI/SOG and LLNL (excluding ground-motion Expert 5) methodologies. The solid curves correspond to the following fractile hazard curves: 0.05 (bottom), 0.15, 0.25, 0.35, 0.45, 0.50, 0.55, 0.65, 0.75, 0.85, 0.95 (top); the dashed curve represents the mean hazard curve.

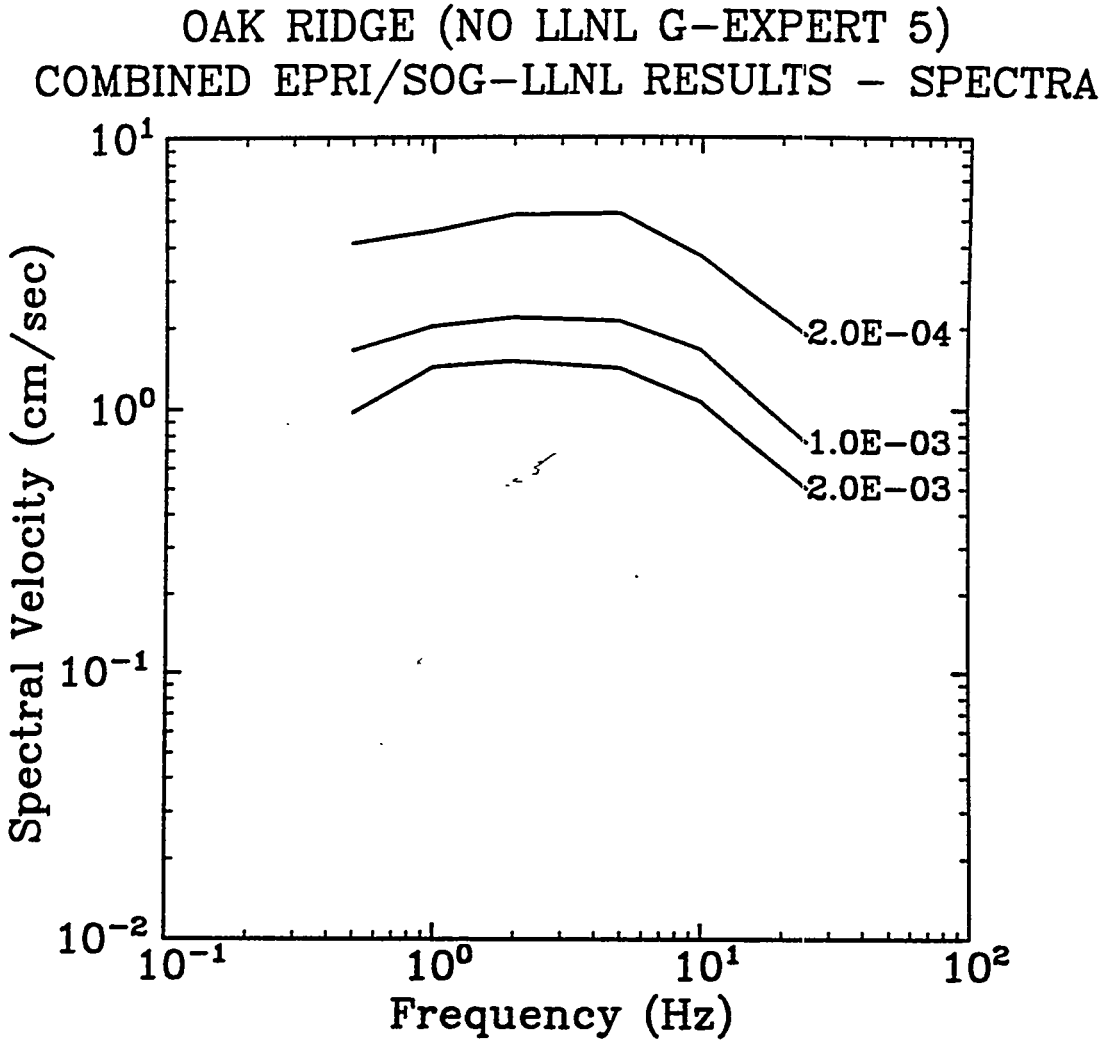

Figure 4-7. Median uniform-hazard spectra (5 % damping) for Oak Ridge obtained by combining results from the EPRI/SOG and LLNL (excluding ground-motion Expert 5) methodologies.

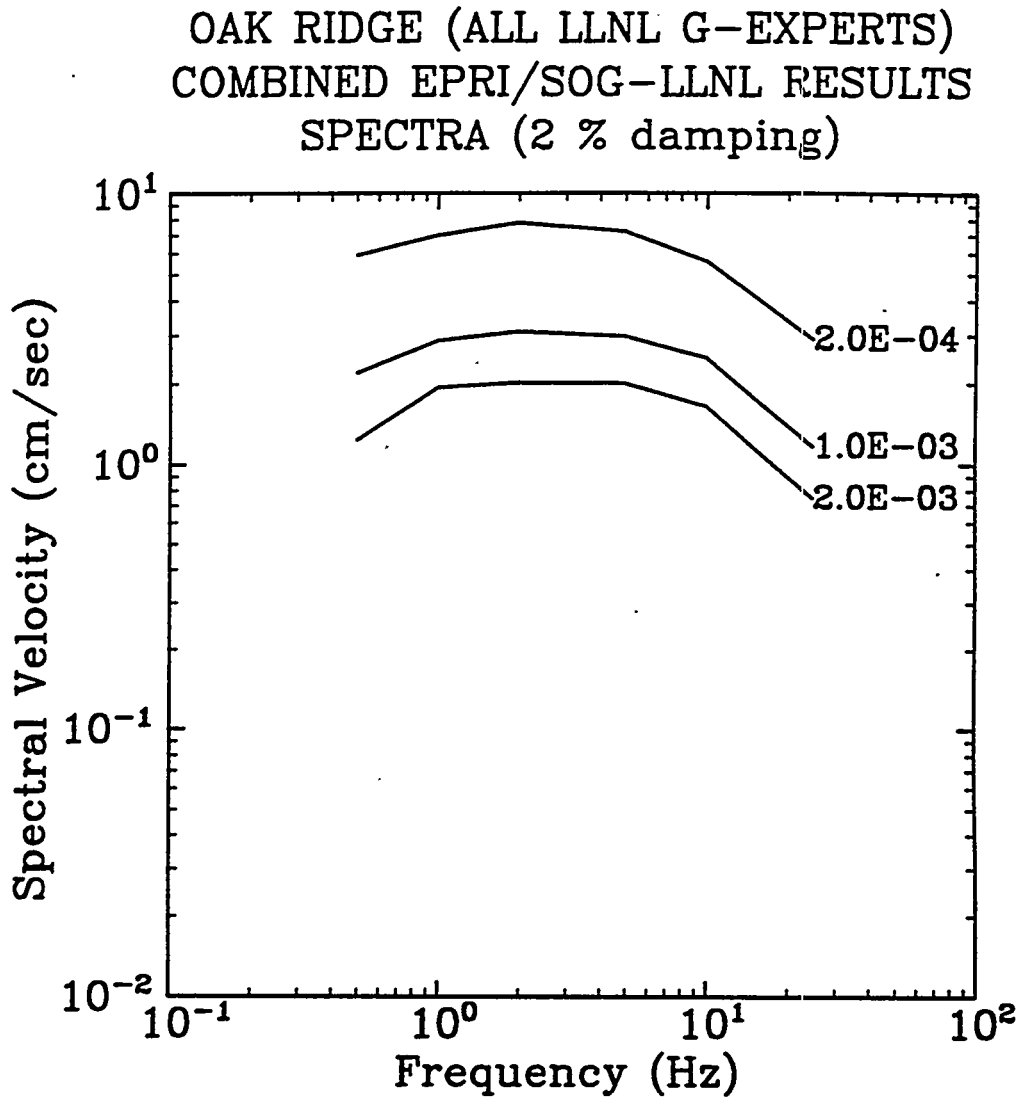

Figure 4-8. Median uniform-hazard spectra (2 % damping) for Oak Ridge obtained by combining results from the EPRI/SOG and LLNL (all ground-motion experts) methodologies.

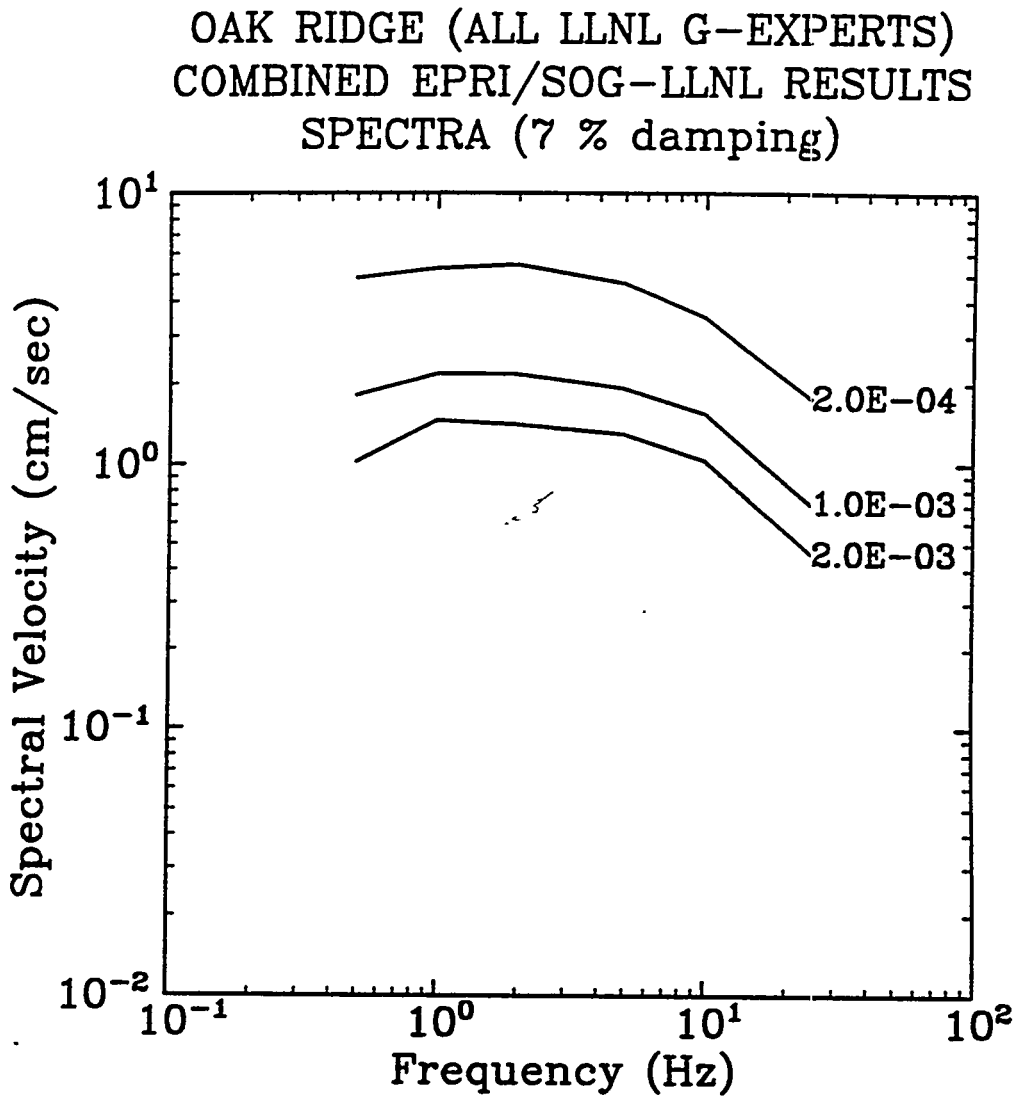

Figure 4-9. Median uniform-hazard spectra (7 % damping) for Oak Ridge obtained by combining results from the EPRI/SOG and LLNL (all ground-motion experts) methodologies.

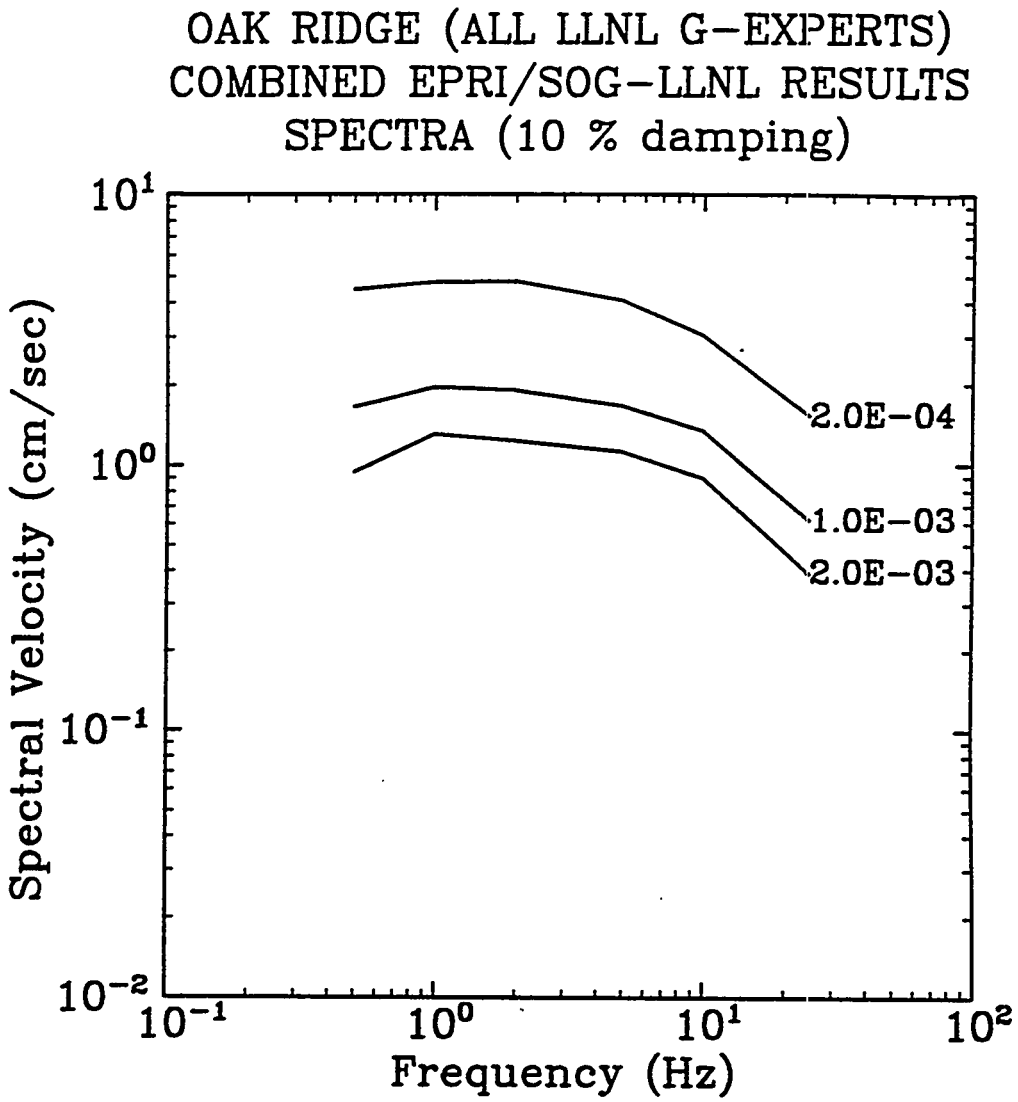

Figure 4-10. Median uniform-hazard spectra (10 % damping) for Oak Ridge obtained by combining results from the EPRI/SOG and LLNL (all ground-motion experts) methodologies.

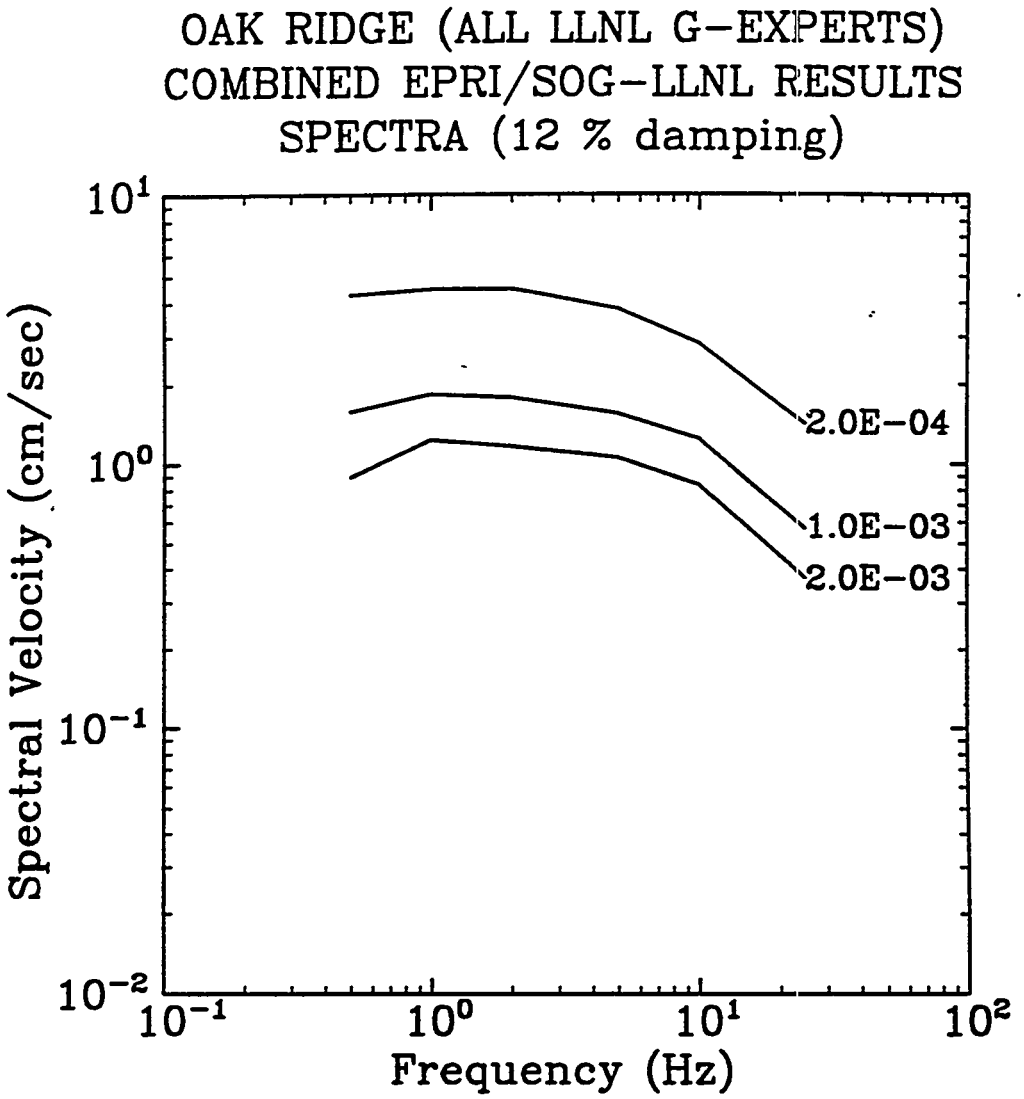

Figure 4-11. Median uniform-hazard spectra (12 % damping) for Oak Ridge obtained by combining results from the EPRI/SOG and LLNL (all ground-motion experts) methodologies.

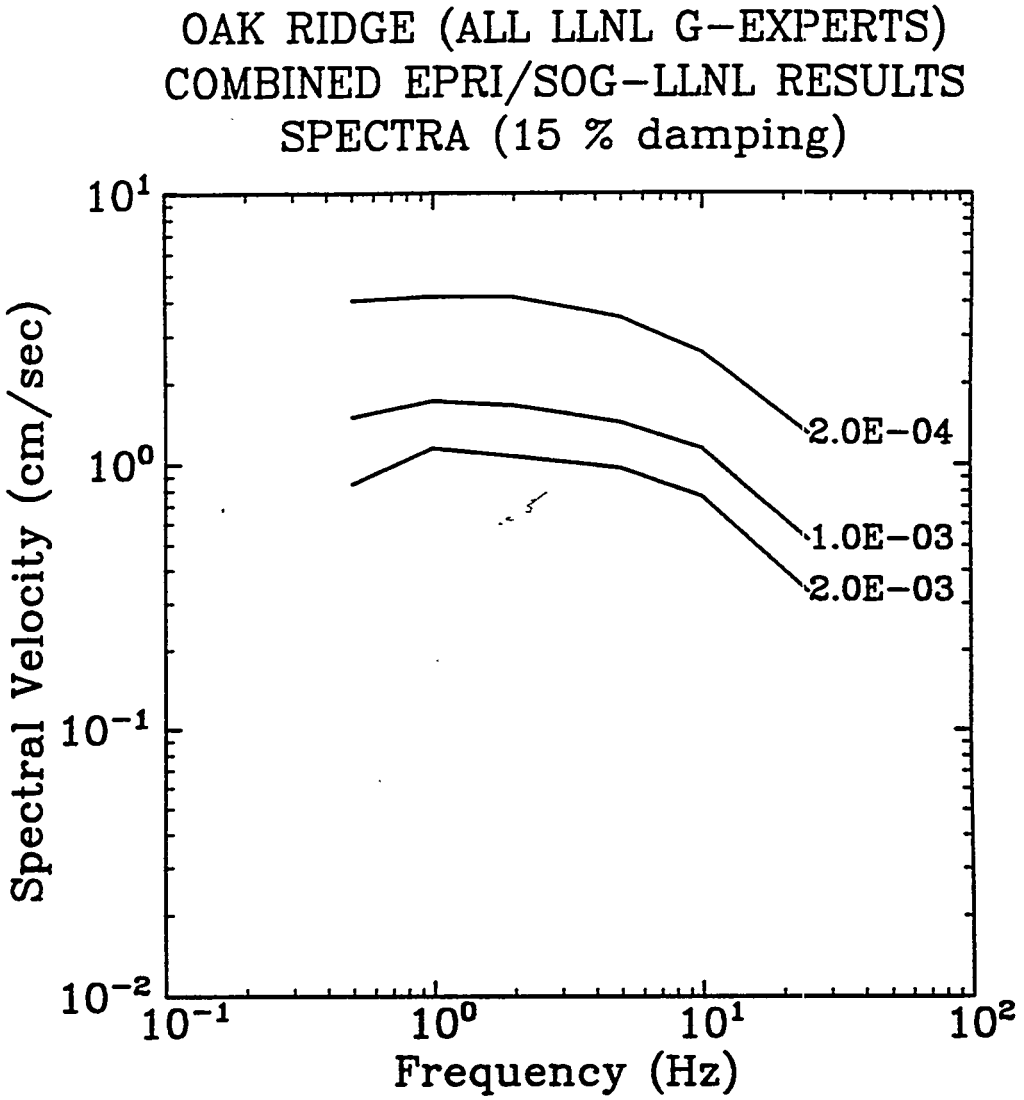

Figure 4-12. Median uniform-hazard spectra (15 % damping) for Oak Ridge obtained by combining results from the EPRI/SOG and LLNL (all ground-motion experts) methodologies.

Section 5

DEVELOPMENT OF SITE-SPECIFIC SPECTRA

5.1 INTRODUCTION

This Section documents the development of deterministic site-specific design spectra for the Oak Ridge site, using the EPRI/SOG and LLNL results presented in Sections 2 and 3, using the Department of Energy (DOE) interim procedure for use of these results (1).

Section 5.2 describes the DOE interim procedure and Section 5.3 documents the application of this procedure to the Oak Ridge site. Section 5.4 compares the resulting deterministic spectrum to spectra from recordings of representative earthquakes in eastern North America (ENA) and northwestern Canada.

5.2 PROCEDURE

The procedure specified DOE interim position (1) is intended to obtain a stable estimate of mean spectra associated with specified non-exceedance probabilities, using the EPRI/SOG and LLNL median results. This procedure consists of the following steps

1. Using the EPRI/SOG and LLNL median hazard curves for PGA and read the accelerations associated with the specified exceedance probability (e.g., 10^{-3} for moderate hazard facilities). Then, compute the geometric average of the two accelerations and multiply this quantity by 1.65 to obtain an estimate of the acceleration associated with the specified mean hazard.

2. Perform the same operation using the hazard curves for the maximum spectral velocity (MSV; in the 1 to 5 Hz range), to obtain the maximum spectral velocity associated with the specified mean hazard.

3. At the exceedance probability of interest (p), calculate the dominant magnitudes and distances for PGA and for MSV. These magnitudes and distances are denoted $M_{PGA,p}$-$R_{PGA,p}$ and $M_{MSV,p}$-$R_{MSV,p}$.

4. Calculate the deterministic response spectral shapes associated with the two magnitude-distance pairs obtained in step 3.

5. Scale the two deterministic spectral shapes to the corresponding PGA and spectral velocity calculated in steps 1 and 2 above. That is, scale the spectral shape associated with $M_{PGA,p}$-$R_{PGA,p}$ to the PGA obtained in step 1 and scale the spectral shape associated with $M_{MSV,p}$-$R_{MSV,p}$ to the MSV obtained in step 2.

6. Envelope the two scaled spectra obtained in step 5 above to create a single response spectrum.

5.3 APPLICATION

We use the hazard results in Sections 2 and 3 to obtain the design spectrum for rock conditions. We consider three values of the annual exceedance probability: 2×10^{-3}, 10^{-3}, and 2×10^{-4} (corresponding to average return periods of 500, 1000, and 5000 years).

Based on the spectra in Figures 2–26 and 3–13, we select the spectral velocity at 2.5 Hz as the maximum spectral velocity. Table 5–1 shows the calculation of design values for PGA and for 2.5 Hz spectral velocity.

Table 5-1

Calculation of Design Values (PGA and 2.5 Hz PSV)

Exceedance Probability	Ground-Motion Measure	EPRI	LLNL	Geometric Mean	×1.65
2×10^{-3}	PGA (cm/sec^2)	41.4	69.2	53.5	88.3
	2.5-Hz PSV (cm/sec)	1.29	3.39	2.09	3.45
10^{-3}	PGA (cm/sec^2)	66.7	99.0	81.3	134.1
	2.5-Hz PSV (cm/sec)	1.93	4.82	3.05	5.03
2×10^{-4}	PGA (cm/sec^2)	153.5	210.0	179.5	296.2
	2.5-Hz PSV (cm/sec)	4.86	10.00	6.97	11.50

The dominant magnitudes and distances associated with peak acceleration are calculated using the mean magnitude and the geometric-mean distance, i.e.,

$$\overline{M}_p = \frac{\sum_k w_k \left[\sum_i \nu_i \iint m P[Y > y_p | m,r] \, f_{M(i)}(m) \, f_{R(i)}(r) \, dm \, dr \right]_k}{\sum_k w_k \left[\sum_i \nu_i \iint P[Y > y_p | m,r] \, f_{M(i)}(m) \, f_{R(i)}(r) \, dm \, dr \right]_k} \qquad (5-1)$$

$$\ln(\overline{R}_p) = \frac{\sum_k w_k \left[\sum_i \nu_i \iint \ln(r) P[Y > y_p | m,r] \, f_{M(i)}(m) \, f_{R(i)}(r) \, dm \, dr \right]_k}{\sum_k w_k \left[\sum_i \nu_i \iint P[Y > y_p | m,r] \, f_{M(i)}(m) \, f_{R(i)}(r) \, dm \, dr \right]_k} \qquad (5-2)$$

where $\sum_k$ indicates summation over all branches of the logic tree of uncertain parameters and assumptions and w_k is the weight associated with branch k. y_p is the ground-motion amplitude associated with a mean exceedance probability p. $\sum_i$ indicates summation over all seismic sources. $P[y_p > y|m,r]$ represents the attenuation function for the ground-motion measure of interest, and $f_{M(i)}(m)$ and $f_{R(i)}(r)$ represent the distributions of earthquake magnitude and distance in source i. The attenuation function, the activity rate ν_i, and the distributions of magnitude and distance are different for the different branches of the logic tree.

We calculate the dominant magnitudes and distances using the EPRI/SOG seismicity models and attenuation functions used in Section 2 and considering 2.5-Hz spectral velocity and PGA. Results are presented in Figures 5–1 through 5–8 as functions of ground-motion amplitude and of mean exceedance probability. The dominant magnitudes and distances for the three probabilities of interest are shown in Table 5–2.

Figures 5–1 through 5–8 and Table 5–2 indicate that moderate magnitudes (m_b 5.6 to 6.1) at distances shorter than 100 km dominate seismic hazard at Oak Ridge for annual exceedance probabilities of 2×10^{-3} to 2×10^{-4}. This is typical of a moderate-seismicity CEUS site located several hundred miles from New Madrid and Charleston.

Because there are very few records from ENA earthquakes at the appropriate magnitudes and distances, we use the attenuation functions of McGuire et al. (2) to construct the spectral shapes. These attenuation functions represent the mean attenuation functions in both the EPRI/SOG and LLNL methodologies.

For each magnitude-distance combination in Table 5–2, we use the McGuire et al. (2) to predict PGA and spectral velocities at multiple frequencies. These predictions are used to

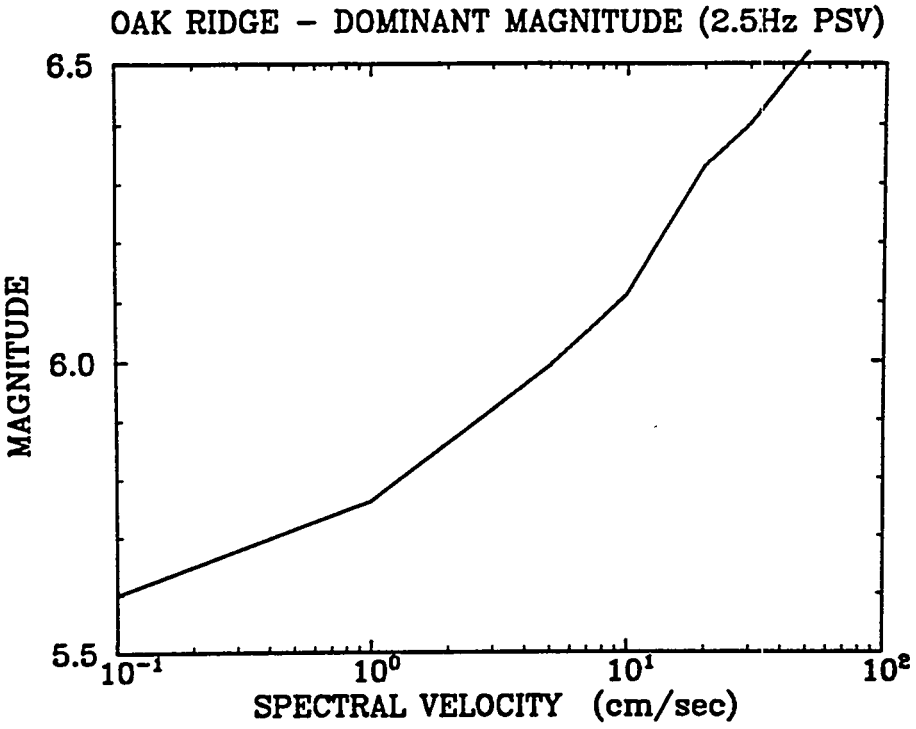

Figure 5-1. Magnitude of earthquakes that dominate the hazard for 2.5-Hz spectral velocity. Results shown as a function of amplitude.

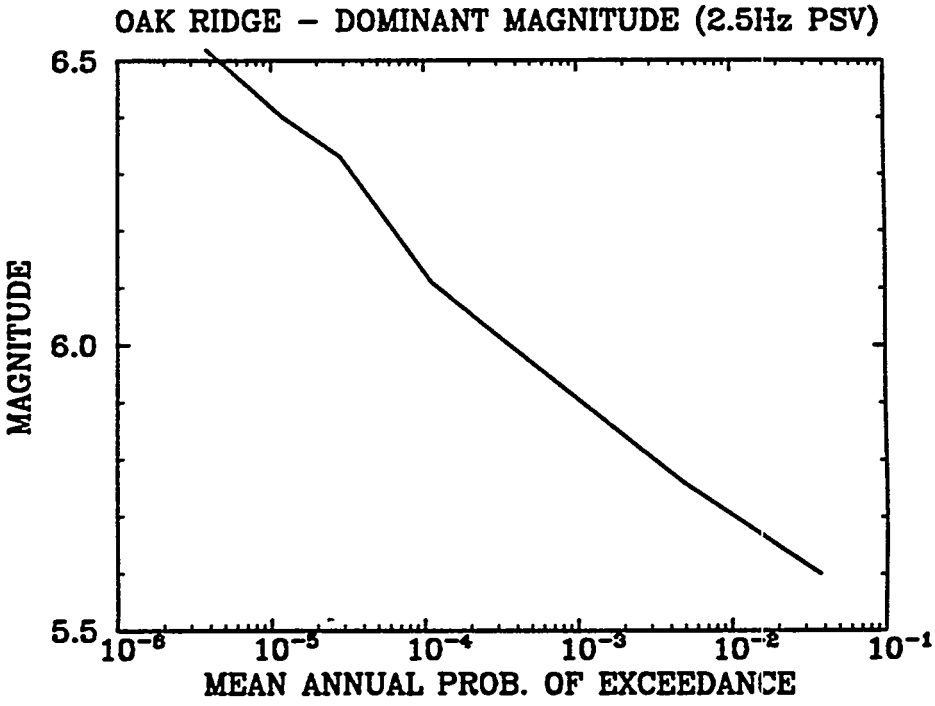

Figure 5-2. Magnitude of earthquakes that dominate the hazard for 2.5-Hz spectral velocity. Results shown as a function of mean hazard.

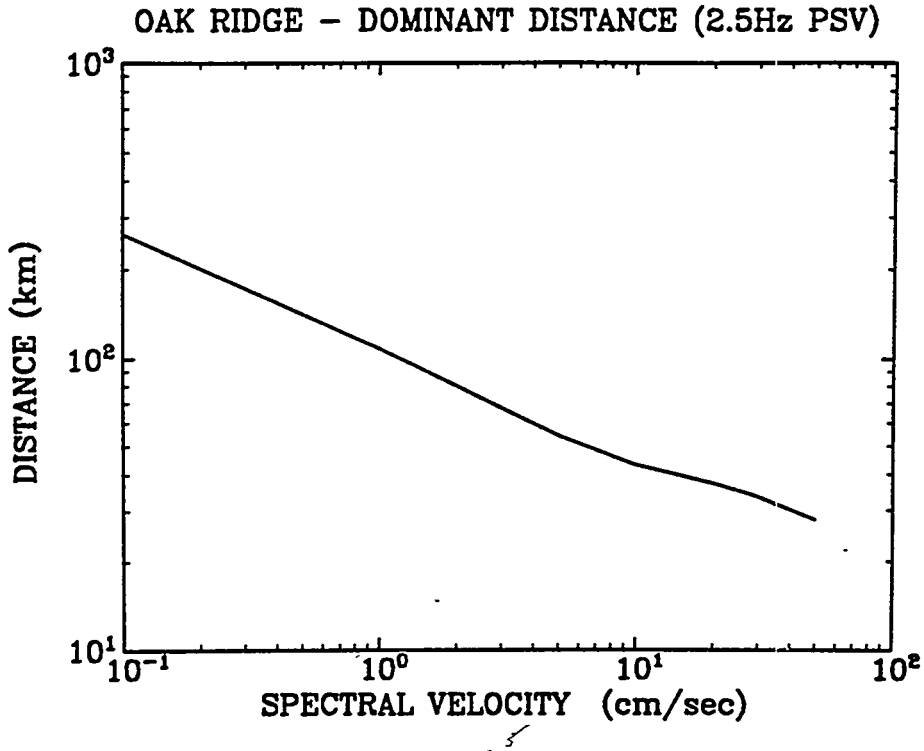

Figure 5-3. Distance of earthquakes that dominate the hazard for 2.5-Hz spectral velocity. Results shown as a function of amplitude.

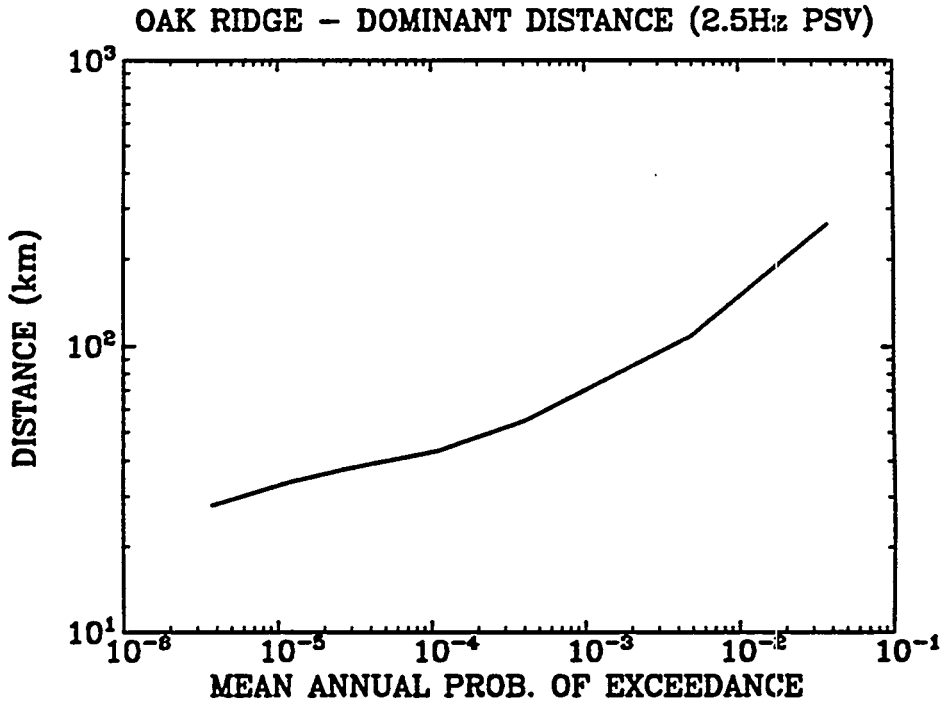

Figure 5-4. Distance of earthquakes that dominate the hazard for 2.5-Hz spectral velocity. Results shown as a function of mean hazard.

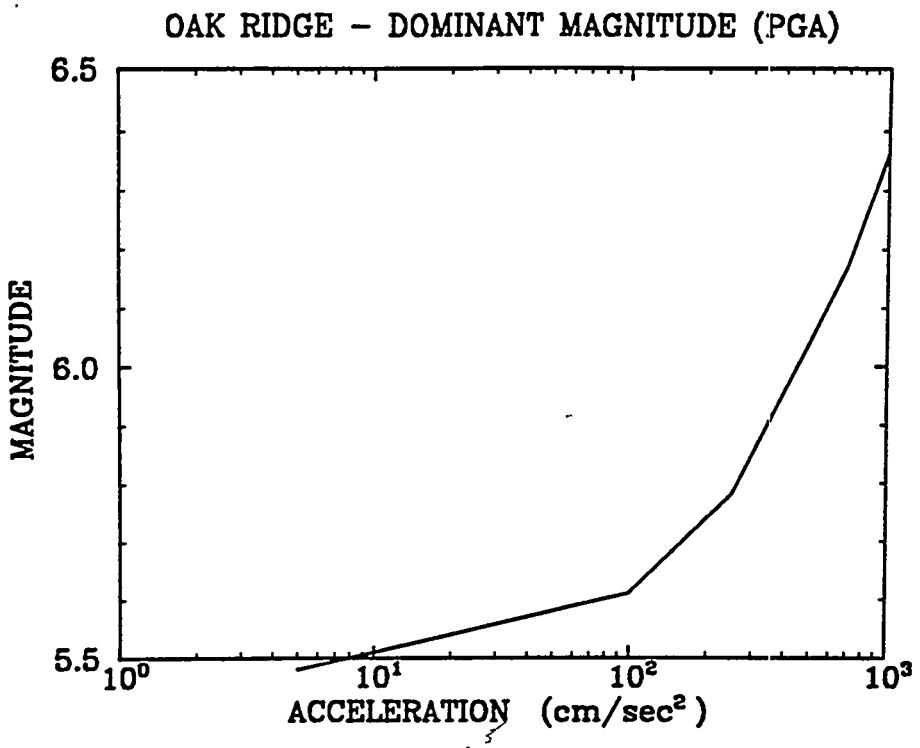

Figure 5-5. Magnitude of earthquakes that dominate the hazard for peak acceleration. Results shown as a function of amplitude.

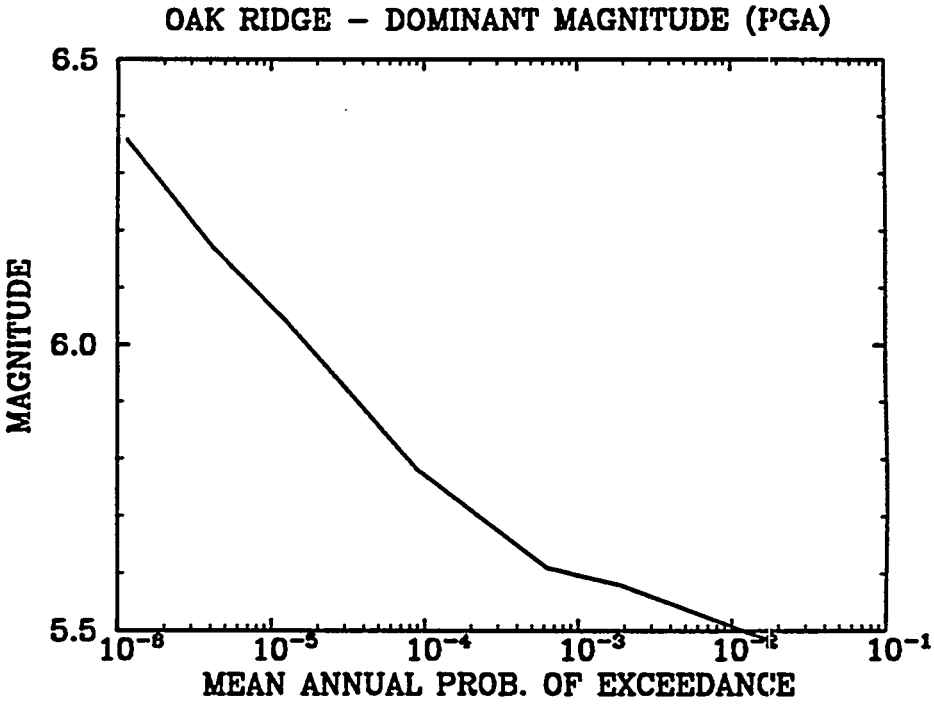

Figure 5-6. Magnitude of earthquakes that dominate the hazard for peak acceleration. Results shown as a function of mean hazard.

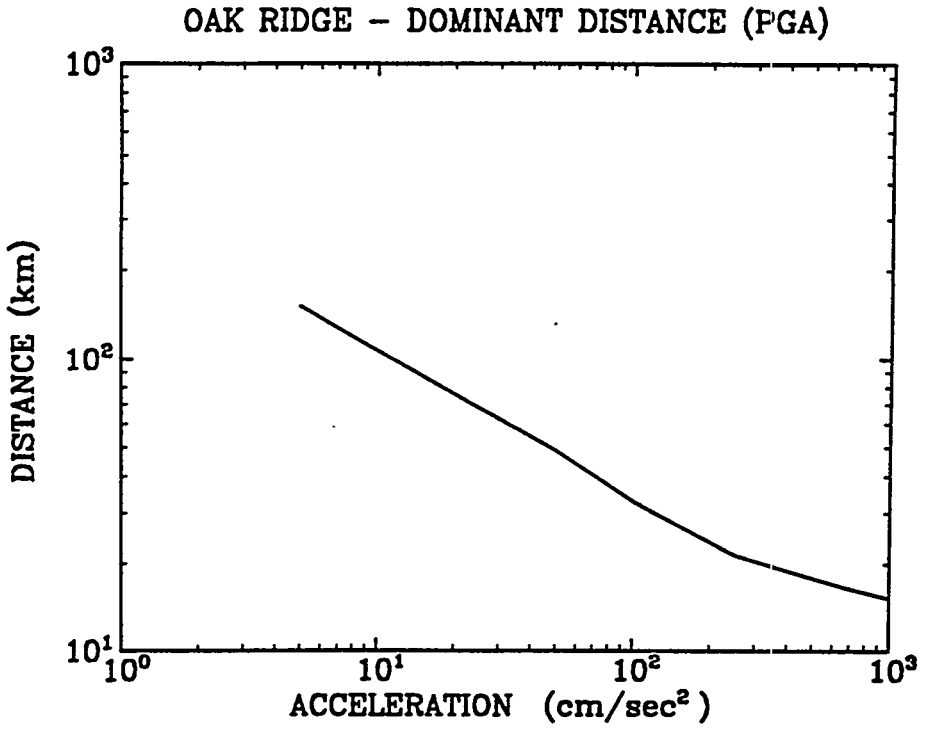

Figure 5-7. Distance of earthquakes that dominate the hazard for peak acceleration. Results shown as a function of amplitude.

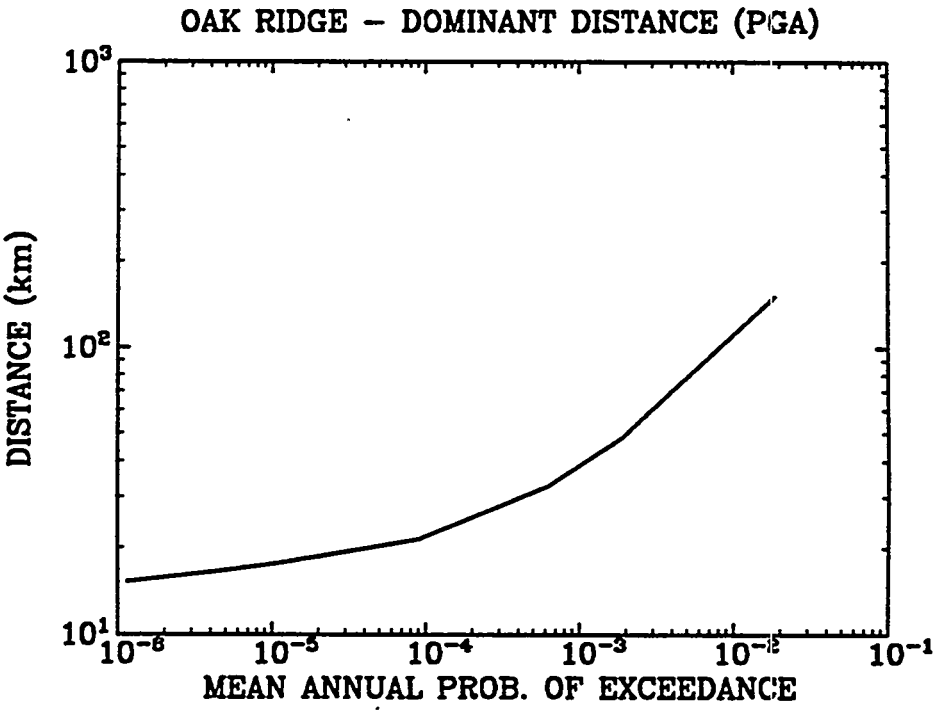

Figure 5-8. Distance of earthquakes that dominate the hazard for peak acceleration. Results shown as a function of mean hazard.

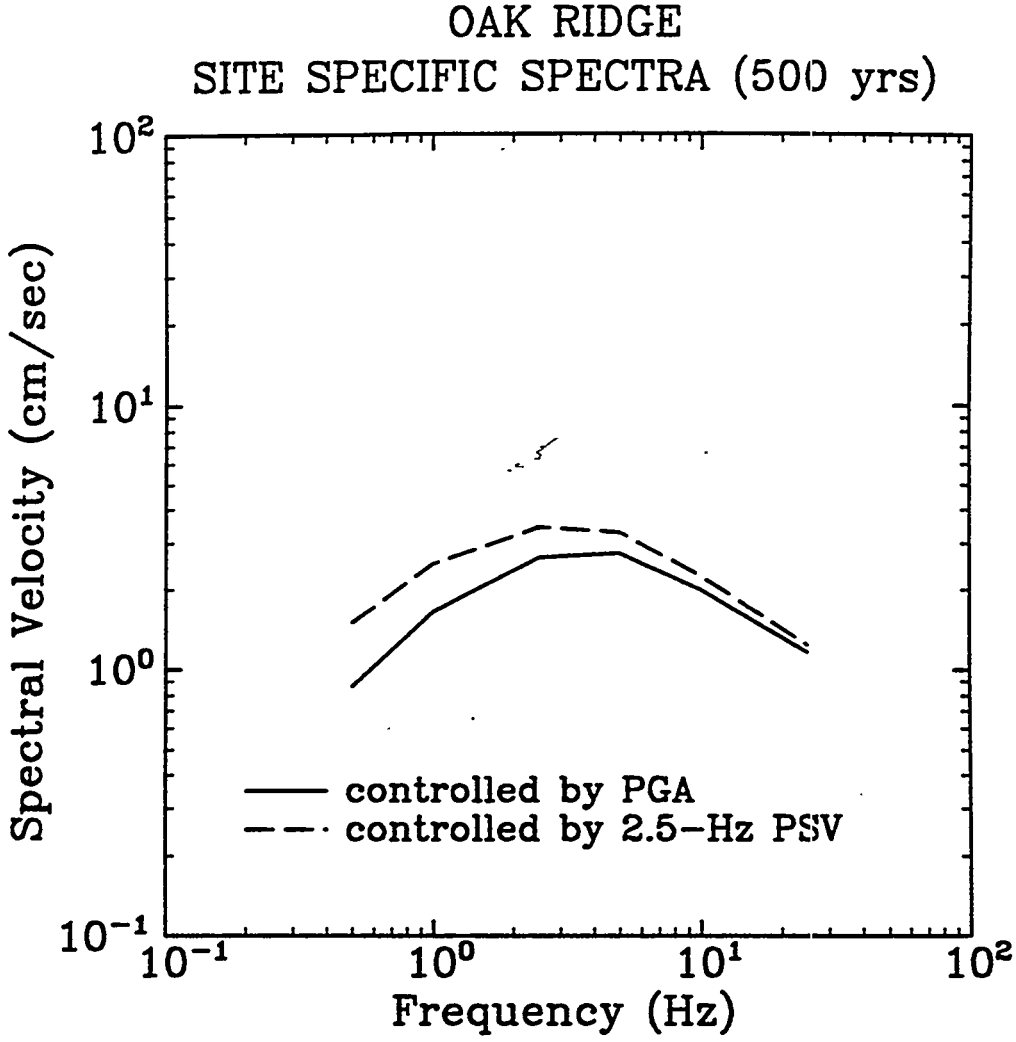

Figure 5-9. Construction of design spectra for 2×10^{-3} annual exceedance probability.

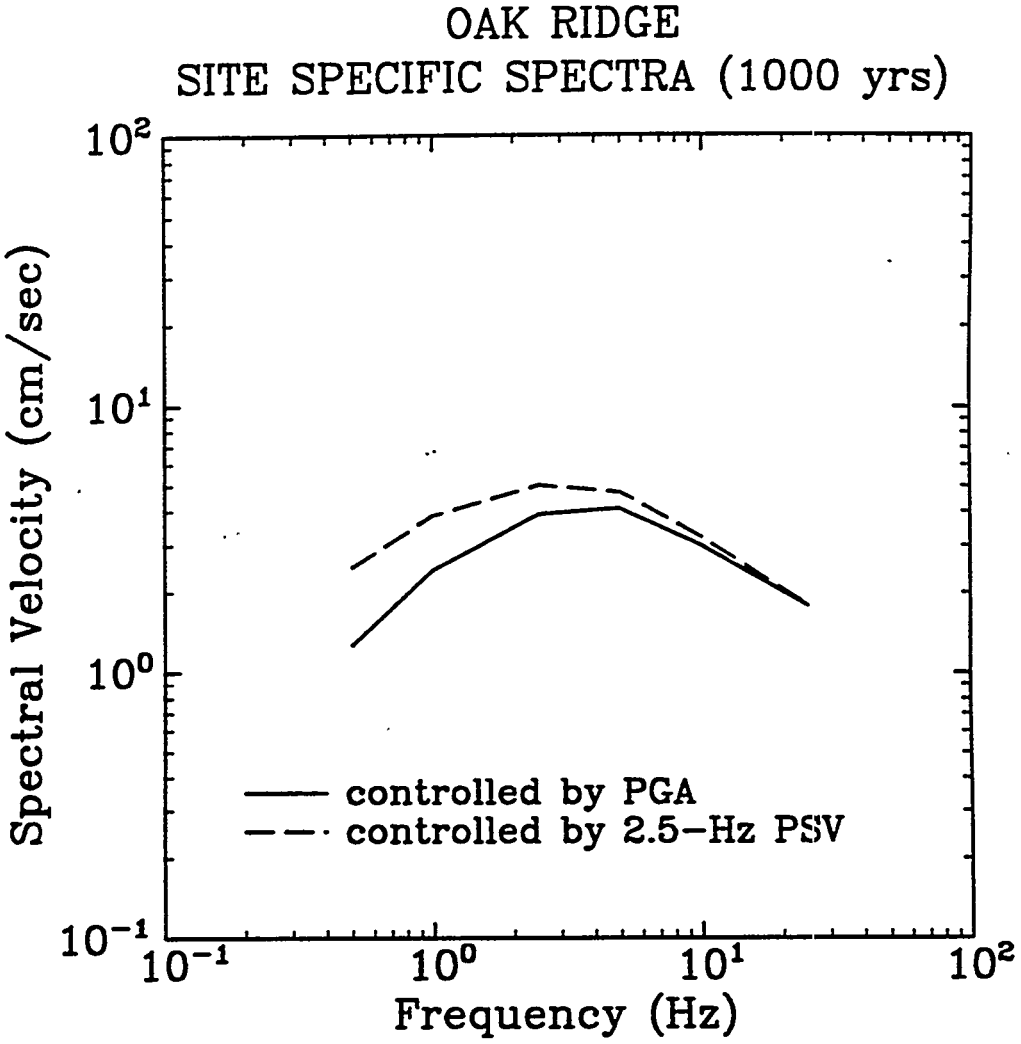

Figure 5-10. Construction of design spectra for 1×10^{-3} annual exceedance probability.

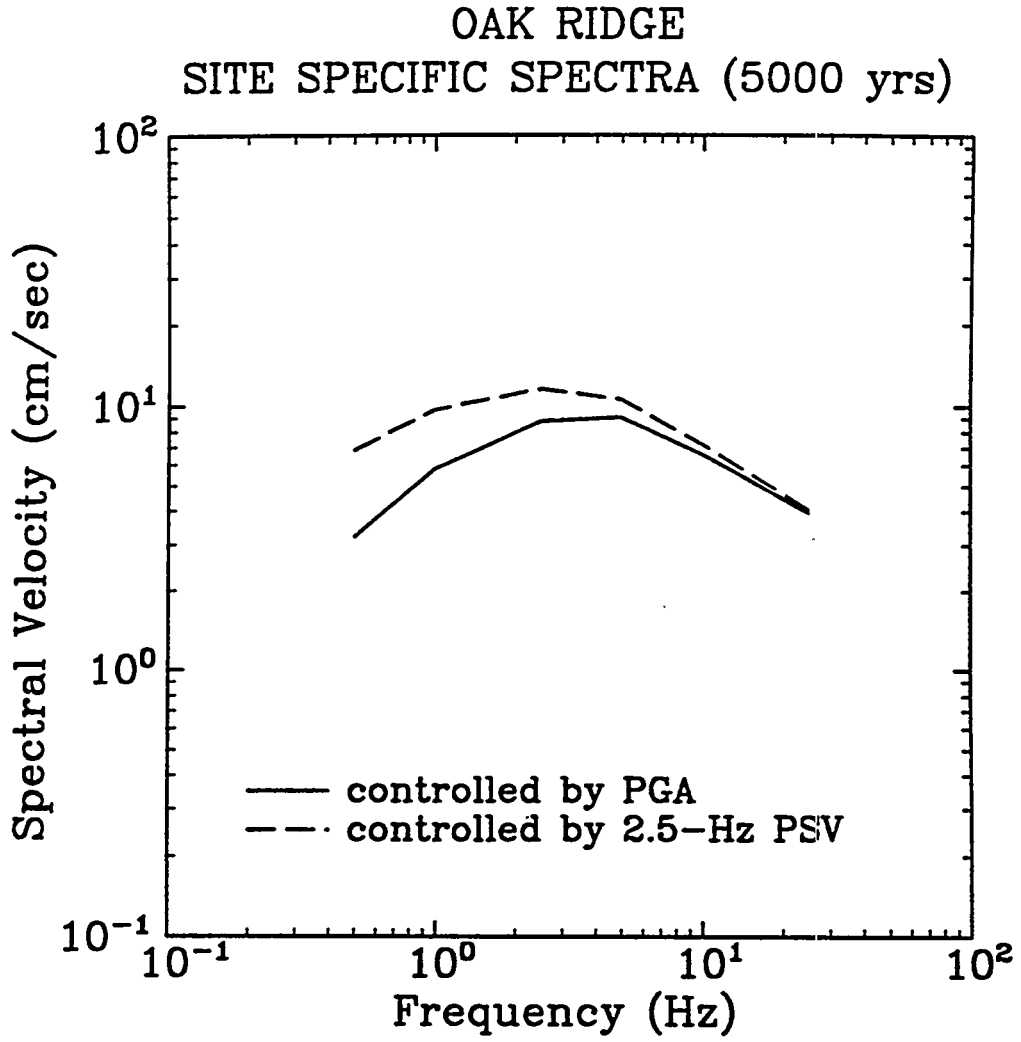

Figure 5-11. Construction of design spectra for 2×10^{-4} annual exceedance probability.

Table 5-2

Dominant Magnitudes and Distances

Exceedance Probability	Ground-Motion Measure	M_p	R_p (km)
2×10^{-3}	PGA (cm/sec^2)	5.6	50.
	2.5-Hz PSV (cm/sec)	5.8	85.
10^{-3}	PGA (cm/sec^2)	5.6	38.
	2.5-Hz PSV (cm/sec)	5.9	70.
2×10^{-4}	PGA (cm/sec^2)	5.7	25.
	2.5-Hz PSV (cm/sec)	6.1	47.

define a spectral shape, which is then scaled to the PGAs and 2.5-Hz spectral velocities in Table 5–1. Table 5–3 shows the original, scaled, and envelope spectra. Figures 5–9 through 5–11 show the scaled spectra for the three probabilities of interest.

Table 5–3 indicates that large scaling factors are required in order to bring the spectra associated with the dominant magnitudes and distances to the desired amplitudes. This is especially true for the spectrum controlled by 2.5-Hz spectral velocity. This suggests that the dominant magnitudes and distances, as computed here, are not appropriate for the definition of "scenario earthquakes" to use as design events. These dominant magnitudes and distances are appropriate, however, for the definition of spectral shapes.

Table 5–3 and Figures 5–9 through 5–11 show that the maximum spectral velocity controls the design spectrum at all frequencies, and for PGA. This suggests that the composite estimate of 2.5-Hz spectral velocity is conservative, perhaps due to the use of Western U.S. spectral shapes by several LLNL ground-motion experts.

We also investigate three alternative procedures for the calculation of design spectrum. These procedures are as follows:

1. Construct the envelope of the unscaled spectra for (M_{PGA}, R_{PGA}) and (M_{PSV}, R_{PSV}), then scale the resulting spectrum to the design PGA in table 5–1.

Table 5-3

Calculation of Site-Specific Spectra

Exceedance Probability	Frequency (Hz)	PGA controlled Spectra		PSV(2.5) controlled Spectra		Envelope
		Unscaled	Scaled	Unscaled	Scaled	
2×10^{-3}	0.5	0.54	0.87	0.53	1.51	1.51
	1.0	1.03	1.66	0.87	2.51	2.51
	2.5	1.65	2.65	1.20	3.45	3.45
	5.0	1.72	2.76	1.15	3.31	3.31
	10.0	1.25	2.01	0.79	2.27	2.27
	25.0	0.73	1.17	0.43	1.24	1.24
	PGA (cm/sec^2)	55.0	88.3	33.7	96.5	96.5
10^{-3}	0.5	0.72	1.27	0.87	2.49	2.49
	1.0	1.39	2.43	1.35	3.87	3.87
	2.5	2.24	3.92	1.76	5.03	5.03
	5.0	2.35	4.12	1.66	4.74	4.74
	10.0	1.72	3.02	1.13	3.24	3.24
	25.0	1.02	1.78	0.63	1.79	1.79
	PGA (cm/sec^2)	76.5	134.0	48.4	138.4	138.4
2×10^{-3}	0.5	1.48	3.22	2.00	6.85	6.85
	1.0	2.68	5.81	2.83	9.70	9.70
	2.5	4.07	8.84	3.38	11.60	11.60
	5.0	4.19	9.10	3.10	10.62	10.62
	10.0	3.06	6.64	2.10	7.22	7.22
	25.0	1.83	3.97	1.19	4.08	4.08
	PGA (cm/sec^2)	136.5	296.2	90.7	311.3	311.3

Units: spectral velocity, cm/sec; PGA, cm/sec^2.

2. Scale the spectra for (M_{PGA}, R_{PGA}) and (M_{PSV}, R_{PSV}) to the design PGA in Table 5–1, then construct the envelope.

3. Scale the EPRI median uniform-hazard spectrum to the design PGA in Table 5–1.

Figure 5–12 shows the spectra obtained using these alternative procedures for a return period of 1000 years and compares them to the procedure specified in (1) and adopted here. The three alternative procedures result in spectra that are similar to or lower than the adopted spectrum, particularly at low frequencies.

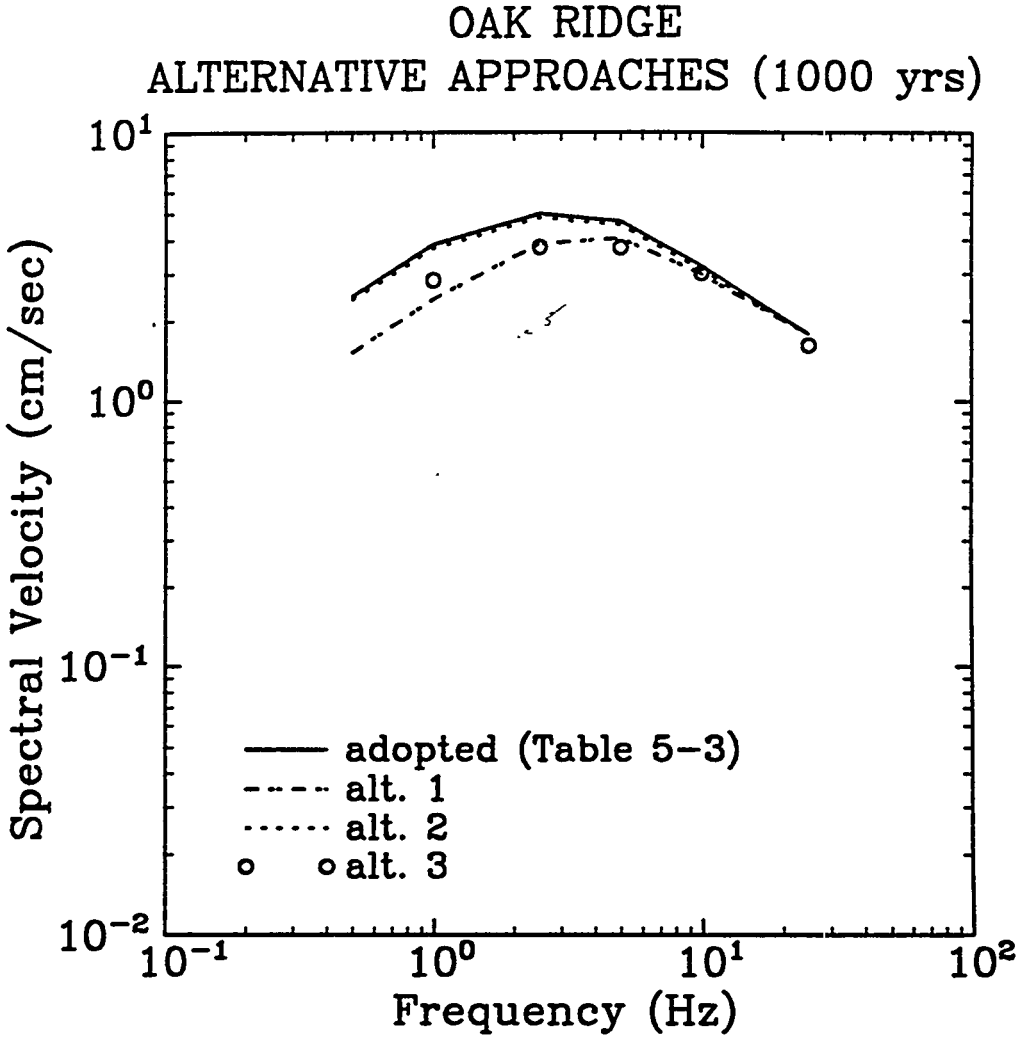

Figure 5-12. Design spectra obtained using alternative procedures; 10^{-3} exceedance probability. See text for description of the various procedures.

We adopt the design spectrum obtained through the procedure in (1), but we note that this procedure may imply additional conservatism at low frequencies, due to the use of Western U.S. spectral shapes by several LLNL ground-motion experts.

5.4 COMPARISON TO SPECTRA FROM RELEVANT RECORDINGS

Even though there are not enough earthquake records from ENA earthquakes with magnitudes and distances near the dominant magnitudes and distances of interest, it is useful to compare the spectral shapes obtained from attenuation functions to the spectra from actual records.

We selected records from ENA and the Nahanni (NWT, Canada) region, with magnitudes and distances near the dominant magnitudes and distances for PGA and 2.5-Hz spectral velocity, for 10^{-3} exceedance probability. Because of the paucity of records available, the selected magnitudes and distances vary over relatively wide ranges. Table 5–4 lists the records used for these comparisons. The spectra from these records are displayed in Appendix B.

Table 5-4

Records Selected for Comparison of Spectral Shapes

Dominant Magnitude and Distance for PGA

Event	Date	m_{Lg}	Station	Distance (km)
N.E. Ohio	01/31/86	5.3	Perry, basement	18
Nahanni, NWT	12/23/85a	5.4	Station 01	16
Nahanni, NWT	12/25/85	5.7	Station 01	24
Nahanni, NWT	12/25/85	5.7	Station 02	24
Nahanni, NWT	12/25/85a	5.4	Station 01	26
Nahanni, NWT	02/13/86	5.4	Station 01	14
Nahanni, NWT	02/13/86	5.4	Station 02	15

Dominant Magnitude and Distance for 2.5-Hz PSV

Event	Date	m_{Lg}	Station	Distance (km)
Nahanni, NWT	12/23/85	6.5	Station 01	22.0
Saguenay, Que	11/25/88	6.5	Station 16	43.0
Saguenay, Que	11/25/88	6.5	Station 17	63.6
Saguenay, Que	11/25/88	6.5	Station 20	90.4
Saguenay, Que	11/25/88	6.5	Station 08	93.0

Records representative of the dominant magnitude and distance for PGA were scaled to the design PGA in Table 5–1 (134.1 cm/sec^2). Similarly, records representative of the dominant

magnitude and distance for 2.5-Hz spectral velocity were scaled to the design PSV in Table 5–1 (5.03 cm/sec). Figures 5–13 and 5–14 show the fractile spectra calculated from the two sets of records, and compare them to the spectral shapes predicted by the McGuire et al. (2) attenuation functions (scaled to the same amplitudes). These figures show consistency between the spectral shapes from actual records and the shapes predicted by the attenuation functions.

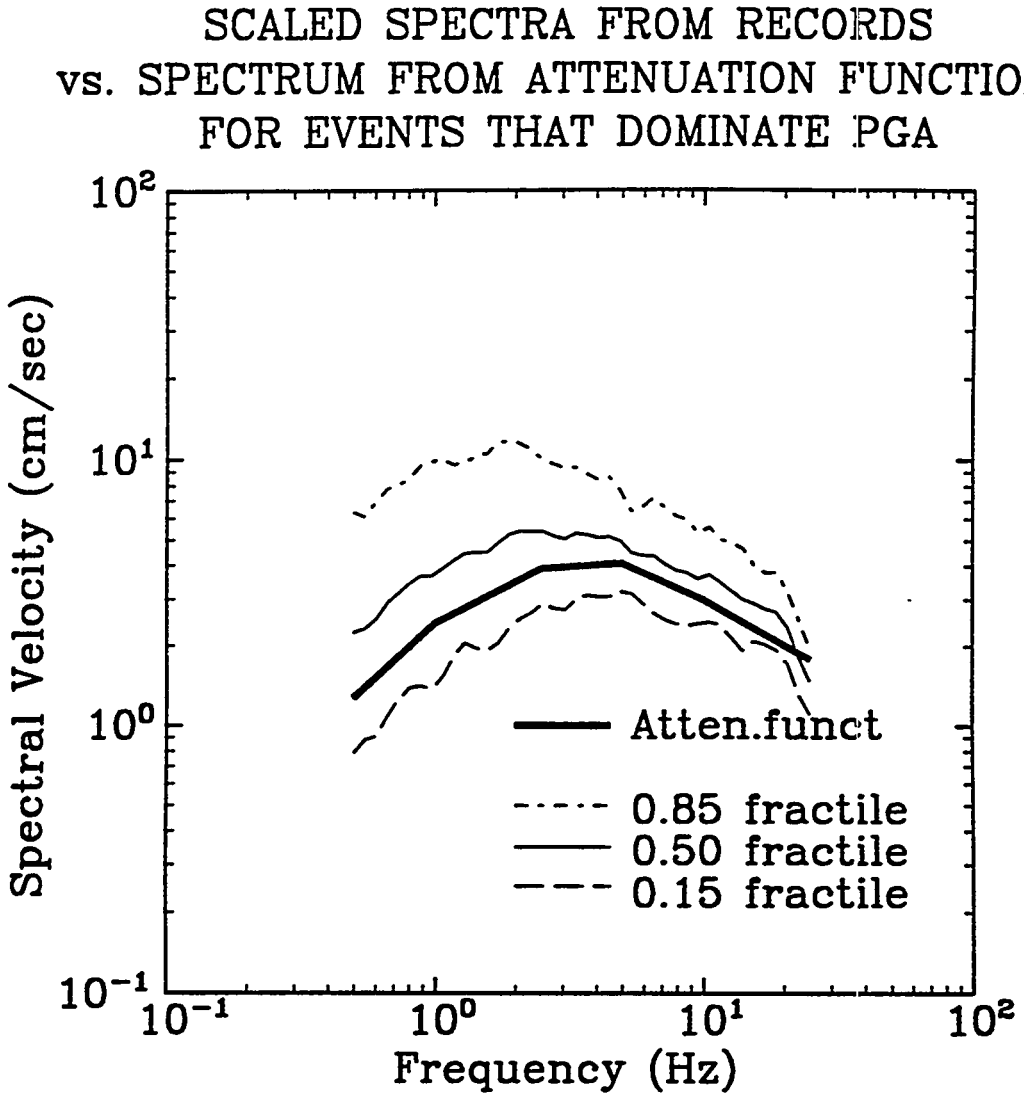

Figure 5-13. Spectra from events representative of the magnitudes and distances that dominate PGA: summary statistics are compared to the shape predicted by the McGuire et al. attenuation functions

Comparing the median spectra in Figures 5–13 and 5–14, one notices that the ratio of low-frequency to high-frequency PSV is higher for the records representative of the magnitudes and distances that dominate PGA, even though these records have lower magnitudes. This observation is contrary to our understanding of seismic-source scaling, but is not unexpected or significant–given the small number of events considered in these comparisons.

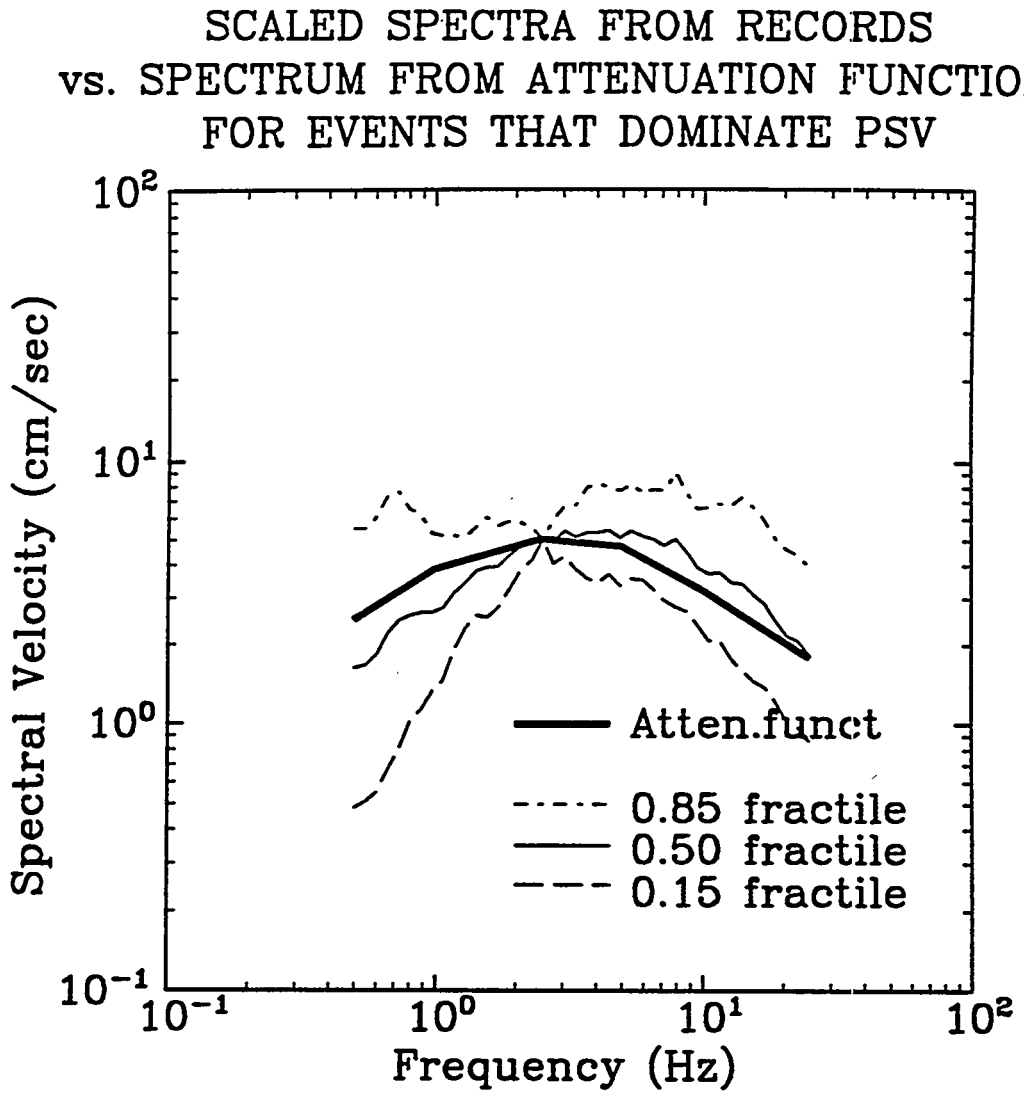

Figure 5-14. Spectra from events representative of the magnitudes and distances that dominate 1.5-Hz PSV: summary statistics are compared to the shape predicted by the McGuire et al. attenuation functions

5.5 SUMMARY AND CONCLUSIONS

This Section has documented the calculation of site-specific design spectra for Oak Ridge using the Department of Energy interim procedure for use of the EPRI/SOG and LLNL (1). Attenuation functions, rather than actual records, were used to generate the spectral shapes. Comparison to the spectra from actual records indicate that the spectral shapes obtained from the attenuation functions are adequate.

5.6 REFERENCES

1. Department of Energy Seismic Working Group. Use of LLNL and EPRI Probabilistic Seismic Hazard Curves: Interim Position. Attachment to Memorandum of W.H. Young to Program Secretarial Officers, dated March 19, 1992. U.S. Department of Energy, 1992.

2. R. K. McGuire, G. R. Toro, and W. J. Silva. *Engineering Model of Earthquake Ground Motion for Eastern North America.* Technical Report NP-6074, Electric Power Research Institute, 1988.

Section 6

CHARACTERISTICS OF CONTROLLING GROUND MOTIONS

6.1 INTRODUCTION

In this Section, we calculate horizontal artificial ground motions compatible with the design spectra calculated in Section 5. In addition, we use the artificial ground motions to calculate the duration characteristics and number of strong-motion cycles that are compatible with these design spectra.

6.2 ARTIFICIAL GROUND MOTIONS

In this Section, we generate ground motions that are typical of the representative magnitudes and distances obtained in Section 5.2 and envelope the design spectra for horizontal ground motions on top of rock, as obtained in Section 5.

We generate the artificial ground motions using the procedure in (1). At the distances of interest for this study, ground-motion duration [as calculated using the methods in (2,3,4,5)] are shorter than the minimum duration of 6 sec specified in (6). Therefore, we generate artificial ground motions with durations slightly longer than 6 sec.

The simulation algorithm uses as inputs the target spectrum and strong-motion duration. The frequency content in these ground motions is then adjusted using an iterative filtering procedure in order to obtain a close match to the design spectra in Table 5–3, while meeting the enveloping requirements (6), with respect to both response spectrum and the power spectrum[1]. Finally, the time history is baseline-corrected to remove trends from the velocity and displacement traces.

We generate artificial ground motions corresponding to design spectra with exceedance probabilities of 2×10^{-3} (500 years), 10^{-3} (1000 years), and 2×10^{-4} (5000 years). The target spectra for the vertical component are taken as 2/3 the horizontal spectra. The assumption

[1]The target power spectrum is calculated following the procedure in the Appendix of (4), which is applied in reverse (i.e., going from response spectrum to power spectrum). The empirical power spectrum is smoothed as suggested in Appendix B of (7), where the smoothed power spectral amplitude at frequency f is the average of all raw power spectral amplitudes within ±20% of f.

about the vertical component is standard practice and is permitted by the NRC Standard Review Plan (6). A recent study on the amplitude of vertical ground motions (8) finds that the ratio of 2/3 is adequate, except for distances shorter than 20 km and very large magnitudes ($M \simeq 8$). Because the dominant ground motions at Oak Ridge are associated with low magnitudes and distances much larger than 20 km, the vertical/horizontal ratio of 2/3 is appropriate. The resulting artificial ground motions, their response spectra, and their power spectra are shown in Figures 5–1 through 5–27.

The less than desirable fit between the actual and target response spectra at low frequencies is due to the power-spectrum enveloping requirements that were introduced in revision 2 of (6). The empirical power spectrum calculated from an earthquake time history (real or artificial) of typical duration often has very deep troughs. In order for these troughs to meet the enveloping requirement, it is necessary to increase the power at low frequencies, usually resulting in a poor fit to the response spectrum at those frequencies. These troughs are due to the combined effect of the finite duration of the time history and the spectral smoothing procedure recommended in (7), not to a deficiency in energy in some frequency range. In fact, these peaks and troughs are present in the power spectra of artificial time histories generated from smooth parent power spectra. It appears that this issue was overlooked in the development of the power-spectrum requirement, as the intent of the requirement was not the introduction of additional conservatism.

6.3 DURATION CHARACTERISTICS

We determine the duration characteristics of the dominant ground motions at Oak Ridge by examining the artificial ground motions generated in Section 5.3. The strong-motion duration is controlled by the requirements in (6); the rise and decay times depend on the strong-motion duration and on the assumed shaping function.

We obtain the rise time, strong-motion duration, and decay time by examining the records and the normalized cumulative energy plots[2] shown in Figure 5–28. We define the strong-motion phase of the record as the interval containing 5 to 75% of the cumulative energy (9,6). The rise time, strong-motion duration, and decay time follow from this definition.

[2]The normalized cumulative energy is defined as

$$\frac{\int_0^t a^2(\tau)d\tau}{\int_0^\infty a^2(\tau)d\tau}$$

where t represents time and $a(t)$ represents the acceleration time history. The plot of normalized cumulative energy as a function of time is sometimes called the Husid plot.

We also compute the number of strong-motion cycles by counting the number of zero up-crossings during the strong-motion phase. Results are presented in Table 5–1.

Because the strong-motion duration is controlled by the requirements in (6), the duration characteristics are the same for the three exceedance probabilities. The number of strong-motion cycles is also the same, as the target spectra for the three exceedance probabilities are similar.

Table 6-1

Duration of Characteristic Ground Motions

Return Period (years)	Rise Time (sec)	Strong Motion Duration (sec)	Decay Time (sec)	Total Duration (sec)	No. of Strong-Motion Cycles
500 to 5000	1.2	6.1	10.2	17.5	133

6.4 REFERENCES

1. R. T. Sewell, G. R. Toro, and R. K. McGuire. *Impact of Ground Motion Characteristics on Conservatism and Variability in Seismic Risk Estimates.* Final Report to the U.S. Nuclear Regulatory Commission, Contract NRC-04-89-098, Risk Engineering, Inc., May 1991.

2. R. B. Herrmann. "An Extension of Random Vibration Theory Estimates of Strong Ground Motion to Large Distances". *Bulletin of the Seismological Society of America*, 75:1447–1453, 1985.

3. D. M. Boore and G. M. Atkinson. "Stochastic Prediction of Ground Motion and Spectral Response Parameters at Hard-Rock Sites in Eastern North America". *Bulletin of the Seismological Society of America*, 77(2):440–467, 1987.

4. G. R. Toro and R. K. McGuire. "An Investigation into Earthquake Ground Motion Characteristics in Eastern North America". *Bulletin of the Seismological Society of America*, 77(2):468–489, April 1987.

5. G. Ou and R. Hermann. "A Statistical Model for Ground Motion Produced by Earthquakes at Local and Regional Distances". *Bulletin of the Seismological Society of America*, 80:1397–1417, 1990.

6. *Standard Review Plan, Revision 1.* NUREG-0800, Nuclear Regulatory Commission, Office of Nuclear Reactor Regulation, July 1981.

7. A. J. Philippacopolous. *Recommendations for Resolution of Public Comments on USI A-40, Seismic Design Criteria.* Technical Report NUREG/CR-5374, U.S. Nuclear Regulatory Commission, June 1989.

8. N. A. Abrahamson and J. J. Litehiser. "Attenuation of Vertical Peak Ground Acceleration". *Bulletin of the Seismological Society of America*, 79(3):549–580, 1989.

9. R. P. Kennedy, S. A. Short, K. L. Merz, F. J. Tokarz, I. M. Idriss, M. S. Power, and K. Sadigh. *Engineering Characterization of Ground Motion, Task I: effects of Caracteristics of Free Field Motions on Structural Response.* Technical Report NUREG/CR-3805, U. S. Nuclear Regulatory Commission, 1984.

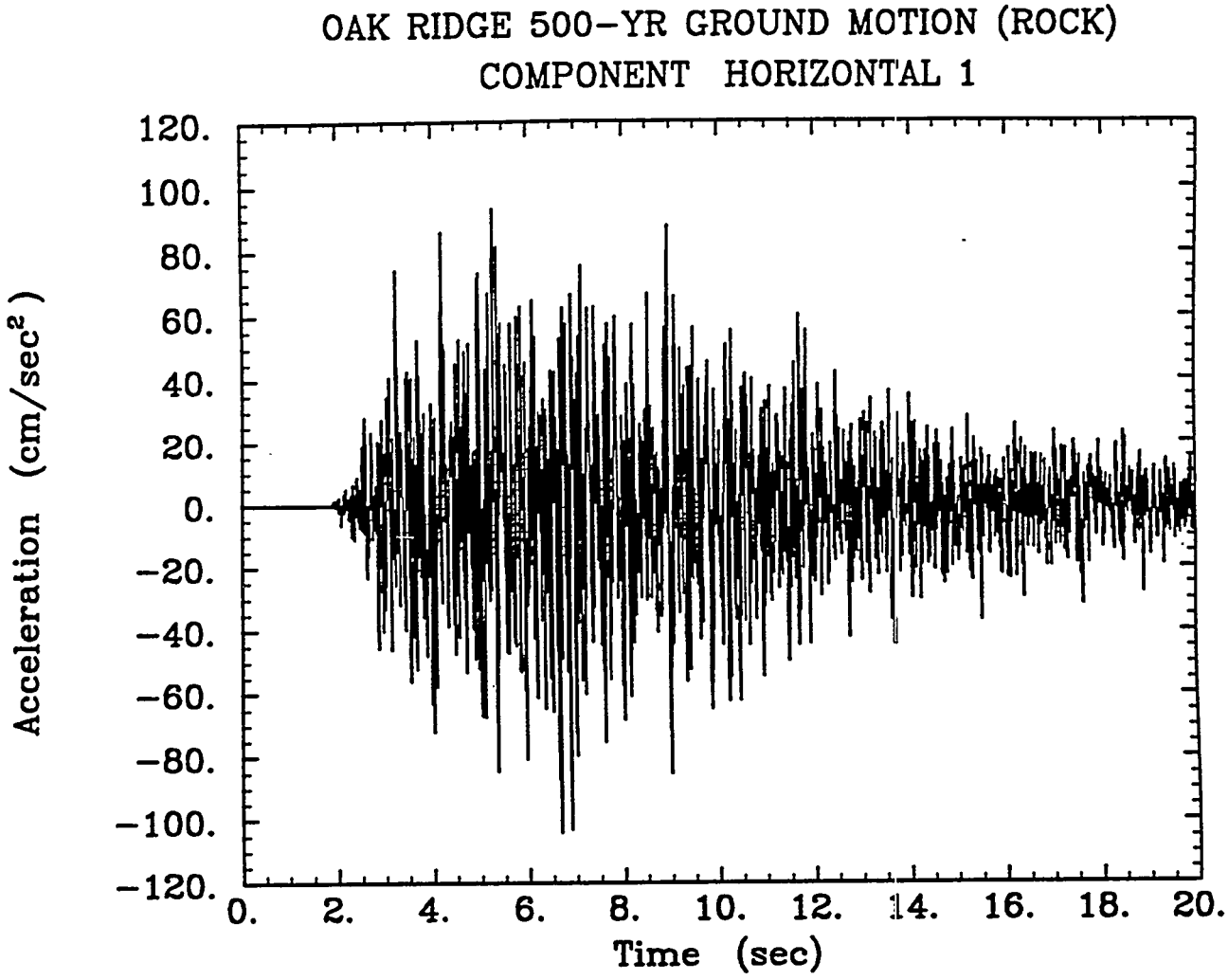

Figure 6-1. Artificial time history for a return period of 500 years; first horizontal component.

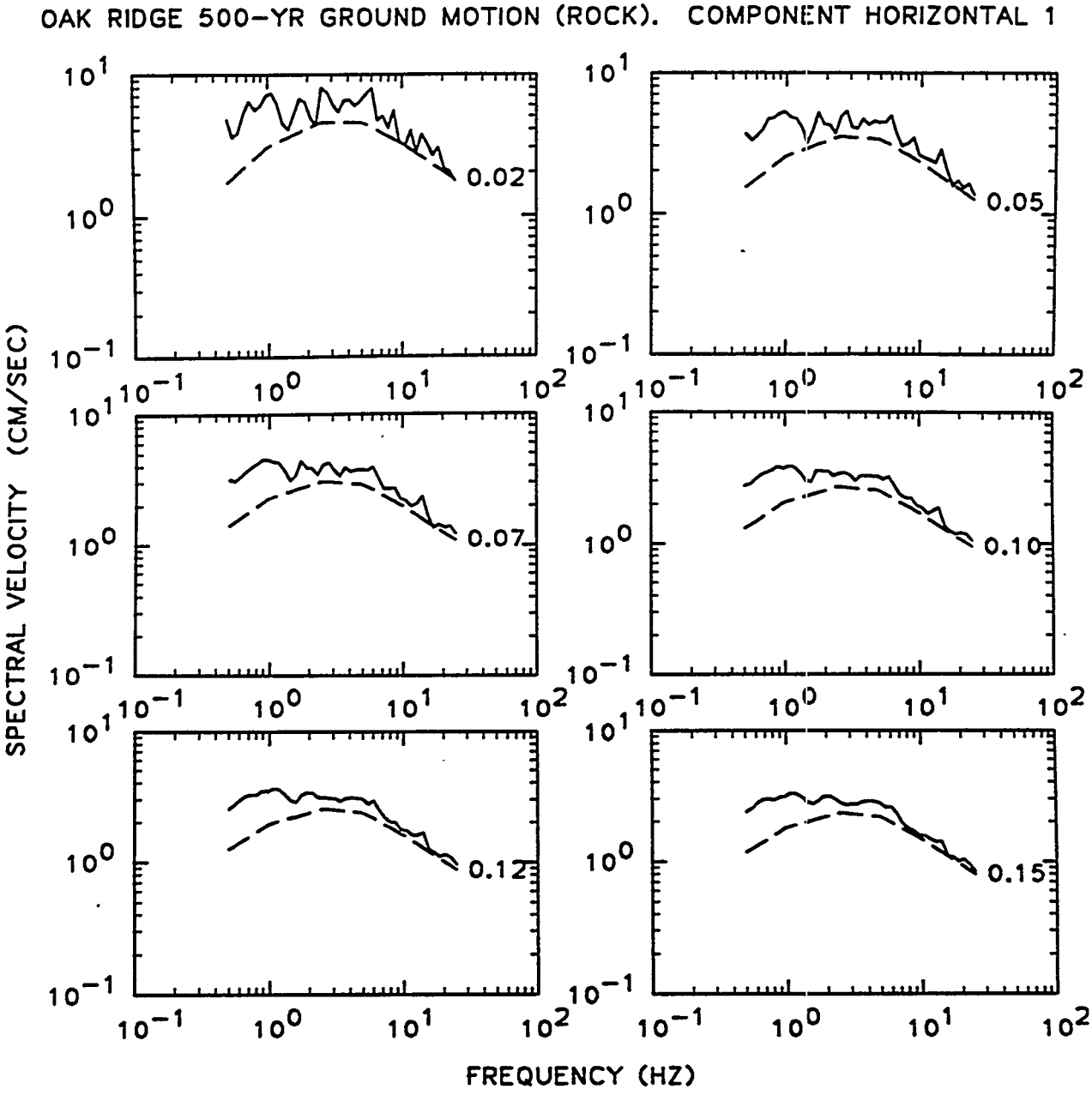

Figure 6-2. Response spectra from artificial time history for a return period of 500 years; first horizontal component. Spectra are shown for six values of damping ratio. Solid lines: response spectra; dashed lines: uniform-hazard spectra.

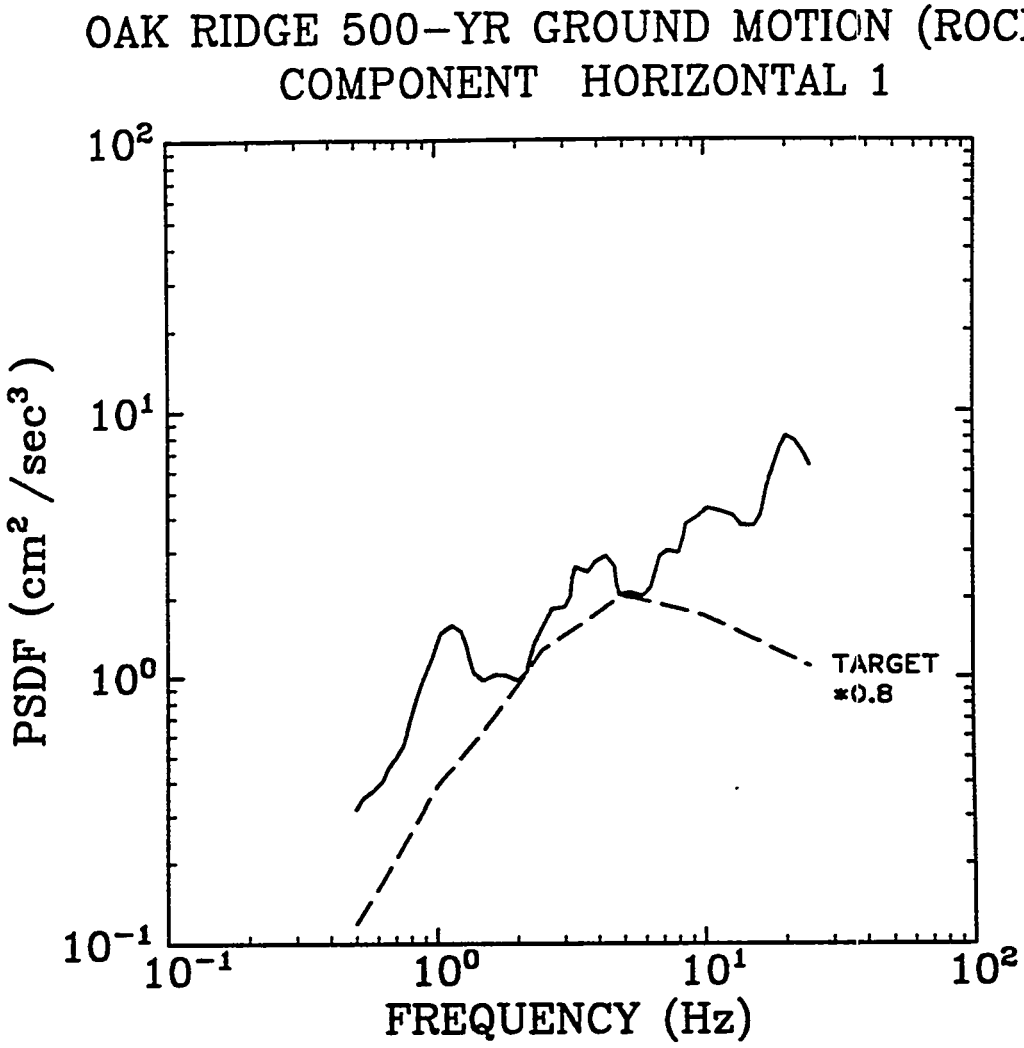

Figure 6-3. Power spectra from artificial time history for a return period of 500 years; first horizontal component. Solid lines: response spectra; dashed lines: uniform-hazard spectra.

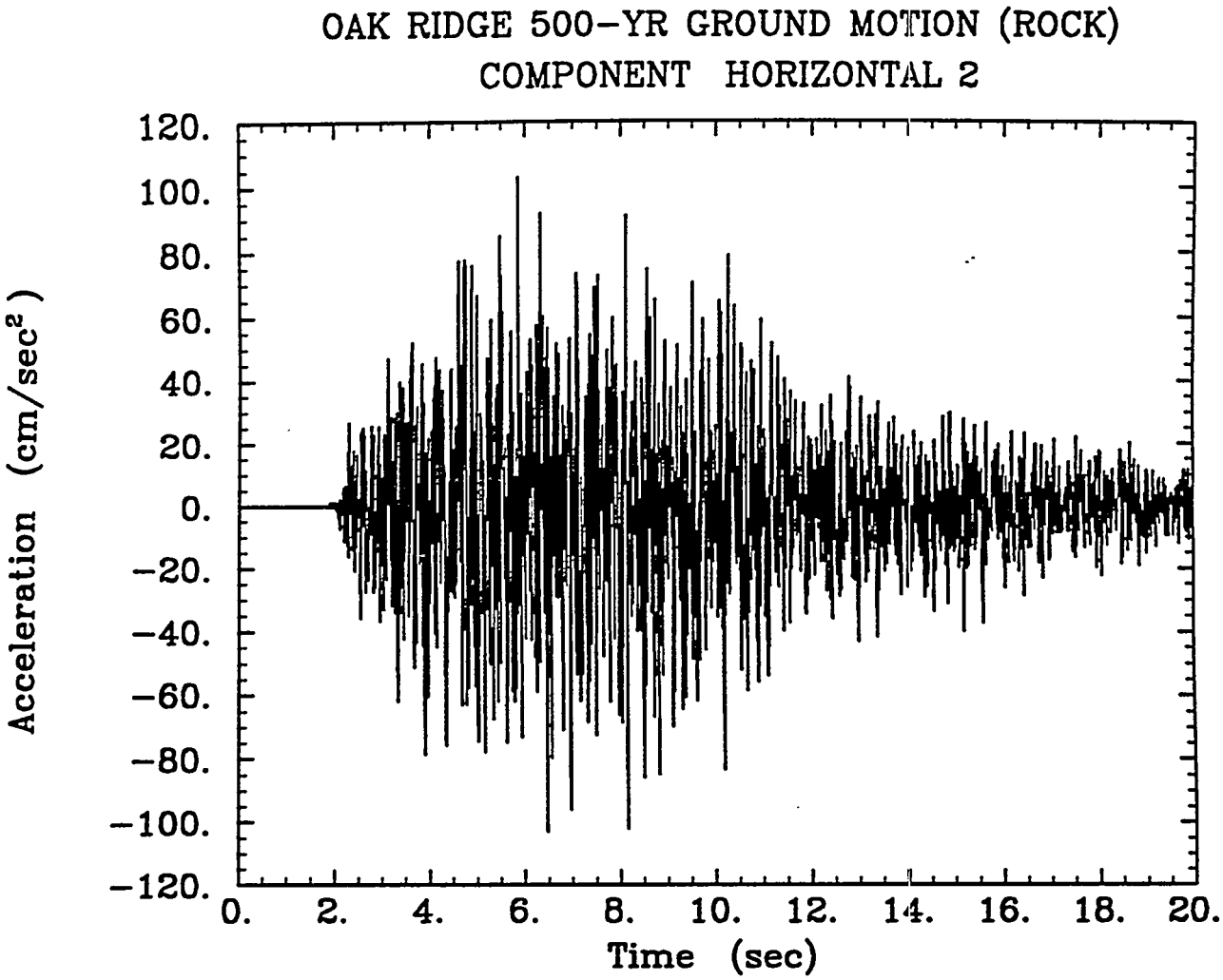

Figure 6-4. Artificial time history for a return period of 500 years; second horizontal component.

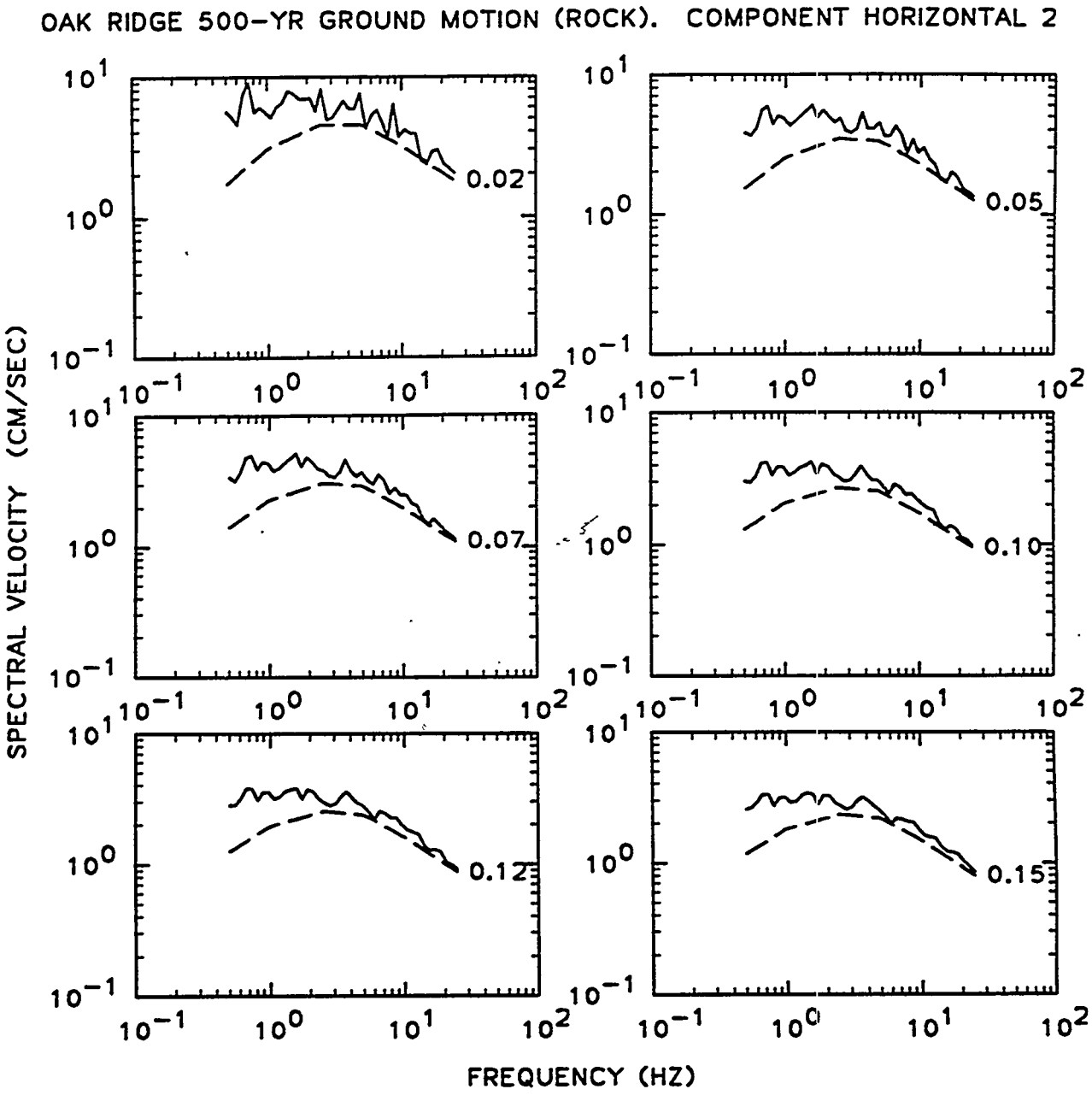

Figure 6-5. Response spectra from artificial time history for a return period of 500 years; second horizontal component. Spectra are shown for six values of damping ratio. Solid lines: response spectra; dashed lines: uniform-hazard spectra.

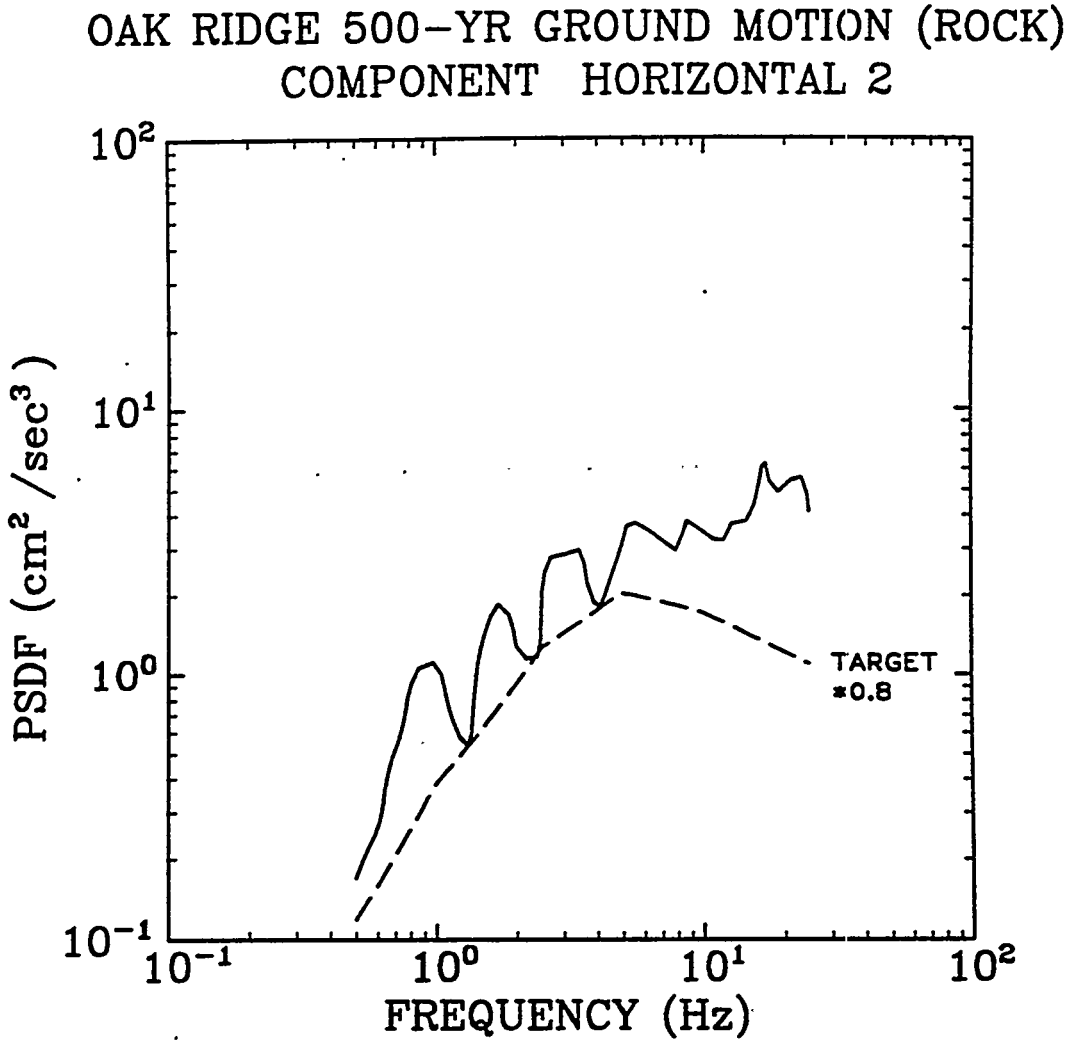

Figure 6-6. Power spectra from artificial time history for a return period of 500 years; second horizontal component. Solid lines: response spectra; dashed lines: uniform-hazard spectra.

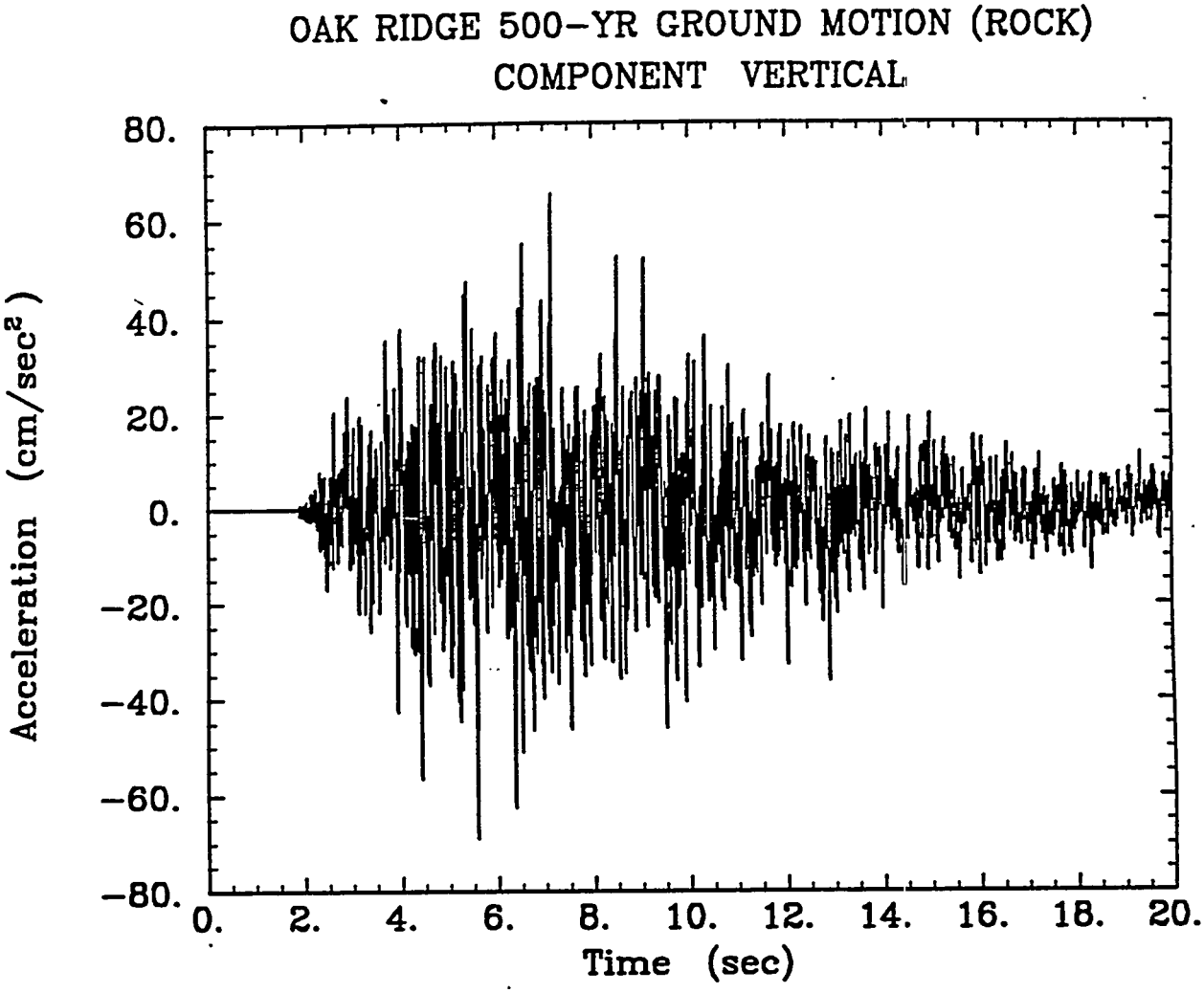

Figure 6-7. Artificial time history for a return period of 500 years; vertical component.

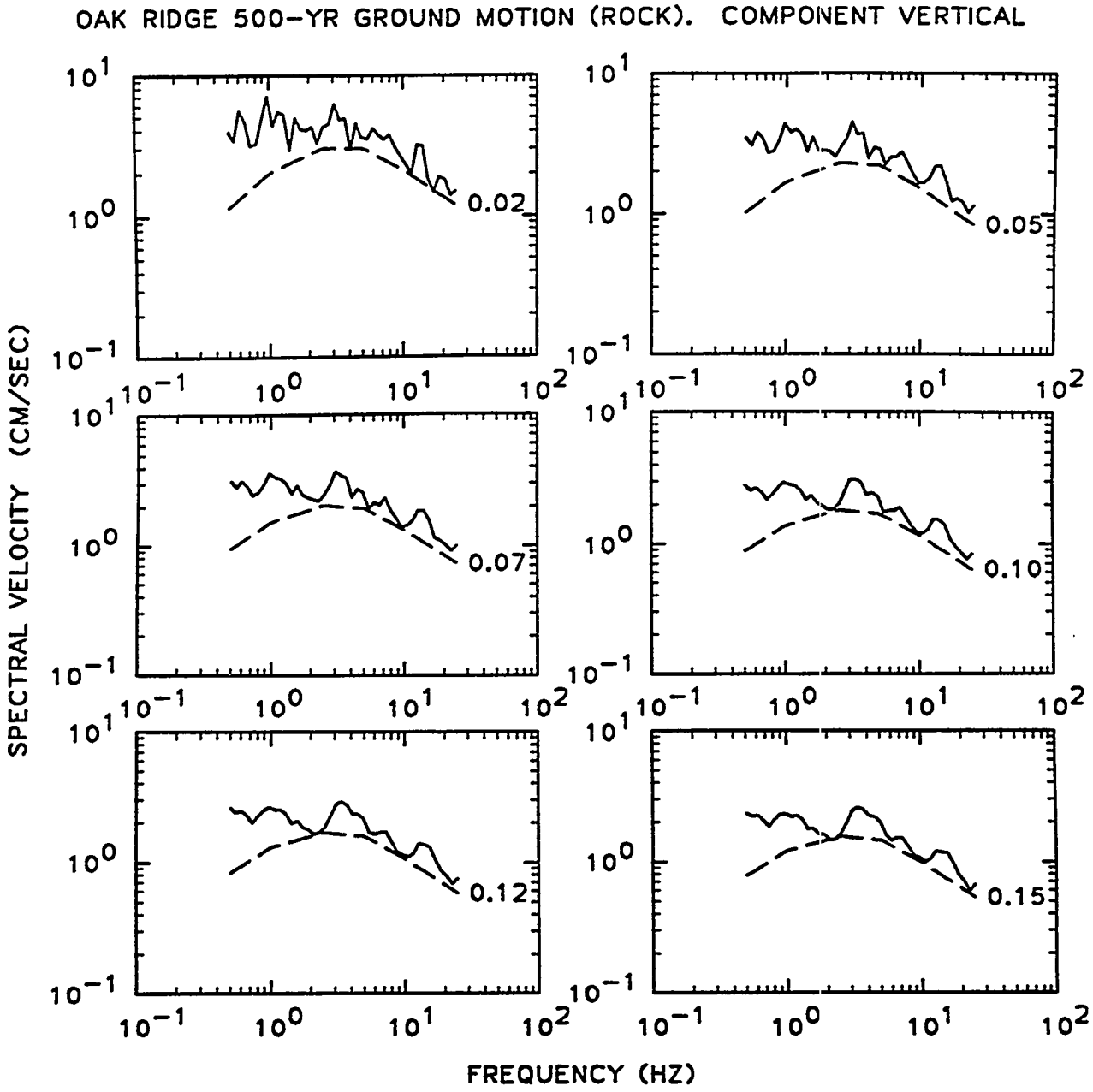

Figure 6-8. Response spectra from artificial time history for a return period of 500 years; vertical component. Spectra are shown for six values of damping ratio. Solid lines: response spectra; dashed lines: uniform-hazard spectra.

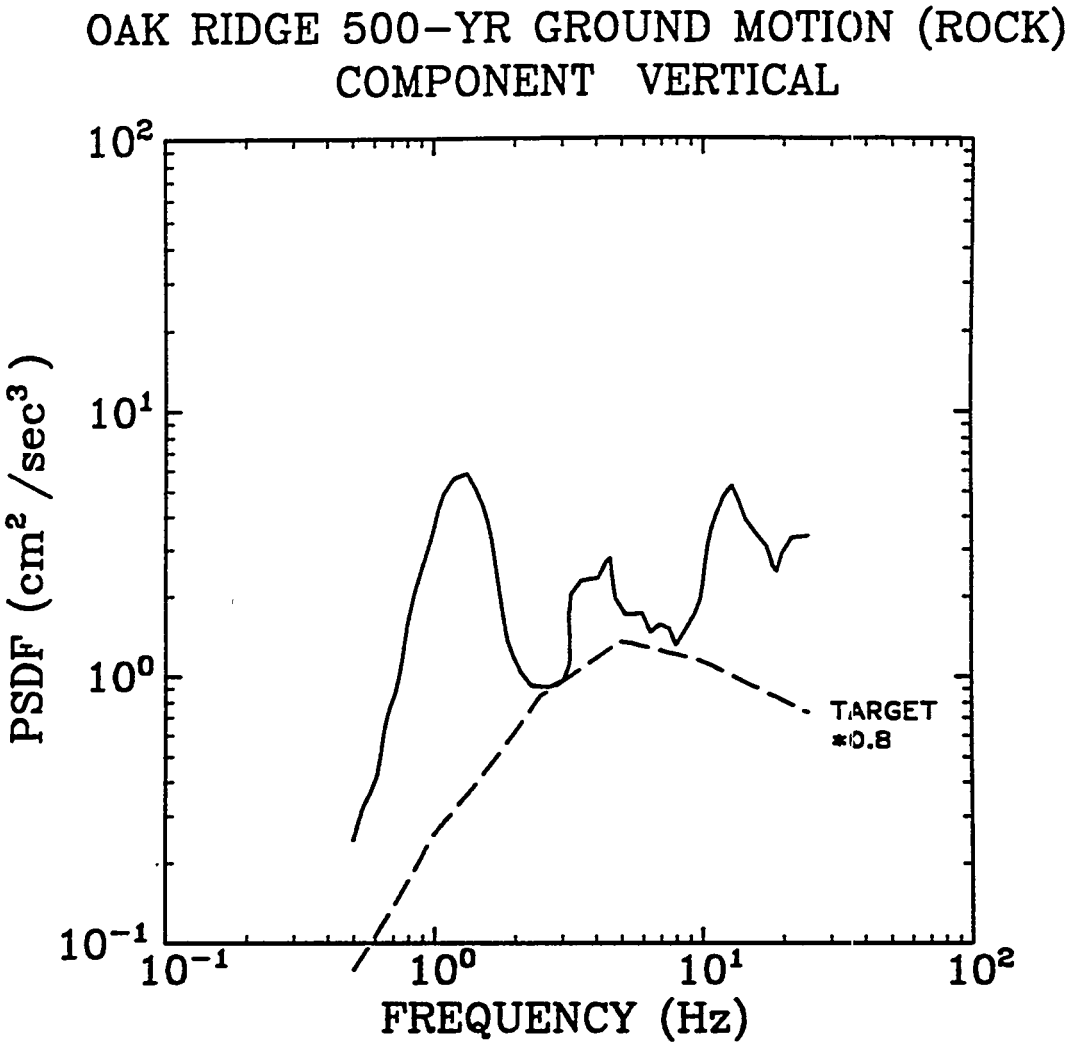

Figure 6-9. Power spectra from artificial time history for a return period of 500 years; vertical component. Solid lines: response spectra; dashed lines: uniform-hazard spectra.

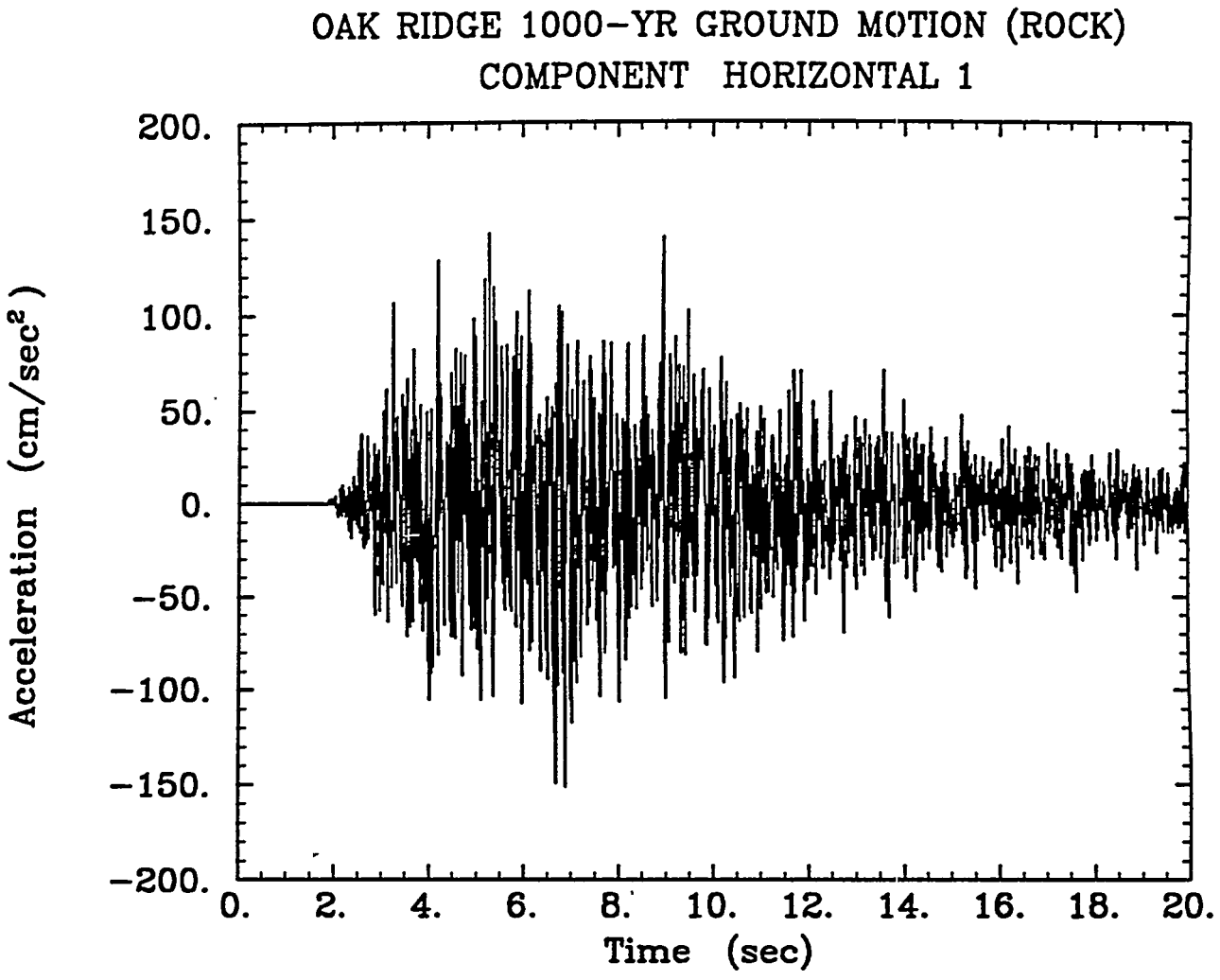

Figure 6-10. Artificial time history for a return period of 1000 years; first horizontal component.

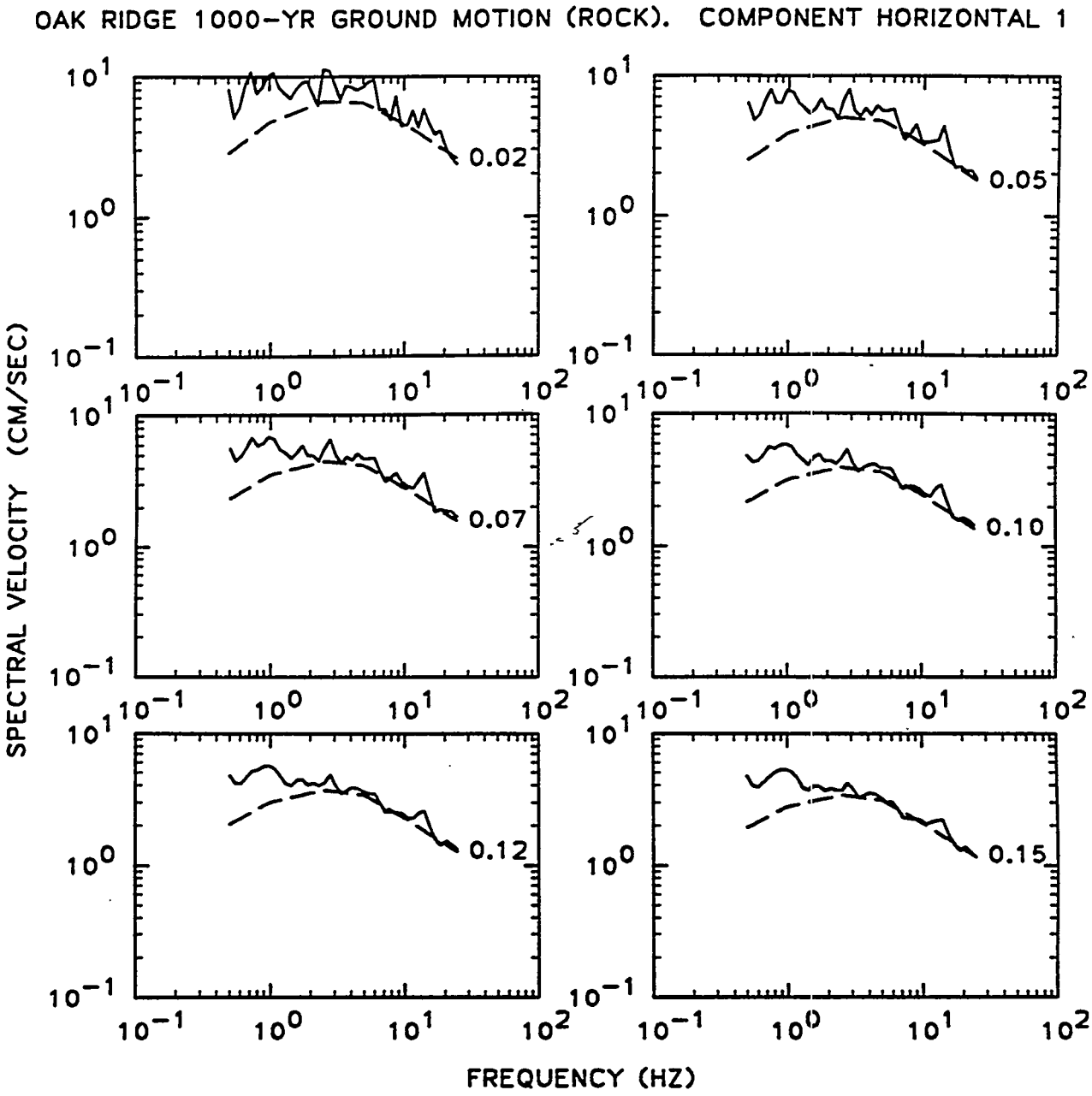

Figure 6-11. Response spectra from artificial time history for a return period of 1000 years; first horizontal component. Spectra are shown for six values of damping ratio. Solid lines: response spectra; dashed lines: uniform-hazard spectra.

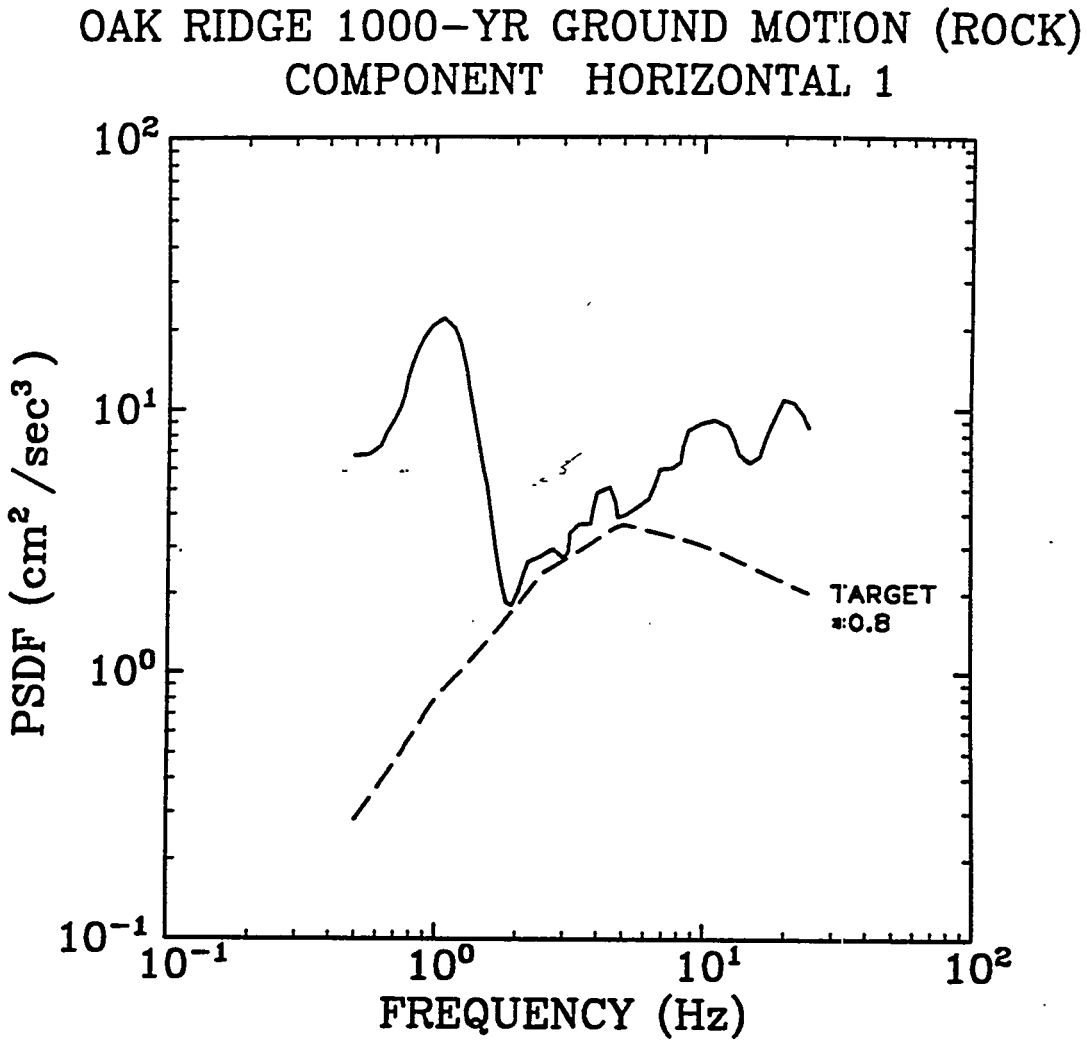

Figure 6-12. Power spectra from artificial time history for a return period of 1000 years; first horizontal component. Solid lines: response spectra; dashed lines: uniform-hazard spectra.

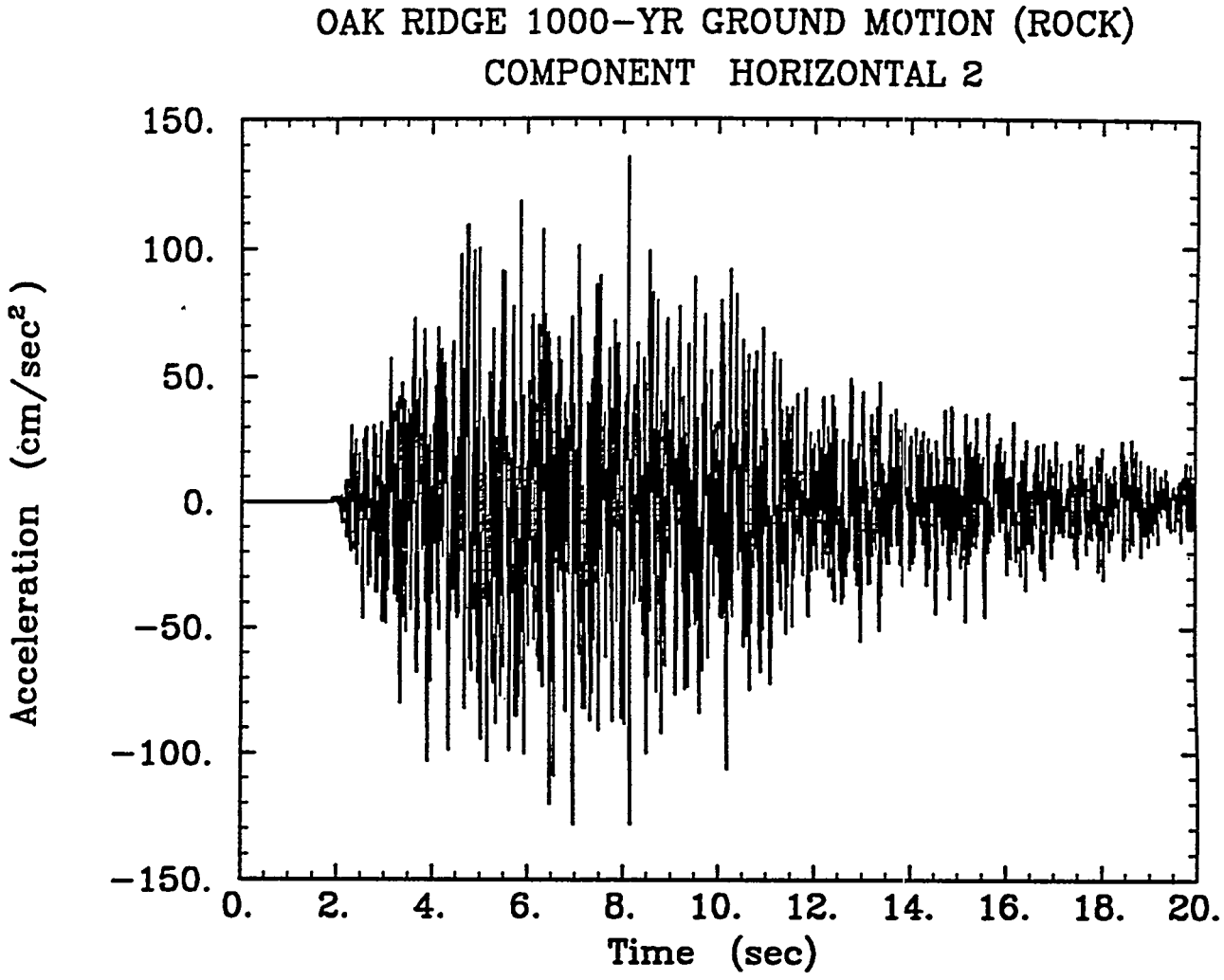

Figure 6-13. Artificial time history for a return period of 1000 years; second horizontal component.

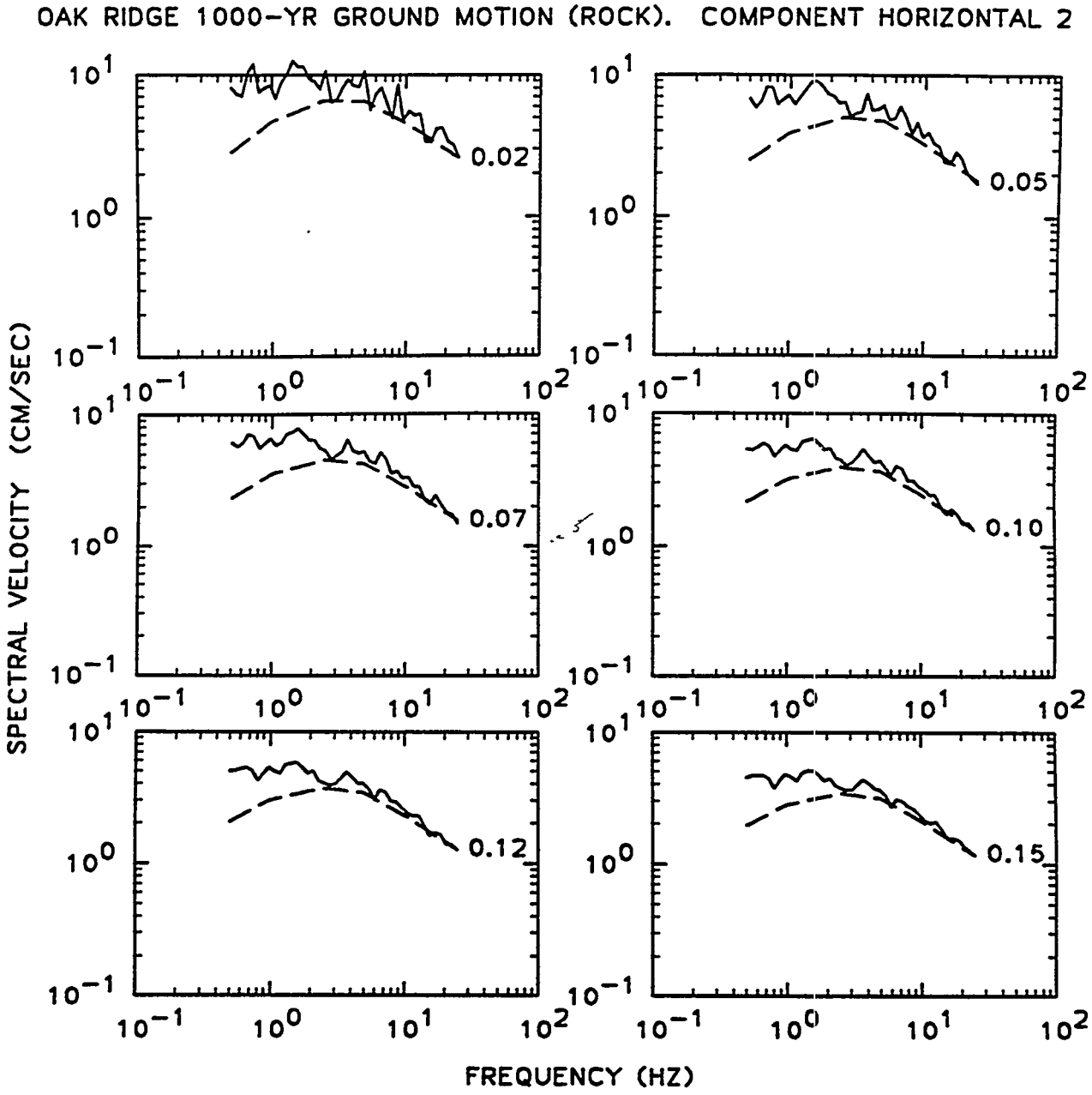

Figure 6-14. Response spectra from artificial time history for a return period of 1000 years; second horizontal component. Spectra are shown for six values of damping ratio. Solid lines: response spectra; dashed lines: uniform-hazard spectra.

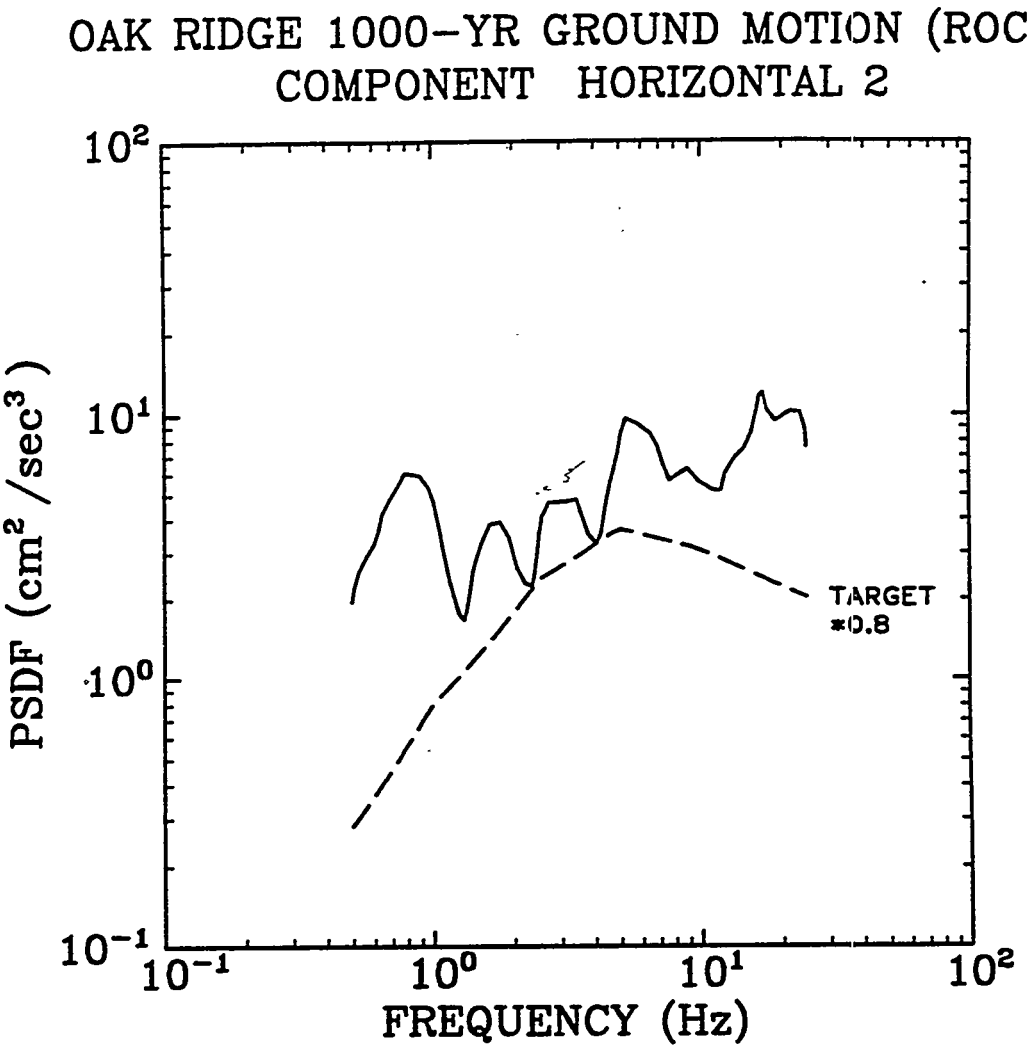

Figure 6-15. Power spectra from artificial time history for a return period of 1000 years; second horizontal component. Solid lines: response spectra; dashed lines: uniform-hazard spectra.

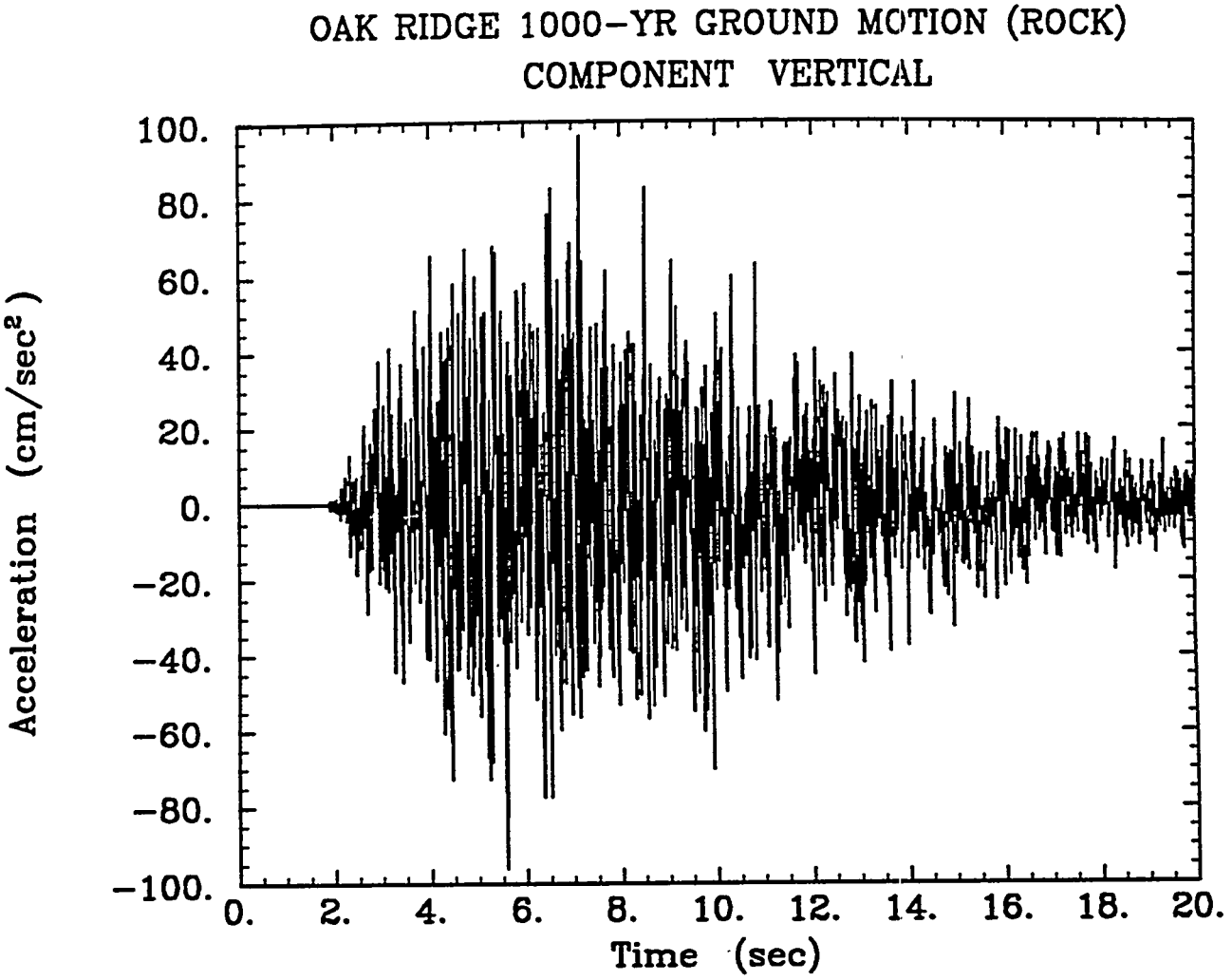

Figure 6-16. Artificial time history for a return period of 1000 years; vertical component.

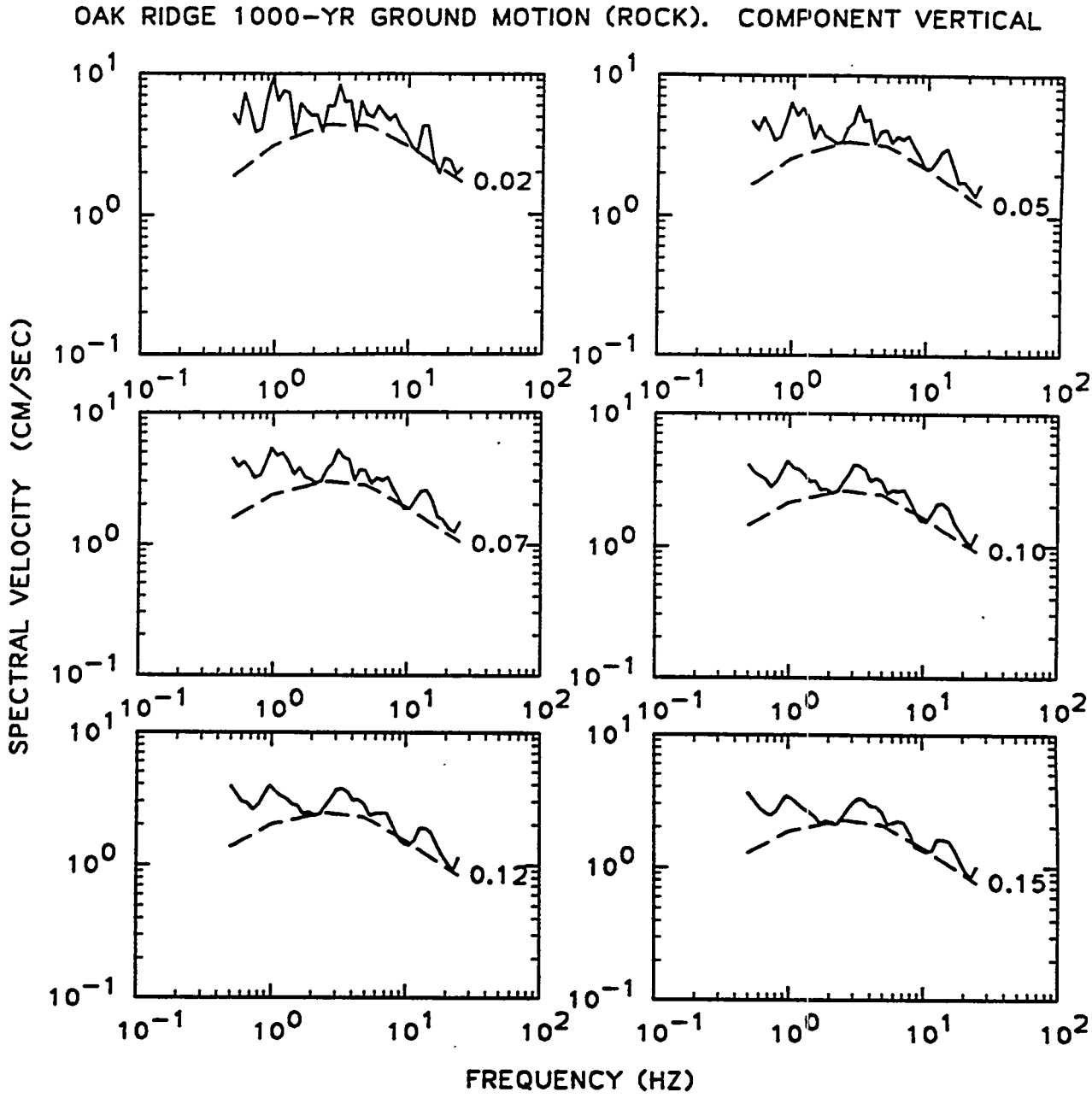

Figure 6-17. Response spectra from artificial time history for a return period of 1000 years; vertical component. Spectra are shown for six values of damping ratio. Solid lines: response spectra; dashed lines: uniform-hazard spectra.

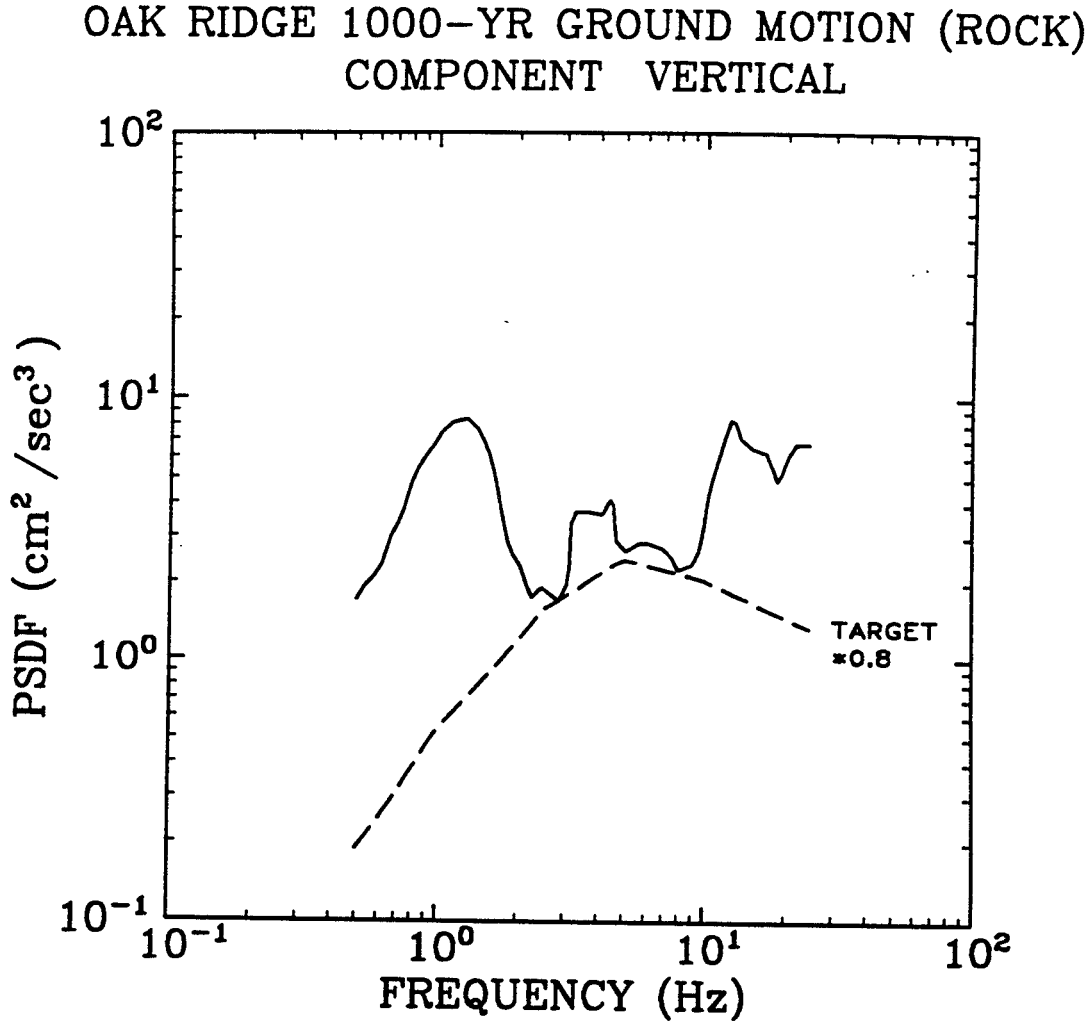

Figure 6-18. Power spectra from artificial time history for a return period of 1000 years; vertical component. Solid lines: response spectra; dashed lines: uniform-hazard spectra.

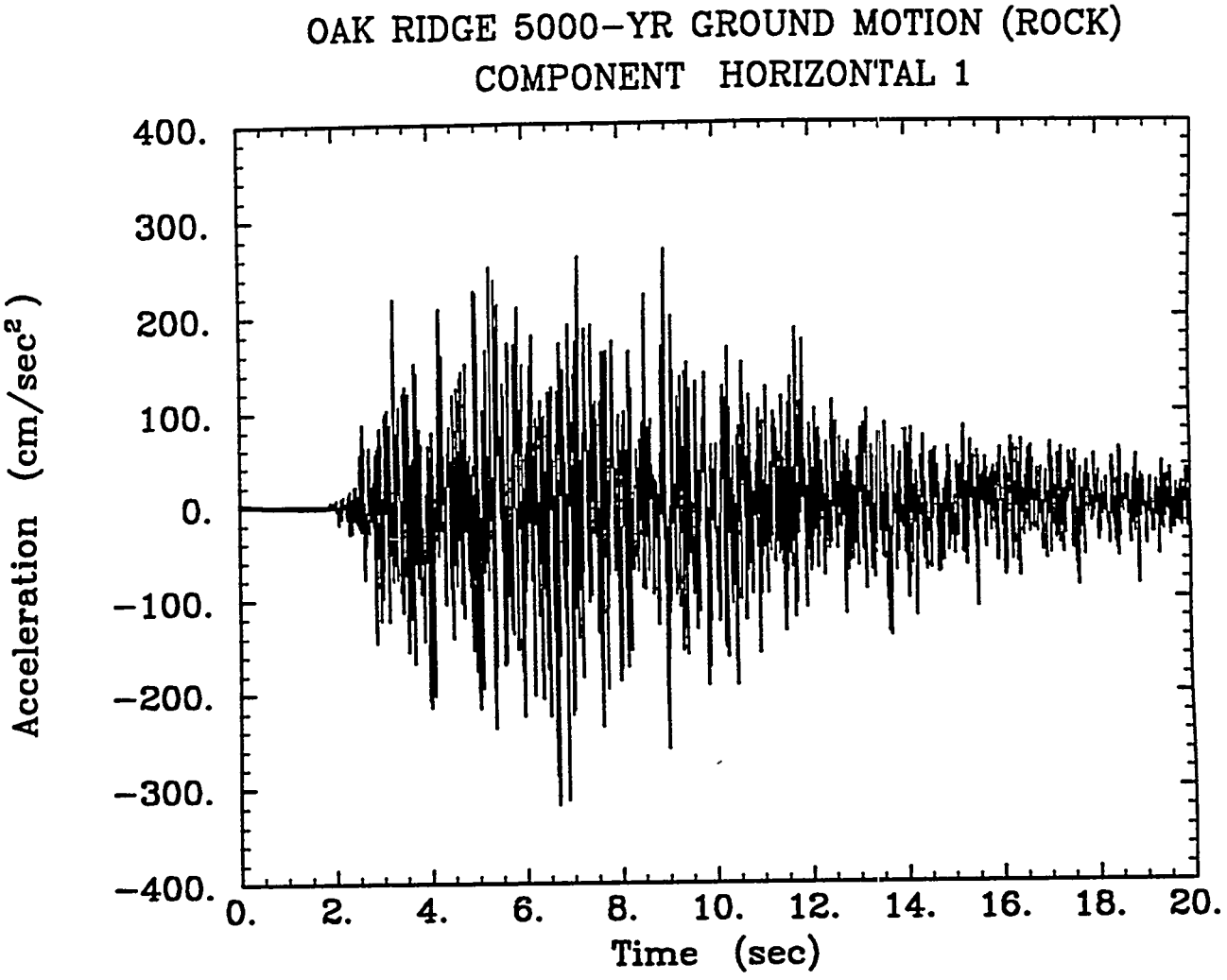

Figure 6-19. Artificial time history for a return period of 5000 years; first horizontal component.

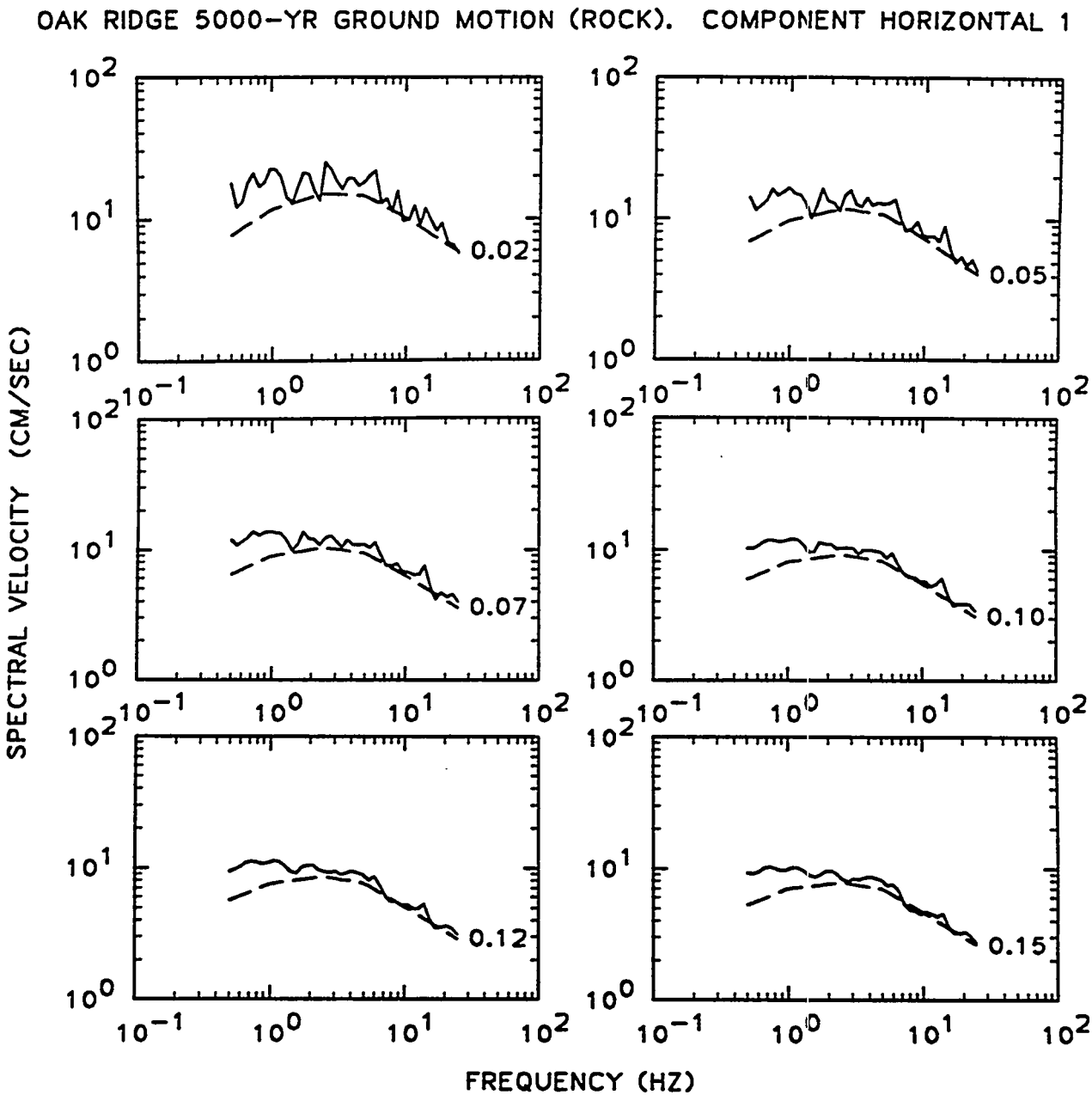

Figure 6-20. Response spectra from artificial time history for a return period of 5000 years; first horizontal component. Spectra are shown for six values of damping ratio. Solid lines: response spectra; dashed lines: uniform-hazard spectra.

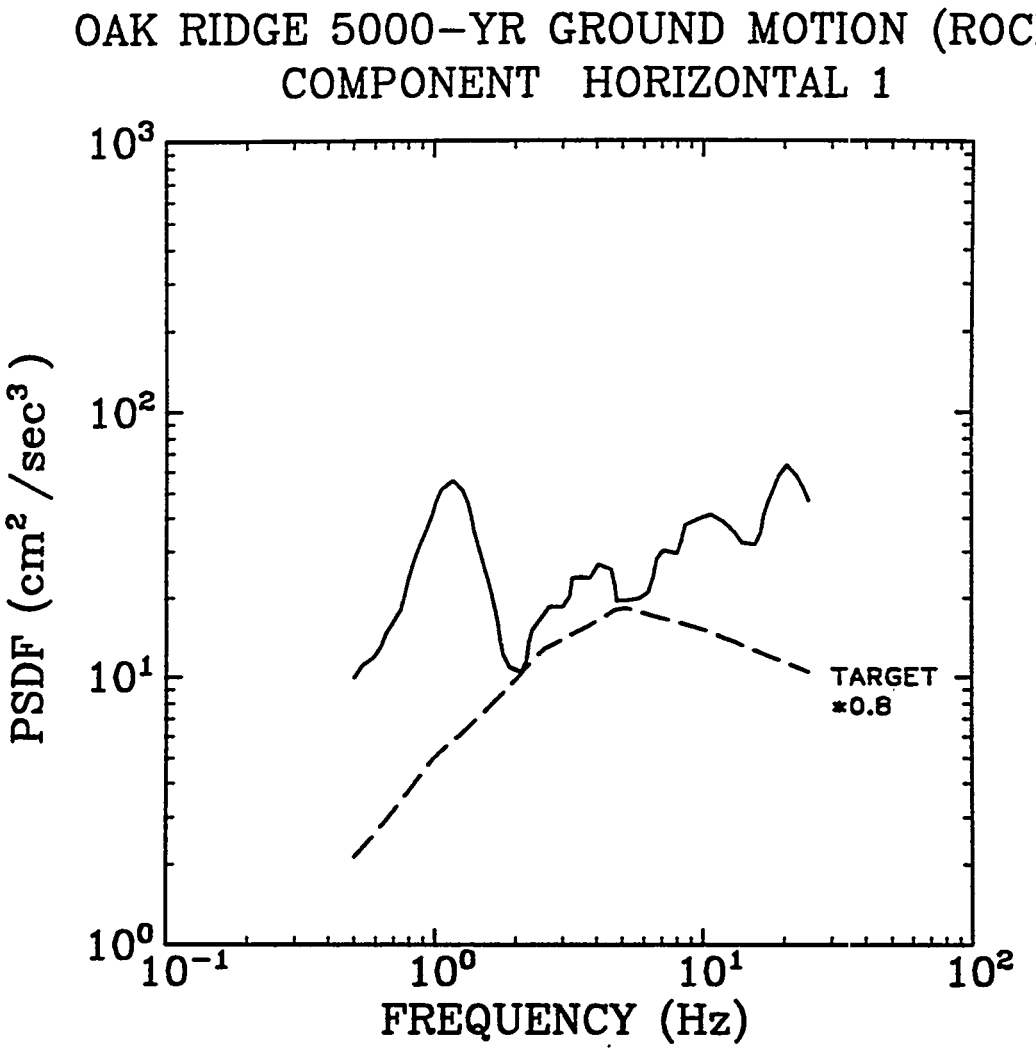

Figure 6-21. Power spectra from artificial time history for a return period of 5000 years; first horizontal component. Solid lines: response spectra; dashed lines: uniform-hazard spectra.

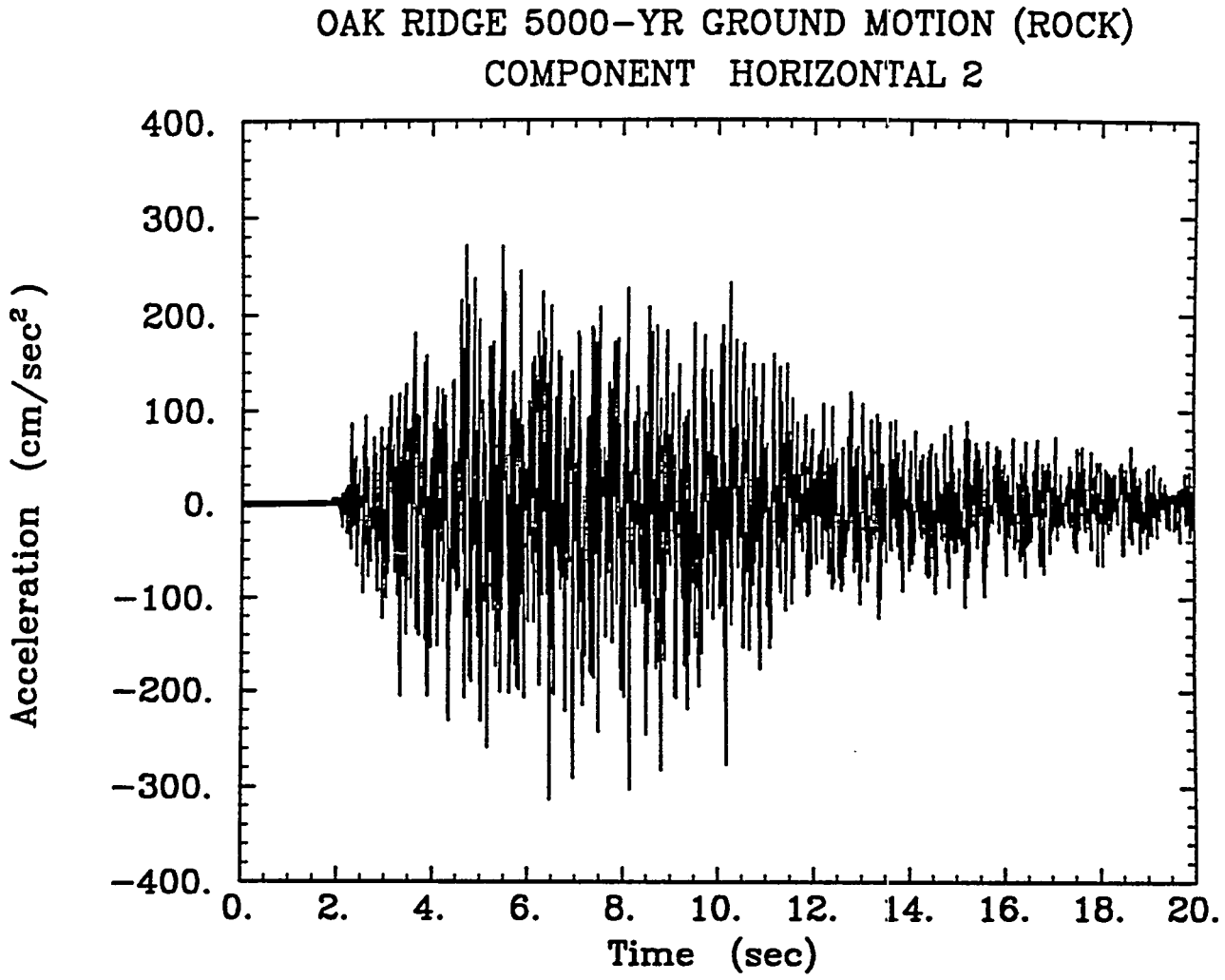

Figure 6-22. Artificial time history for a return period of 5000 years; second horizontal component.

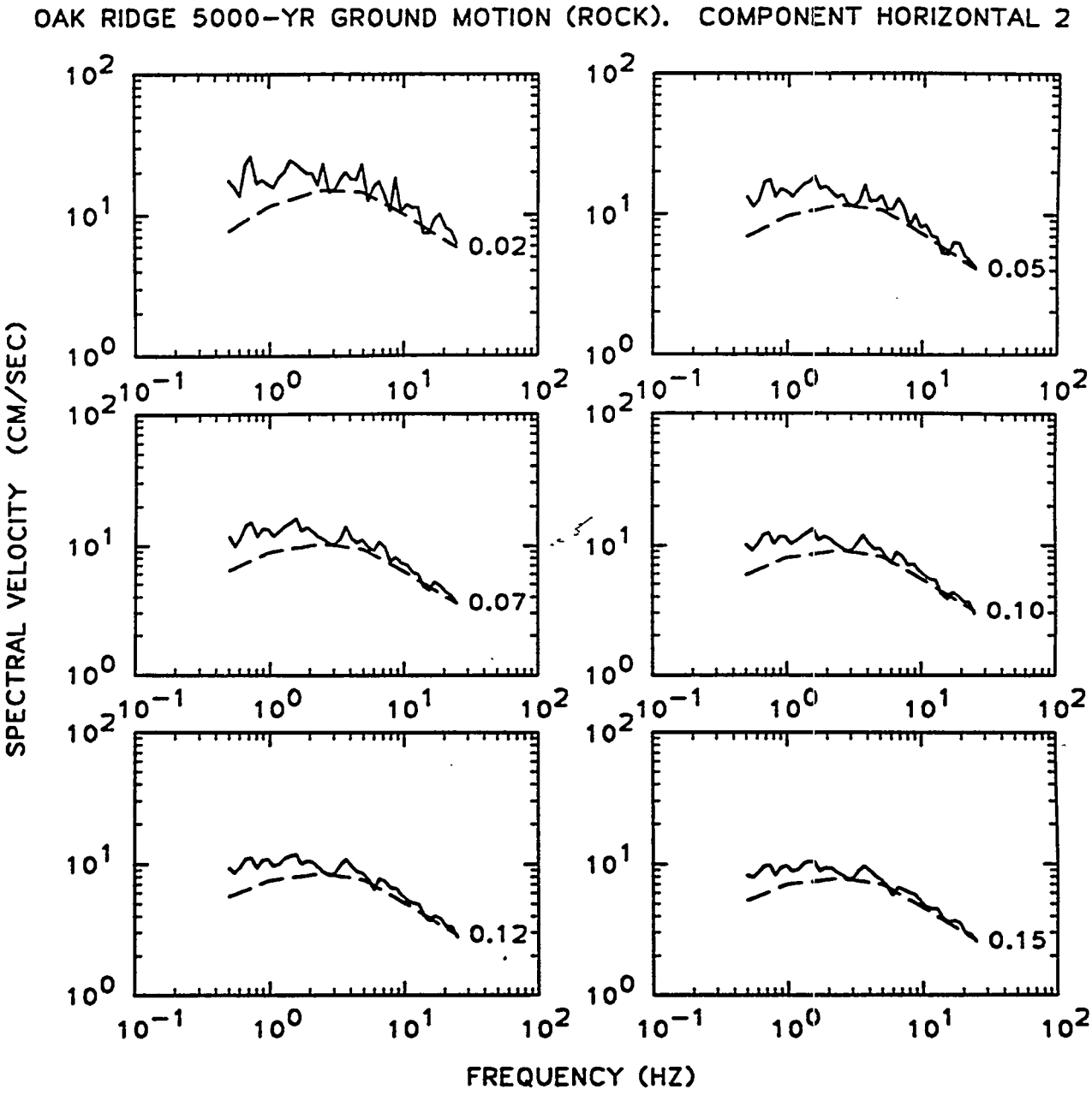

Figure 6-23. Response spectra from artificial time history for a return period of 5000 years; second horizontal component. Spectra are shown for six values of damping ratio. Solid lines: response spectra; dashed lines: uniform-hazard spectra.

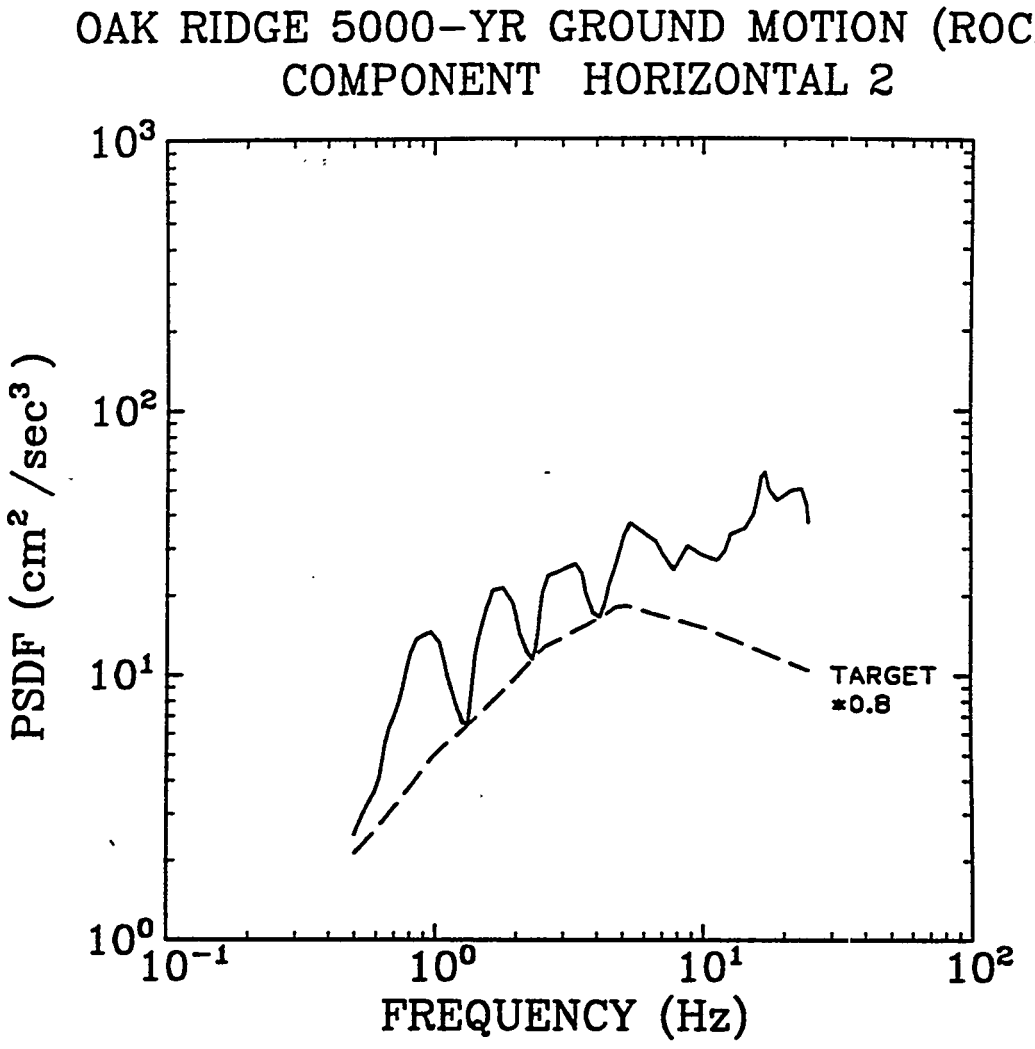

Figure 6-24. Power spectra from artificial time history for a return period of 5000 years; second horizontal component. Solid lines: response spectra; dashed lines: uniform-hazard spectra.

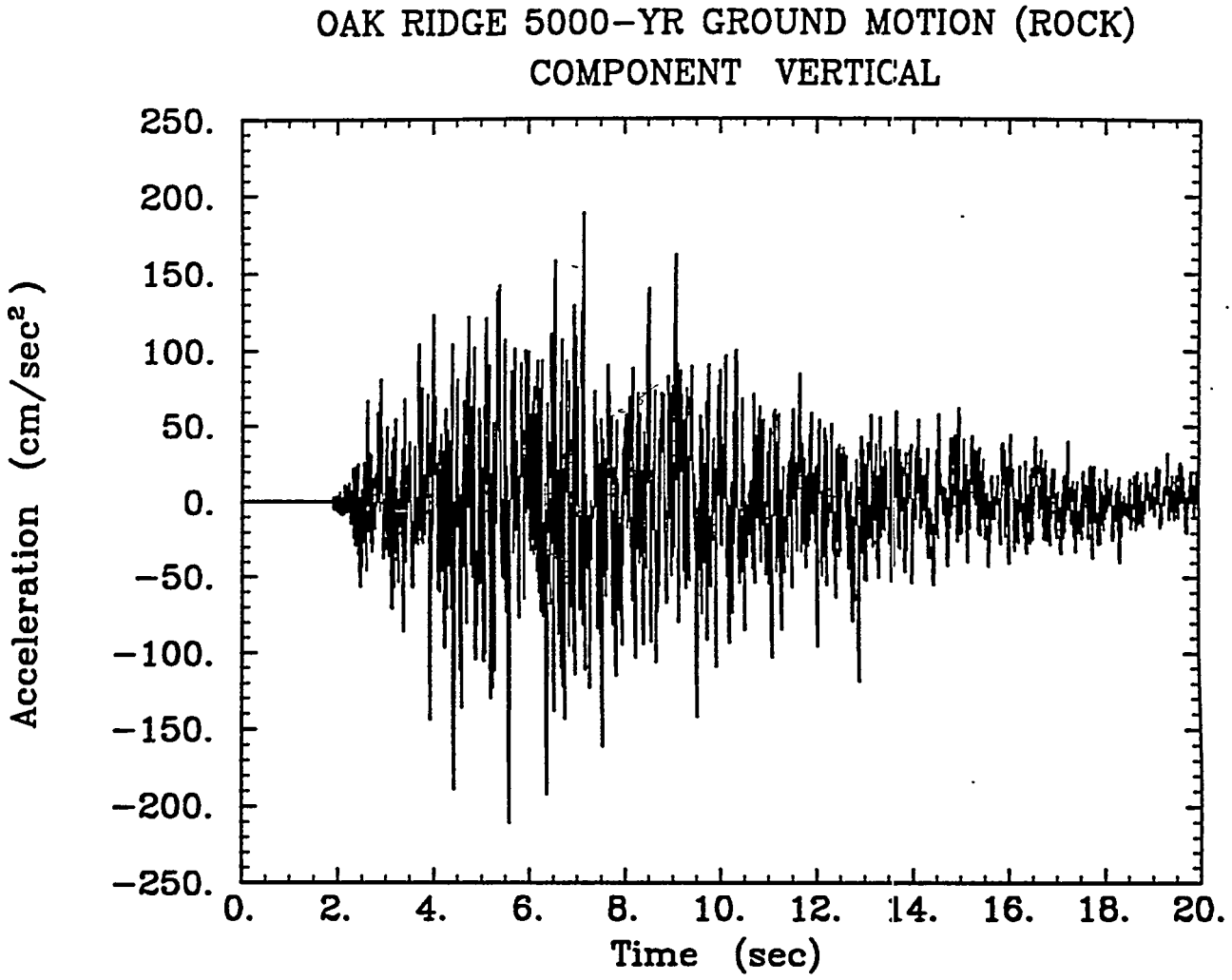

Figure 6-25. Artificial time history for a return period of 5000 years; vertical component.

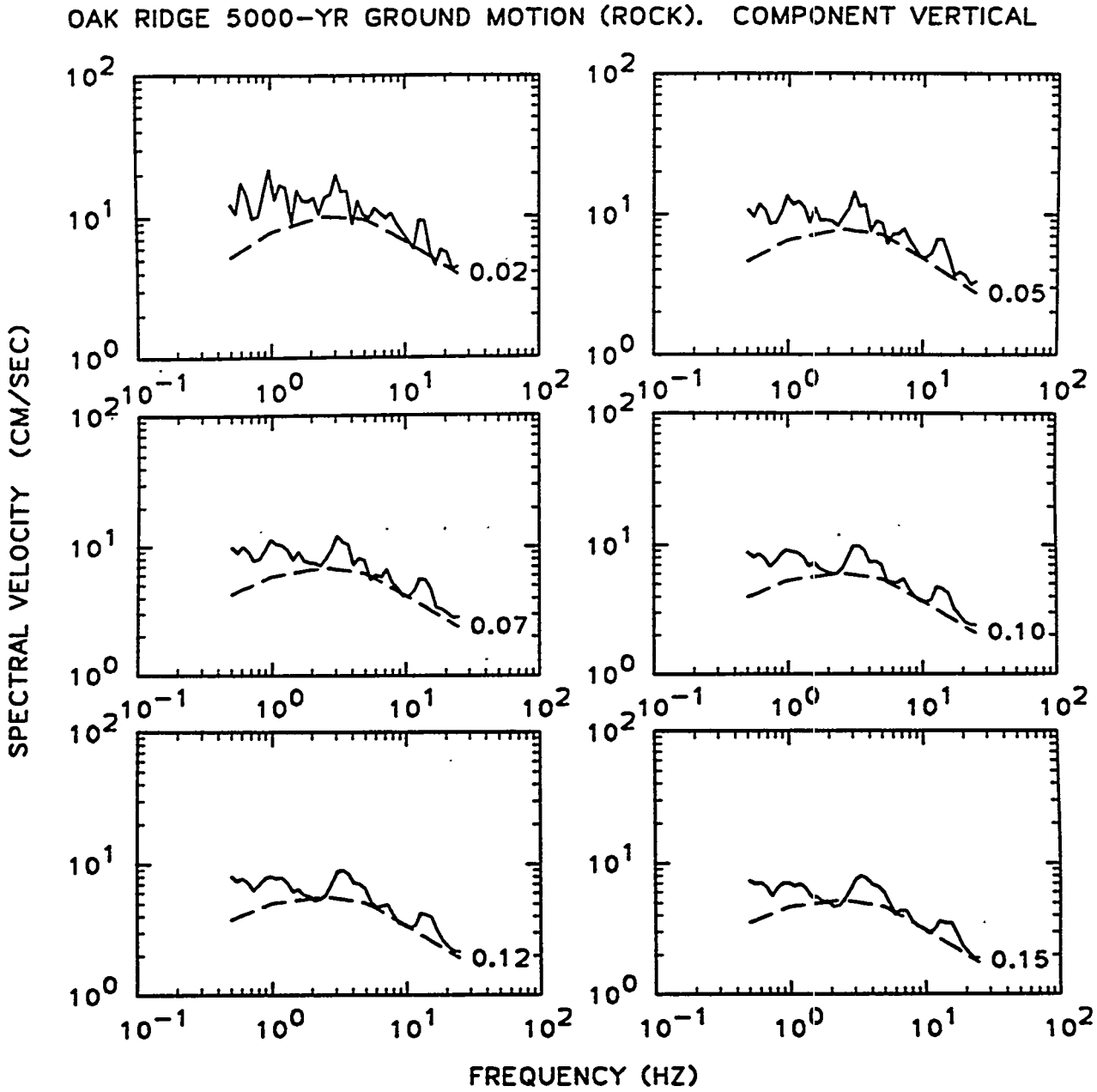

Figure 6-26. Response spectra from artificial time history for a return period of 5000 years; vertical component. Spectra are shown for six values of damping ratio. Solid lines: response spectra; dashed lines: uniform-hazard spectra.

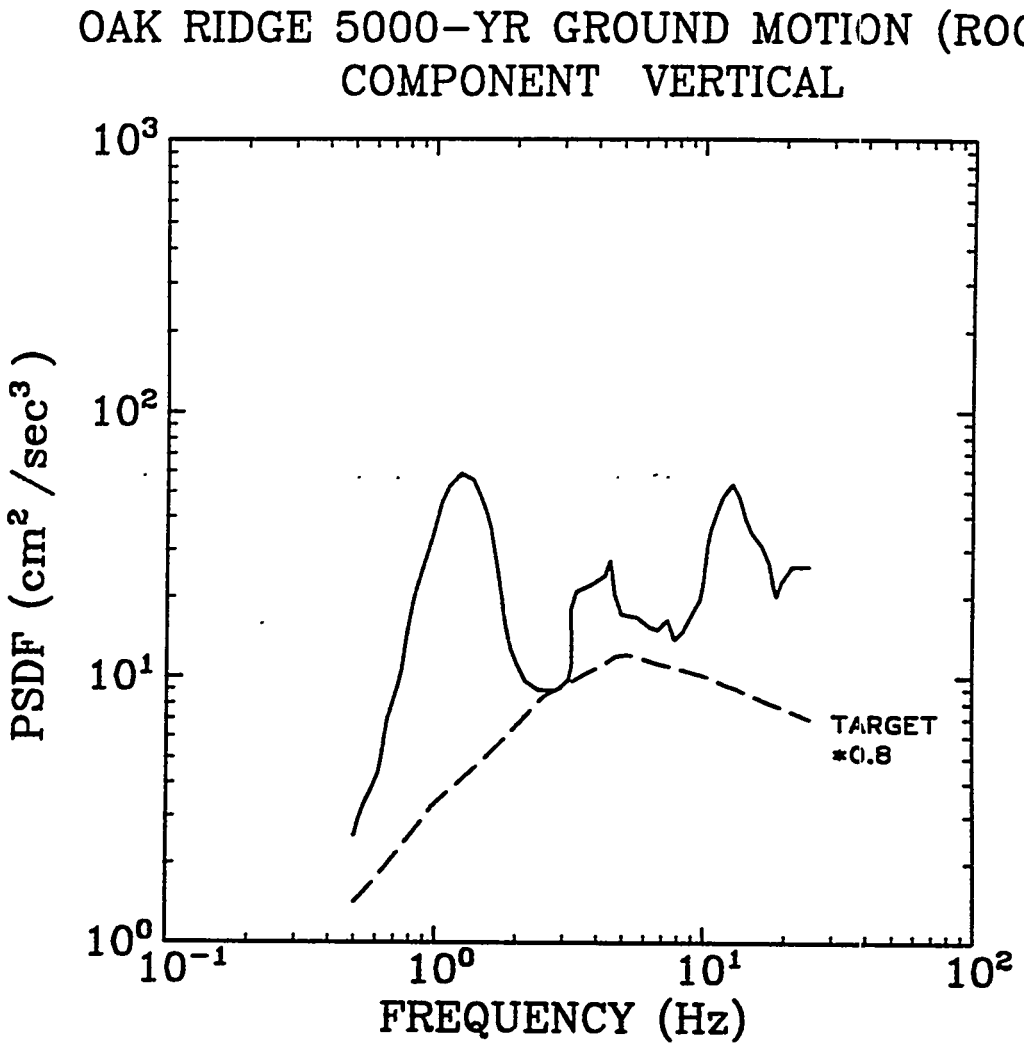

Figure 6-27. Power spectra from artificial time history for a return period of 5000 years; vertical component. Solid lines: response spectra; dashed lines: uniform-hazard spectra.

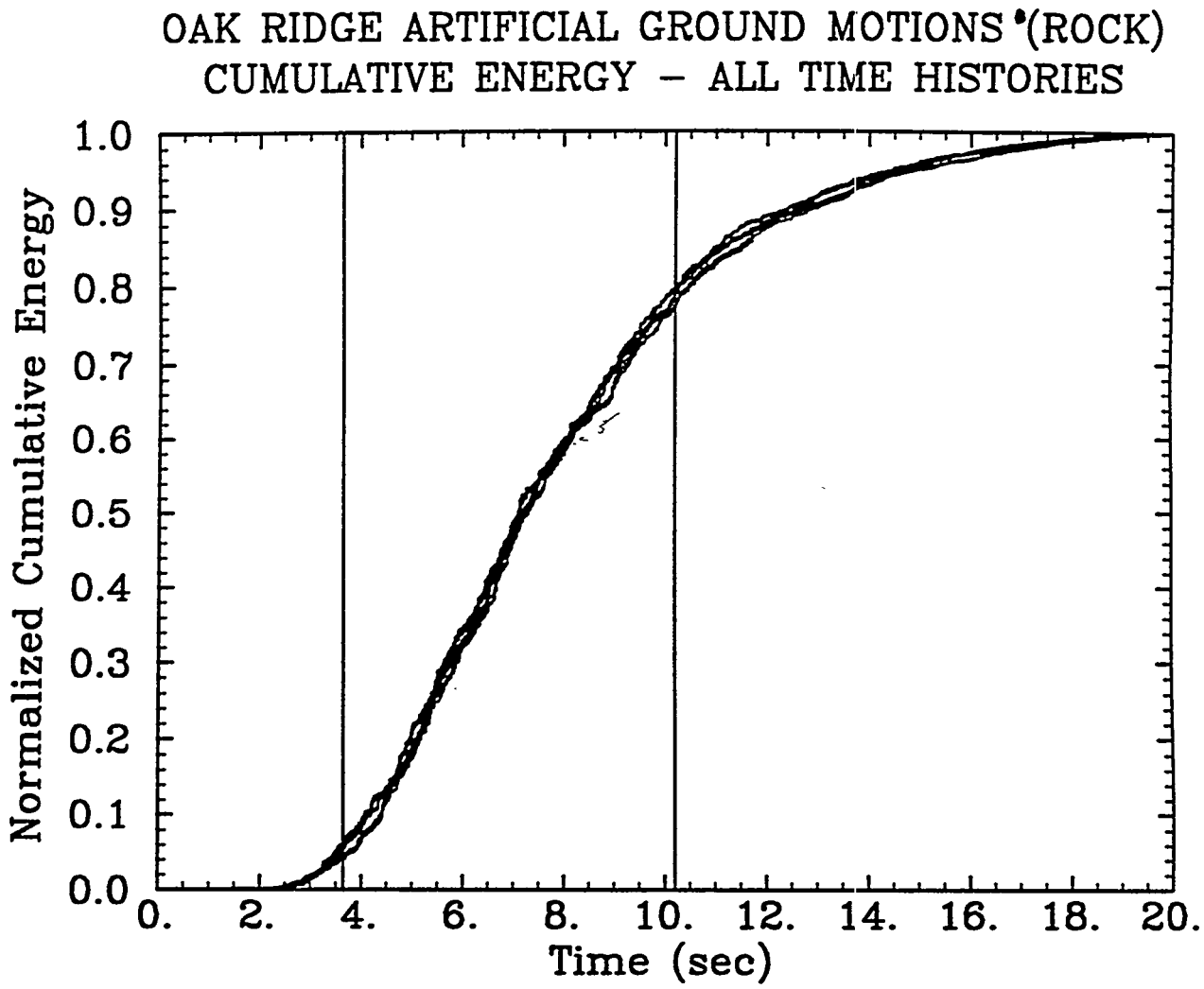

Figure 6-28. Cumulative energy plot for all artificial ground motions (all components). The vertical bars indicate the beginning and end of the strong-motion phase

Section 7

CONCLUSIONS

In this study we have derived a set of seismic hazard curves that represent the frequency of exceedance of various PGA levels at the Oak Ridge Reservations, and the uncertainty in that frequency of exceedance. These results are represented as a family of fractile hazard curves. We have also characterized the types of earthquakes associated with selected return periods and generated compatible artificial ground motions.

The EPRI/SOG (1) and LLNL (2) methods of seismic hazard evaluation for the central and eastern U.S. (CEUS) have been used as input for this study. For the EPSI/SOG work, an analysis has been conducted using the seismological inputs and ground motion equations described in the EPSI/SOG study. For the LLNL method, calculations were performed by LLNL for the Oak Ridge site and transmitted to us for use in this study. We have weighted the two studies equally, and have generated combined EPRI/SOG-LLNL results with and without LLNL attenuation model G16-A3. Model G16-A3 is the most significant source of differences between the EPRI/SOG and LLNL results.

For the sake of comparison, Table 7–1 presents the median results for peak ground acceleration and 1-Hz spectral velocity, as obtained from all seismic hazard analyses reported here.

We have also calculated design spectra for exceedance probabilities of 2×10^{-3}, 10^{-3}, and 2×10^{-4}, by applying the Department of Energy (DOE) interim procedure for use of the EPSI/SOG and LLNL seismic hazard results (3). We have also generated artificial ground motions that are compatible with these design spectra and meet the requirements of (4).

It should be noted that both the EPSI/SOG study and the LLNL study were undertaken with low and moderate levels of ground motion in mind (PGA levels up to 0.5g or so). At those levels, certain effects such as truncation of the ground motion distribution and decrease of the scatter in ground motion with increasing earthquake magnitude can and were ignored, because they have a minor effect. (The LLNL study allowed the ground motion experts to specify a truncation on the ground motion distribution, but only two experts chose to

Table 7-1

Ground-Motion Amplitudes for Selected Values of the Median Annual Exceedance Probability

Ground Motion Measure	Annual Exceedance Probability	EPRI	LLNL (4 GX†)	LLNL (5 GX†)	Combined EPRI+LLNL (4 GX†)	Combined EPRI+LLNL (5 GX†)
Peak Ground Acceleration (g)	2×10^{-3} (500 yr)	0.041	0.050	0.068	0.043	0.051
	1×10^{-3} (1000 yr)	0.068	0.073	0.100	0.068	0.076
	2×10^{-4} (5000 yr)	0.153	0.162	0.209	0.153	0.170
1-Hz Spectral Velocity (cm/sec)	2×10^{-3} (500 yr)	0.96	2.46	3.38	1.42	1.60
	1×10^{-3} (1000 yr)	1.45	3.38	4.74	2.01	2.37
	2×10^{-4} (5000 yr)	3.67	7.03	10.2	4.55	5.76

† 4GX and 5GX denote results obtained considering 4 and 5 LLNL ground-motion experts

do so, and the limits they specified have virtually no effect even at 2g.) If results from these two methodologies are relied upon for higher accelerations (1g and above), and those results are critical for seismic safety decisions, the effects of limits on ground motion may be quite important. In this sense the current results are conservative, in that they generally ignore factors that might reduce the frequency of occurrence of these large amplitude ground motions. In this case studies should be undertaken to refine the EPSI/SOG and LLNL hazard curves at these high amplitudes to account for truncation and other causes that would reduce the frequencies compared to current results.

7.1 REFERENCES

1. *Seismic Hazard Methodology for the Central and Eastern United States.* Technical Report NP-4726-A, Electric Power Research Institute, July 1986. Revised, 1988. Vol. 1, Part 1: Methodology, Vol. 1, Part 2: Theory, Vol. 2: EQHAZARD Programmer's Manual, Vol. 3: EQHAZARD User's Manual, Vol. 4: Applications, Vols. 5 through 10: Tectonic Interpretations, Vol. 11: Nuclear Regulatory Commission Safety Review.

2. D. L. Bernreuter, J. B. Savy, R. W. Mensing, and J. C. Chen. *Seismic Hazard Characterization of 69 Plant Sites East of the Rocky Mountains.* Technical Report NUREG/CR5250, UCID-21517, U. S. Nuclear Regulatory Commission, 1988.

3. Department of Energy Seismic Working Group. Use of LLNL and EPRI Probabilistic Seismic Hazard Curves: Interim Position. Attachment to Memorandum of W.H. Young to Program Secretarial Officers, dated March 19, 1992. U.S. Department of Energy, 1992.

4. *Standard Review Plan, Revision 1.* NUREG-0800, Nuclear Regulatory Commission, Office of Nuclear Reactor Regulation, July 1981.

Appendix A

TABULATED RESULTS

This appendix presents the results from Sections 2 and 4 in tabular form. Results are organized by section.

A.1 RESULTS FROM THE EPRI/SOG ANALYSIS

Table A-1

Peak Ground Acceleration Hazard Curves

AMPLITUDE	MEAN	FRACTILES						
(cm/sec2)		0.100	0.150	0.300	0.500	0.700	0.850	0.900
5.00	1.88E-02	6.56E-03	7.72E-03	9.87E-03	1.43E-02	2.05E-02	3.13E-02	3.28E-02
50.00	1.90E-03	4.00E-04	6.26E-04	9.49E-04	1.61E-03	2.33E-03	3.44E-03	3.83E-03
99.98	6.29E-04	1.17E-04	1.84E-04	2.85E-04	5.13E-04	7.81E-04	1.12E-03	1.30E-03
249.88	9.02E-05	1.07E-05	1.59E-05	3.45E-05	6.82E-05	1.05E-04	1.70E-04	1.81E-04
500.20	1.27E-05	5.35E-07	1.09E-06	2.84E-06	7.90E-06	1.35E-05	2.65E-05	3.02E-05
699.94	4.18E-06	7.41E-08	1.87E-07	5.89E-07	1.93E-06	4.26E-06	8.90E-06	1.05E-05
1000.24	1.14E-06	6.30E-09	2.03E-08	8.68E-08	3.79E-07	9.67E-07	2.60E-06	2.94E-06

Table A-2

0.5-Hz Spectral Velocity Hazard Curves

AMPLITUDE	MEAN	FRACTILES						
(cm/sec)		0.100	0.150	0.300	0.500	0.700	0.850	0.900
0.05	3.64E-02	1.08E-02	1.18E-02	1.80E-02	2.30E-02	3.86E-02	6.26E-02	7.14E-02
0.10	2.65E-02	6.64E-03	7.78E-03	1.06E-02	1.40E-02	2.38E-02	5.47E-02	6.21E-02
1.00	3.84E-03	3.97E-04	4.86E-04	8.16E-04	1.28E-03	1.88E-03	1.07E-02	1.28E-02
5.00	4.63E-04	5.42E-06	1.24E-05	3.53E-05	1.04E-04	2.03E-04	1.48E-03	1.73E-03
10.00	1.51E-04	2.29E-07	8.05E-07	4.43E-06	1.91E-05	6.93E-05	3.98E-04	6.28E-04
20.01	4.04E-05	3.42E-09	4.07E-08	2.25E-07	3.23E-06	1.92E-05	9.08E-05	1.59E-04
40.00	8.48E-06	1.32E-11	2.13E-10	1.89E-09	3.56E-07	3.48E-06	1.61E-05	2.37E-05
69.97	2.17E-06	1.44E-14	6.75E-14	1.36E-11	2.39E-08	2.51E-07	2.88E-06	5.11E-06

Table A-3

1-Hz Spectral Velocity Hazard Curves

AMPLITUDE	MEAN	FRACTILES						
(cm/sec)		0.100	0.150	0.300	0.500	0.700	0.850	0.900
0.10	3.32E-02	1.07E-02	1.19E-02	1.83E-02	2.23E-02	3.57E-02	5.45E-02	6.21E-02
1.00	4.31E-03	5.71E-04	7.87E-04	1.43E-03	1.91E-03	2.88E-03	1.07E-02	1.28E-02
5.00	4.68E-04	6.11E-06	1.90E-05	4.97E-05	1.17E-04	2.66E-04	1.45E-03	1.68E-03
10.00	1.37E-04	1.69E-07	1.59E-06	6.48E-06	2.63E-05	8.55E-05	3.32E-04	5.40E-04
20.01	3.28E-05	1.30E-09	6.68E-08	4.29E-07	4.12E-06	1.45E-05	4.68E-05	1.20E-04
40.00	7.34E-06	3.28E-10	9.93E-10	1.12E-08	3.45E-07	1.76E-06	8.32E-06	1.96E-05

Table A-4

2.5-Hz Spectral Velocity Hazard Curves

AMPLITUDE	MEAN	FRACTILES						
(cm/sec)		0.100	0.150	0.300	0.500	0.700	0.850	0.900
0.10	3.73E-02	1.23E-02	1.57E-02	2.42E-02	2.70E-02	4.48E-02	5.87E-02	6.33E-02
1.00	4.83E-03	1.14E-03	1.44E-03	2.20E-03	3.11E-03	4.37E-03	1.01E-02	1.16E-02
5.00	4.06E-04	2.73E-05	4.46E-05	9.57E-05	1.92E-04	3.63E-04	1.00E-03	1.23E-03
10.00	1.12E-04	2.67E-06	3.58E-06	1.28E-05	3.11E-05	8.04E-05	2.04E-04	3.72E-04
20.01	2.83E-05	6.98E-08	1.35E-07	9.23E-07	3.04E-06	1.34E-05	3.40E-05	8.67E-05
29.99	1.20E-05	4.47E-09	9.78E-09	1.31E-07	6.54E-07	3.53E-06	1.33E-05	3.26E-05
50.00	3.74E-06	3.30E-10	4.17E-10	6.00E-09	5.45E-08	5.92E-07	3.14E-06	8.35E-06

Table A-5

5-Hz Spectral Velocity Hazard Curves

AMPLITUDE (cm/sec)	MEAN	FRACTILES 0.100	0.150	0.300	0.500	0.700	0.850	0.900
0.10	3.31E-02	1.05E-02	1.13E-02	1.80E-02	2.43E-02	3.66E-02	5.32E-02	6.09E-02
1.00	4.16E-03	8.24E-04	1.26E-03	1.93E-03	3.10E-03	4.39E-03	7.76E-03	9.18E-03
5.00	3.47E-04	2.52E-05	5.17E-05	8.51E-05	1.90E-04	3.53E-04	7.52E-04	9.66E-04
10.00	8.62E-05	2.05E-06	5.34E-06	1.09E-05	3.27E-05	7.17E-05	1.64E-04	2.71E-04
20.01	1.74E-05	5.62E-08	1.91E-07	5.91E-07	2.91E-06	1.01E-05	2.54E-05	5.25E-05
29.99	6.12E-06	4.09E-09	1.55E-08	6.32E-08	4.22E-07	2.41E-06	7.83E-06	1.65E-05

Table A-6

10-Hz Spectral Velocity Hazard Curves

AMPLITUDE (cm/sec)	MEAN	FRACTILES 0.100	0.150	0.300	0.500	0.700	0.850	0.900
0.10	2.39E-02	8.21E-03	8.83E-03	1.28E-02	1.74E-02	2.53E-02	3.95E-02	4.30E-02
1.00	2.69E-03	5.55E-04	8.91E-04	1.24E-03	1.98E-03	2.83E-03	5.01E-03	5.93E-03
2.00	9.57E-04	1.52E-04	2.52E-04	4.07E-04	6.70E-04	1.06E-03	1.97E-03	2.31E-03
5.00	1.62E-04	1.69E-05	2.48E-05	5.47E-05	1.02E-04	1.65E-04	3.22E-04	3.97E-04
10.00	2.82E-05	9.18E-07	1.89E-06	6.44E-06	1.37E-05	2.73E-05	5.18E-05	7.15E-05
20.01	3.34E-06	1.73E-08	4.23E-08	2.64E-07	7.21E-07	2.75E-06	5.67E-06	7.95E-06
29.99	7.88E-07	9.45E-10	2.65E-09	2.33E-08	1.03E-07	4.78E-07	1.02E-06	1.96E-06

Table A-7

25-Hz Spectral Velocity Hazard Curves

AMPLITUDE	MEAN	FRACTILES						
(cm/sec)		0.100	0.150	0.300	0.500	0.700	0.850	0.900
0.10	1.13E-02	5.09E-03	6.45E-03	7.82E-03	1.00E-02	1.30E-02	1.70E-02	1.90E-02
0.50	2.15E-03	6.93E-04	9.70E-04	1.48E-03	2.18E-03	2.72E-03	3.18E-03	3.41E-03
1.00	7.61E-04	1.95E-04	2.86E-04	5.07E-04	7.35E-04	9.94E-04	1.22E-03	1.36E-03
2.00	2.11E-04	4.03E-05	5.89E-05	1.17E-04	2.00E-04	2.77E-04	3.70E-04	4.16E-04
5.00	2.20E-05	1.58E-06	2.75E-06	5.91E-06	1.84E-05	2.69E-05	4.61E-05	5.44E-05
10.00	2.25E-06	3.91E-08	8.38E-08	2.04E-07	1.20E-06	2.47E-06	5.27E-06	7.26E-06
20.01	1.32E-07	4.91E-10	8.55E-10	1.76E-09	2.77E-08	1.12E-07	2.96E-07	4.79E-07

Table A-8

Median uniform-hazard spectra (5 % damping)

FREQ	ANNUAL EXCEEDANCE PROBABILITY			
(Hz)	2E-3	1E-3	2E-4	1E-4
0.50	0.651	1.17	3.29	5.08
1.00	0.958	1.45	3.67	5.38
2.50	1.29	1.93	4.89	6.41
5.00	1.29	1.92	4.86	6.43
10.00	0.989	1.54	3.60	5.04
25.00	0.530	0.823	1.99	2.60

A.2 COMBINED RESULTS FROM EPRI/SOG AND LLNL ANALYSES

Table A-9

Peak Ground Acceleration Hazard Curves (all LLNL G-experts)

AMPLITUDE (cm/sec2)	MEAN	0.050	0.150	0.250	0.350	0.450	0.500	0.550	0.650	0.750	0.850	0.950
5.000E+00	3.543E-01	6.457E-03	9.120E-03	1.334E-02	1.698E-02	2.570E-02	2.851E-02	3.273E-02	8.035E-02	1.778E-01	6.607E-01	9.333E-01
5.000E+01	1.044E-02	1.549E-04	5.188E-04	8.710E-04	1.365E-03	1.679E-03	2.065E-03	2.291E-03	2.630E-03	4.571E-03	1.288E-02	6.531E-02
9.998E+01	3.356E-03	4.467E-05	1.445E-04	2.512E-04	4.365E-04	5.188E-04	6.166E-04	7.586E-04	9.661E-04	1.413E-03	3.846E-03	2.089E-02
2.499E+02	5.392E-04	5.248E-06	1.698E-05	3.631E-05	5.689E-05	6.761E-05	8.913E-05	9.550E-05	1.603E-04	1.778E-04	4.842E-04	3.350E-03
5.002E+02	8.874E-05	4.074E-07	1.622E-06	3.467E-06	5.623E-06	7.943E-06	9.441E-06	1.202E-05	2.089E-05	2.851E-05	7.762E-05	5.559E-04
6.999E+02	3.353E-05	6.998E-08	3.199E-07	7.852E-07	1.514E-06	2.065E-06	2.818E-06	3.236E-06	6.457E-06	1.047E-05	2.754E-05	2.113E-04
1.000E+03	1.100E-05	6.683E-09	3.388E-08	1.216E-07	2.512E-07	3.802E-07	5.370E-07	7.079E-07	1.318E-06	2.818E-06	7.943E-06	6.531E-05
1.300E+03	4.400E-06	6.839E-10	5.070E-09	2.239E-08	5.309E-08	8.318E-08	1.349E-07	1.905E-07	3.311E-07	8.128E-07	2.630E-06	2.661E-05

Table A-10

Median uniform-hazard spectra (5 % damping, all LLNL G-experts)

FREQ	ANNUAL EXCEEDANCE PROBABILITY			
(Hz)	2E-3	1E-3	2E-4	1E-4
0.50	1.09	1.92	5.18	8.21
1.00	1.60	2.37	5.76	8.03
2.00	1.57	2.41	6.05	8.18
5.00	1.47	2.17	5.27	7.09
10.00	1.18	1.77	3.98	5.41
25.00	0.522	0.818	2.02	2.63

Table A-11

Peak Ground Acceleration Hazard Curves (4 LLNL G-experts)

AMPLITUDE (cm/sec2)	MEAN	0.050	0.150	0.250	0.350	0.450	0.500	0.550	0.650	0.750	0.850	0.950
5.000E+00	1.907E-01	6.457E-03	9.120E-03	1.334E-02	1.698E-02	2.089E-02	2.851E-02	2.951E-02	4.467E-02	9.550E-02	2.344E-01	7.328E-01
5.000E+01	4.422E-03	1.349E-04	4.519E-04	7.328E-04	1.000E-03	1.622E-03	1.679E-03	2.065E-03	2.455E-03	3.715E-03	5.623E-03	2.239E-02
9.998E+01	1.329E-03	3.631E-05	1.216E-04	2.344E-04	3.090E-04	4.677E-04	5.188E-04	6.166E-04	7.852E-04	1.072E-03	1.738E-03	6.683E-03
2.499E+02	1.930E-04	4.571E-06	1.288E-05	2.570E-05	4.169E-05	6.310E-05	6.761E-05	8.913E-05	1.096E-04	1.603E-04	2.512E-04	9.661E-04
5.002E+02	2.560E-05	3.548E-07	1.148E-06	2.630E-06	4.571E-06	6.918E-06	8.222E-06	9.441E-06	1.429E-05	2.089E-05	3.162E-05	1.259E-04
6.999E+02	7.882E-06	6.095E-08	2.692E-07	6.166E-07	1.148E-06	1.862E-06	2.138E-06	2.723E-06	4.266E-06	7.161E-06	1.047E-05	4.315E-05
1.000E+03	1.874E-06	5.623E-09	3.273E-08	8.913E-08	1.778E-07	3.548E-07	3.802E-07	5.188E-07	9.561E-07	1.862E-06	3.126E-06	1.202E-05
1.300E+03	5.762E-07	5.012E-10	4.571E-09	1.479E-08	3.388E-08	7.244E-08	8.318E-08	1.303E-07	2.512E-07	5.370E-07	1.109E-06	4.121E-06

Table A-12

Median uniform-hazard spectra (5 % damping, 4 LLNL G-experts)

FREQ	ANNUAL EXCEEDANCE PROBABILITY			
(Hz)	2E-3	1E-3	2E-4	1E-4
0.50	0.97	1.63	4.10	6.04
1.00	1.42	2.01	4.55	6.49
2.00	1.49	2.17	5.21	7.15
5.00	1.41	2.11	5.26	6.94
10.00	1.07	1.65	3.66	5.04
25.00	0.499	0.752	1.87	2.49

Table A-13

Median uniform-hazard spectra (other damping ratios, rock, all LLNL G-experts)

PSV (cm/sec)

DAMPING RATIO (%)	FREQ. (Hz)	ANNAUL EXCEEDANCE PROBABILITY 2.E-3	1.E-3	2.E-4	1.E-4
2	0.5	1.24	2.18	5.88	9.32
	1.0	1.93	2.86	6.95	9.70
	2.0	2.02	3.09	7.77	10.50
	5.0	2.01	2.97	7.20	9.69
	10.0	1.66	2.49	5.60	7.61
	25.0	0.75	1.17	2.90	3.77
7	0.5	1.02	1.80	4.84	7.68
	1.0	1.46	2.17	5.26	7.34
	2.0	1.41	2.16	5.43	7.34
	5.0	1.30	1.92	4.65	6.26
	10.0	1.04	1.55	3.49	4.75
	25.0	0.46	0.71	1.76	2.30
10	0.5	0.94	1.65	4.46	7.06
	1.0	1.31	1.95	4.73	6.60
	2.0	1.24	1.91	4.80	6.49
	5.0	1.13	1.67	4.06	5.46
	10.0	0.90	1.35	3.03	4.12
	25.0	0.39	0.62	1.53	1.99
12	0.5	0.89	1.58	4.25	6.74
	1.0	1.24	1.84	4.47	6.23
	2.0	1.17	1.79	4.49	6.08
	5.0	1.06	1.56	3.78	5.09
	10.0	0.84	1.25	2.82	3.83
	25.0	0.37	0.57	1.42	1.85
15	0.5	0.84	1.48	3.99	6.33
	1.0	1.15	1.71	4.15	5.78
	2.0	1.07	1.65	4.14	5.60
	5.0	0.97	1.43	3.47	4.66
	10.0	0.76	1.15	2.58	3.51
	25.0	0.33	0.52	1.30	1.69

Appendix B

SPECTRA FROM RECORDS USED IN SECTION 5

This appendix contains the response spectra for the records that were used in Section 5 to investigate the spectral shapes associated with the dominant magnitudes and distances. These spectra were calculated for all three components of motion and for damping ratios of 2, 5, 7, 10, 12, and 15 percent of critical. The figures follow the same sequence as Table 5–4. For the sake of clarity, the time of occurrence (in Universal Time) is specified for the multiple earthquakes that occurred in Nahanni on December 23 and 25, 1985.

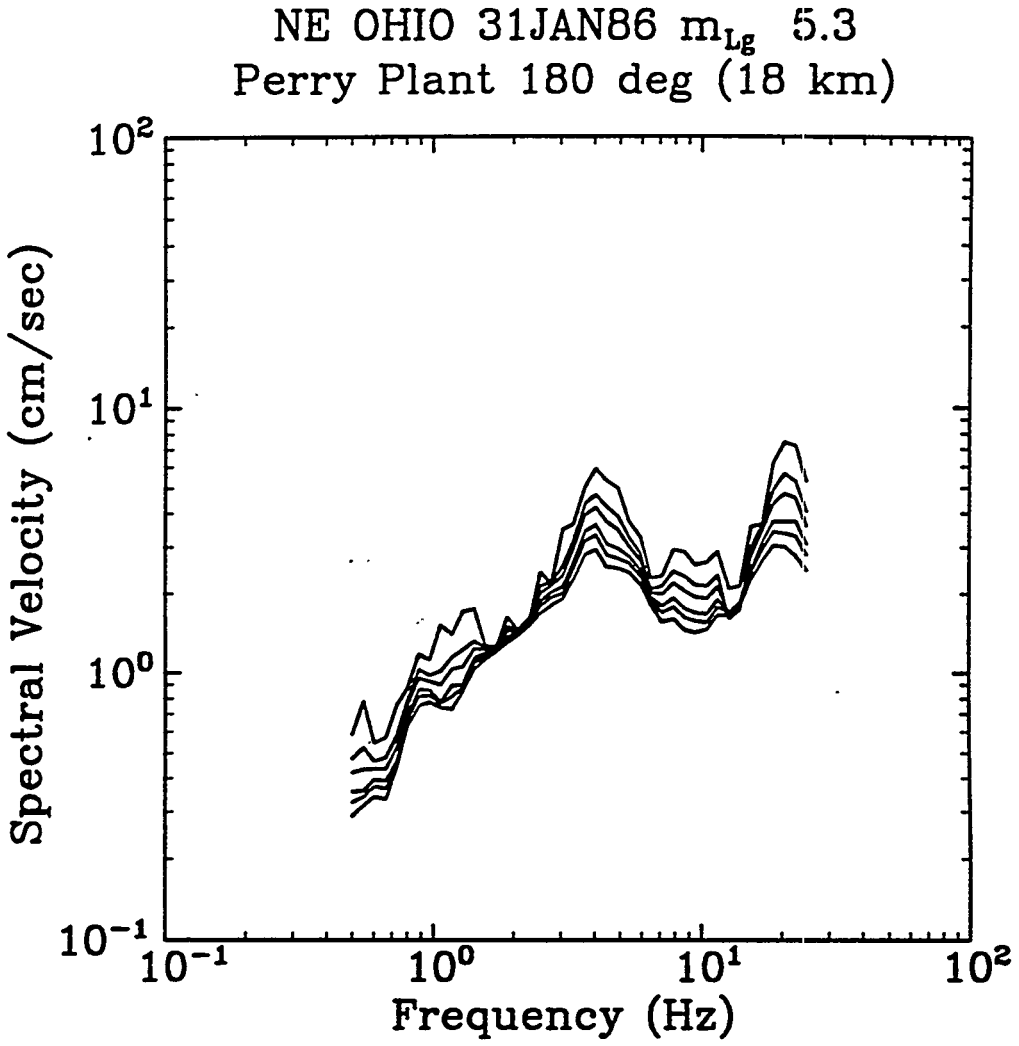

Figure B-1. Response spectra from the 31 January 1986, NE Ohio earthquake recorded at the Perry Plant; 180-degree component. Damping ratios: 2 (top), 5, 7, 10, 12, and 15 percent of critical (bottom).

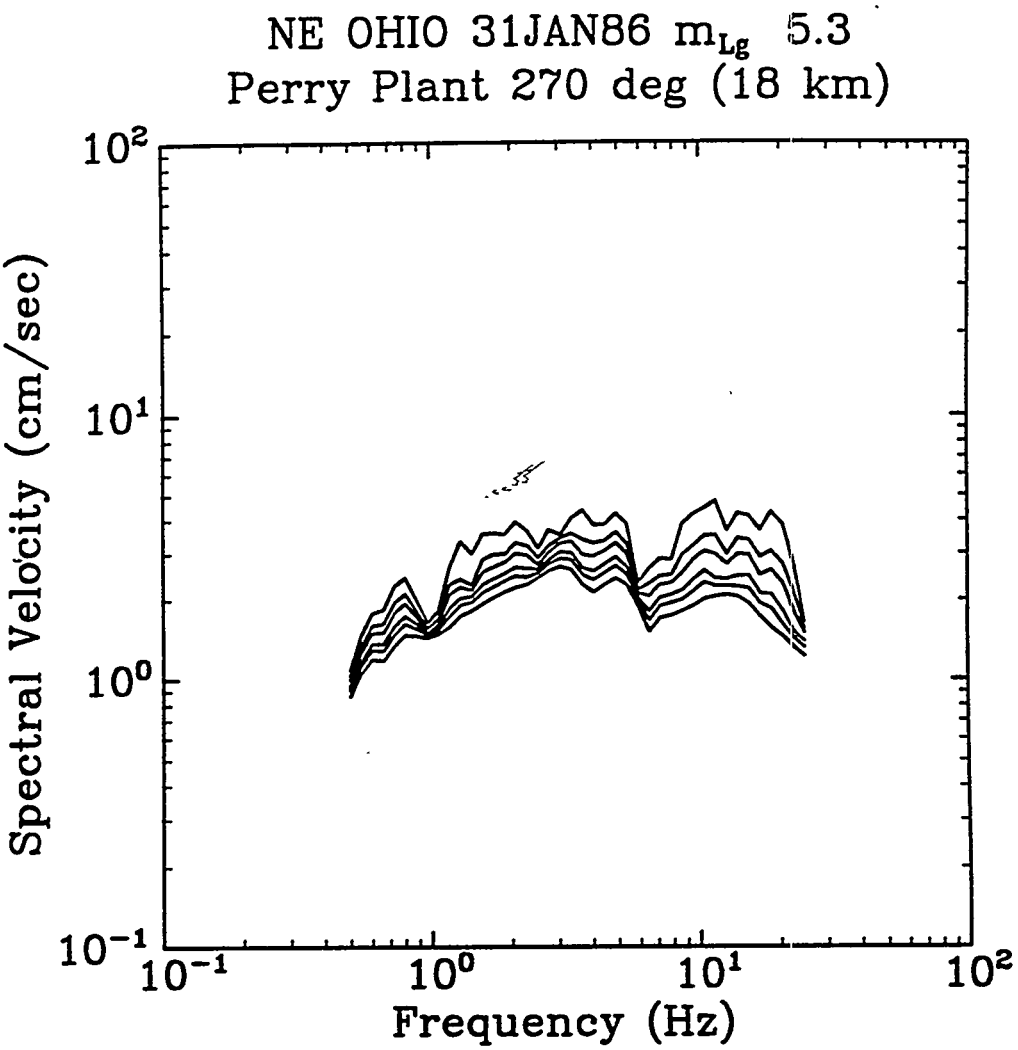

Figure B-2. Response spectra from the 31 January 1986, NE Ohio earthquake recorded at the Perry Plant; 270-degree component. Damping ratios: 2 (top), 5, 7, 10, 12, and 15 percent of critical (bottom).

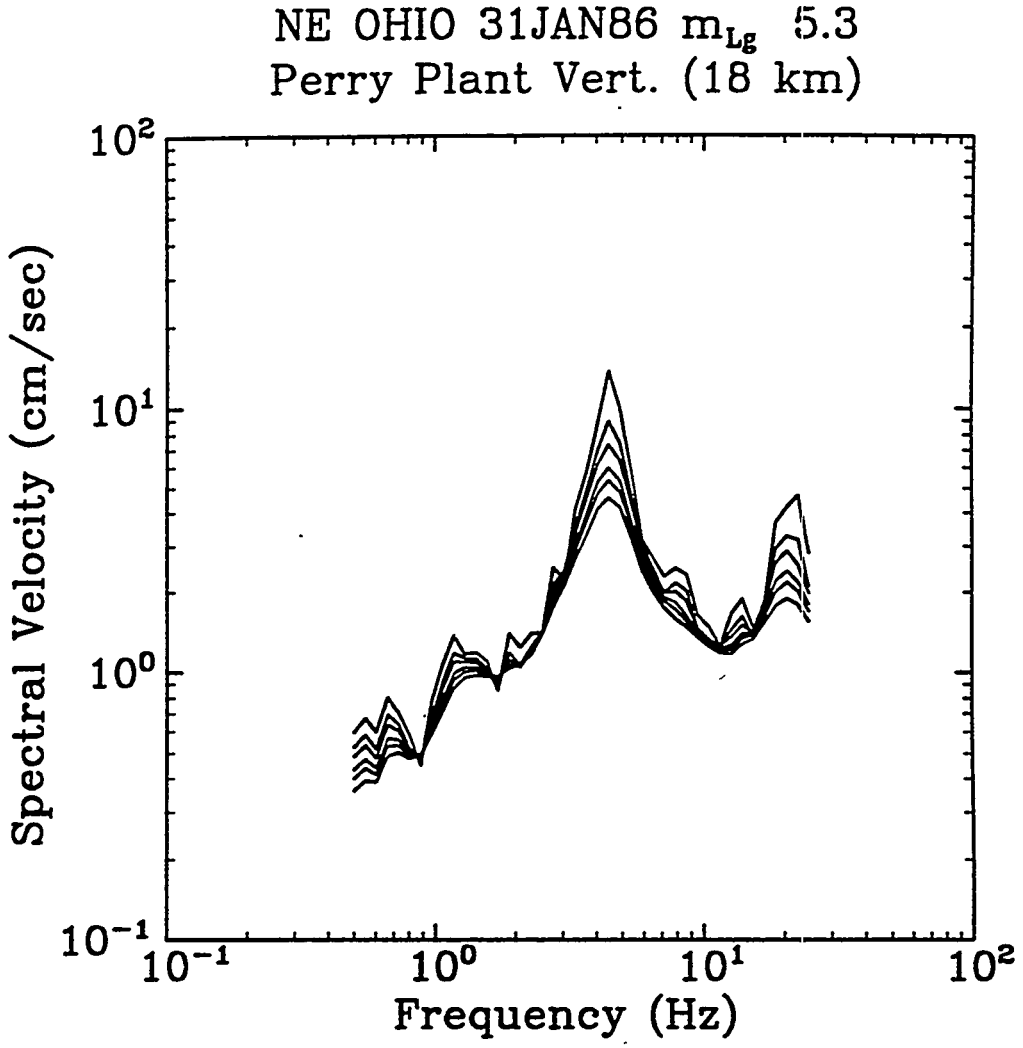

Figure B-3. Response spectra from the 31 January 1986, NE Ohio earthquake recorded at the Perry Plant; vertical component. Damping ratios: 2 (top), 5, 7, 10, 12, and 15 percent of critical (bottom).

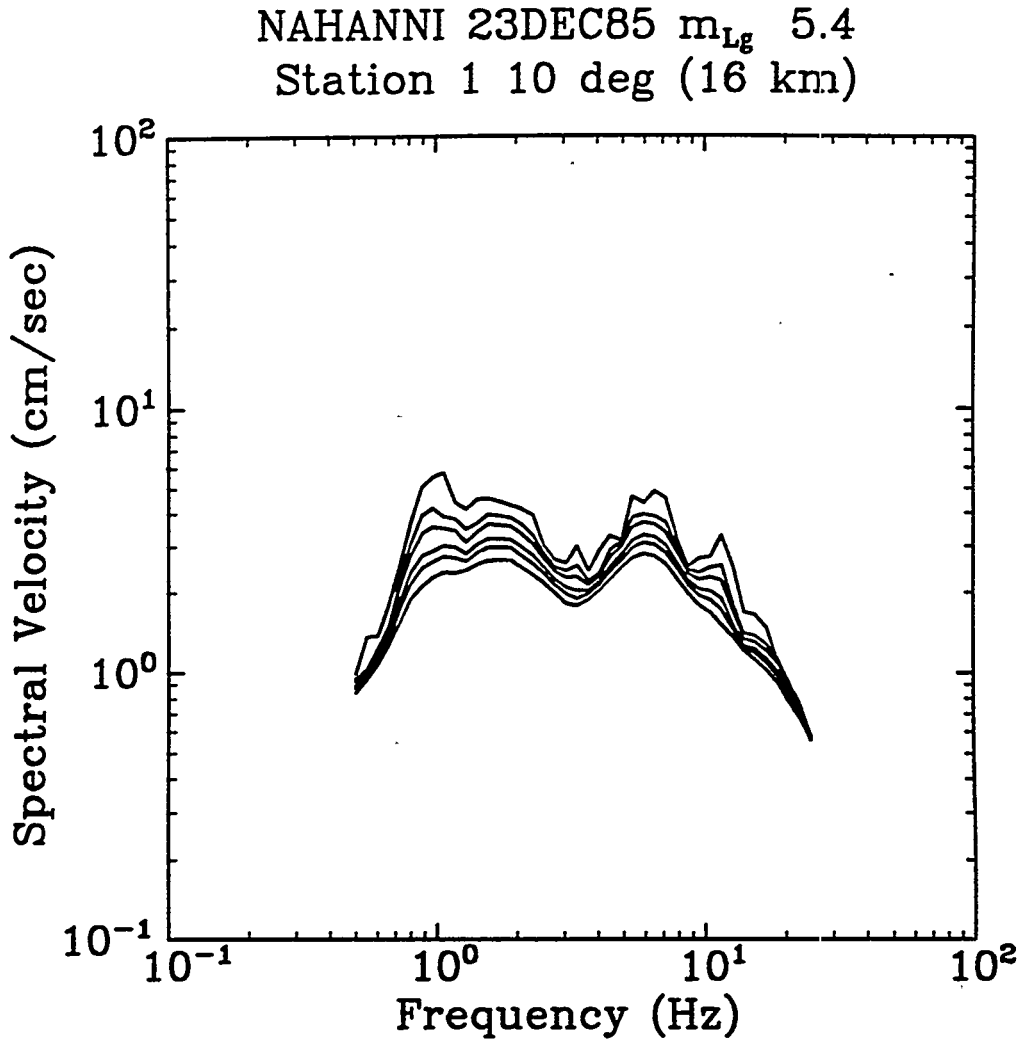

Figure B-4. Response spectra from the 23 December 1985 (19:37 UT), Nahanni earthquake recorded at station 1; 10-degree component. Damping ratios: 2 (top), 5, 7, 10, 12, and 15 percent of critical (bottom).

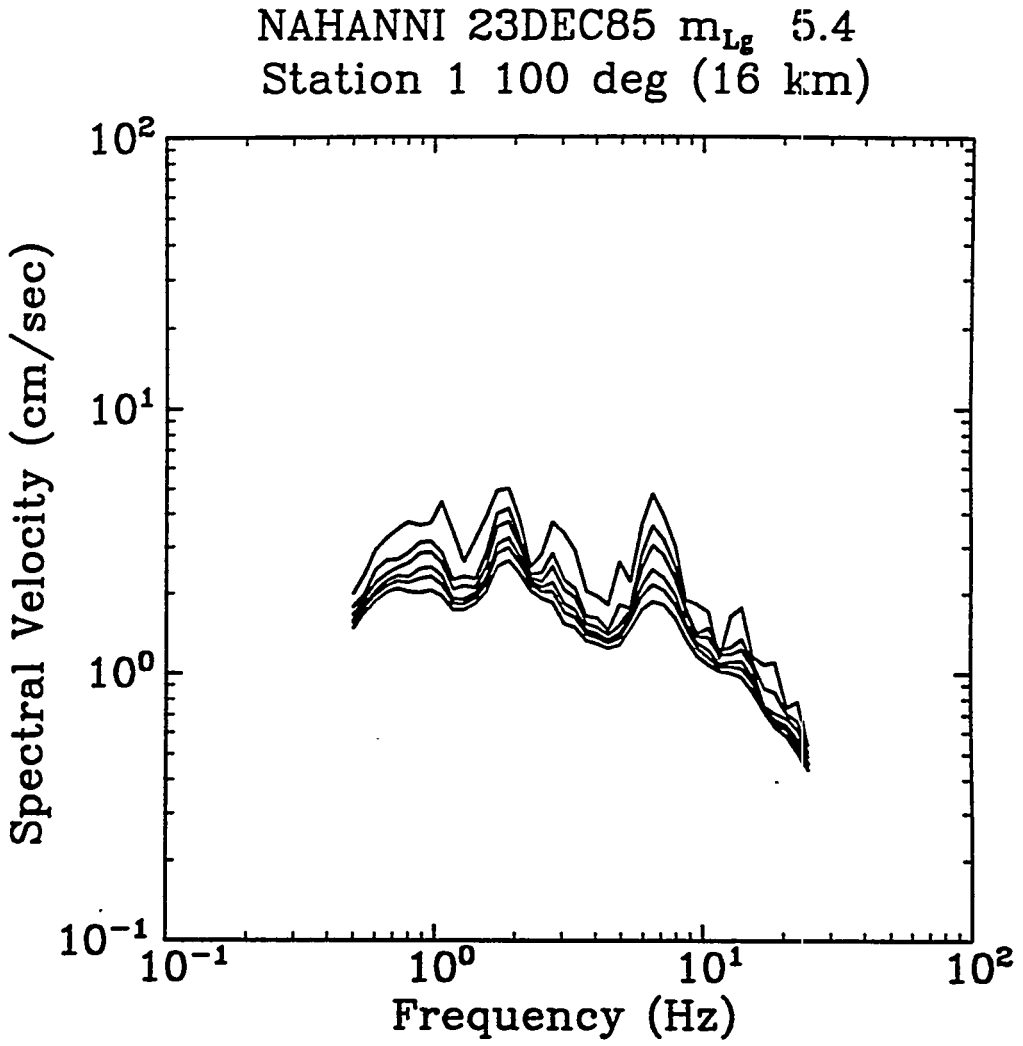

Figure B-5. Response spectra from the 23 December 1985 (19:37 UT), Nahanni earthquake recorded at station 1; 100-degree component. Damping ratios: 2 (top), 5, 7, 10, 12, and 15 percent of critical (bottom).

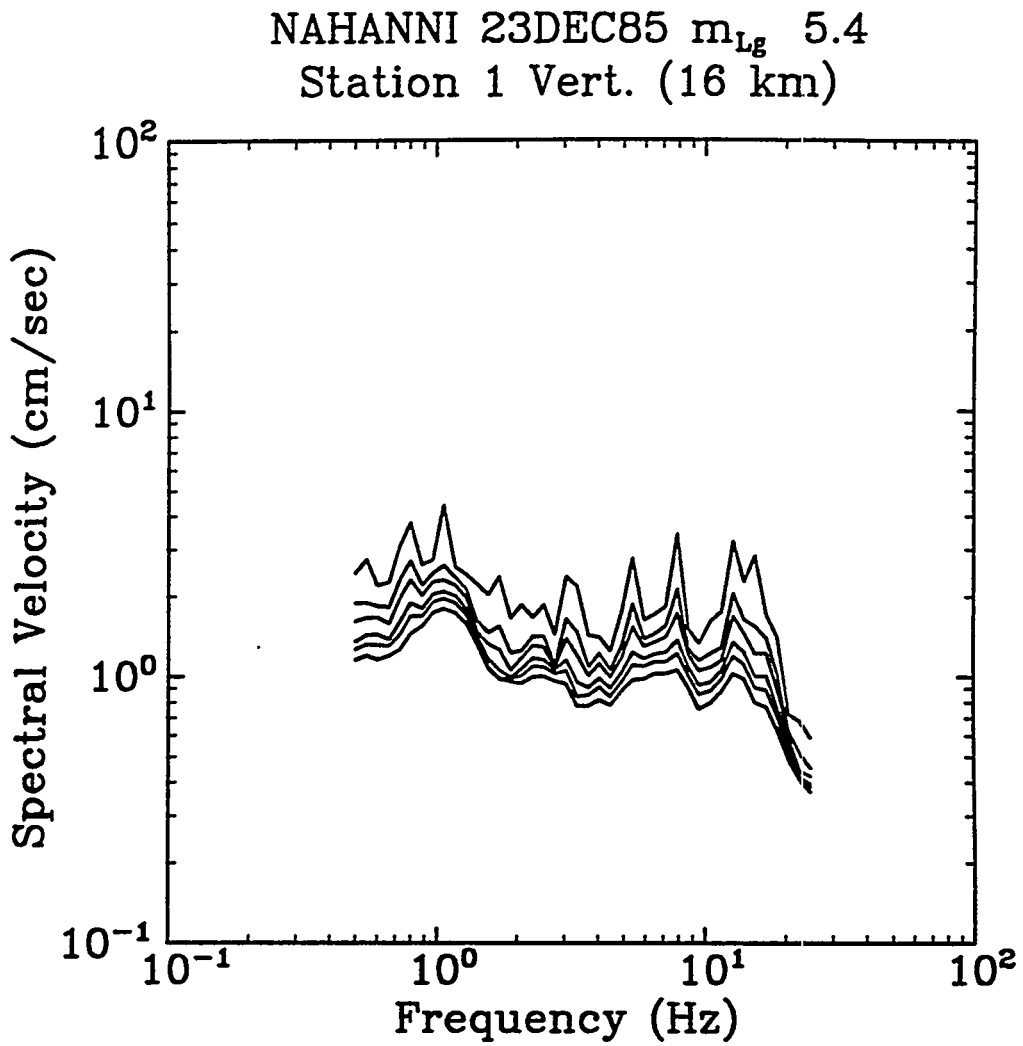

Figure B-6. Response spectra from the 23 December 1985 (19:37 UT), Nahanni earthquake recorded at station 1; vertical component. Damping ratios: 2 (top), 5, 7, 10, 12, and 15 percent of critical (bottom).

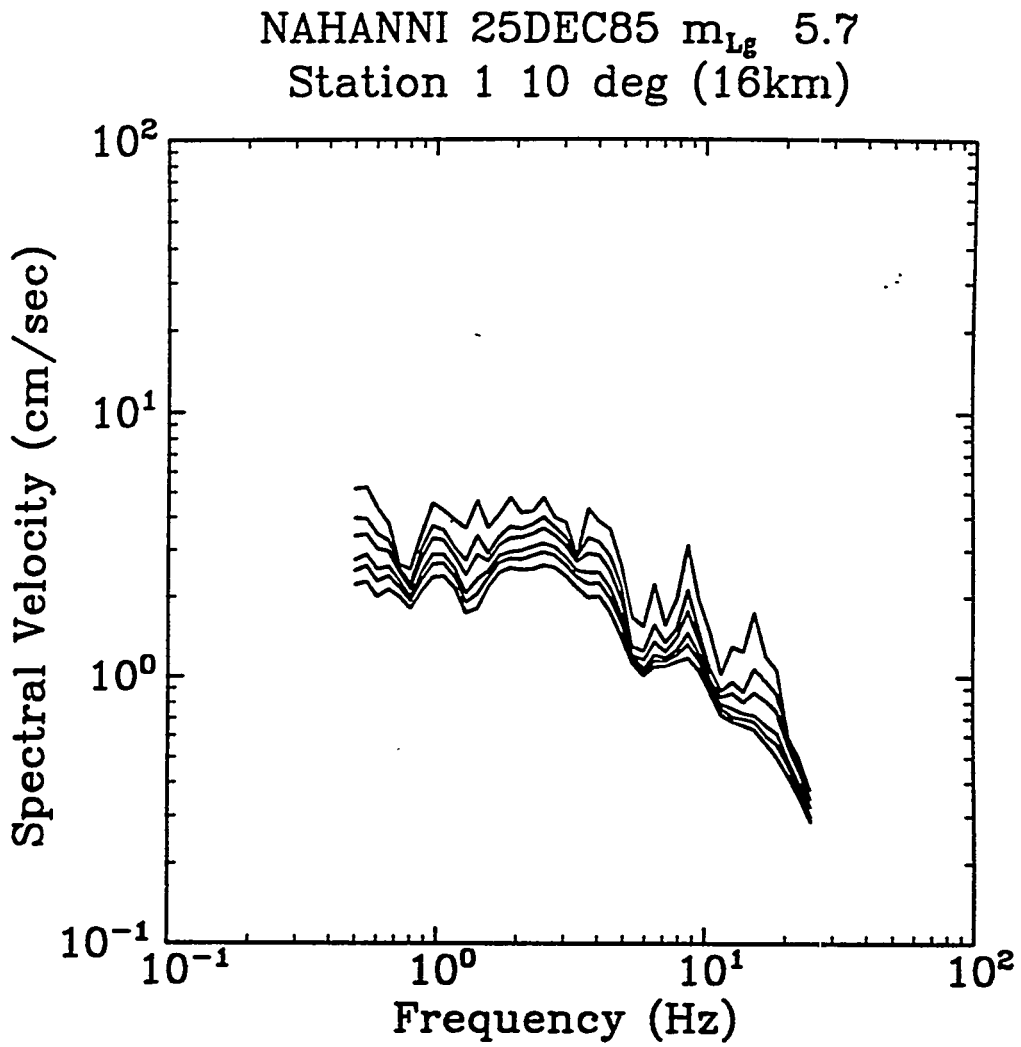

Figure B-7. Response spectra from the 23 December 1985 (15:42 UT), Nahanni earthquake recorded at station 1; 10-degree component. Damping ratios: 2 (top), 5, 7, 10, 12, and 15 percent of critical (bottom).

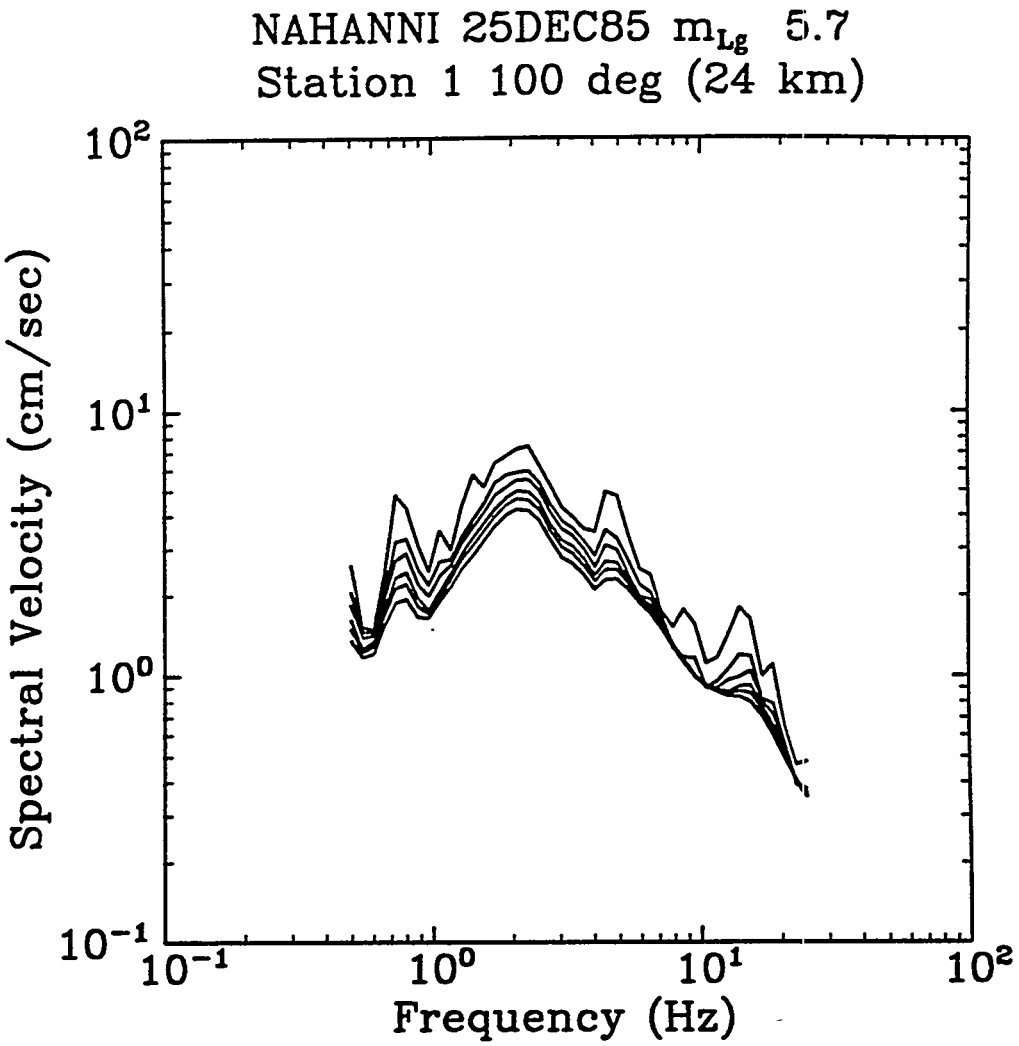

Figure B-8. Response spectra from the 23 December 1985 (15:42 UT), Nahanni earthquake recorded at station 1; 100-degree component. Damping ratios: 2 (top), 5, 7, 10, 12, and 15 percent of critical (bottom).

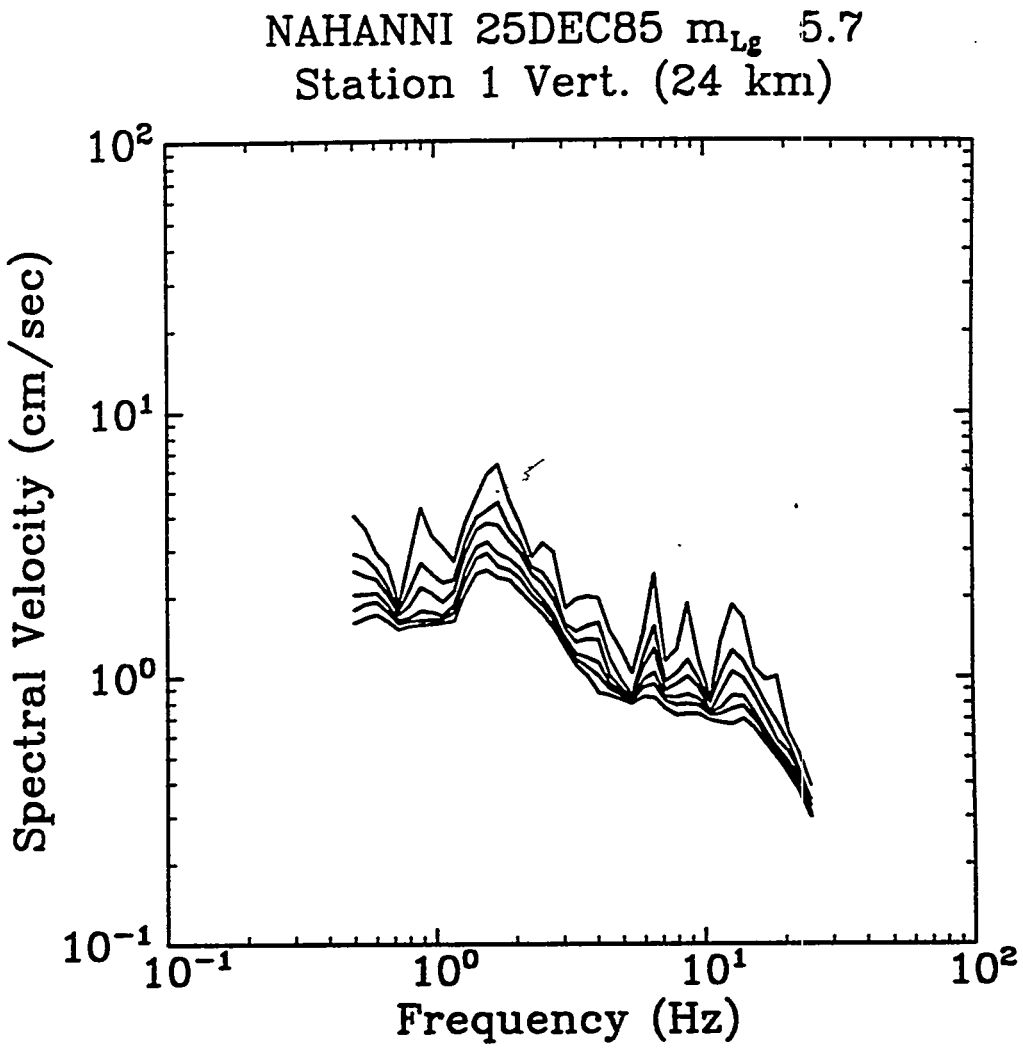

Figure B-9. Response spectra from the 23 December 1985 (15:42 UT), Nahanni earthquake recorded at station 1; vertical component. Damping ratios: 2 (top), 5, 7, 10, 12, and 15 percent of critical (bottom).

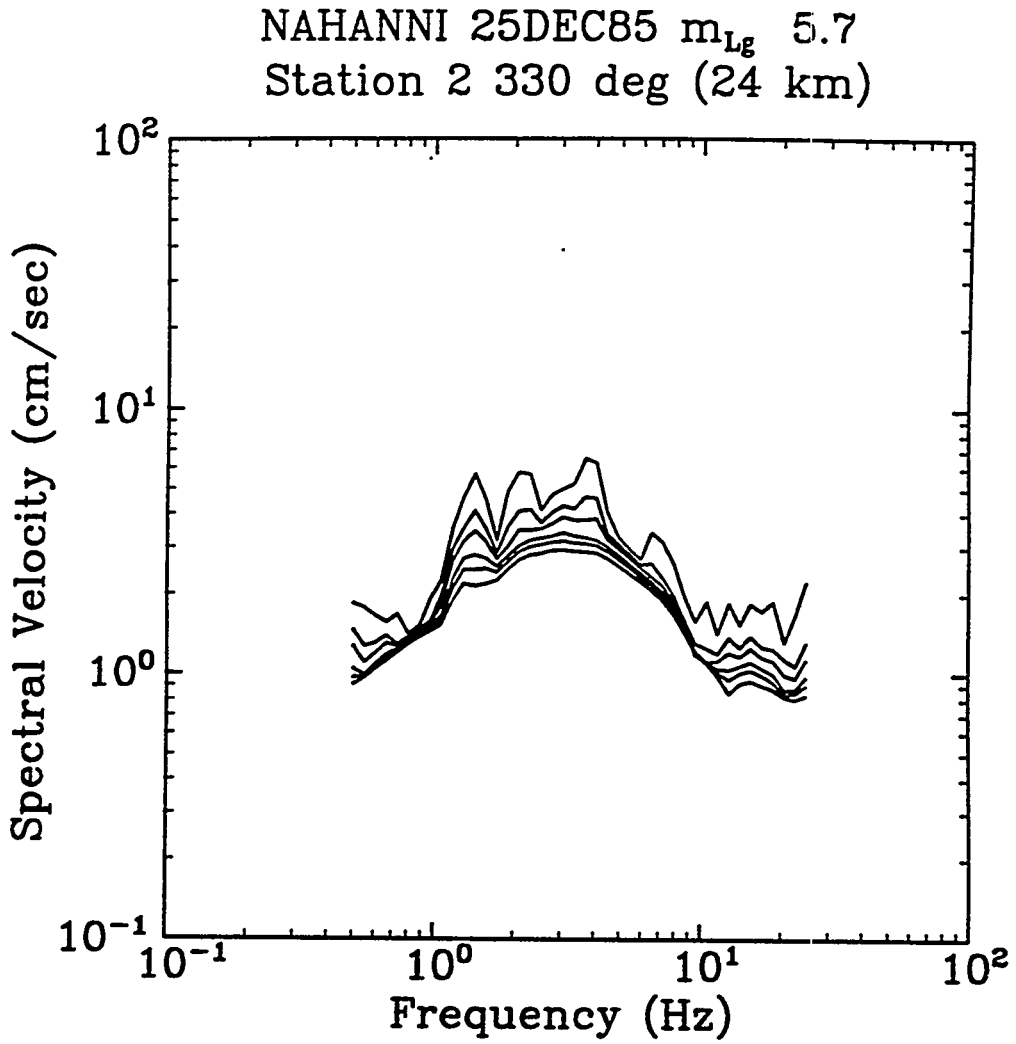

Figure B-10. Response spectra from the 23 December 1985 (15:42 UT), Nahanni earthquake recorded at station 2; 330-degree component. Damping ratios: 2 (top), 5, 7, 10, 12, and 15 percent of critical (bottom).

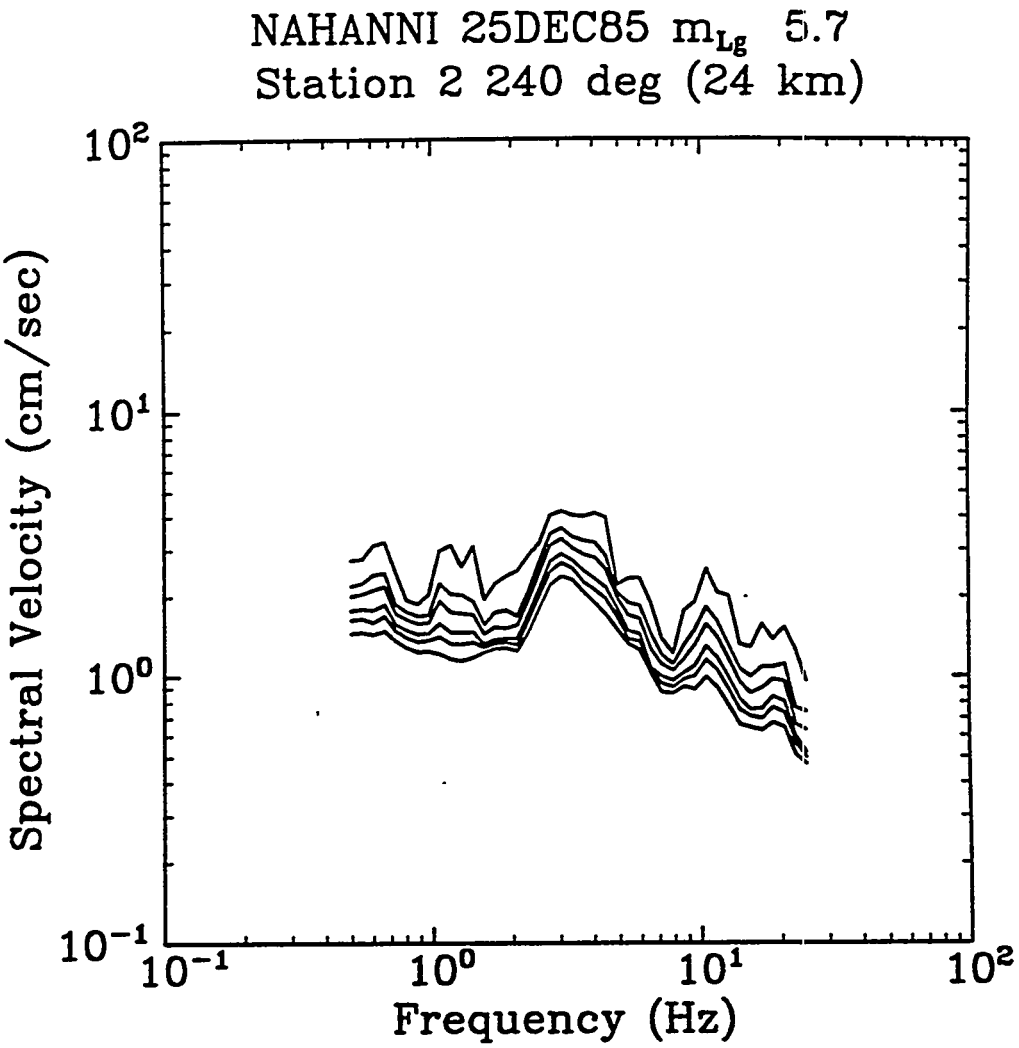

Figure B-11. Response spectra from the 23 December 1985 (15:42 UT), Nahanni earthquake recorded at station 2; 240-degree component. Damping ratios: 2 (top), 5, 7, 10, 12, and 15 percent of critical (bottom).

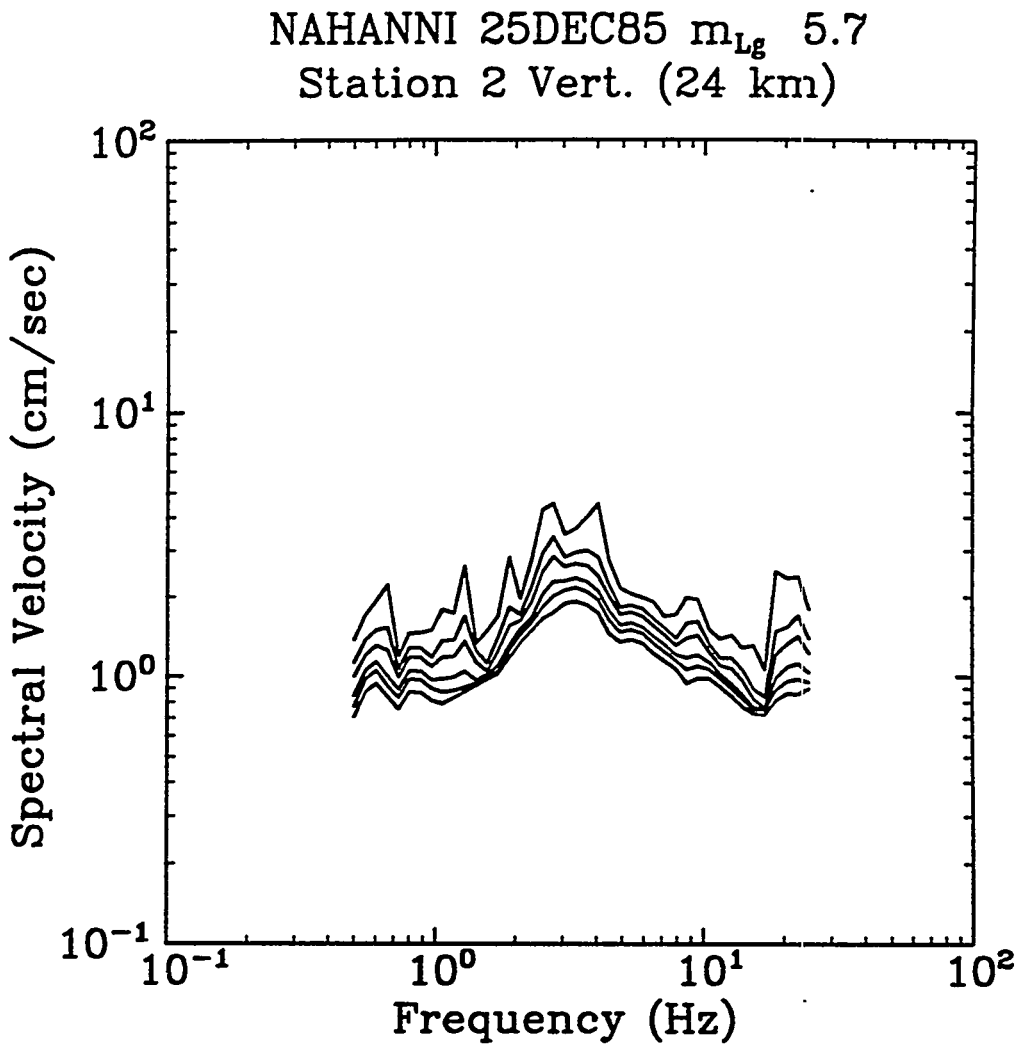

Figure B-12. Response spectra from the 23 December 1985 (15:42 UT), Nahanni earthquake recorded at station 2; vertical component. Damping ratios: 2 (top), 5, 7, 10, 12, and 15 percent of critical (bottom).

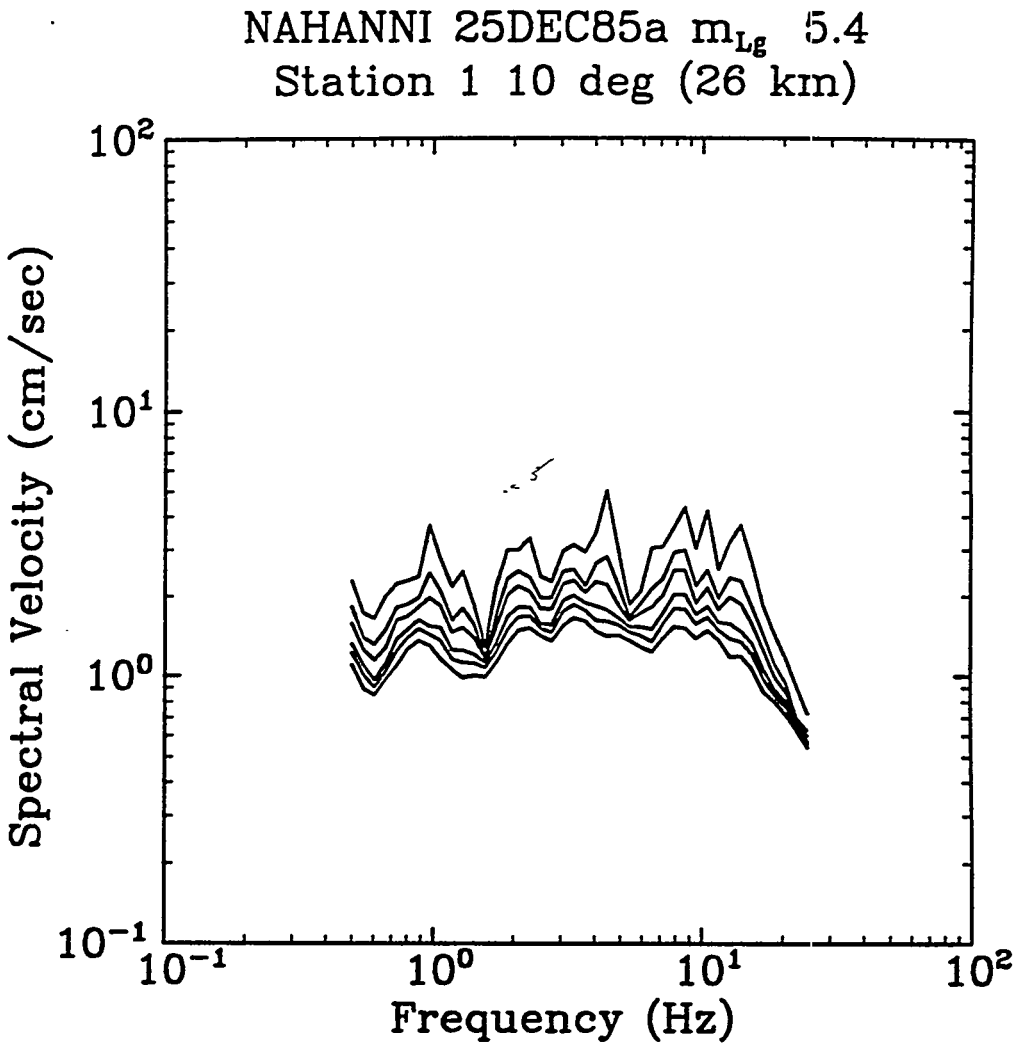

Figure B-13. Response spectra from the 23 December 1985 (18:49 UT), Nahanni earthquake recorded at station 1; 10-degree component. Damping ratios: 2 (top), 5, 7, 10, 12, and 15 percent of critical (bottom).

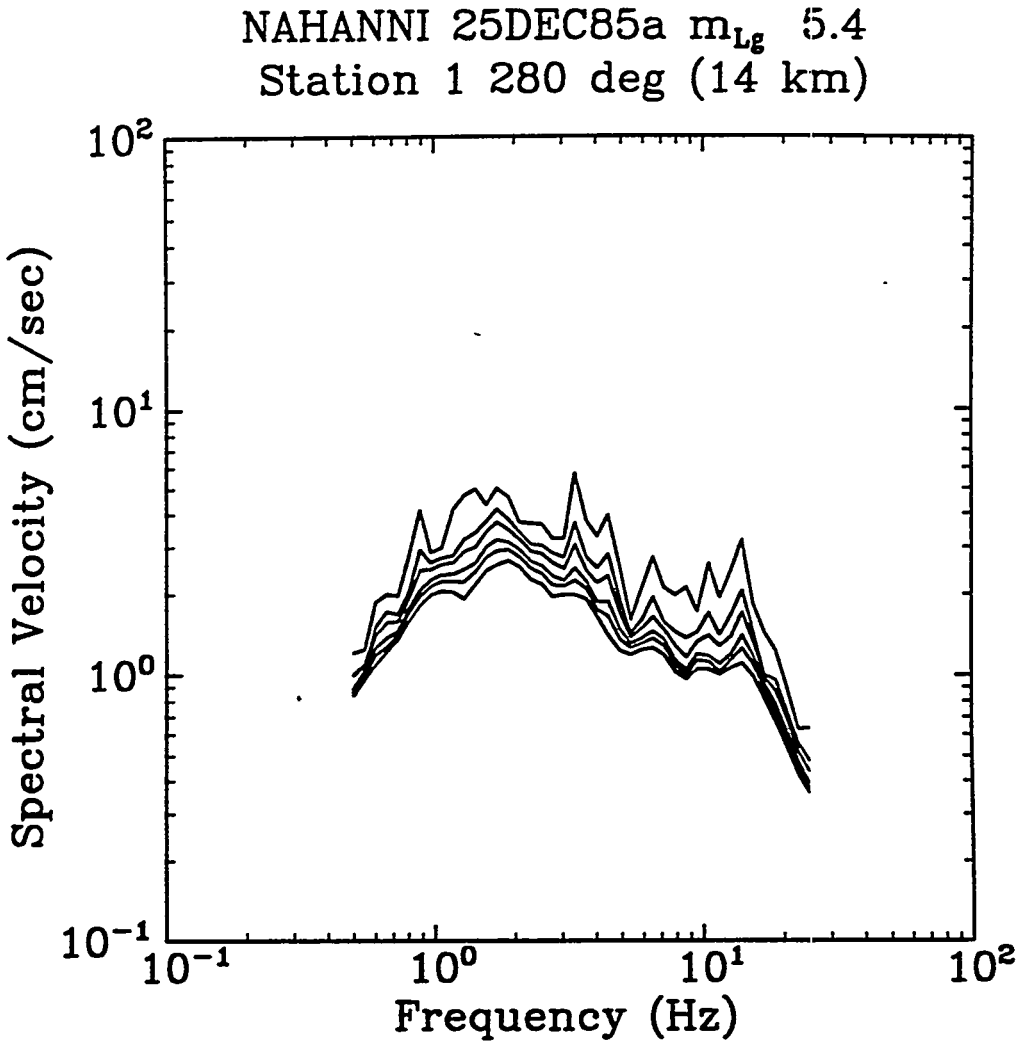

Figure B-14. Response spectra from the 23 December 1985 (18:49 UT), Nahanni earthquake recorded at station 1; 100-degree component. Damping ratios: 2 (top), 5, 7, 10, 12, and 15 percent of critical (bottom).

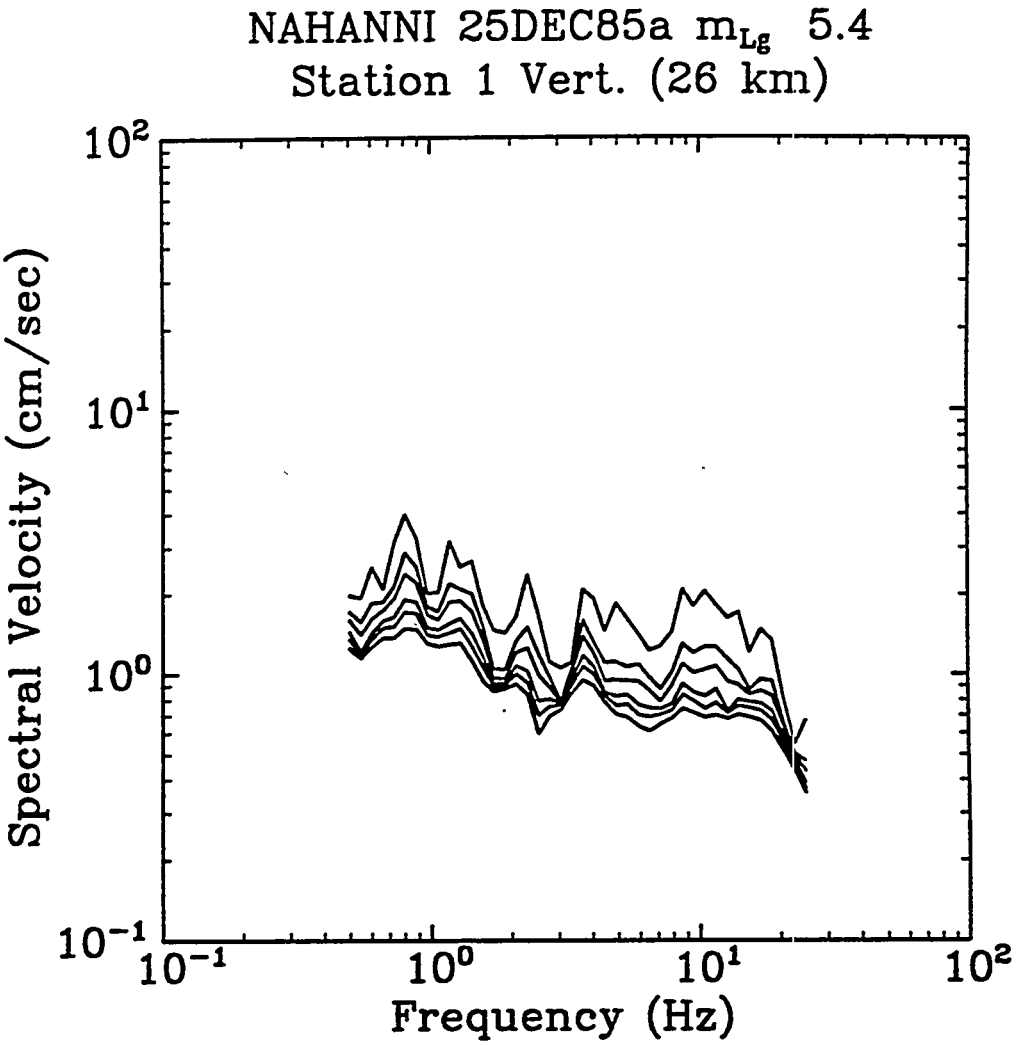

Figure B-15. Response spectra from the 23 December 1985 (18:49 UT), Nahanni earthquake recorded at station 1; vertical component. Damping ratios: 2 (top), 5, 7, 10, 12, and 15 percent of critical (bottom).

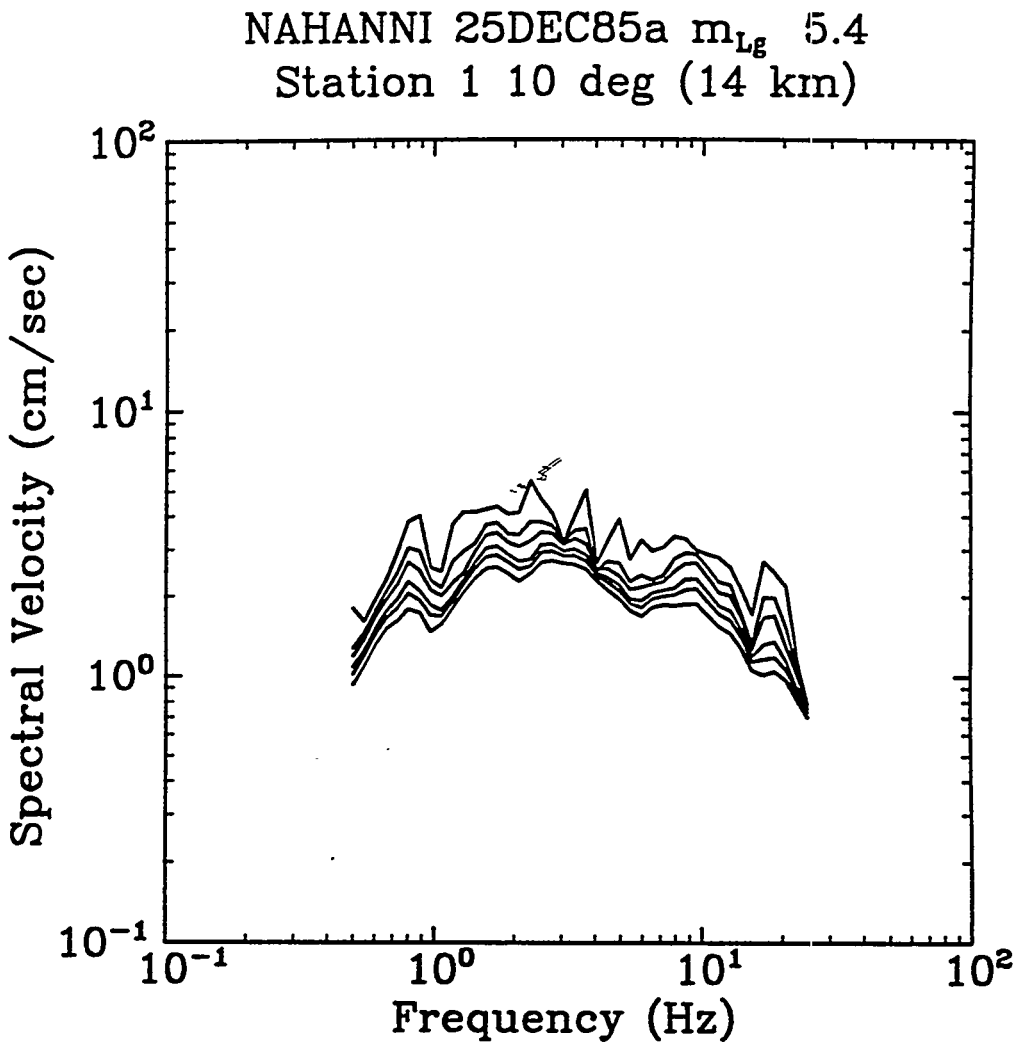

Figure B-16. Response spectra from the 13 February 1986, Nahanni earthquake recorded at station 1; 10-degree component. Damping ratios: 2 (top), 5, 7, 10, 12, and 15 percent of critical (bottom).

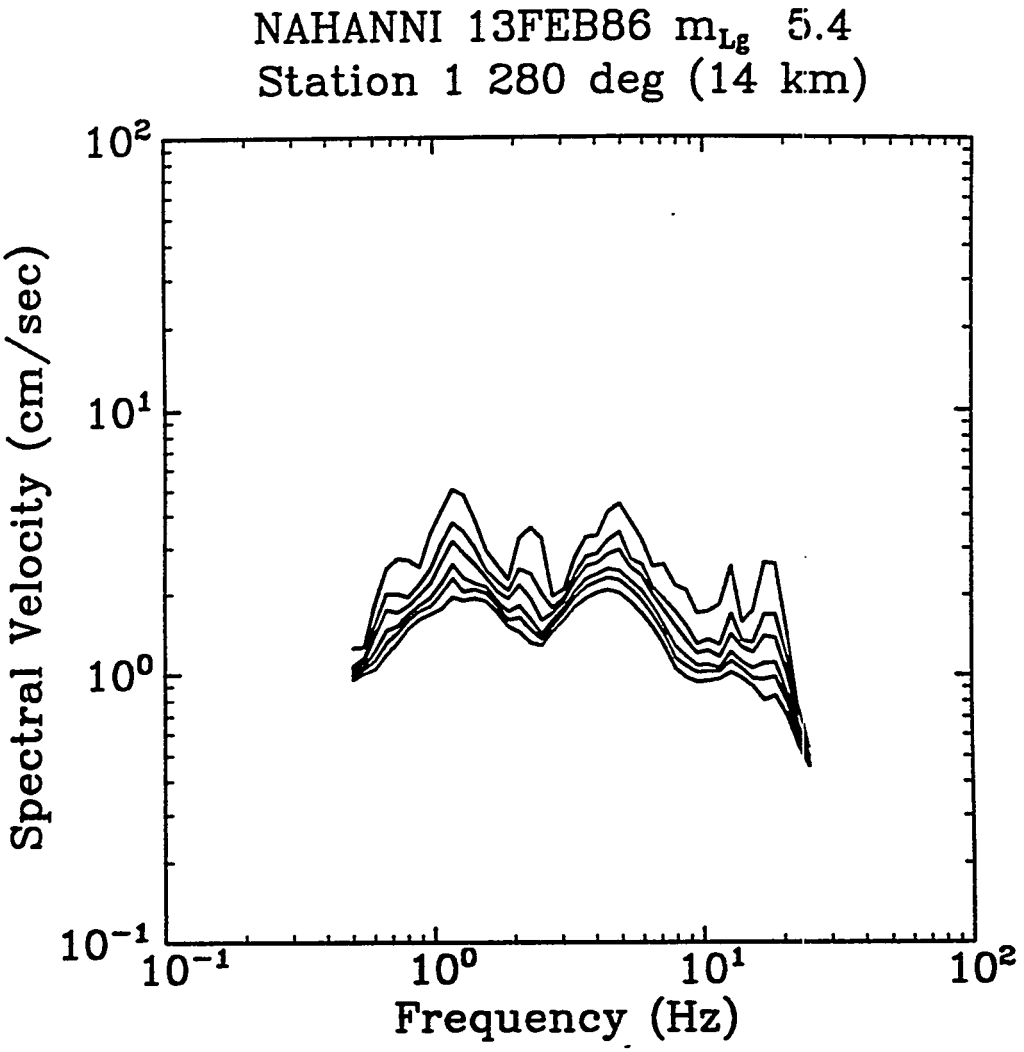

Figure B-17. Response spectra from the 13 February 1986, Nahanni earthquake recorded at station 1; 100-degree component. Damping ratios: 2 (top), 5, 7, 10, 12, and 15 percent of critical (bottom).

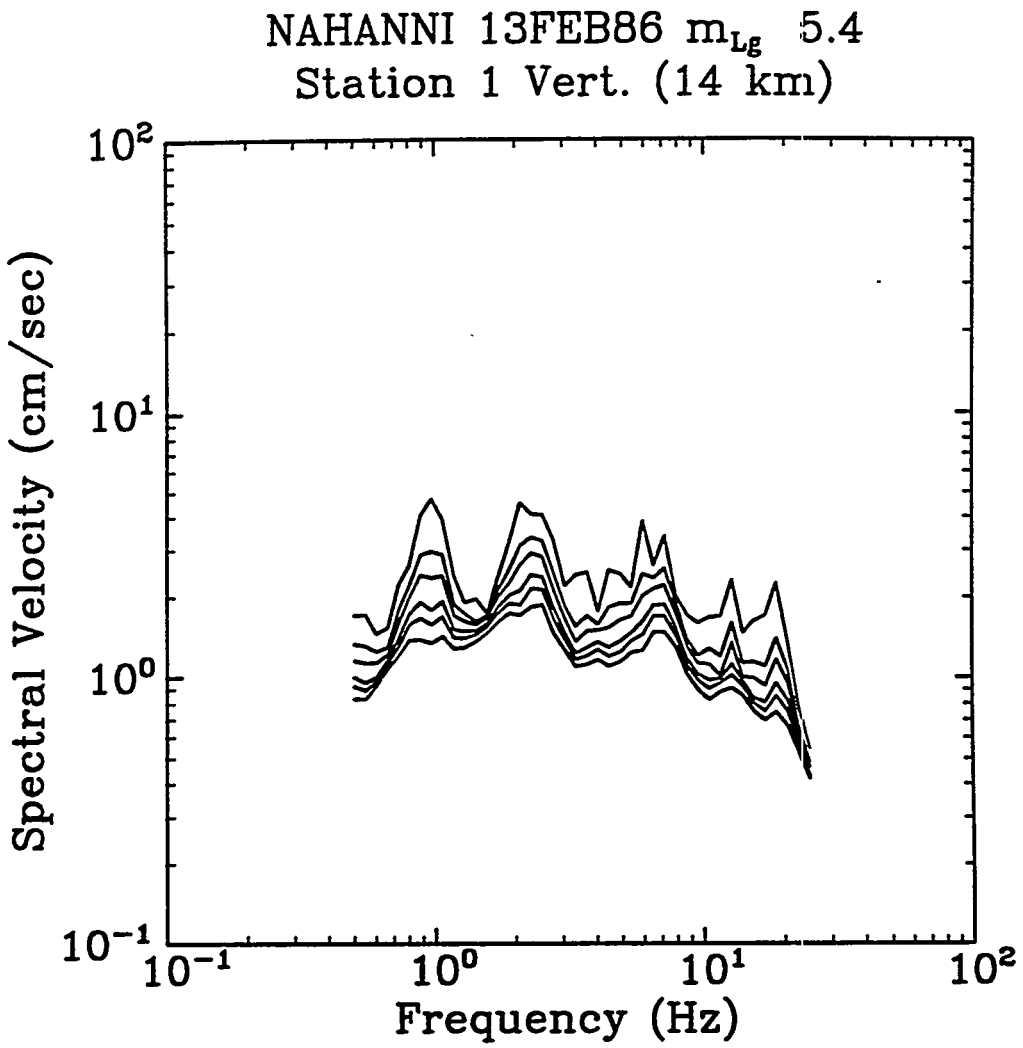

Figure B-18. Response spectra from the 13 February 1986, Nahanni earthquake recorded at station 1; vertical component. Damping ratios: 2 (top), 5, 7, 10, 12, and 15 percent of critical (bottom).

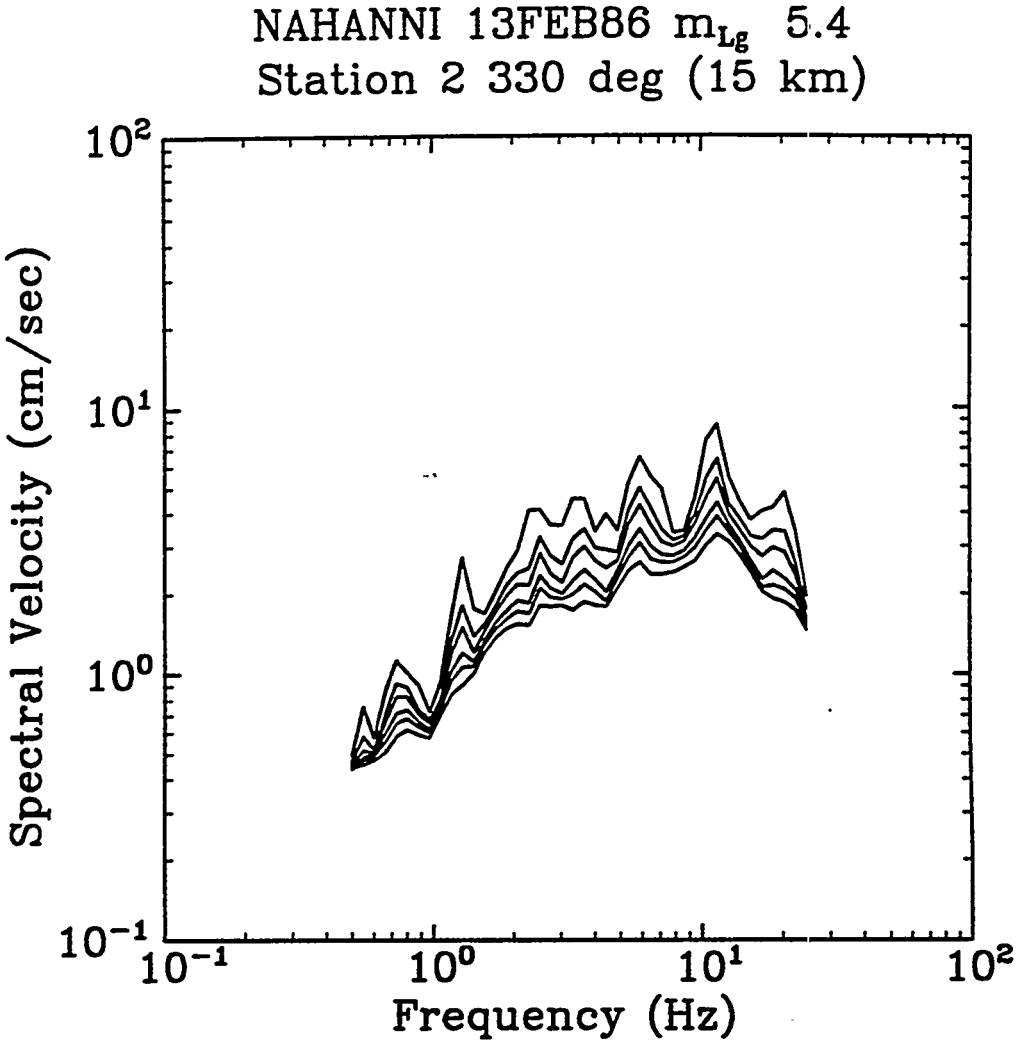

Figure B-19. Response spectra from the 13 February 1986, Nahanni earthquake recorded at station 2; 330-degree component. Damping ratios: 2 (top), 5, 7, 10, 12, and 15 percent of critical (bottom).

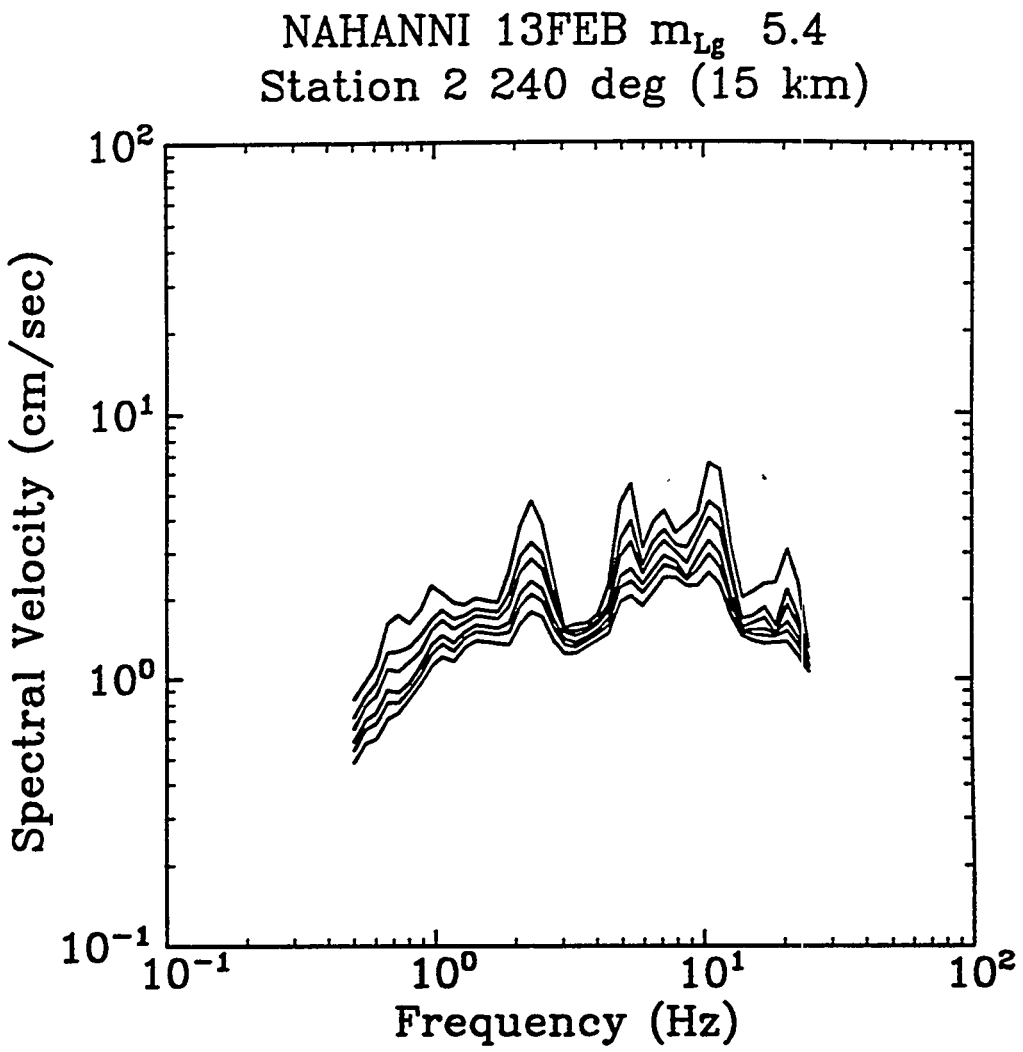

Figure B-20. Response spectra from the 13 February 1986, Nahanni earthquake recorded at station 2; 240-degree component. Damping ratios: 2 (top), 5, 7, 10, 12, and 15 percent of critical (bottom).

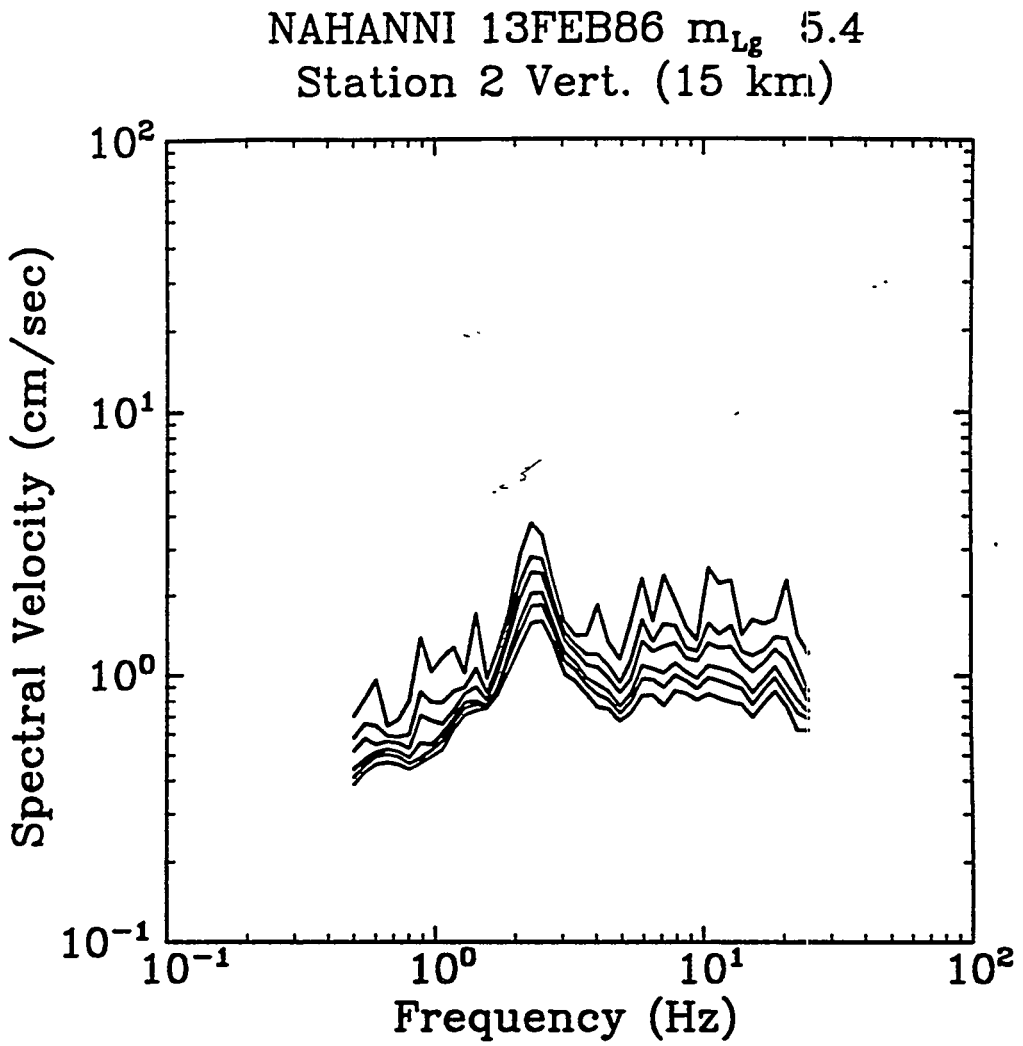

Figure B-21. Response spectra from the 13 February 1986, Nahanni earthquake recorded at station 2; vertical component. Damping ratios: 2 (top), 5, 7, 10, 12, and 15 percent of critical (bottom).

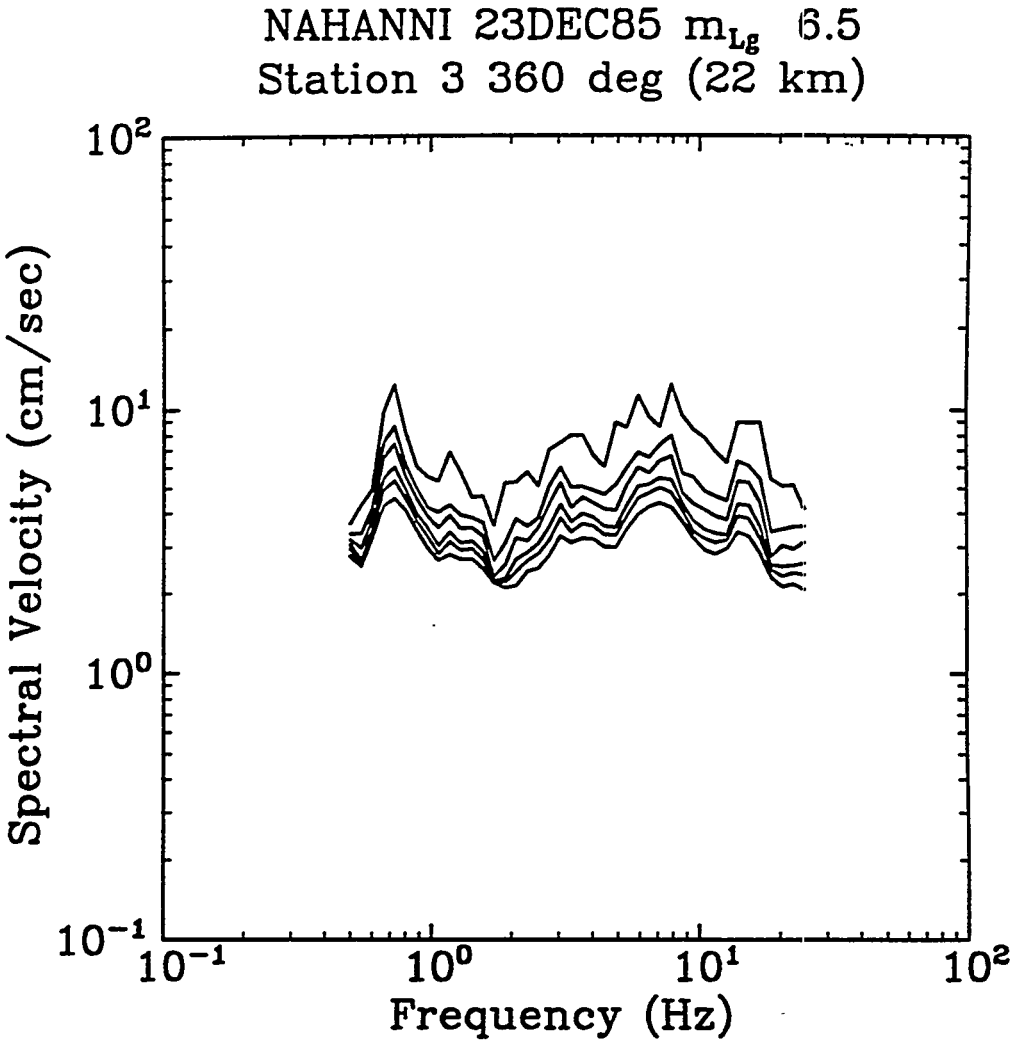

Figure B-22. Response spectra from the 23 December 1985 (05:16 UT), Nahanni earthquake recorded at station 3; 360-degree component. Damping ratios: 2 (top), 5, 7, 10, 12, and 15 percent of critical (bottom).

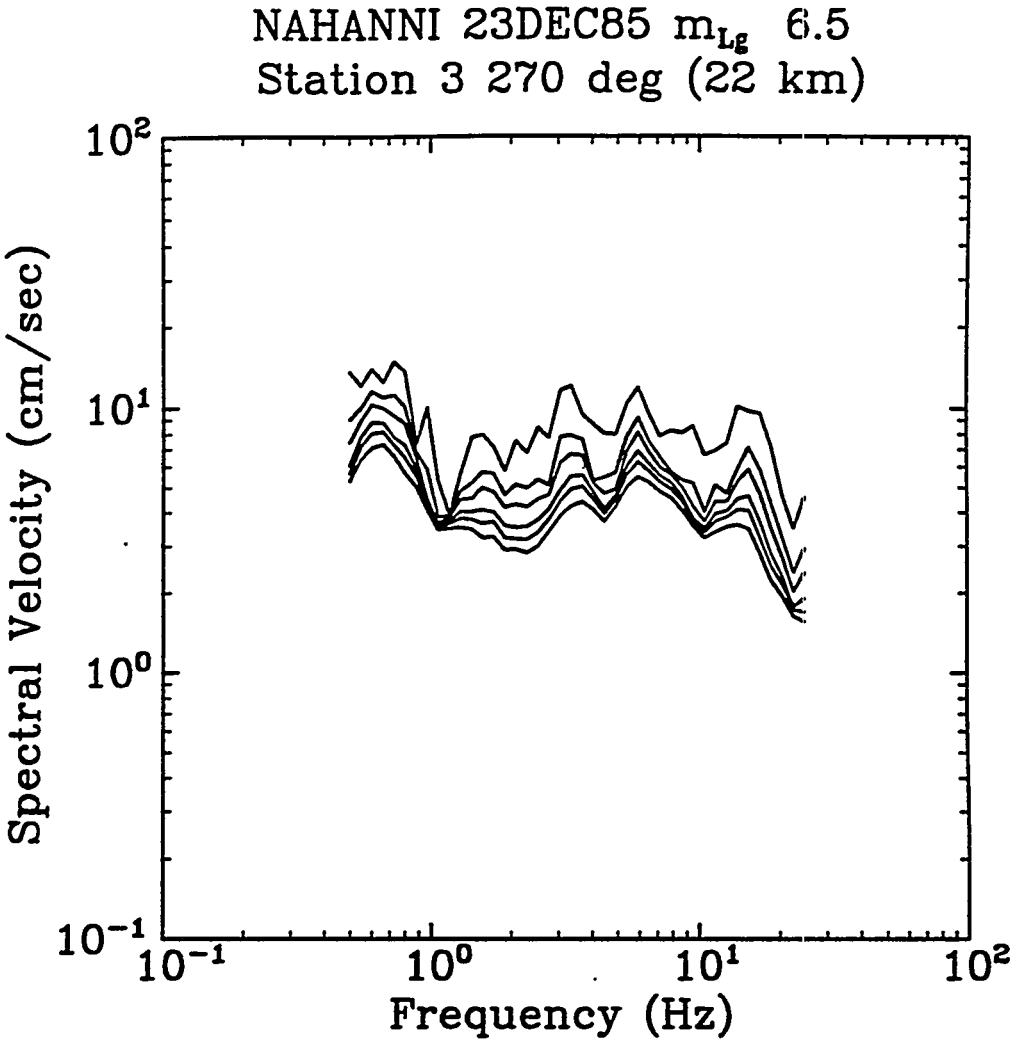

Figure B-23. Response spectra from the 23 December 1985 (05:16 UT), Nahanni earthquake recorded at station 3; 270-degree component. Damping ratios: 2 (top), 5, 7, 10, 12, and 15 percent of critical (bottom).

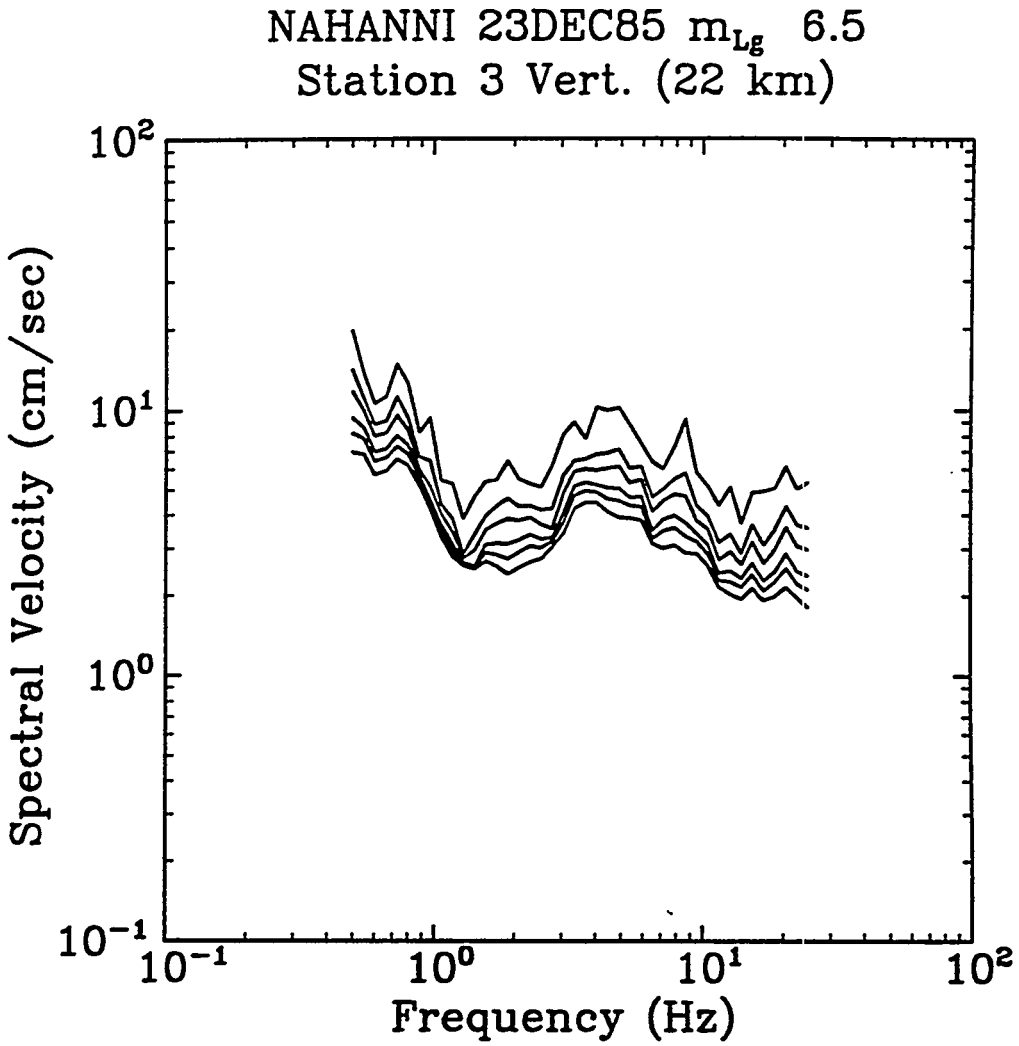

Figure B-24. Response spectra from the 23 December 1985 (05:16 UT), Nahanni earthquake recorded at station 3; vertical component. Damping ratios: 2 (top), 5, 7, 10, 12, and 15 percent of critical (bottom).

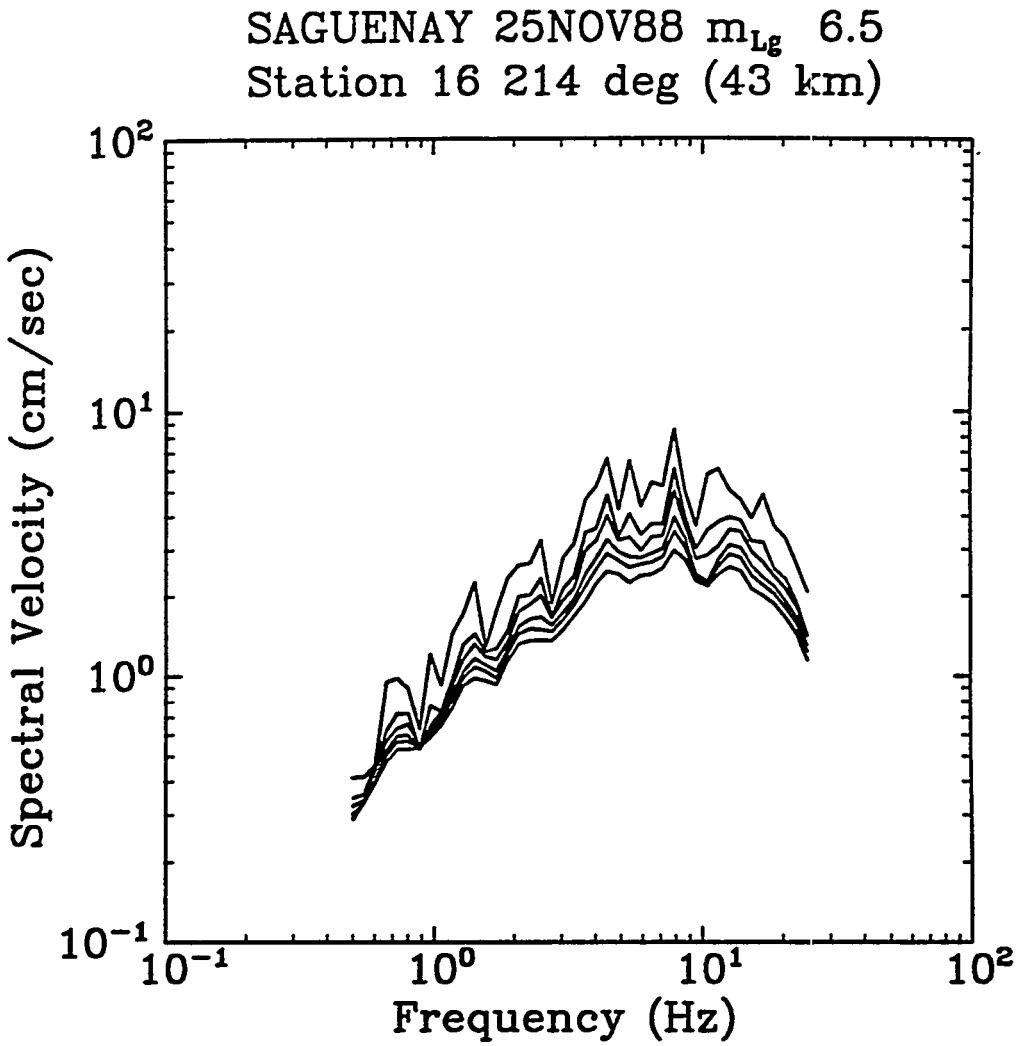

Figure B-25. Response spectra from the 25 November 1988, Saguenay earthquake recorded at station 16; 214-degree component. Damping ratios: 2 (top), 5, 7, 10, 12, and 15 percent of critical (bottom).

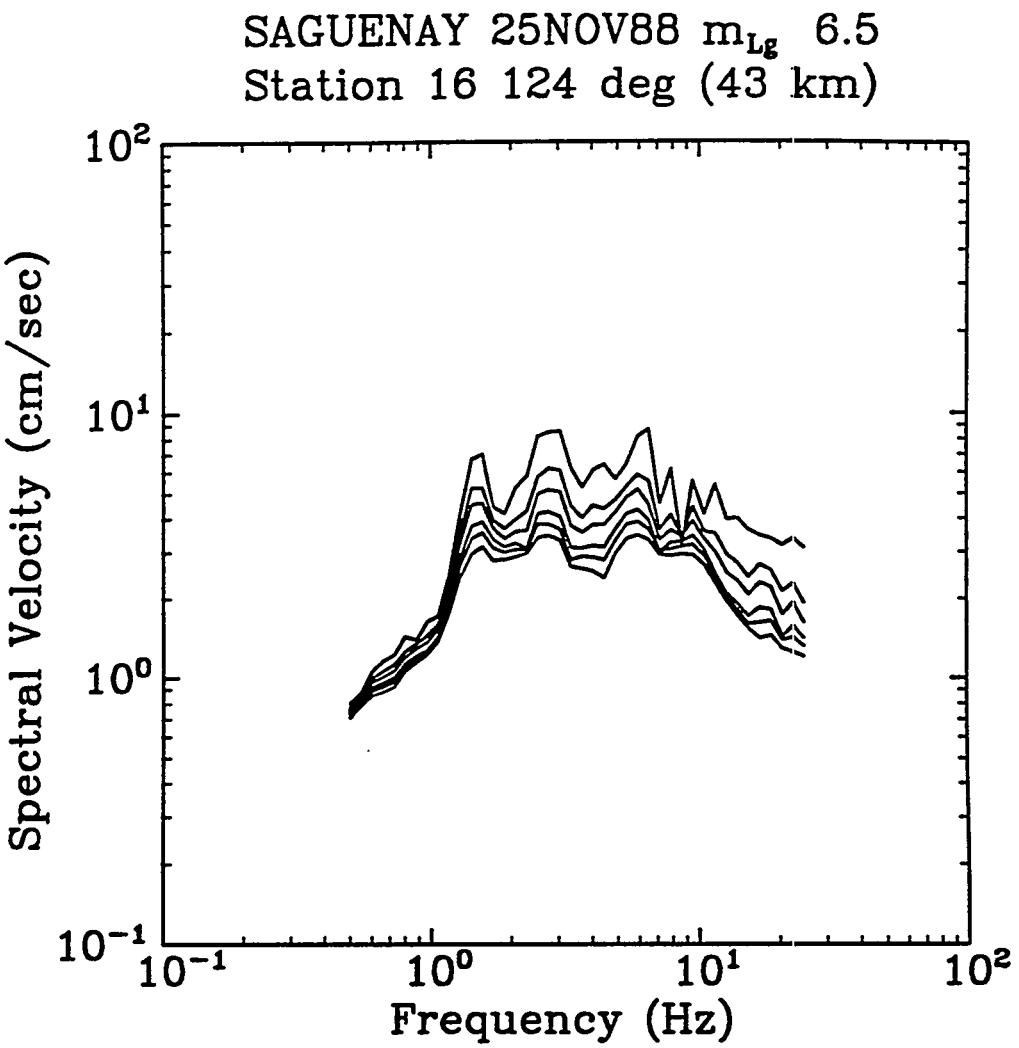

Figure B-26. Response spectra from the 25 November 1988, Saguenay earthquake recorded at station 16; 124-degree component. Damping ratios: 2 (top), 5, 7, 10, 12, and 15 percent of critical (bottom).

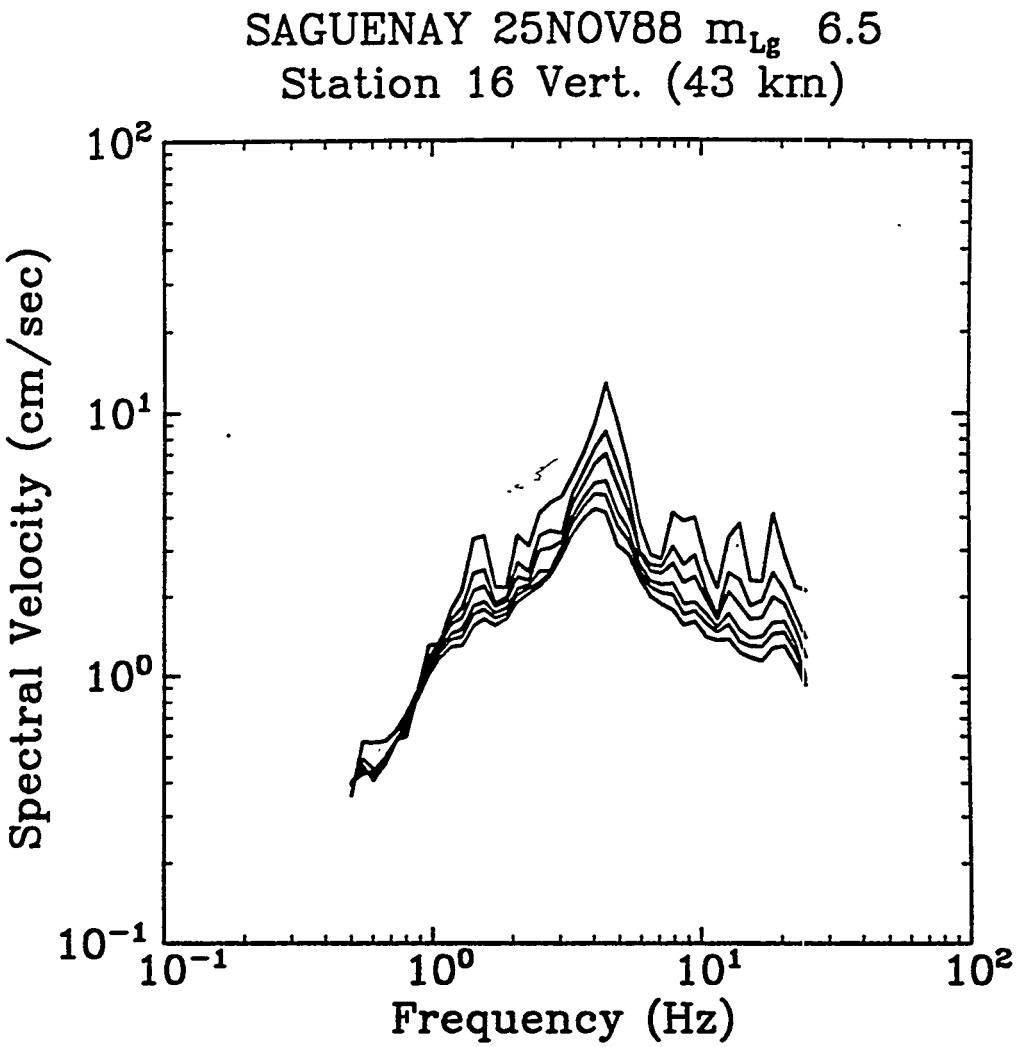

Figure B-27. Response spectra from the 25 November 1988, Saguenay earthquake recorded at station 16; vertical component. Damping ratios: 2 (top), 5, 7, 10, 12, and 15 percent of critical (bottom).

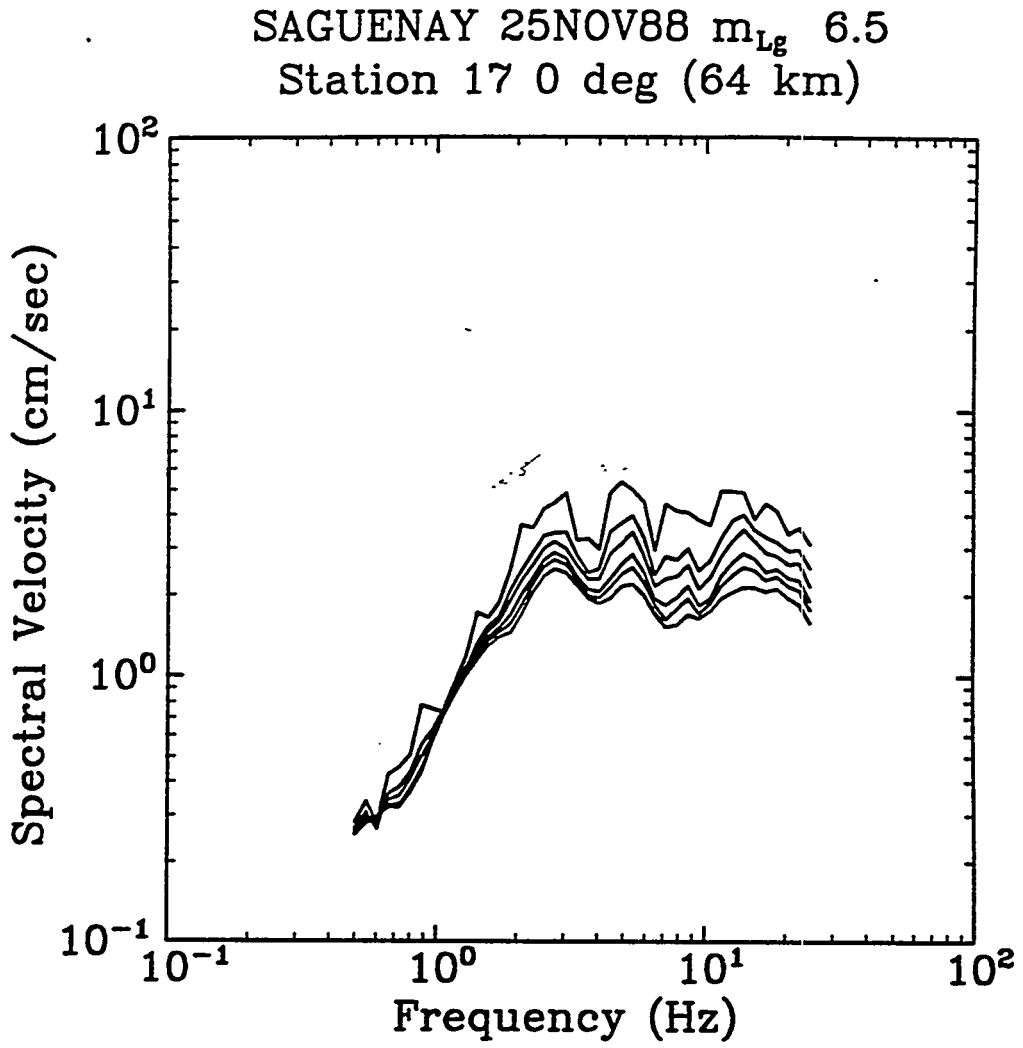

Figure B-28. Response spectra from the 25 November 1988, Saguenay earthquake recorded at station 17; 0-degree component. Damping ratios: 2 (top), 5, 7, 10, 12, and 15 percent of critical (bottom).

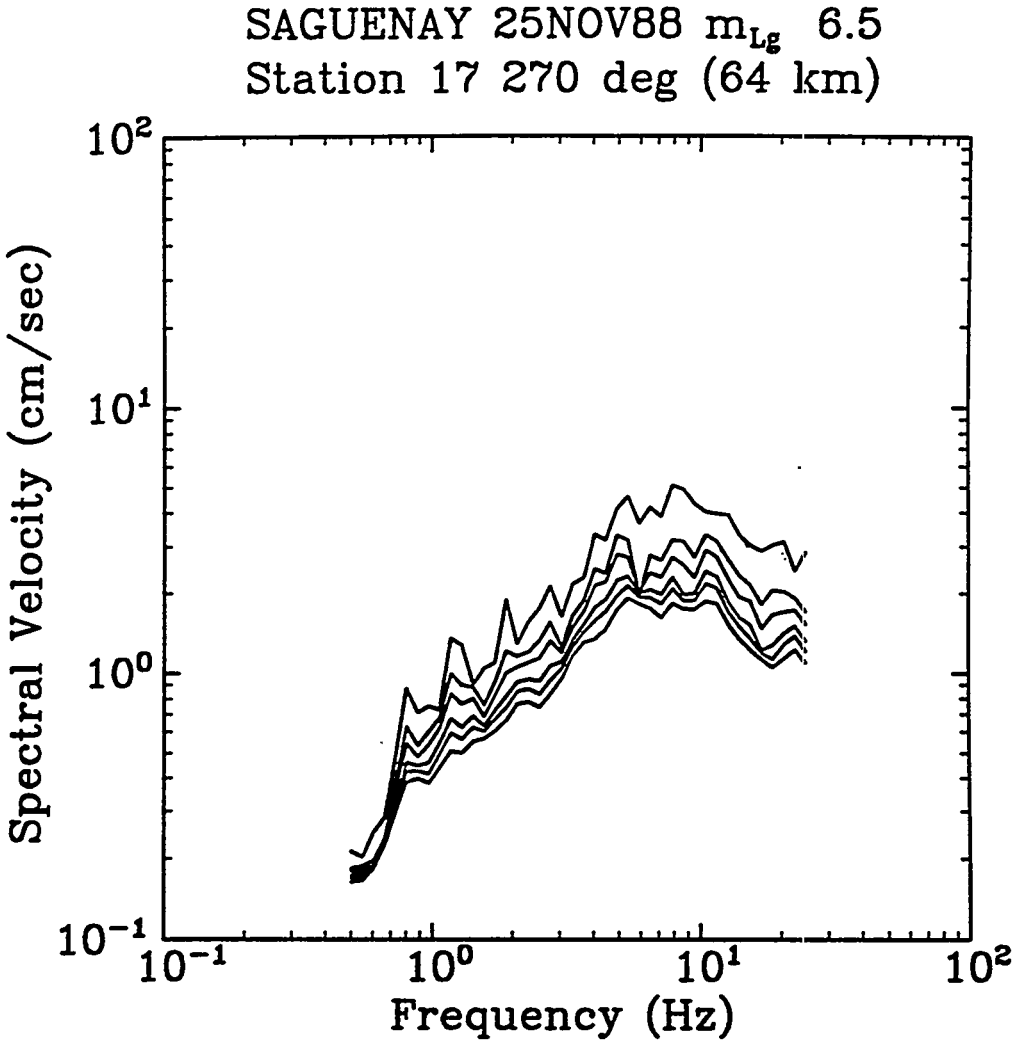

Figure B-29. Response spectra from the 25 November 1988, Saguenay earthquake recorded at station 17; 270-degree component. Damping ratios: 2 (top), 5, 7, 10, 12, and 15 percent of critical (bottom).

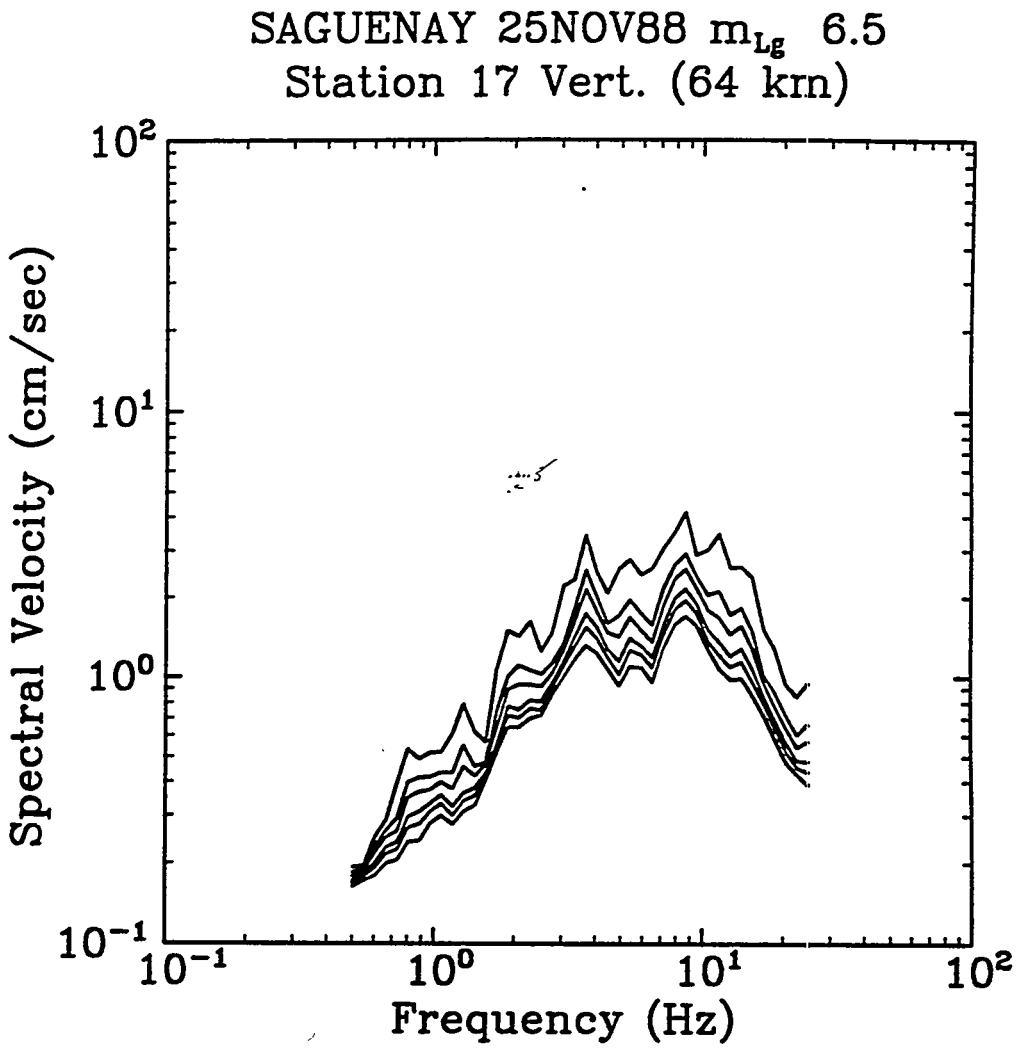

Figure B-30. Response spectra from the 25 November 1988, Saguenay earthquake recorded at station 17; vertical component. Damping ratios: 2 (top), 5, 7, 10, 12, and 15 percent of critical (bottom).

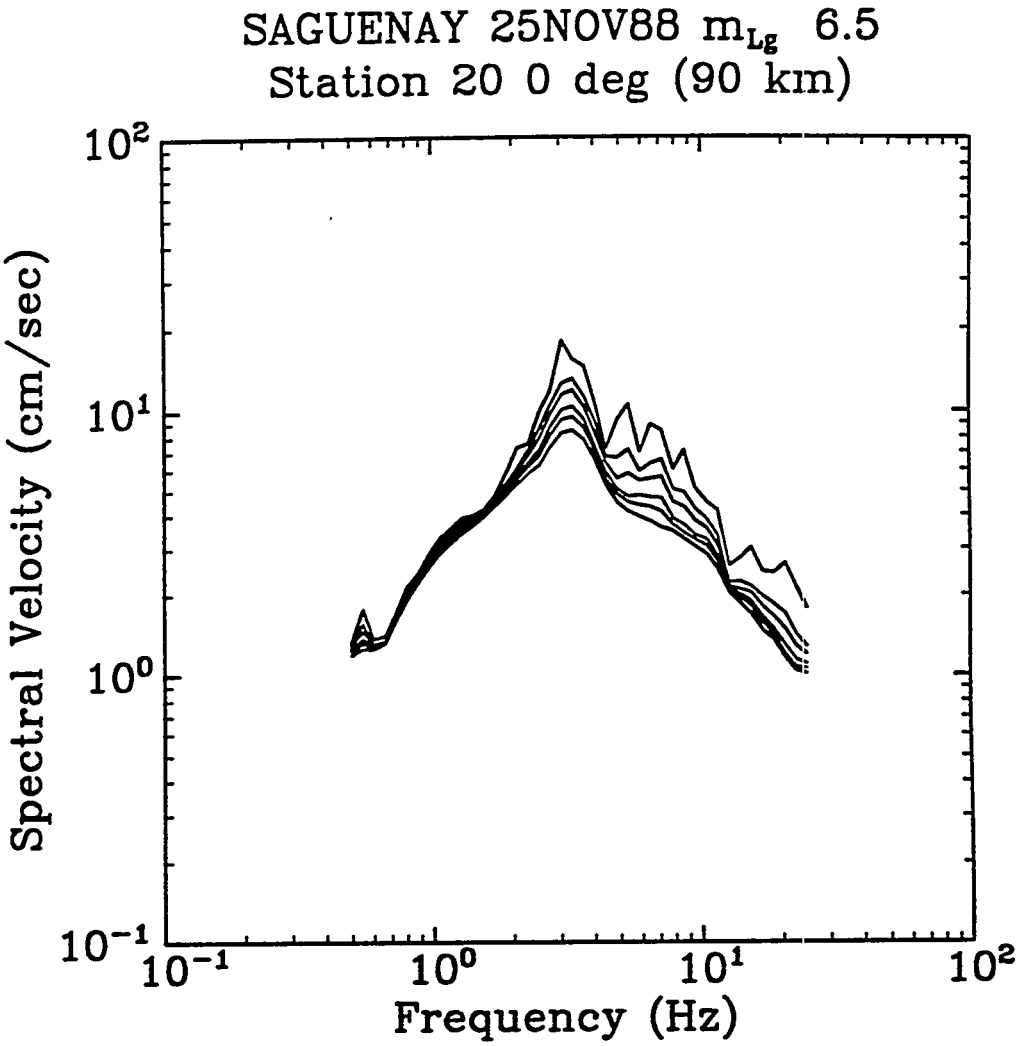

Figure B-31. Response spectra from the 25 November 1988, Saguenay earthquake recorded at station 20; 0-degree component. Damping ratios: 2 (top), 5, 7, 10, 12, and 15 percent of critical (bottom).

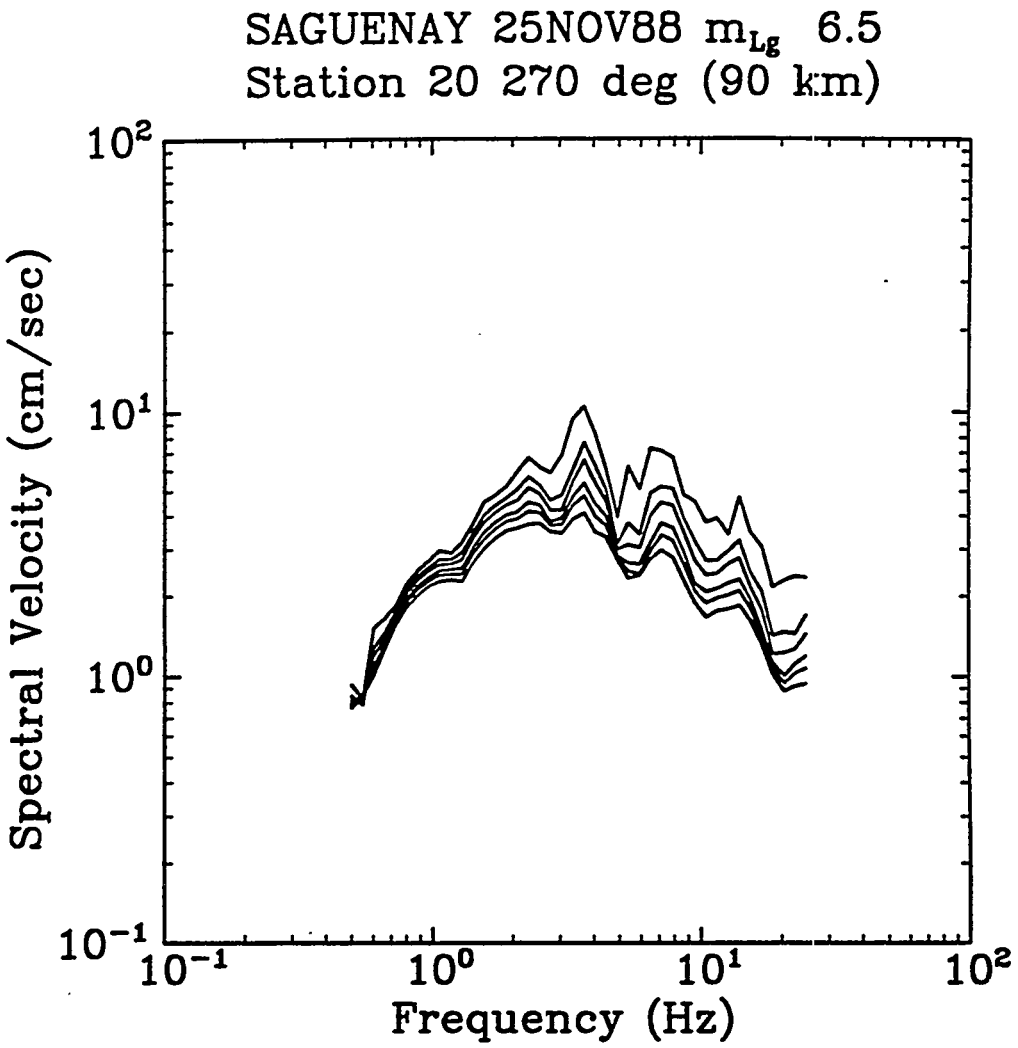

Figure B-32. Response spectra from the 25 November 1988, Saguenay earthquake recorded at station 20; 270-degree component. Damping ratios: 2 (top), 5, 7, 10, 12, and 15 percent of critical (bottom).

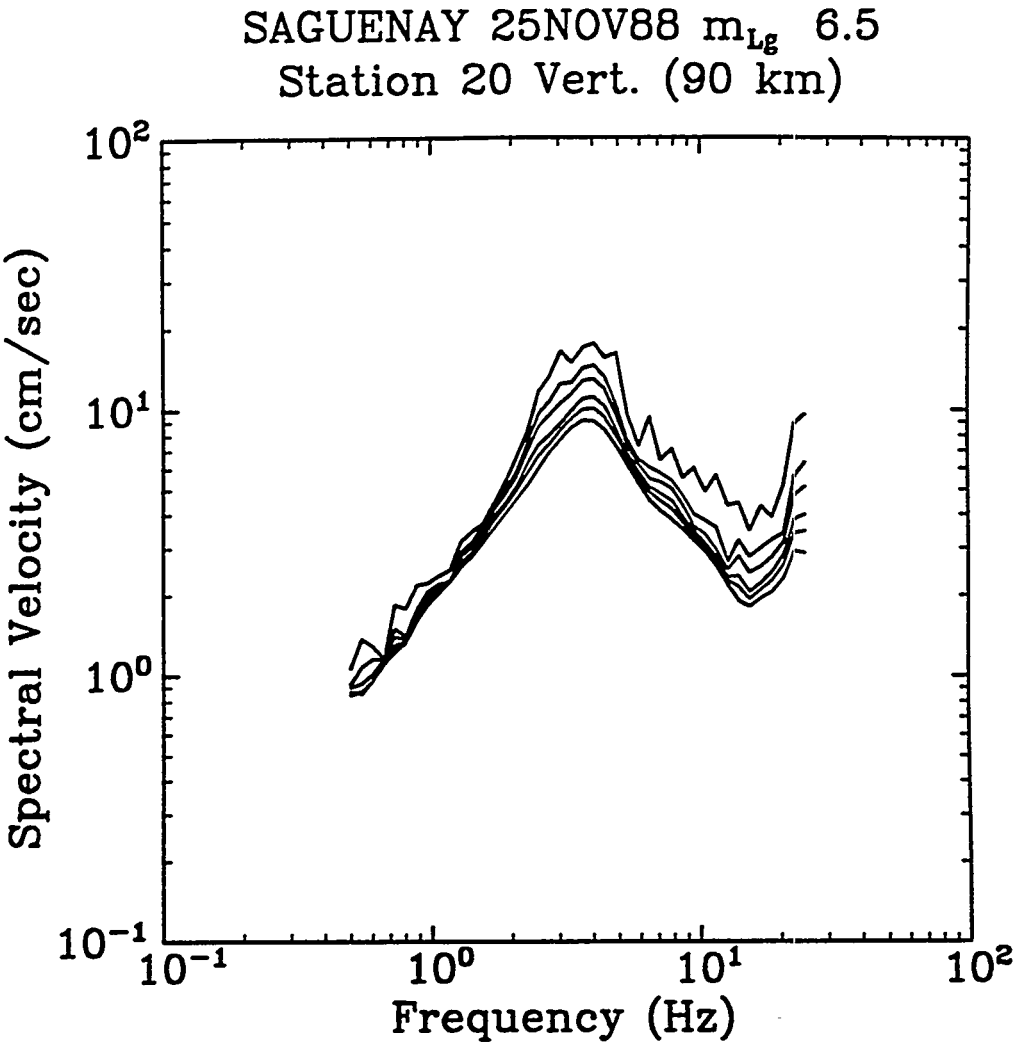

Figure B-33. Response spectra from the 25 November 1988, Saguenay earthquake recorded at station 20; vertical component. Damping ratios: 2 (top), 5, 7, 10, 12, and 15 percent of critical (bottom).

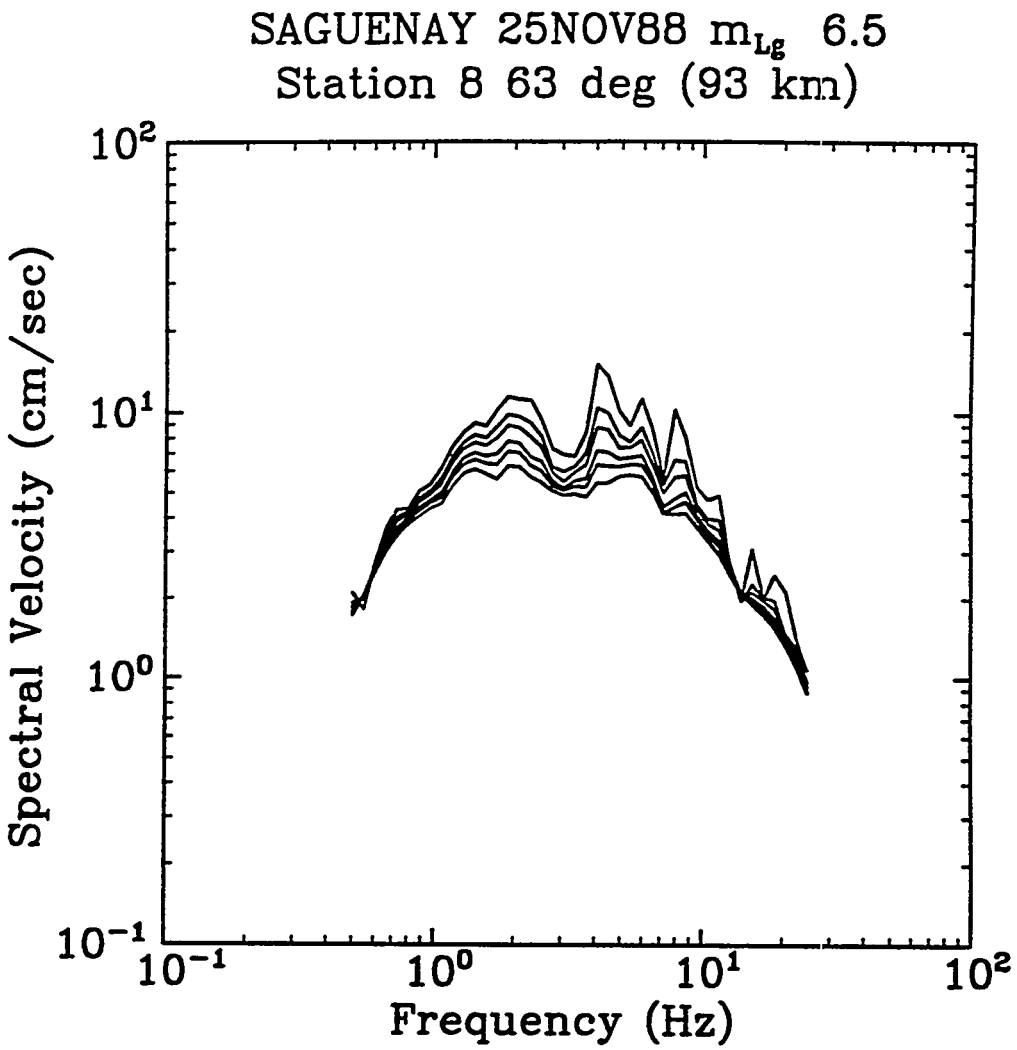

Figure B-34. Response spectra from the 25 November 1988, Saguenay earthquake recorded at station 08; 63-degree component. Damping ratios: 2 (top), 5, 7, 10, 12, and 15 percent of critical (bottom).

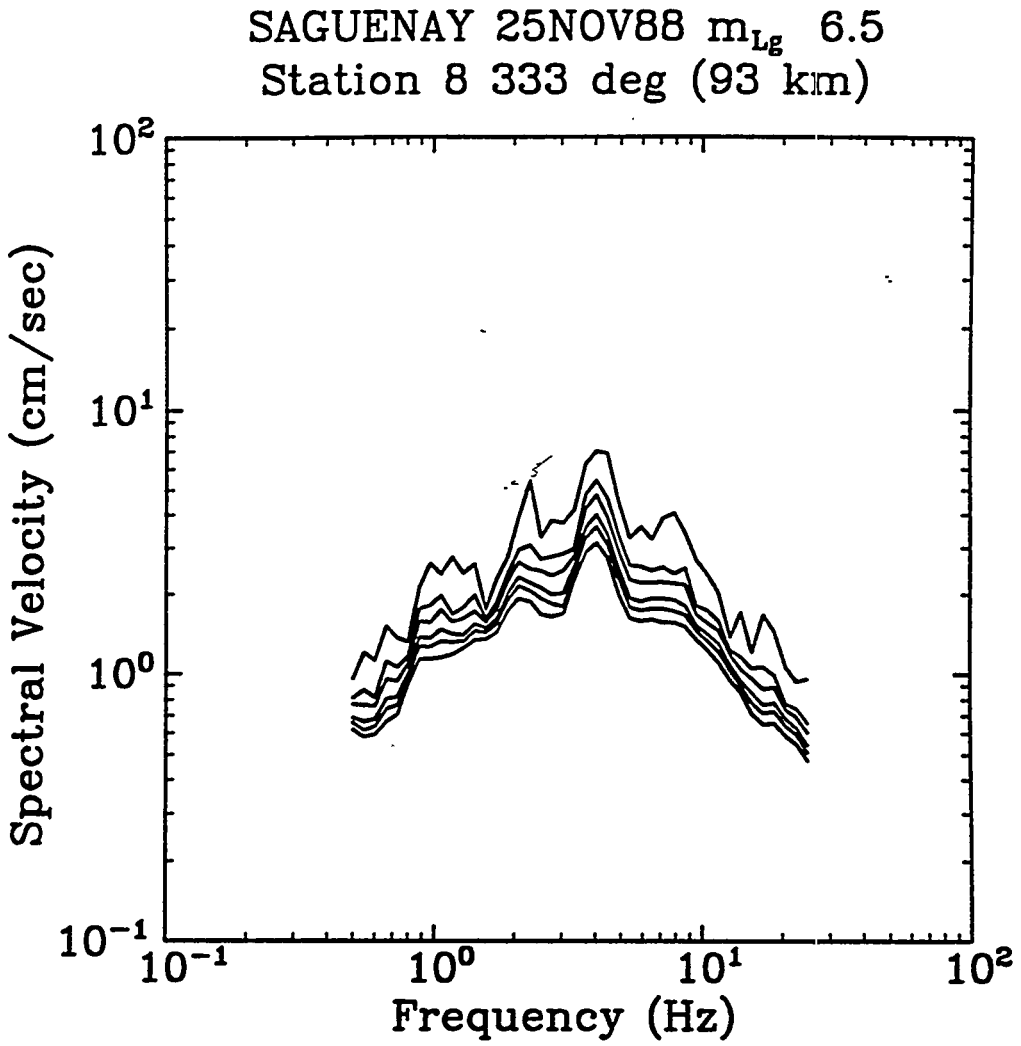

Figure B-35. Response spectra from the 25 November 1988, Saguenay earthquake recorded at station 08; 333-degree component. Damping ratios: 2 (top), 5, 7, 10, 12, and 15 percent of critical (bottom).

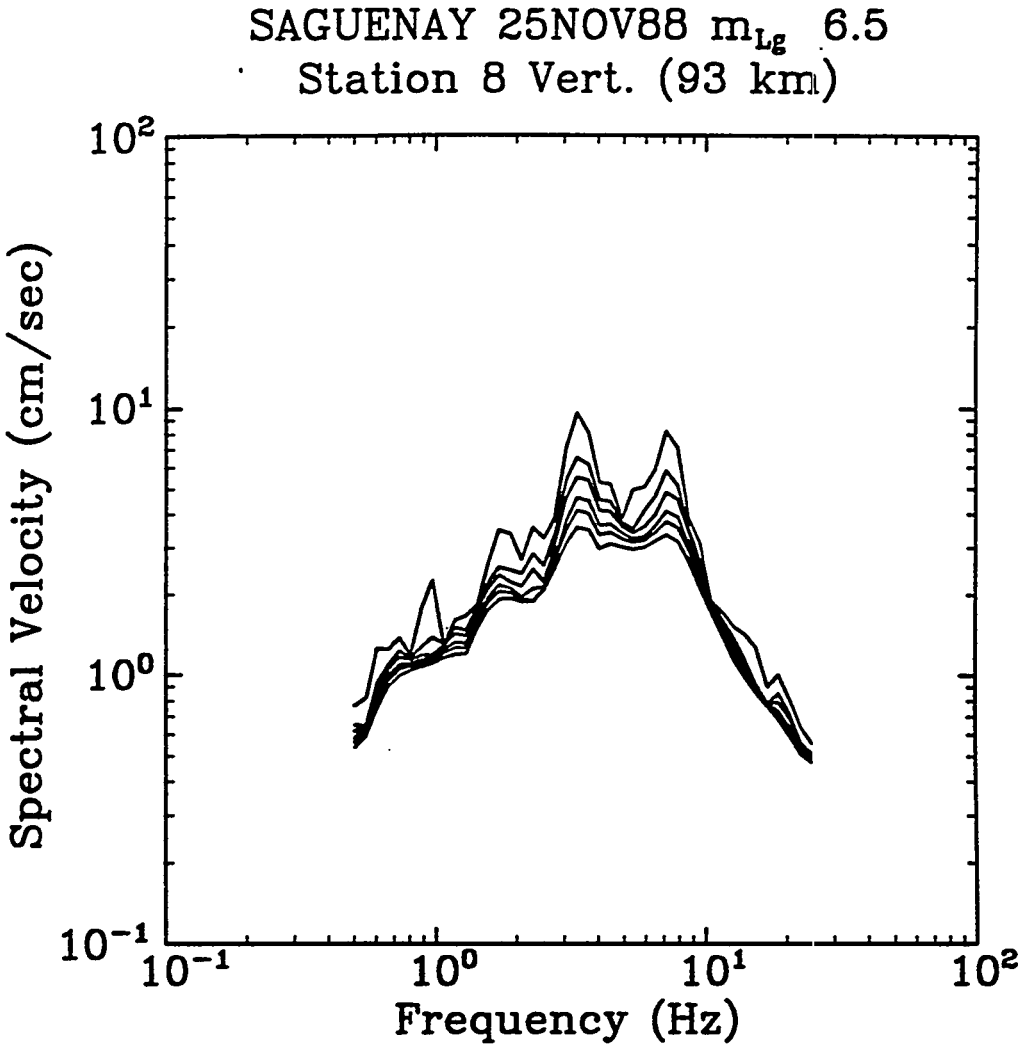

Figure B-36. Response spectra from the 25 November 1988, Saguenay earthquake recorded at station 08; vertical component. Damping ratios: 2 (top), 5, 7, 10, 12, and 15 percent of critical (bottom).